unesp

PROGRAMA DE PÓS-GRADUAÇÃO EM GEOCIÊNCIAS E MEIO AMBIENTE

Análise de sistemas deposicionais não convencionais: evolução sedimentar da Formação Corumbataí, Permiano Superior da Bacia do Paraná

BEATRIZ CHRISTOFOLETTI

Instituto de Geociências e Ciências Exatas
Campus de Rio Claro

Rio Claro - SP
2024

UNIVERSIDADE ESTADUAL PAULISTA

"Júlio de Mesquita Filho"
Instituto de Geociências e Ciências Exatas
Câmpus de Rio Claro

BEATRIZ CHRISTOFOLETTI

ANÁLISE DE SISTEMAS DEPOSICIONAIS NÃO CONVENCIONAIS: EVOLUÇÃO SEDIMENTAR DA FORMAÇÃO CORUMBATAÍ, PERMIANO SUPERIOR DA BACIA DO PARANÁ

Dissertação de Mestrado apresentada ao Instituto de Geociências e Ciências Exatas do Câmpus de Rio Claro, da Universidade Estadual Paulista "Júlio de Mesquita Filho", como parte dos requisitos para obtenção do título de Mestre em Geociências e Meio Ambiente

Orientador: Lucas Veríssimo Warren

Coorientador: Filipe Giovanini Varejão

Rio Claro - SP

2024

C556a

Christofoletti, Beatriz
Análise de sistemas deposicionais não convencionais: evolução sedimentar da Formação Corumbataí, Permiano Superior da Bacia do Paraná / Beatriz Christofoletti. -- Rio Claro, 2024
143 f.

Dissertação (mestrado) - Universidade Estadual Paulista (Unesp), Instituto de Geociências e Ciências Exatas, Rio Claro
Orientador: Lucas Veríssimo Warren
Coorientador: Filipe Giovanini Varejão

1. Mega-lagos. 2. Formação Corumbataí. 3. Tufo vulcânico. 4. Permiano Superior. I. Título.

Sistema de geração automática de fichas catalográficas da Unesp. Biblioteca do Instituto de Geociências e Ciências Exatas, Rio Claro. Dados fornecidos pelo autor(a).

IMPACTO DA PESQUISA

Os novos conhecimentos aqui apresentados sobre a evolução e os depósitos sedimentares de lagos de escala continental (mega lagos) poderão servir como base de dados para, no futuro, gerar soluções para problemas relacionados a reservatórios de hidrocarbonetos, já que grande parte das jazidas brasileiras estão em depósitos lacustres, ou sobre as modificações que grandes mudanças climáticas podem causar nesses ambientes.

POTENTIAL IMPACT OF THIS RESEARCH

The new knowledge presented here about the evolution and sedimentary deposits of continental-scale lakes (mega lakes) could serve as a database to, in the future, generate solutions to problems related to hydrocarbon reservoirs since a large part of Brazilian deposits are in lake deposits, or about the changes that major climate changes can cause in these environments.

UNIVERSIDADE ESTADUAL PAULISTA
"Júlio de Mesquita Filho"
Instituto de Geociências e Ciências Exatas
Câmpus de Rio Claro

BEATRIZ CHRISTOFOLETTI

ANÁLISE DE SISTEMAS DEPOSICIONAIS NÃO CONVENCIONAIS: EVOLUÇÃO SEDIMENTAR DA FORMAÇÃO CORUMBATAÍ, PERMIANO SUPERIOR DA BACIA DO PARANÁ

Dissertação de Mestrado apresentada ao Instituto de Geociências e Ciências Exatas do Câmpus de Rio Claro, da Universidade Estadual Paulista "Júlio de Mesquita Filho", como parte dos requisitos para obtenção do título de Mestre em Geociências e Meio Ambiente

Comissão Examinadora

Prof. Dr. LUCAS VERÍSSIMO WARREN
IGCE / UNESP/Rio Claro (SP)

Prof. Dr. CLAUDIO RICCOMINI
IEE / USP/São Paulo (SP)

Prof. Dr. ERNESTO LUIZ CORREA LAVINA
UNISINOS / São Leopoldo (RS)

Conceito: Aprovado.

Rio Claro (SP), 12 de Janeiro de 2024.

AGRADECIMENTOS

Ao meu grande professor, orientador e amigo Prof. Dr. Lucas Warren, pelo imenso conhecimento compartilhado, pelos momentos de descontração sempre acompanhado de uma Heineken gelada, por todas as dicas e conselhos de vida e por sempre me incentivar a encarar novos desafios. Ao Prof. Dr. Filipe Varejão por ter aceitado embarcar nessa jornada, pelas ótimas ideias e sugestões, por aguentar minhas intermináveis dúvidas sobre estratigrafia e por ter se tornado também um grande amigo. Vocês fizeram com que eu entendesse meu amor pela ciência. Seguiremos juntos por mais alguns anos!

Ao Programa de Recursos Humanos da Agência Nacional do Petróleo, Gás Natural e Biocombustíveis – PRH-ANP, suportado com recursos provenientes do investimento de empresas petrolíferas qualificadas na Cláusula P, D & I da Resolução ANP n° 50/2015.

As amigas geólogas Mariza Rodrigues e Paloma Promenzio por todo suporte e boas conversas. Aos professores Mário Assine, Marcello Simões, Lucía Gómez-Peral, Cristiano Lana, Cláudio Riccomini, Bernardo Tavares e Ernesto Lavina por contribuírem para a melhora deste trabalho.

Aos meus pais, irmãos e sobrinhos, pelo amor incondicional. As minhas grandes grandes amigas de infância e vida, Lívia, Milena, Natália, Flávia, Larissa e Laura, presentes em todas as fases especiais da minha vida.

Ao UNESPetro e Departamento de Geologia pelo fornecimento do espaço e equipamentos fundamentais na realização desta dissertação.

RESUMO

Durante o Permiano, o desenvolvimento de uma barreira orográfica na margem sudoeste de Gondwana, levou à restrição das conexões marinhas entre o Panthalassa e as bacias Paraná-Karoo, resultando na formação de um mar aprisionado (*trapped sea*) que evoluiu para um lago de escala continental, no qual foi depositado o Grupo Passa Dois. Nesse contexto, destaca-se a Formação Corumbataí, composta por sucessão mista carbonática-siliciclástica com espessuras de até 120 m. Desde meados do do século XX, diversos cenários paleoambientais foram propostos para esta unidade, incluindo marinho raso, deltaico, lacustre e planície de maré. Face ao panorama exposto, este trabalho buscou aplicar abordagem calcada na análise multi-indicadores (sedimentologia, icnologia, estratigrafia de sequências, geocronologia e geoquímica) dos depósitos da Formação Corumbataí, a fim de investigar quais processos sedimentares e controles de sedimentação são responsáveis pelos produtos deposicionais observados neste sistema não-convencional estabelecido durante o Permiano. Neste contexto, é proposto novo modelo deposicional, contemplando a evolução estratigráfica, bem como o refinamento geocronológico e bioestratigráficoda Formação Corumbataí. Os dados apresentados nesta dissertação apontam para sedimentação em um mega lago endorreico, caracterizado por acentuadas variações hidrológicas e salinas que condicionaram estágios de preenchimento *ballanced-fill* a *overfilled*, e intimamente associado aos tratos dos sistemas transgressivo e regressivo. Soma-se a este cenário, evidências da influência de ondas, marés metereológicas (seiche) e tempestades na sedimentação. A presença de um nível de tufo vulcânico no topo da Formação Corumbataí forneceu nova idade U-Pb e contribuiu para a compreensão da evolução geológica do Gondwana ocidental, traçando cenário mais realista da evolução *in situ* de moluscos endêmicos, com implicações cronoestratigráficas.

Palavras-chave: Mega-lagos; Formação Corumbataí; tufo vulcânico; Permiano Superior

ABSTRACT

During the Permian, the development of an orographic barrier on the southwestern margin of Gondwana led to the restriction of marine connections between the Panthalassic Ocean and the Paraná-Karoo basins, resulting in the formation of a trapped sea that evolved into a megalake in which the Passa Dois Group was deposited. In this context, highlights the up to 120 m-thick mixed carbonate-siliciclastic succession from the Corumbataí Formation. Since the mid-20th century, several paleoenvironmental scenarios have been proposed for this unit, including shallow marine, deltaic, lacustrine and tidal flat. Considering this context, the present research used a multi-proxy approach (sedimentology, ichnology, sequence stratigraphy, geochronology and geochemistry) applied to the deposits of the Corumbataí Formation, in order to investigate which sedimentary processes and controls were responsible for the depositional products observed in this unconventional system established during the Permian. A new depositional model, as well as stratigraphic evolution, geochronological and biostratigraphic refinement are proposed. The data presented in this dissertation point to sedimentation in an endorheic megalake, characterized by accentuated hydrological and saline variations that conditioned the development of balanced-fill to overfilled stages, in close association with transgressive and regressive system tracts. In this scenario, there is evidence of the influence of waves, meteorological tides (seiche) and storms in deposition. The presence of a volcanic tuff bed at the top of the Corumbataí Formation provided a new U-Pb age and contributed to understanding the geological evolution of SW Gondwana, outlining a more realistic scenario to the *in situ* evolution of endemic mollusks.

Key-words: Megalakes; Corumbataí Formation; volcanic tuff; late Permian.

ORGANIZAÇÃO DA DISSERTAÇÃO

Esta dissertação intitulada "Análise de sistemas deposicionais não convencionais: evolução sedimentar da Formação Corumbataí, Permiano Superior da Bacia do Paraná", foi concebida e organizada em forma de artigos científicos. Estes encontram-se redigidos em língua inglesa e possuem listas de referências bibliográficas individuais cuja formatação atende aos padrões específicos de cada periódico para qual foram submetidos. Um breve resumo em língua portuguesa é feito antes de cada artigo a fim de contextualizar a produção no âmbito do presente documento.

O **Capítulo 1** apresenta as problemáticas acerca do ambiente de deposição e idade da Formação Corumbataí, uma breve contextualização da área estudado em seu âmbito geológico, bem como uma revisão sobre a evolução dos conhecimentos sobre a unidade estudada e as principais metodologias aplicadas. Está dividido em: 1. Introdução, 2. Objetivos, 3. Metodologia, 4. Contextualização Geológica.

O **Capítulo 2** apresenta a integração dos principais resultados sedimentológicos e estratigráficos da Foormação Corumbataí. Os dados constam no manuscrito intitulado: "*Sedimentation and accommodations controls on the facies stacking and lateral distribution of a Permian unconventional megalake*". Este trabalho aborda a evolução da estratigrafia da unidade, bem como os principais fatores controladores da sedimentação. Também é dissertado sobre o novo modelo de deposição proposto para a sedimentação em lagos de grandes dimensões e batimetrias diminutas.

O **Capítulo 3** apresenta a primeira datação radiométrica de camada de tufo vulcânico da Formação Corumbataí para a porção norte da Bacia do Paraná. Esses dados são apresentados como manuscrito, redigido em língua inglesa, intitulado: *"Rising mollusk bivalves from the ashes: geologic, biostratigraphy and evolutionary implications from tuff data in the Permian Corumbataí Formation, Paraná Basin, Brazil"*, sob revisão no periódico *Journal of South American Earth Science*.

O **Capítulo 4** apresenta as conclusões parciais e considerações adicionais desta dissertação. No **Apêndice I** são disponibilizadas todas as seções colunares medidas com seus respectivos diagramas de Fischer, bem como a correlação lateral proposta para elas. No **Apêndice II** constam os dados obtidos das análises geocronológicas e geoquímicas dos grãos de zircão coletados no nível de tufo. No **Apêndice III**, consta o manuscrito intitulado *"Rising* *mollusk bivalves from the ashes: geologic, biostratigraphy and evolutionary implications from tuff data in the Permian Corumbataí Formation, Paraná Basin, Brazil"* publicado no períodico *Journal of South American Earth Science*.

SUMÁRIO

1. CONSIDERAÇÕES INICIAIS

1.1. Introdução

Durante o Permiano, o mar epicontinental que banhava o sudeste do continente Gondwana passou por condições progressivas de continentalização (Lavina, 1991; Milani et al., 2007; Holz et al., 2010; Limarino et al., 2013; Kern et al., 2021) devido ao soerguimento do cinturão orogênico Gondwanides (Keidel, 1916; Ramos et al., 1986). Na América do Sul e África, este capítulo único na história evolutiva das bacias do Paraná e Huab/Karoo é registrado pelas formações Irati e White Hill (Kungurian; ~277 Ma). Este vasto mar aprisionado tectonicamente ("*trapped sea*", sensu Palcu et al., 2021) cobria uma grande área do SW Gondwana correspondendo originalmente a três vezes o tamanho do Mar Cáspio e uma vez e meia o tamanho do Golfo do México (Runnegar e Newell, 1971). Devido às restritas conexões oceânicas, esta enorme massa de água provavelmente foi fortemente estratificada e influenciada por ingressões marinhas pontuais com períodos de acentuada hipersalinidade e produção de carbonatos (Bastos et al., 2021; Brito et al., 2023). Posteriormente, durante a Época Guadalupiana, a Bacia do Paraná foi completamente desvinculada do Panthalassa, tornando-se um megalago que cobria uma área superior a 1,7 milhão de km^2 (Rohn, 1994), correspondendo atualmente a parte do Brasil, Uruguai, Paraguai, Namíbia, e África do Sul.

Este mega lago no interior no supercontinente foi caracterizado por acentuadas variações hidrológicas e de salinidade que condicionaram o desenvolvimento de uma fauna endêmica única de bivalves, gastrópodes, peixes e répteis (Runnegar e Newell, 1971; Simões et al., 1998). A evolução deste imenso corpo d'água antes da total continentalização do Gondwana, está registrado na Formação Corumbataí. Esta unidade aflora na forma de um arco delgado que margeia as bordas leste e norte-noroeste da Bacia do Paraná, restringindo-se aos estados de São Paulo, Goiás e Mato Grosso.

A Formação Corumbataí tem sido alvo de grande número de estudos desde o início do século passado, os quais especularam diferentes cenários paleoambientais para a sedimentação siliciclástica-carbonática neste intervalo. No entanto, não existe ainda consenso quanto ao ambiente deposicional desta unidade, com interpretações que seguem uma tendência cronológica, variando de sistema marinho dominado por maré (Salamuni, 1963; Northfleet et al., 1969; Schneider et al., 1974; Fúlfaro et al., 1978; Gama Jr., 1979; Fúlfaro et al., 1980; Zaine, 1980; Sousa, 1985) à lacustre com influência de tempestades (Suguio et al., 1974; Petri e Coimbra, 1982; Petri e Fúlfaro, 1983; Lavina, 1991; Rohn, 1994).

Embora existam atualmente mares fechados e interiores distribuídos em diversas regiões do planeta (e.g., mares Cáspio e Negro na Eurásia; Palcu et al., 2021), a dimensão, condições climáticas e características deposicionais destes corpos d´água durante o Permiano conferem caráter único à Bacia do Paraná. Deste modo, análogos modernos funcionam apenas como sistemas comparáveis do ponto de vista fisiográfico, já que os mecanismos de deposição são desconhecidos e modelos de fácies são basicamente inexistentes para estes tipos de sistema. Em função destas particularidades, os mares interiores e fechados (ou mega lagos) são muito pouco compreendidos do ponto de vista de seus sistemas deposicionais dificultando muitas vezes sua correta interpretação no registro geológico. Por exemplo, padrões de circulação de correntes e dispersão de sedimento comuns em análogos atuais, à exemplo do fenômeno meteorológico seiche, semelhante às marés, são completamente desprezados (ou não reconhecidos) no registro geológico. Seiches são formados quando ventos fortes, gerados por mudanças rápidas na pressão atmosférica, empurram a água de uma margem do corpo d'água para outra, aumentando consideravelmente o nível da água. Quando os ventos cessam, a massa de água recua na direção oposta, expondo a margem anteriormente inundada, efeito este que faz a água continuar a oscilar para frente e para trás por horas ou até dias (Ichinose et al., 2000)

Considerando o acima exposto, esta pesquisa buscou elucidar quais os processos sedimentares que atuaram na deposição da Formação Corumbataí. Para isso, propõem-se estabelecer, pela primeira vez, o arcabouço litoestratigráfico, bioestratigráfico e de estratigrafia de sequencias da unidade, bem como gerar um modelo de fácies coerente a fim de possibilitar a interpretação de seu sistema deposicional não convencional. Além disso, embora exista extenso volume bibliográfico produzido até hoje acerca do posicionamento cronológico da unidade, este foi embasado principalmente em dados paleontológicos (i.e., palinomorfos; Daemon e Quadros, 1970). Desta forma, faz necessário a integração de dados bioestratigráficos com dados geocronológicos no intuito de compreender a correlação temporal das formações Teresina e Corumbataí e contribuir para o entendimento das taxas deposicionais da unidade para melhor entendimento da dinâmica sedimentar do complexo sistema que recobria boa parte do supercontinente Gondwana durante o Permiano.

1.2. Objetivos

A presente dissertação teve como objetivo estabelecer a evolução sedimentar da Formação Corumbataí e um modelo de fácies adequado para sistemas deposicionais desenvolvidos em mega lagos de batimetria reduzida e com influência de seiche. A integração desses dados permitiu delinear um novo modelo deposicional para a unidade, com implicações relevantes para a compreensão da sedimentação dos mega lagos e parte da história deposicional das bacias paleozoicas do Gondwana. Com a descoberta de um nível de cinzas vulcânicas, tornou-se objetivo secundário desta dissertação aferir a idade deposicional da Formação Corumbataí a fim de refinar a correlação temporal entre esta unidade e as formações Teresina e Rio do Rasto, bem como compreender as implicações bioestratigráficas desta nova idade radiométrica.

1.3. Metodologia

1.3.1. Análise de fácies sedimentares e seções colunares

O termo fácies sedimentar designa um corpo rochoso com um conjunto de características (texturas, geometrias, estruturas sedimentares e fósseis) distintas dos corpos adjacentes, e que foi depositado sob determinado processo sedimentar relativamente constante (Walker e James, 1992; Miall, 1999). As fácies ocorrem naturalmente agrupadas, ou seja, geneticamente relacionadas entre si e com um significado paleoambiental. Dessa forma, através da associação de fácies é possível estabelecer modelos que servem como parâmetro de comparação, além de permitir interpretações ambientais mais abrangentes (Walker e James, 1992). Através do levantamento de seções colunares é possível caracterizar as fácies sedimentares e evidenciar como estas se agrupam e variam vertical e lateralmente nos diferentes ambientes deposicionais.

As seções colunares foram adquiridas em escala de semi-detalhe (1:50), seguindo a metodologia de Miall (1996), na qual são descritas as fácies sedimentares reconhecidas e coletadas amostras estratigraficamente posicionadas para análise em laboratório. O grau de bioturbação foi estimado com base no esquema de Taylor e Goldring (1993), que definiu um índice de bioturbação (BI), variando de zero (sem bioturbação) a seis (completamente bioturbação). Ao todo foram adquiridas vinte e cinco seções colunares buscando caracterizar as associações de fácies da Formação Corumbataí em escala local, regional e de bacia (Tabela 1). Todas as seções colunares, bem como a correlação regional, são apresentadas no Anexo I.

Tabela 1 - Seções colunares medidas nos estados de Mato Grosso, Goiás e São Paulo em afloramentos da Formação Corumbataí. Cód.: código; **baseada no trabalho de Santos (2011).

Cód.	Seção	Cidade/Estado	Coordenadas Geográficas		Espessura (m)
			Latitude	Longitude	
0	Império**	Alto Garças	16° 55.595'S	53° 30.962'O	21.3
1	Pedreira Mentel	Alto Garças/MT	16° 55.817'S	53° 30.802'O	10.9
2	Lageadinho	Alto Garças/MT	16° 56.336'S	53° 29.764'O	44
3	Córrego Cuiabano	Santa Rita do Araguaia/GO	17° 12.702'S	53° 4.051'O	56.7
4	A-Evaporitos	Mineiros/GO	17° 32.669'S	52° 33.491'O	3.8
	B- Mineiros Tufo	Mineiros/GO	17° 32.607'S	52° 33.931'O	5.9
	C-Mineiros Meninas	Mineiros/GO	17° 32.449'S	52° 33.572'O	6.5
	D-Mineiros Pedreira	Mineiros/GO	17° 31.757'S	52° 33.548'O	15
5	Pedreira Sucal	Perolândia/GO	17° 28.698'S	52° 3.518'O	10.1
6	Corumbataí	Corumbataí/SP	22° 13.314'S	47° 37.182'O	7.3
7	Zarko's	Rio Claro/SP	22°20'57.85"S	47°33'51.29"O	16.9
8	Batalha	Rio Claro/SP	22°21'36.97"S	47°35'24.10"O	18.9
9	Trevo	Rio Claro/SP	22° 22.821'S	47° 36.537'O	31.1
10	Usipedra	Ipeúna/SP	22°22'56.49"S	47°38'28.33"O	20.8
11	Pedreira Ipeúna	Ipeúna/SP	22° 23.993'S	47° 37.308'O	42.2
12	Ipeúna-Charqueada	Ipeúna/SP	22°22'58.47"S	47°38'16.73"O	13.7
13	Camaquã	Rio Claro/SP	22° 22.433'S	47° 38.637'O	4.3
14	Calcário Cruzeiro	Limeira/SP	22°32'27.00"S	47°26'42.39"O	31.8
15	Rod. Bandeirantes	Limeira/SP	22°32'21.00"S	47°27'12.00"O	30
16	Onça	Charqueada/SP	22° 33.978'S	47° 45.685'O	21.7
17	CHQ-Pira	Charqueada/SP	22° 34.736'S	47° 42.769'O	25.1
18	Rotatória Artemis	Piracicaba/SP	22° 39.315'S	47° 47.314'O	18.4
19	Piracicaba-São Pedro	Piracicaba/SP	22°40'5.30"S	47°46'35.80"O	19.6
20	Onça 2	Charqueada/SP	22°32'20.50"S	47°45'51.30"O	9.1
21	Ajapi-Ferraz	Rio Claro/SP	22°15'34.20"S	47°34'33.20"O	19.3
22	Santa Luzia	Charqueada/SP	22°35'5.10"S	47°43'45.10"O	41.1
23	Laras	Laras/SP	22°55'34.90"S	47°53'43.80"O	11.4
24	Conchas	Conchas/SP	23° 0'42.70"S	47°59'44.60"O	5.9
25	Conchas	Conchas/SP	23° 0'23.50"S	47°59'24.00"O	14.1

O empilhamento e correlação das seções colunares foi baseado principalmente na identificação de superfícies estratigráficas e correlação das associações de fácies, visto que, principalmente no Estado de São Paulo (região do Domo de Pitanga), há uma grande quantidade de falhas que não permitem o empilhamento e correlação baseado em dados topográficos. Para a confecção das três seções compostas da Formação Corumbataí foram selecionadas aquelas mais completas e representativas para cada região estudada, a saber: Seção Composta I – seções 14, 15, 16, 17, 18, 19, 20 e 22 (Anexo I.I); Seção Composta II – seções 6, 7, 8, 9, 10, 11, 12, 13 e 21 (Anexo I.II); Seção Composta 3 – 0, 1, 2, 3, 4A, 4B, 4C, 4D e 5 (Anexo I.III).

Além disso, foram desenvolvidas curvas de acomodação através de diagramas de Fischer, que indicam tendências arquitetônicas na sucessão estudada e contribuem para a correlação de trechos geograficamente distantes. Os gráficos de Fischer são amplamente utilizados na pesquisa paleoambiental como representações gráficas das mudanças no nível do mar ou lago (Ocakoğlu et al., 2012; Muniz et al., 2015; Yang et al., 2018; Brito et al., 2018; Cardoso et al., 2019) por meio do desvio cumulativo da espessura média dos ciclos em relação ao número total de ciclos medidos. Fischer (1964) introduziu este método gráfico de exibição de mudanças relativas no nível do mar (ou seja, a mudança no nível do mar representada como a soma da subsidência e da eustasia) derivadas de sucessões cíclicas de carbonatos. Sadler et al. (1993) revisaram o uso dos gráficos de Fisher e sugeriram que, em vez de uma escala de tempo originalmente usada, o eixo horizontal dos gráficos deveria ser rotulado pelo número do ciclo, para evitar o problema de um controle deficiente do tempo absoluto no registro estratigráfico. Sadler et al. (1993) recomendam a utilização de pelo menos 50 ciclos para separar flutuações não aleatórias (alogenéticas) de flutuações aleatórias (autogenéticas). Seguindo esse conceito, foram identificados o número e a espessura das sucessões granocrescente ascendentes (sequências de raseamento) registradas nas seções colunares da Formação Corumbataí e correlacionados gráficos de Fischer. Com o objetivo de identificar as flutuações de alta frequência do nível de base e definir as principais superfícies estratigráficas, a correlação das seções compostas foi realizada primeiro nas seções proximais e depois na escala da bacia (Fischer, 1964; Read e Goldhammer, 1988; Day, 1997).

1.3.2. Análise petrográfica de rochas siliciclásticas e carbonáticas

A descrição petrográfica de lâminas delgadas complementou a descrição macroscópica das amostras e permitiu a classificação das microfácies carbonáticas e evaporíticas descritas nas porções de topo da Formação Corumbataí. No total, foram confeccionadas quinze lâminas delgadas, as quais foram descritas por microscopia ótica utilizando luz transmitida com o microscópio Zeiss Axio Imager A.2, do Laboratório de Petrografia Microscopia de Departamento de Geologia (DEGEO) da Universidade Federal de Ouro Preto (UFOP) e imageadas no Centro de Pesquisas Aplicadas ao Petróleo (Unespetro), na Universidade Estadual Paulista (UNESP). A descrição macroscópica e petrográfica das rochas carbonáticas se baseou nas classificações propostas por Dunham (1962) e Embry & Klovan (1971).

1.3.3. Datação Radiométrica U-Pb de zircões

Uma amostra de tufo vulcânico foi coletada na “Seção Mineiros Tufo” (ver no Anexo I.III – Seção 4B) intercalada a camadas arenosas e siltitos da Formação Corumbataí. O afloramento está localizado em um corte de estrada (coordenadas: 17°32.607’S / 52°33.931’O), na cidade de Mineiros, no Estado de Goiás (porção norte da Bacia do Paraná).

Os grãos de zircão foram extraídos de aproximadamente 2 kg de amostra, através de técnicas convencionais para concentração de minerais pesados, passando por britagem, moagem, peneiramento, bateamento, separação através de Bromoformio e, por fim, coleta manual em lupa estereoscópica (aproximadamente 430 grãos). Após o processo de separação, os grãos de zircão foram montados em discos de resina epóxi e polidos para expor o centro dos cristais. Os grãos selecionados foram imageados por catodoluminescência (CL) em Microscópio Eletrônico de Varredura JEOL 6510 no DEGEO/UFOP, para examinar as características morfológicas dos grãos de zircão e para selecionar áreas para análises pontuais por LA-MC-ICP-EM.

As análises U-Pb foram realizadas no Laboratório de Geoquímica Isotópica da Universidade Federal de Ouro Preto, utilizando um multicoletor Thermo-Finnegan Neptune ICP-MS acoplado a um sistema Photon-Machines 193 nm excimer laser (LA-MC-ICP-EM), sob os cuidados do Prof. Dr. Cristiano Lana. Foram selecionados aleatóriamente 45 grãos de zircão e os dados foram adquiridos usando o modo automático com medição de fundo durante 20 segundos, ablação do zircão durante 40 segundos e tamanho de ponto de 20 µm. O padrão de zircão GJ-1 (Jackson et al., 2004) foi usado como padrão primário para este estudo e o padrão Plešovice (206Pb/238U = 337 Ma, 207Pb/235U = 337 Ma e 207Pb/206Pb = 339 Ma; Sláma et al., 2008) como secundário. A redução dos dados foi feita no software SATURN® (Silva et al., 2022), enquanto os diagramas de concordia, e as idades médias ponderadas foram gerados pelo software Excel Isoplot (Ludwig, 2003). Dos 43 grãos de zircão datados, seis foram desconsiderados (grãos: 23, 43, 45, 65, 69, 73) por apresentarem idades discordantes (entre 558 e 2018 Ma) (todos os dados são apresentados no Anexo II.I).

1.3.4. Análise isotópica Lu-Hf

Devido ao comportamento geoquímico semelhante, o elemento Háfnio (Hf) pode substituir o Zircônio (Zr) na estrutura cristalina do zircão. Somente durante a geração do magma, ocorre o fracionamento do Lutécio (Lu) em relação ao Hf, assim, tais elementos podem ser utilizados como traçadores da história da diferenciação geoquímica de crosta e manto (Kinny & Maas, 2003). Desta maneira, é possível obter informações sobre a origem da fonte sedimentar usando a idade modelo e o parâmetro petrogenético εHf do magma gerador da rocha através dos isótopos de Hf modelado para uma determinada idade.

A razão isotópica de Hf pode ser expressa pela notação Épsilon (εHf), determinada para um período (T) calculado, expressa pela Equação 1.

$$\varepsilon \text{Hf} = \left[\frac{(176Hf/177Hf)t}{(176Hf/177Hf)condrito - 1}\right] \cdot 10$$

Este parâmetro determina se a composição inicial é maior ou menor que o condrito, para o qual valores positivos indicam que sua fonte é mantélica e valores negativos indicam fontes crustais (Faure, 1986).

Análises de Hf foram realizadas em 17 grãos de zircão da mesma amostra submetida a datação U-Pb, usando o espectrômetro de massa Neptune do Laboratório de Geoquímica Isotópica da Universidade Federal de Ouro Preto. O spot do laser usado foi de 40 μm de diâmetro com ablação de 60 segundos, taxa de repetição de 8 Hz e 0.3 He gás. A precisão e reprodutibilidade externa dos resultados Lu-Hf das amostras foram monitoradas através da análise dos padrões de zircão: Temora (176Hf/177Hf = 0.282680 ± 0.000031; Black et al., 2003; Wu et al., 2006), Blue Berry (176Hf/177Hf = 0.281674 ± 0.000018; Santos et al., 2017), Mud Tank (176Hf/177Hf = 0.282504 ± 0.000044; Black e Gulson, 1978; Woodhead e Hergt, 2005), e GJ-1 (176Hf/177Hf = 0.282000 ± 0.000005; Jackson et al., 2004), os quais apresentaram razões médias de 176Hf/177Hf iguais a: 0.28260 ± 0.000014 (n = 10), 0.281692 ± 0.000017 (n = 10), 0.282516 ± 0.000015 (n = 10) e 0.282005 ± 0.000019 (n = 10), respectivamente (±2SD). Todos os valores aferidos encontram-se dentro das incertezas e em boa concordância com as proporções padrão aceitas.

As proporções iniciais de isótopos de Hf foram recalculadas para a idade de 206Pb/238U de cada respectivo grão de zircão. Para o cálculo dos valores de εHf(t), foram utilizados os valores condriticos apresentados por Chauvel et al. (2008) de 176Hf/177Hf = 0.283164 e 176Lu/177Hf = 0.0270. Para calcular as idades modelo (TDM) com base em uma fonte de manto esgotada, foram usadas as razões atuais de 176Hf/177Hf = 0.282313 e 176Lu/177Hf = 0.000311 (Blichert-Toft, 2008). A constante de decaimento λ para 176Lu usada é 1,867x10−11/ano (Söderlund et al., 2004). Todos os dados são apresentados no Anexo II.II.

1.3.5. Mineralogia de rocha total e geoquímica ICP-MS

A mineralogia de rocha total e argila da amostra de tufo foi determinada a partir de padrões de difratometria de raios-X (XRD). As análises foram realizadas em um difratômetro PANalytical X'Pert PRO no Centro de Investigaciones Geológicas (CIG CONICET-UNLP, La Plata, Argentina), utilizando radiação de Cu (Kα=1,5 Å), um filtro de Ni, e configurações de geração de 40 kV e 40mA. As rotinas *air-dried* foram executadas entre 2 e 32°2θ a uma velocidade de varredura de 2°2θ/min. As amostras foram solvatadas com etilenoglicol sem prétratamento de saturação e aquecidas a 550 °C, e foram analisadas de 2 a 27°2θ e 3–15°2θ, respectivamente, a uma velocidade de varredura de 2°2θ/min. A metodologia utilizada para preparação das amostras segue Brown & Brindley (1980), e a semiquantificação dos minerais foi obtida considerando a intensidade do pico principal de cada mineral (Biscaye, 1965; Moore & Reynolds, 1999 incluindo padrões de laboratório).

Elementos terras raras e teores de ítrio (REY), expressos em ppm, foram obtidos da amostra de tufo usando espectrometria de massa com plasma indutivamente acoplado quadrupolo Perkin-Elmer (ICP-MS) equipado com um nebulizador concêntrico Meinhardt no CIG. Na preparação para análises elementares, alíquotas de pó inteiro foram digeridas por 2 h em HNO_3 a 2% de grau metálico. As concentrações de REE foram normalizadas para valores de condrito (Sun e McDonough, 1989) e comparadas ao geopadrão REE certificado de riolito (RGM-1). Todos os resultados obtidos da amostra estão apresentados nos Anexos II.III e II.IV.

1.4. Contexto Geológico

Durante o Paleozoico, a parte sudoeste do supercontinente Gondwana esteve sujeita a complexos eventos regionais geotectônicos e paleoclimáticos. Durante o Permiano, a orogênese San Rafaelica resultou no soerguimento do Cinturão Gondwanides (Keidel, 1916; Ramos, 1986). Neste período, tal barreira orográfica pode ter restringido as conexões marítimas das águas do Panthalassa ao sul com o mar epírico das bacias do Paraná e Karoo (Warren et al., 2008; Holz et al., 2010), promovendo uma progressiva continentalização e aridização da parte interna do sudoeste de Gondwana (Milani et al., 2007; Limarino et al., 2013).

Na Bacia do Paraná, este período de transição de ambiente marinho pós-glacial para continental é registrado pelo Grupo Passa Dois, o qual encontra-se delimitado pelas formações Tatuí e Pirambóia, base e topo, respectivamente. Esta sucessão permo-triássica é composta pelas formações Irati, Serra Alta, Corumbataí/Teresina e Rio do Rasto. A Formação Irati compreende folhelhos ricos em matéria orgânica e camadas carbonáticas que foram depósitados em ambiente com ligação restrita com o Panthalassa (Araújo, 2001; Holz et al., 2010; Brito et al., 2023). Acima, a sucessão monótona de siltitos cinza escuro da Formação Serra Alta é interpretada como sendo depositada em um mar epírico fechado sob condições disóxicas a anóxicas (Holz et al., 2010; Warren et al., 2015), e corresponde ao último evento transgressivo de terceira ordem da bacia (Warren et al., 2015). A presença de bivalves endêmicos e a ausência de fósseis marinhos (Runnegar e Newell, 1971; Maranhão e Petri, 1996; Simões et al., 1998; Ghilardi e Simões, 2002) constituem fortes evidências de que a Formação Serra Alta já estava isolada do Panthalassa (Simões et al., 2012; Warren et al., 2015). A sucessão mista siliciclástica-carbonática sobrejacente da Formação Teresina representa a transição do ambiente de águas mais profundas da Formação Serra Alta para um ambiente deposicional totalmente óxico e raso (Holz et al., 2010; Warren et al., 2015; Matos et al., 2017; Ng et al., 2019). Devido a uma acentuada variação lateral de fácies, esta unidade é reconhecida como Formação Corumbataí nos estados de São Paulo, Mato Grosso e Goiás (Rohn, 1994). Por fim, o caráter predominantemente progradacional do Grupo Passa Dois culminou com a total colmatação do corpo d´água, propiciando o desenvolvimento de sistemas deposicionais deltaicos e eólicos da Formação Rio do Rasto (Lavina, 1992; Warren et al., 2008).

1.4.1. Evolução dos conhecimentos sobre a Formação Corumbataí

A denominação "Folhelho Estrada Nova" foi utilizada inicialmente por White (1908), para as fácies finas (argilitos e siltitos), areníticas e carbonáticas descritas entre a porção superior do "Folhelho Irati" e a base do Grupo São Bento, na Serra do Rio do Rasto (Santa Catarina). O termo Corumbataí foi utilizado pela primeira vez em 1916, pela antiga Comissão Geográfica e Geológica, mas somente com o trabalho de Pacheco (1939) estabeleceu-se a aplicação desta denominação às rochas localizadas entre o topo da Formação Irati e a base das, então denominadas, Camadas Pirambóia (parte inferior do "Arenito Botucatu"; Pacheco, 1939).

Desde a sua introdução na literatura geológica, os termos Estrada Nova e Corumbataí causam controvérsia, principalmente em relação a tentativa de correlação entre a Formação Estrada Nova, presente nos estados do Paraná e Santa Catarina, e aquela aflorante em São Paulo (Sousa, 1985). No Estado de São Paulo, a Formação Estrada Nova foi reconhecida como indivisível em trabalhos como os de Fulfaro (1970), Landim (1970) e Zaine (1980). No entanto, para Lellis (1970) a subdivisão da Formação Estrada Nova, aplicável a Santa Catarina e Paraná, também foi reconhecida até o centro-sul de São Paulo. Mais tarde, Vieira (1973) denominou Grupo Estrada Nova ao conjunto das formações Irati, Serra Alta e Teresina.

No trabalho de revisão litoestratigráfica da Bacia do Paraná de Schneider et al. (1974), proposta mais aceita até o momento (Milani et al., 2007; Holz et al., 2010), a Formação Corumbataí passou a ser concebida como equivalente lateral das formações Serra Alta, Teresina e parte do Rio do Rasto (Membro Serrinha) nos estados de São Paulo, Goiás e Mato Grosso. Mais recentemente, a Formação Serra Alta foi mapeada como unidade independente no Estado de São Paulo (Warren et al., 2015), sendo que as formações Corumbataí e Teresina foram finalmente confirmadas como correlatas lateralmente.

1.4.2. Ocorrência e relações de contato

A Formação Corumbataí ocorre em superfície nos estados de: (i) São Paulo, à norte do Domo de Gibóia (Rio das Pedras – SP), em uma faixa de afloramento na direção SSW-NNE; (ii) Minas Gerais, apenas no município de Monte Santo de Minas; (iii) Goiás, em uma faixa E-W entre Montividiu e Mineiros, e (iv) Mato Grosso, entre as cidades de Alto Araguaia e Itiquira. O contato inferior com a Formação Serra Alta é considerado transicional (Castro et al., 1993; Hachiro, 1996; Araújo, 2001; Warren et al., 2015), materializando mudança gradual de ambiente profundo pouco oxigenado para ambiente de águas cada vez mais rasas, agitadas e oxigenadas (Mendes, 1984; Warren et al., 2015). No Estado de São Paulo, a Formação Pirambóia encontra-se sobreposta discordantemente aos depósitos da Formação Corumbataí (Christofoletti et al., 2021). Nos estados de Goiás e Mato Grosso, a Formação Corumbataí encontra-se diretamente sotoposta à Formação Botucatu ou recoberta por sedimentos cenozoicos (CPRM, 2004). O contato entre as formações Corumbataí e Teresina é interpretado como transicional, marcado pelo afinamento gradual das camadas carbonáticas que passam lateralmente a apresentar cores avermelhadas, sugerindo contemporaneidade e coexistência entre os ambientes de sedimentação (Matos, 1995; Meglhioratti, 2006; Warren et al., 2015).

1.4.3. Conteúdo fossilífero e idade

Desde o relatório pioneiro de White (1908), atribuiu-se idade permiana ao Grupo Passa Dois; o que foi confirmado a posteriori por dados palinológicos por Daemon e Quadros (1970), que indicaram idade kanzaiana (Permiano Superior) para o topo deste grupo. Estudos paleomagnéticos na região de Ártemis-Piracicaba, posicionaram a Formação Corumbataí no Permiano Superior (Valencio et al., 1975). Ragonha (1984) atribuiu ao topo da unidade idade carniana (Triássico), baseado em restos de peixe xenacantódios. Datações radiométricas realizadas para a Formação Corumbataí, incluem idades U-Pb em zircões de 257,5 ± 2 Ma, supostamente obtida de uma camada de tufo vulcânico 34 m abaixo da “Camada Porangaba”, nos arredores da cidade de Limeira (SP) (Fernandes, 2007; Rocha-Campos et al., 2019) e idades U-Pb em zircões detríticos da “Camada Porangaba” (contato em algumas localidades entre as formações Corumbataí e Pirambóia), de 253,0 ± 3,0 Ma (Tohver et al., 2018). Mais recentemente, novos levantamentos paleomagnéticos indicaram que a unidade se depositou entre 274 e 254 Ma (Aragão e Sacardia, 2021).

O registro fossilífero da Formação Corumbataí é dominado por conchas de bivalves que já foram objeto de estudos tafonômicos detalhados (Rohn, 1994; Simões et al., 1996; Klein, 1997; Simões e Kowalewski, 1998; Torello, 1999; Simões et al., 2000) apresentando uma história de acumulação, distribuição estratigráfica, taxonomia e paleoecologia bem conhecidas (Sousa, 1985; Rohn, 1988, 1994; Lavina, 1991; Maranhão, 1995; Klein, 1997; Simões et al., 1997, 1998; Mello et al., 1998; Mello, 1999; Ghilardi, 1999; Simões et al., 2000; Ghilardi & Simões, 2002). Mendes (1949; 1952) propôs as primeiras zonas bioestratigráficas formais para os bivalves da Formação Corumbataí no Estado de São Paulo: Zona Pinzonela illusa–Plesiocyprinella carinata e a Zona *Pinzonella neotropica–Jacquesia brasiliensis*, que mais tarde foram estendidas para a porção sul da Bacia do Paraná (Rohn, 1994).

No entanto, a evolução da Classe Bivalvia durante a deposição do Grupo Passa Dois, constitui um capítulo único (Runnegar e Newell, 1971). A bacia experimentou diferentes condições de salinidade, oxigenação e variações climáticas. Dessa forma, os ambientes bentônicos rasos desse vasto mar interior foram provavelmente estressantes para a maioria dos macroinvertebrados totalmente marinhos, sendo colonizados principalmente por bivalves endêmicos (Simões et al., 1998) que irradiaram na bacia especialmente após o evento anóxico do Artinskiano (Mendes, 1952; Beurlen, 1954; Runnegar e Newell, 1971; Simões et al., 1997, 1998; Wesselingh, 2007; Matos et al., 2017).

O estudo de ostracodes resultou em divergências paleoambientais: primeiramente foram atribuídos a ambientes de água doce (Sohn e Rocha-Campos, 1990; Maranhão, 1995) e mais tarde como marinhos e cosmopolitas (Almeida e Do Carmo, 2005). Alguns outros microfósseis "marinhos", como foraminíferos raros, espículas de esponjas e até mesmo conodontes, foram citados, mas nunca descritos formalmente (Holz et al., 2010).

Fragmentos de peixes são abundantes na Formação Corumbataí (i.e., escamas de peixe, dentes, placas dentárias e outros) dispersos em forma de lentes fosfatizadas ou em *bone beds* (Toledo, 2001). Alguns desses restos de vertebrados indicam ambientes de água doce (por exemplo, petalodontes e raros restos de anfíbios); no entanto, estes restos podem representar fragmentos parautóctones ou alóctones que podem ter sido transportados para ambientes deposicionais mais salinos (Toledo, 2001).

Os fitofósseis também são abundades na Formação Corumbataí, ocorrendo desde folhas e esporos até troncos (Carvalho, 2019), representados principalmente por licófitas Lepidodendrales (*L. derbyi)* e gimnospermas (*Glossopteris sp*). A presença de carbonato de cálcio em alguns fósseis estudados de *Lycopodiopsis cf. derbyi* indica que tais plantas habitavam o entorno de lagos rasos salobros, com uma concentração de sais superior a média atual da água do mar (Carvalho, 2019).

1.4.4. Aspectos sedimentares e ambiente deposicional

Do ponto de vista litológico, a Formação Corumbataí apresenta predominância de siltito e argilito na base e arenito fino no topo. São também comuns fácies heterolíticas e intercalações rítmicas de siltito arroxeado e avermelhado com camadas tabulares de arenito fino com laminação cruzada por onda, ou mais raramente, estratificação cruzada de pequeno porte (Schneider et al., 1974). Ocasionalmente, ocorrem coquinas de bivalves e siltito laminado contendo gretas de contração intercalados com bancos carbonáticos de oóides e raros estromatólitos (Schneider et al., 1974; Simões e Torello, 2003). A unidade apresenta também, corpos discordantes de arenito maciço associados à extrusão de diques clásticos relacionados à atividade sísmica contemporânea à sedimentação (Perinotto et al., 2008; Turra, 2009).

O ambiente de sedimentação da Formação Corumbataí há muito tempo é objeto de discussão entre os pesquisadores da Bacia do Paraná. O tema divide-se entre os autores que defendem sua deposição em ambiente marinho (planície de maré, laguna e praia) e aqueles favoráveis a ideia de um ambiente continental (fluvial, planície de inundação e lacustre). Nos trabalhos pioneiros acerca da Formação Estrada Nova (formações Serra Alta, Teresina/Corumbataí e Rio do Rasto) mencionava-se deposição em ambiente de águas altamente salinas (Washburne, 1930; Moraes Rego, 1940). Beurlen (1954; 1955), embasado em dados paleontológicos, foi o primeiro a interpretar a existência de um mar intracontinental, de água salobra, com ligação restrita com o Oceano Panthalassa. Os "folhelhos Irati" e as "Camadas Serra Alta" teriam sido depositados em um ambiente de águas tranquilas, distante da costa e em profundidade relativamente grande. A passagem para as "Camadas Teresina" (= Corumbataí), composta por siltito, arenito com marcas de onda e calcário oolítico, indicaria regressão do mar, com deposição em águas agitadas e mais proximais. Mais tarde, Barbosa e Gomes (1958) e Vieira (1973) corroboraram com essa hipótese. Em contraposição, Mendes (1952), alegava a inexistência de fósseis tipicamente marinhos na unidade. Ademais, Mendes (1952) interpretava a presença de restos vegetais e troncos silicificados com fósseis animais (peixes, pelecípodes, gastrópodes, conchostráceos e ostracodes) como sugestiva de ambiente continental.

Na década seguinte, a presença de estruturas sedimentares como gretas de contração, laminações cruzadas por onda e brechas intraformacionais, levaram Salamuni (1963) a interpretar o ambiente deposicional como de planície de maré. Diversos outros autores seguiram essa mesma interpretação (ver Northfleet et al., 1969; Schneider et al., 1974; Fúlfaro et al., 1978; Gama Jr., 1979; Fúlfaro et al., 1980; Zaine, 1980). Suguio et al. (1974) e Petri e Coimbra (1982), com base na descrição de fácies com estratificação cruzada, laminação cruzada por onda, presença de gretas de contração, e oolitos nas pedreiras em Taguaí (SP), propuseram à Formação Estrada Nova ambiente marinho restrito ou lagunar, de águas rasas e ocasionalmente atingidas por tempestades. Suguio et al. (1974) analisando dados restritos de isótopos de oxigênio (O^{18}/O^{16}), concluíram que o clima à época de deposição era quente, favorecendo altas taxas de evaporação. De acordo com Petri e Fúlfaro (1983) a comunicação restrita com o Oceano Panthalassa estaria situada na região sul-ocidental da Bacia do Paraná. Para os mesmos autores, o ambiente deposicional da “Fácies Teresina” seria lagunar e a exposição subaérea registrada nas fácies com gretas de contração e outras estruturas estariam relacionadas a flutuações de pluviosidade.

Após décadas de opiniões contrastantes, Mendes (1984) admitiu a possibilidade de os ambientes deposicionais das formações Teresina e Corumbataí terem apresentado comunicação restrita com o oceano; porém, os equivalentes marinhos francos não estariam preservados na Bacia do Paraná. Sousa (1985) voltou a aventar um sistema dominado por macro-marés para as formações Estrada Nova (a sul da atual calha do rio Tietê) e Corumbataí (correlata a norte da calha), evoluindo de condições marinhas mais profundas para mais rasas, mas com variações do nível relativo do mar. Para Lavina (1991), a Formação Teresina teria sido depositada em um imenso lago ou “mar” interior, influenciado por tempestades, com pelo menos dois episódios marcantes de queda do nível de base, seguido por “*onlap*”, inseridos num intervalo geral regressivo. Além disso, nenhuma evidência clara da atuação de marés foi encontrada.

No trabalho de Rohn (1994), a Formação Serra Alta é interpretada como o primeiro grande ciclo transgressivo-regressivo, o qual se estende até a parte inferior da Formação Teresina, correlacionável à Zona *Pinzonella illusa* da Formação Corumbataí no Estado de São Paulo. Durante esse intervalo, Rohn (1994) propõe a possibilidade da existência de alguma comunicação com a Bacia do Karoo, porém não mais com o Oceano Panthalassa, e que, os raros fósseis que evocam paleoambiente "marinho" teriam sido originados de organismos marinhos euritópicos (ou seja, espécies encontradas em grandes áreas e que não são afetadas pelas mudanças de ambiente) bem mais antigos. O desenvolvimento de carbonatos nas margens deste enorme “mar interior” seria indicativo de fases de grande aridez durante a deposição da Formação Teresina/Corumbataí. A extensa distribuição geográfica de *Pinzonella neotropica* indicaria períodos de inundação acarretados por novas subidas do nível de base (Rohn, 1994). Por fim, o acentuado aumento da pluviosidade teria controlado o último ciclo transgressivo-regressivo reconhecido para a Formação Teresina, o qual promoveu a extinção dos bivalves da Zona *P. neotropica*, provavelmente causada por diminuição da salinidade (Rohn, 1994). Ademais, durante a existência desse “lago-mar” progressivamente mais raso, a água era frequentemente agitada por tempestades (Rohn, 1994).

1.5. Referências

Almeida, C.M., Do Carmo, D.A. 2005. Taxonomia e paleoecologia de ostracodes do Permiano da Bacia do Paraná, Estado de Goiás, Brasil. *In:* 19° Congresso Brasileiro de Paleontologia; 6°Congresso Latino-Americano de Paleontologia, Aracaju. Resumos.

Aragão, M. e Scardia, G. 2021. Middle–Late Permian magnetostratigraphy and the onset of the Illawarra Reversals in the northeastern Parana Basin, South America. Geophysical Journal International, 225:860-871.

Araújo, L.M. 2001. Análise da expressão estratigráfica dos parâmetros de geoquímica orgânica e inorgânica nas sequencias Irati. Tese de Doutoramento, Universidade Federal do Rio Grande do Sul, Porto Alegre.

Barbosa, O. e Gomes, F.A. 1958. Pesquisa de petróleo da bacia do Rio Corumbataí, Estado de São Paulo. DNPM, Boletim 171, Rio de Janeiro, 40p.

Bastos, L.P.H., Rodrigues, R., Pereira, E., Bergamaschi, S., Alferes, C.L.F., Augland, L.E., Domeier, M., Planke, S. and Svensen, H.H. 2021. The birth and demise of the vast epicontinental Permian Irati-Whitehill Sea: evidence from organic geochemistry, geochronology, and paleogeography. Palaeogeography, Palaeoclimatoogy,. Palaeoecology, 562, Article 110103.

Beurlen, K. 1954. As faunas de lamelibrânquios do Sistema Gonduânico no Paraná. *In:* Volume Comemorativo do 1° Centenário do Estado do Paraná (F.W. Lange ed.), p.p. 107–136.

Beurlen, K. 1955. As formações Gondwânicas do sul do Estado do Paraná. Div. Geol. Min., Bol. 153, Rio de Janeiro, 52p

Biscaye, P.E. 1965. Mineralogy and Sedimentation of Recent Deep-Sea Clay in the Atlantic Ocean and Adjacent Seas and Oceans. Geological Society of America Bulletin, 76, 803–832

Black, L.P. and Gulson, B.L. 1978. The age of the Mud Tank carbonatite, Strangeways Range, Northern Territory. BMR Journal of Australian Geology and Geophysics, 3, 227–232.

Black, L.P., Kamo, S.L., Allen, C.M., Aleinikoff, J.N., Davis, D.W., Korsch, R.J., Foudoulis, C. 2003. TEMORA 1: a new zircon standard for Phanerozoic U–Pb geochronology. Chemical Geology, 200, 155-170.

Blichert-Toft, J. 2008. The Hf isotopic composition of zircon reference material 91500. Chemical Geology, 253, 252-257.

Brito, A.S., Nogueira, A.C.R., de Almeida, L.T.G. and de Lima, S.G. 2023. Orbital-scale cyclicity and organic matter production in a Permian shallow mixed carbonate-siliciclastic system: Paraná Basin, Brazil. Marine and Petroleum Geology, 147, 105987.

Brown, G., and Brindley, G.W. 1980. X-ray diffraction procedures for clay mineral identification. *In:* Crystal structures of clay minerals and their X-ray identification (G.W. Brindley and G. Brown ed.). Mineralogical Society of Great Britain and Ireland, p.p. 305-359.

Cardoso, A.R., Nogueira, A.C.R. and Rabelo, C.E.N. 2019. Lake cyclicity as response to thermal subsidence: A post-CAMP scenario in the Parnaíba Basin, NE Brazil. Sedimentary Geology, 385, 96–109

Carvalho, T.S. 2019. Assembleia Fitofossilífera de Lycopodiopsis cf. Derbyi da Formação Corumbataí, Bacia do Paraná, São Paulo, Brasil. Dissertação de Mestrado, Universidade Federal de São Carlos, São Paulo.

Castro, J.C., Maciel, U., Alves, C.F.C., Grecchi, R.C. 1993. O Grupo Guatá na margem nordeste da Bacia do Paraná: uma revisão. *In:* 1º Simpósio sobre a cronoestratigrafia da Bacia do Paraná, Rio Claro. Boletim de Geociências, p. 55-56.

Chauvel, C., Lewin, E., Carpentier, M., Arndt, N.T. and Marini, J.C. 2008. Role of recycled oceanic basalt and sediment in generating the Hf–Nd mantle array. Nature Geoscience, 1, 64-67.

Christofoletti, B., Peixoto, B.C., Warren, L.V., Inglez, L., Fernandes, M.A., Alessandretti, L., Perinotto, J.A.J., Simões, M.G., Assine, M.L. 2021. Dinos among the dunes: dinoturbation in the Pirambóia Formation (Paraná Basin), São Paulo State and comments on cross-section tracks. Journal of South American Earth Sciences, 109, Article 103252.

CPRM – SERVIÇO GEOLÓGICO DO BRASIL. 2004. Cartas geológicas do Brasil ao milionésimo.

Daemon, R.F. and Quadros, L.P. 1970. Bioestratigrafia do Neopaleozoico da Bacia do Paraná. *In:* 24° Congresso Brasileiro de Geologia, Brasília (DF), Anais, p. 359-412.

Day, P.I. 1997. The Fischer diagram in the depth domain: a tool for sequence stratigraphy. Journal of Sedimentary Research, 67, 982–984.

Dunham, R.J. 1962. Classification of carbonate rocks according to depositional textures.

Embry, A.F. and Klovan, J.E. 1972. Absolute water depth limits of Late Devonian paleoecological zones. Geologische Rundschau, 61, 672-686.

Faure, G. 1986. Isotope systematics in two-component mixtures. Principles of Isotope Geology, pp.141- 153.

Fernandes, M.T. 2007. Ocorrência de material vulcanoclástico na Formação Corumbataí (Neopaleozoico), Bacia do Paraná. Trabalho de Conclusão de Curso, Universidade de São Paulo, São Paulo.

Fischer, A.G. 1964. The Lofer cyclothems of the Alpine Triassic. Geological Survey of Kansas Bulletin, 169, 107-149.

Fulfaro, V.J. 1970. Contribuição à geologia da região de Angatuba, Estado de São Paulo. DNPM - Div. Geol. Min., Boletim 253, Rio de Janeiro, p. 1-82.

Fulfaro, V.J., Saad, A.R., Campanha, V.A. and Canuto, J.R. 1978. Considerações sobre a gênese da Formação Estrada Nova (P) da Bacia do Paraná. *In:* Anais do Congresso Brasileiro de Geologia, 30, pp.158.

Fulfaro, V.J., Gama Jr., E.G. and Soares, P.C. 1980. Revisão estratigráfica da Bacia do Paraná. *Relatório BP 008/80*, Paulipetro, São Paulo, 115p.

Gama Jr., E.G. 1979. A sedimentação do Grupo Passa Dois (exclusive Formação Irati): um modelo geomórfico. Revista Brasileira de Geociências, 9, 1-16.

Ghilardi, R.P. 1999. Paleoautoecologia dos bivalves do Grupo Passa Dois (Neopermiano) no Estado de São Paulo: bivalves fósseis como indicadores da dinâmica sedimentar. Dissertação de Mestrado, Instituto de Geociências, Universidade de São Paulo, 160p.

Ghilardi, R.P. and Simões, M.G. 2002. Foram os bivalves do Grupo Passa Dois (exclusive Formação Rio do Rasto) moluscos dulcícolas? Pesquisas em Geociências, 29, 91-92.

Hachiro, J. 1996. O Subgrupo Irati (Neopermiano) da Bacia do Paraná. Tese de Doutoramento, Universidade de São Paulo, São Paulo, 196p.

Holz, M., França, A.B., Souza, P.A., Iannuzzi, R. and Rohn, R. 2010. A stratigraphic chart of the late Carboniferous/Permian succession of the eastern border of the Paraná Basin, Brazil, South America. Journal of South American Earth Science, 29, 381-399.

Ichinose, G.A., Anderson, J.G., Satake, K., Schweickert, R.A. and Lahren, M.M. 2000. The potential hazard from tsunami and seiche waves generated by large earthquakes within Lake Tahoe, California-Nevada. Geophysical Research Letters, 27, 1203-1206.

Jackson, S.E., Pearson, N.J., Griffin, W.L., Belousova, E.A. 2004. The application of laser ablation-inductively coupled plasma-mass spectrometry to in-situ U-Pb zircon geochronology. Chemical Geology, 211, 47–69.

Keidel, J. 1916. La geología de las Sierras de la Provincia de Buenos Aires y sus relaciones con las montañas de Sudáfrica y Los Andes. Ministerio de Agricultura de La Nación, Sección Geología, Mineralogía y Minería, 11, 1-78.

Kern, H.P., Lavina, E.L.C., Paim, P.S.G., Girelli, T.J. and Lana, C. 2021. Paleogeographic evolution of the southern Paraná Basin during the Late Permian and its relation to the Gondwanides. Sedimentary Geology, 415, Article 105808.

Kinny, P.D. and Maas, R. 2003. Lu–Hf and Sm–Nd isotope systems in zircon. Reviews in Mineralogy and Geochemistry, 53, 327-341.

Klein, C. 1997. Contribuição ao estudo das concentrações fossilíferas do Grupo Passa Dois na região de Tiarajú, RS e suas implicações paleoambientais. Dissertação de Mestrado, Universidade do Vale do Rio dos Sinos, 136 p.

Landim, P.M.B. 1970. O Grupo Passa Dois (P) na bacia do Rio Corumbataí (SP). DNPM - Div. Geol. Min., Boletim 252, Rio de Janeiro, 103 p.

Lavina, E.L. 1991. Geologia sedimentar e paleogeografa do Neopermiano e Eotriássico (intervalo Kazaniano–Citiano) da Bacia do Paraná. Tese de Doutoramento, Universidade Federal do Rio Grande do Sul, Porto Alegre.

Lellis, H.S. 1970. Contribuição a geologia da região de Pereiras - Cesário Lange - Bofete, Estado de São Paulo. Dissertação de Mestrado, Universidade de São Paulo, São Paulo.

Limarino, C.O., Césari, S.N., Spalletti, L.A., Taboada, A.C., Isbell, J.L., Geuna, S. and Gulbranson, E.L. 2013. A paleoclimatic review of southern South America during the late Paleozoic: a record from icehouse to extreme greenhouse conditions. Gondwana Research, 25, 1396-1421.

Ludwig, K.R., 2003. User's Manual for Isoplot 3.00: A Geochronological Toolkit for Microsoft Excel. Berkeley Geochronology Center, Special Publication, pp. 1–70.

Maranhão, M.S.A.S. 1995. Fósseis das formações Corumbataí e Estrada Nova do Estado de São Paulo: subsídios ao conhecimento paleontológico e bioestratigráfico. Tese de Doutoramento, Universidade de São Paulo, São Paulo.

Maranhão, M.S.A.S. and Petri, S. 1996. Novas ocorrências de fósseis nas formações Corumbataí e Estrada Nova do Estado de São Paulo e considerações preliminares sobre seus significados paleontológicos e bioestratigráficos. Revista do Instituto Geológico, 17, 33-54.

Matos, S.L.F. 1995. O contato entre o Grupo Passa Dois e a Formação Piramboia na borda Leste da Bacia do Paraná no Estado de São Paulo. Dissertação de Mestrado, Universidade de São Paulo, São Paulo.

Matos, S.A., Warren, L.V., Varejão, F.G., Assine, M.L. and Simões, M.G. 2017. Permian endemic bivalves of the "Irati anoxic event", Paraná Basin, Brazil: Taphonomical, paleogeographical and evolutionary implications. Paleogeography, Paleoclimatology, Paleoecology, 469, 18–33.

Meglhioratti, T. 2006. Estratigrafia de sequências das Formações Serra Alta, Teresina e Rio do Rasto (Permiano, Bacia Do Paraná) na porção nordeste do Paraná e centro-sul de São Paulo. Dissertação de Mestrado, Universidade Estadual Paulista "Júlio de Mesquita Filho", Rio Claro.

Mello, L.H.C., Ghilardi, R.P., Torello, F.F., Simoes, M.G. 1998. Some biostratinomic aspects of carbonate concretions from Serra Alta Formation (Late Permian), Paraná Basin, Brazil. *In:* Congresso Brasileiro de Geologia, 40, Anais, p. 452.

Mello, L.H.C. 1999. Análise cladística dos bivalves do Grupo Passa Dois (Neopermiano), Bacia do Paraná, Brasil: Implicações taxonômicas, evolutivas e paleobiogeográficas. Dissertação de Mestrado, Universidade de São Paulo.

Mendes, J.C. 1949. Novos Lamelibrânquios fósseis da Série Passa Dois, sul do Brasil. Boletim da Divisão de Geologia e Mineralogia, 133, 1–40.

Mendes, J.C. 1952. A Formação Corumbataí na região do Rio Corumbataí. Estratigrafia e descrição dos lamelibrânquios. Boletim USP, 145, 119p.

Mendes, J.C. 1984. Sobre os paleoambientes deposicionais do Grupo Passa Dois. Revista do Instituto Geológico, 5, 15-24.

Miall, A.D. 1996. The Geology of Fluvial Deposits. Springer-Verlag, Berlin.

Miall, A.D. 1999. Principles of Sedimentary Basin Analysis, 3ª ed. Springer-Verlag, New York

Milani, E.J., Melo, J.H.G, Souza, P.A., Fernades, L.A. and França, A.B. 2007. Bacia do Paraná. Boletim de Geociências da Petrobrás, 15, 265–287.

Moore, D.M. and Reynolds Jr, R.C. 1997. X-ray Diffraction and the Identification and Analysis of Clay Minerals, 2nd ed. Oxford University Press, Oxford.

Moraes Rego, L.F. 1940. A geologia do Estado de São Paulo. Boletim do Departamento de Estradas de Rodagem (DER), 2, 155-174.

Muniz, M.C. and Bosence, D.W.J. 2015. Pre-salt microbialites from the Campos Basin (offshore Brazil): image log facies, facies model and cyclicity in lacustrine carbonates. Geological Society of London Special Publications, 418, 221-242.

Ng, C., Vega, C.S. and Maranhão, M.S.A.S. 2019. Mixed carbonate-siliciclastic microfacies from Permian deposits of Western Gondwana: evidence of gradual marine to continental transition or episodes of marine ingressions? Sedimentary Geology, 390, 62-82.

Northfleet, A.A., Medeiros, R.A. and Muhlmann, H. 1969. Reavaliação dos dados geológicos do Paraná. Boletim Técnico da Petrobrás, 12, 291-346.

Ocakoğlu, F., Açıkalın, S., Yılmaz, İÖ., Şafak, Ü. and Gökçeoğlu, C. 2012. Evidence of orbital forcing in lake-level fluctuations in the Middle Eocene oil shale-bearing lacustrine successions in the Mudurnu-Göynük Basin, NW Anatolia (Turkey). Journal of Asian Earth Science, 56, 54–72.

Pacheco, J. 1939. Geologia do petróleo do estado de São Paulo, por Chester W. Washburne; traduzido, comentado e ampliado por Joviano Pacheco. Rio de Janeiro, Brasil, Oficinas gráficas do Serviço de publicidade agrícola

Palcu, D.V., Patina, I.S., Şandric, I., Lazarev, S., Vasiliev, I., Stoica, M. and Krijgsman, W. 2021. Late Miocene megalake regressions in Eurasia. Scientific Reports, 11, 11471.

Perinotto, J.A.D.J., Etchebehere, M.L.D.C., Simões, L.S.A., Zanardo, A. 2008. Diques clásticos na Formação Corumbataí (P) no nordeste da Bacia do Paraná, SP: Análise sistemática e significações estratigráficas, sedimentológicas e tectônicas. Geociências, 27, 469-491.

Petri, S. and Coimbra, A.M. 1982. Estruturas sedimentares das Formações Irati e Estrada Nova (Permiano) e sua contribuição para elucidação dos seus paleoambientes geradores. In: 5º Congresso Latinoamericano de Geologia, Anais, 353-371.

Petri, S. and Fulfaro, V.J. 1983. Geologia do Brasil (Fanerozoico). Ed. Universidade de São Paulo, São Paulo, 631p.

Ragonha, E.W. 1984. Taxonomia de dentes e espinhos isolados de Xenacanfhodii (condrichfhyes, elasmobranchii) da Formação Corumbataí: considerações cronológicas e paleoambientais. Tese de Doutoramento, Universidade de São Paulo, São Paulo.

Ramos, V.A., Jordan, T., Allmendinger, R., Mpodozis, C., Kay, S., Cortez, J. and Palma, M. 1986. Paleozoic terranes of the central Argentina–Chilean Andes. Tectonics, 5, 855–880.

Read, J.F. and Goldhammer, R.K. 1988. Use of Fischer plots to define third-order sea-level curves in peritidal carbonates, Ordovician, Appalachians. Geology, 16, 895-899.

Rocha-Campos, A.C., Basei, M.A.S., Nutman, A.P., Santos, P.R.D., Passarelli, C.R., Canile, F.M., Rosa, O.C.R., Fernandes, M.T., Santa Ana, H. and Veroslavsky, G. 2019. U-Pb zircon dating of ash fall deposits from the paleozoic Paraná basin of Brazil and Uruguay: a reevaluation of the stratigraphic correlations. The Journal of Geology, 127, 167-182.

Rohn, R. 1994. Evolução Ambiental da Bacia do Paraná durante o Neopermiano no leste de Santa Catarina e do Paraná. Tese de Doutoramento, Universidade de São Paulo, São Paulo.

Runnegar, B. and Newell, N.D. 1971. Caspian-like relict molluscan fauna in the South American Permian. Bulletin of the American Museum of Natural History, 146, 1–66.

Sadler, P.M., Osleger, D.A. and Montanez, I.P. 1993. On the labeling, length, and objective basis of Fischer plots. Journal of Sedimentary Research, 63, 360-368.

Salamuni, R. 1963. Estruturas sedimentares singenéticas e sua significação na Série Passa Dois, Paraná. Boletim do Instituto Geológico, 12, 89p.

Santos, M.M., Lana, C., Scholz, R., Buick, I., Schmitz, M.D., Kamo, S.L., Gerdes, A., Corfu, F., Tapster, S., Lancaster, P., Storey, C.D., Basei, M.A.S., Tohver, E., Alkmim, A., Nalini, H., Krambrock, K., Fantini, C. and Wiedenbeck, M. 2017. A new appraisal of Sri Lankan BB zircon as a reference material for LA- ICP-MS U- Pb geochronology and Lu- Hf isotope tracing. Geostandards and Geoanalytical Research, 41, 335-358.

Santos, A.P.M.R. 2011. A Formação Corumbataí na porção norte da Bacia do Paraná: litofácies e composição mineral para correlação regional e base para interpretação do contexto deposicional. Dissertação de Mestrado. Universidade de Brasília, Brasília.

Schneider, R.L., Mühlmann, H., Tomassi, E., Medeiros, R.A., Daemon, R.F. and Nogueira, A.A. 1974. Revisão Estratigráfica da Bacia do Paraná. Anais do Congresso Brasileiro de Geologia, 28, 41–65.

Silva, J. P., Lana, C., Mazoz, A., Buick, I., Scholz, R. 2022. U-Pb Saturn: New U-Pb/Pb-Pb Data Reduction Software for LA-ICP-MS. Geostandards and Geoanalytical Research, 47, 49-66

Simões, M.G., Marques, A.C., Mello, L.H.C., Anelli, L.E. 1997. Phylogenetic analysis of the genera of the extinct Family Megadesmidae (Pelecypoda, Anomalodesmata), with remarks on its paleoecology and taxonomy. Journal of Comparative Biology, 2, 75–90.

Simões, M. G. and Kowalewski, M. 1998. Shell beds as paleoecological puzzles: a case study from the Upper Permian of the Paraná Basin, Brazil. Facies, 38, 175-195.

Simões, M.G., Torello, F.F., Mello, L.H.C., Ghilardi, R.P. 2000. O conteúdo fossilífero de novos afloramentos do Grupo Passa Dois (Neopermiano), nas porções centro-sul e nordeste do Estado de São Paulo: implicações bioestratigráficas e paleoecológicas. Acta Geologica Leopoldensia, 23, 61-90.

Simões, M.G., Quaglio, F., Warren, L.V., Anelli, L.E., Stone, P., Riccomini, C., Grohmann, C.H. and Chamani, M.A.C. 2012. Permian non marine bivalves of the Falkland Islands and their paleoenvironmental significance. Alcheringa, 36, 543-554.

Sláma, J., Košler, J., Condon, D.J., Crowley, J.L., Gerdes, A., Hanchar, J.M., Horstwood, M.S.S., Morris, G.A., Lutz, N., Norberg, N., Schaltegger, U., Schoene, B., Tubrett, M.N., Whitehouse, M.J. 2008. Plešovice zircon—a new natural reference material for U–Pb and Hf isotopic microanalysis. Chemical Geology, 249, 1-35.

Söderlund, U., Patchett, P.J., Vervoort, J.D. and Isachsen, C.E. 2004. The ^{176}Lu decay constant determined by Lu–Hf and U–Pb isotope systematics of Precambrian mafic intrusions. Earth and Planetary Science Letters 219, 311-324.

Sohn, I.G. and Rocha-Campos, A.C. 1990. Late Paleozoic (Gondwanan) ostracodes in the Corumbataí Formation, Paraná Basin, Brazil. Journal of Paleontology, 64, 116–128.

Sousa, S.H.M. 1985. Fácies sedimentares das formações Estrada Nova e Corumbataí no Estado de São Paulo. Dissertação de Mestrado, Universidade de São Paulo, São Paulo.

Suguio, K., Salati, C. and Barcelos, J.H. 1974. Calcários oolíticos de Taguaí, SP e seu possível significado paleoambeintal na deposição da Formação Estrada Nova. Revista Brasileira de Geociências, 4, 142-160.

Sun, S. and McDonough, W.F. 1989. Chemical and Isotopic Systematics of Oceanic Basalts: Implications for Mantle Composition and Processes. *In:* Magmatism in the Ocean Basins (AD Saunders and MJ Norry Eds.). Geological Society of London Special Publications 42, 313–345.

Taylor, A.M. and Goldring, R. 1993. Description and analysis of bioturbation and ichnofabric. Journal of the Geological Society, 150, 141–148.

Tohver, E., Schmieder, M., Lana, C., Mendes, P.S., Jourdan, F., Warren, L., Riccomini, C. 2018. End-Permian impactogenic earthquake and tsunami deposits in the intracratonic Paraná Basin of Brazil. GSA Bulletin, 130, 1099-1120.

Toledo, C.E.V. 2001. Análise paleoictiológica da Formação Corumbataí na região de Rio Claro, Estado de São Paulo. Dissertação de Mestrado, Universidade Estadual Paulista "Julio de Mesquita Filho", Rio Claro.

Torello, F. F. 1999. Bioestratinomia de concentrações fossilíferas da assembléia de Pinzonella neotropica (Reed), Formação Corumbataí (Permiano), Tambaú, SP. 130p. Dissertação de Mestrado, Universidade de São Paulo, São Paulo.

Turra, B.B. 2009. Diques clásticos da Formação Corumbataí, Bacia do Paraná, no contexto da Tectônica Permotriássica do Gondwana Ocidental. Dissertação de Mestrado, Universidade de São Paulo, São Paulo.

Valencio, D.A., Rocha-Campos, A.C. and Pacca, I.G. 1975. Paleomagnetism of some sedimentary rocks of the late Paleozoic Tubarão and Passa Dois Groups from the Paraná Basin, Brazil. Revista Brasileira de Geociencias, 5, 186–197.

Vieira, A.J. 1973. Geologia do centro e nordeste do Paraná e centro-sul de São Paulo. In: Congresso Brasileiro de Geologia, Aracaju, Anais, p. 259-277.

Walker, R.G., James, N.P. 1992. Facies models: response to sea level change. Geological Association of Canada, Ontario, Canadá, p. 454.

Warren, L.V., Almeida, R.P., Hachiro, J., Machado, R., Roldan, L.F., Steiner, S.S. and Chamani, M.A.C. 2008. Evolução Sedimentar da Formação Rio do Rasto (Permo-Triássico da Bacia do Paraná) na porção centro-sul do Estado de Santa Catarina, Brasil. Revista Brasileira de Geociências, 38, 213–227.

Warren, L.V., Assine, M.L., Simões, M.G., Riccomini, C. and Anelli, L.E. 2015. A Formação Serra Alta, Permiano, no centro-leste do Estado de São Paulo, Bacia do Paraná, Brasil. Brazilian Journal of Geology, 45, 109-126.

Washburne, C.W. 1930. Petroleum geology of the State of São Paulo. Boletim Comissão Geográfica e Geológica, 22, 272p.

Wesselingh, F.P. 2007. Long-lived lake mollusks as island faunas: a bivalve perspective. *In:* Biogeography, Time and Place: Distributions, Barriers and Islands (W. Remena ed.), Springer, Dordrecht, 275–314.

White, D. 1908. Relatório sobre a flora fóssil das camadas carboníferas do Brasil. In: White, I.C. (ed.) Relatório final da Comissão de estudo das minas de carvão de pedra do Brasil. DNPM. Brasília. p. 338-617.

Woodhead, J.D. and Hergt, J.M. 2005. A preliminary appraisal of seven natural zircon reference materials for in situ Hf isotope determination. Geostandards and Geoanalytical Research, 29, 183-195.

Wu, F.Y., Yang, Y.H., Xie, L.W., Yang, J.H. and Xu, P. 2006. Hf isotopic compositions of the standard zircons and baddeleyites used in U–Pb geochronology. Chemical Geology, 234, 105-126.

Yang, D., Huang, Y., Guo, W., Huang, Q., Ren, Y. and Wang, C. 2018. Late Santonian-early Campanian lake-level fluctuations in the Songliao Basin, NE China and their relationship to coeval eustatic changes. Cretaceous Research, 92, 138-149.

Zaine, M.F. 1980. Uma barreira geográfica no Paleozoico Superior na região de Fartura, SP. Dissertação de Mestrado, Universidade de São Paulo, São Paulo.

2. CONTROLES DEPOSICIONAIS E EVOLUÇÃO DO MEGA LAGO PERMIANO: NOVAS INTERPRETAÇÕES PARA A FORMAÇÃO CORUMBATAÍ (BACIA DO PARANÁ)

A Formação Corumbataí, depositada durante o Permiano médio a superior, registra um capítulo único na evolução do sudoeste de Gondwana. Durante todo o Permiano, a margem sul do supercontinente esteve sujeita a esforços compressivos, que resultou no soerguimento do Cinturão Gondwanides (Keidel, 1916), levando à restrição das conexões marítimas entre o Panthalassa e as bacias do Paraná e Karoo. Isso resultou na formação de um "*trapped sea*" que evoluiu para um mega-lago (sensu Palcu et al., 2021), no qual foram depositadas as formações Irati, Serra Alta, Teresina/Corumbataí e Rio do Rasto (parte intermediária a superior da Supersequência Gondwana I, Milani et al., 2007). Neste contexto, desde meados do século XX, múltiplos cenários paleoambientais têm sido propostos para a deposição da Formação Corumbataí, incluindo ambientes marinhos rasos restritos, deltaicos, lacustres e influenciados por marés. Apesar da ausência de estudos sedimentológicos e estratigráficos detalhados nesta unidade, o conteúdo fóssil endêmico (Runnegar e Newell, 1971; Maranhão e Petri, 1996; Simões et al., 1998; Ghilardi e Simões, 2002) e a ocorrência de fácies siliciclásticas, carbonáticas e evaporíticas indicam que a história deposicional desta unidade é muito mais complexa do que se pensava anteriormente. No presente capítulo são descritas e associadas as fácies sedimentares da Formação Corumbataí, integrando-as ao conceito de estratigrafia de sequências para lagos, a fim de elaborar arcabouço completo para intepretações paleoambientais e paleogeográficas. Os dados adquiridos inauguram novas perspectivas para os controles alo e autogênicos da unidade e da Bacia do Paraná durante o mencionado período. Os resultados constituem o manuscrito intitulado *"Sedimentation and accommodations controls on the facies stacking and lateral distribution of a Permian unconventional megalake"*.

Referências

Ghilardi, R.P. e Simões, M.G. 2002. Foram os bivalves do Grupo Passa Dois (exclusive Formação Rio do Rasto) moluscos dulcícolas? Pesquisas em Geociências, 29, 91-92.

Keidel, J. 1916. La geología de las Sierras de la Provincia de Buenos Aires y sus relaciones con las montañas de Sudáfrica y Los Andes. Ministerio de Agricultura de La Nación, Sección Geología, Mineralogía y Minería, 11, 1-78.

Maranhão, M.S.A.S. e Petri, S. 1996. Novas ocorrências de fósseis nas formações Corumbataí e Estrada Nova do Estado de São Paulo e considerações preliminares sobre seus significados paleontológicos e bioestratigráficos. Revista do Instituto Geológico, 17, 33-54.

Milani, E.J., Melo, J.H.G, Souza, P.A., Fernades, L.A., França, A.B. 2007. Bacia do Paraná. Boletim de Geociências da Petrobrás, 15, 265–287.

Palcu, D.V., Patina, I.S., Ş D.V., I., Lazarev, S., Vasiliev, I., Stoica, M., Krijgsman, W. 2021. Late Miocene megalake regressions in Eurasia. Scientific Reports, 11, 11471.

Runnegar, B. e Newell, N.D. 1971. Caspian-like relict molluscan fauna in the South American Permian. Bulletim of American Museum of Natural History, 146, 1–66.

Simões, M.G., Rocha-Campos, A.C., Anelli, L.E. 1998. Paleoecology and evolution of Permian pelecypod assemblages (Paraná Basin) from Brazil. In: *Bivalves – An Eon of Evolution- Paleobiological Studies Honoring Norman D. Newell* (Eds. P.A. Johnston and J.W. Haggart). University of Calgary Press, Calgary, pp. 443–452.

Sedimentation and accommodations controls on the facies stacking and lateral distribution of a Permian unconventional megalake

Abstract

The Permian succession of the Paraná Basin records the disconnection of the Panthalassa global ocean and the epicontinental sea that bathed the SW Gondwana. The development of an orographic barrier (Gondwanides Belt) led to the restriction of the marine connections and resulted in the formation of a trapped sea that evolved to a megalake. This contribution presents an interpretation of the evolution of fourth-order depositional sequence comprising a mixed siliclastic-carbonate deposits, the sedimentation and accommodations controls on the unconventional megalake, represented by the Corumbataí Formation (Paraná Basin, Brazil). This continental-scale aquatic body was characterized by hydrological and saline variations that conditioned the development of a unique endemic fauna. Data suggests that these unit was deposited in an endorheic megalake that went through balanced-fill to overfilled stages, intimately associated to the transgressive and regressive systems tracts. The first transgressive system tract is characterized by offshore settings deposited in a freshwater ballanced-fill lake. The first regressive system tract is represented by the progradation of coastal system with shoreface to offshore-transition facies in a freshwater overfilled lake. The overlying deposits comprise a brackish water balanced-fill lake that records the landward migration of the system and the deposition of offshore-transition deposits over the shoreface facies, due to positive water balance that allowed the rise of the lake level and accommodation, resulting in the second transgressive system tract. Finally, the second regressive system tract mark the saline overfilled lake stage, characterized by the progressive intensification of arid climate and a relatively shallow water level conditions, that is evidenced by the presence of evaporite deposits (saline flat facies association) and dominance of shoreface facies. Furthermore, the Corumbataí Formation records the seiche influence in reduced bathymetry megalakes sedimentation and the relevant implications for understanding part of the depositional history of the Gondwanan Paleozoic basins.

Keywords: Megalake; Seiche; Facies Models; Paraná Basin

2.1. Introduction

Megalakes are characterized by lakes greater than 10,000 km^2 in area (Quade et al., 2018) that are also termed “inland seas”, although they do not behave like small oceans, at least in the stratigraphic or geochemical sense (e.g., Bohacs, 1999; Bohacs et al., 2000c; Buoniconti, 2001). Bohacs et al. (2003), based on numerous observations of modern large lakes (e.g., Caspian, Baikal, Great Canadian Lakes, Tanganyika, Victoria, among others) and Phanerozoic lacustrine strata, suggested that lake size, shape, chemistry, and ecology are not simple functions of climatic humidity or tectonic subsidence. In fact, a lake’s size, chemistry, and biota can vary rapidly, and lake strata are punctuated by many widespread breaks (Gierlowski-Kordesch and Kelts, 1994; Sladen, 1994; Bohacs et al., 2000a). In these continental-scale lakes, the sedimentary filling depends mainly on the nonlinear interaction of rates of potential accommodation (space available for sediment accumulation below a lake’s sill or spillpoint) increase and supply of sediment and water (Carroll and Bohacs, 1999).

A prominent process acting in lakes is a seiche (Trebitz, 2006; Matishov and Inzhebeikin, 2009; Medvedev et al., 2018), a large-scale stationary wave originated by the amplification of other waves commonly formed by winds. In an enclosed (e.g., Great Canadian Lakes and Azov Sea) or semi-enclosed (e.g., Adriatic Sea) basins, seiche forms when strong winds and rapid changes in atmospheric pressure push water from one margin of water body to the other, considerably raising the water level. When the winds cease, the water mass moves back in the opposite direction, exposing the previously flooded margin (Ichinose et al., 2000). Then the water continues to oscillate back and forth for hours or even days (Ichinose et al., 2000). In a similar way, earthquakes, tsunamis, or severe storm surge may also cause these mega-scale stationary waves.

Very rare in the past and currently present in some parts of Eurasia (e.g., Caspian, Azov, and Black seas; Palcu et al., 2021), megalakes are understudied regarding their sedimentary processes, auto and allogenic depositional controls and general basin architecture. This gap on the knowledge extends to the known Paleozoic examples, with the absence of an adequate facies model for this particular depositional system, especially one comprehending the recognition of seiche effects in sedimentation. Thus, the available modern analogs function only as comparable from the physiographic perspective (Matishov and Inzhebeikin, 2009; Kosyan and Krylenko, 2019; Palcu et al., 2021), remaining unanswered, questions about the influence of size variation, bathymetry, climatic conditions, sediment dispersion and circulation patterns in their depositional patterns.

The epicontinental sea that bathed the southeastern Gondwana continent following the Permo-Carboniferous deglaciation event, went through progressive conditions of continentalization during the Permian (Lavina, 1991; Milani et al., 2007; Holz et al., 2010; Limarino et al., 2013; Kern et al., 2021) due to the uplift of the Gondwanides orogenic belt (Keidel, 1916; Ramos et al., 1986) (Fig. 1). In the South America and Africa continents, this unique chapter in the evolutionary history of the Paraná and Huab/Karoo basins is recorded by the Irati and White Hill formations (Kungurian; ~277 Ma). This vast tectonically trapped sea (sensu Palcu et al., 2021) covered a large area of the SW Gondwana originally corresponding to three times the size of the Caspian Sea and one and a half times the size of the Gulf of Mexico (Runnegar and Newell, 1971). Due to the restricted ocean connections, this huge water mass was probably strongly stratified and influenced by punctual marine ingressions with periods of pronounced hypersalinity and carbonate production (Bastos et al., 2021; Brito et al., 2023). Later, during the Guadalupian Epoch, the intracratonic Paraná Basin was completely disconnected from the Panthalassic Ocean, becoming a megalake that covered an area greater than 1.7 million km^2 (Rohn, 1994), currently corresponding to part of Brazil, Uruguay, Paraguay, Namibia, and South Africa. This landlocked megalake was characterized by marked hydrological and saline variations that conditioned the development of a unique endemic fauna of bivalves, gastropods, fishes, and reptiles (Runnegar and Newell, 1971; Simões et al., 1998) in a similar mode to what occurred during the Miocene of Eurasia (Palcu et al., 2021).

Considering this scenario, in this contribution we analyze the depositional aspects and sedimentary evolution of the Corumbataí Formation, an emblematic Permian unit of the Paraná Basin interpreted as deposited in a closed water body (Runnegar and Newell, 1971; Maranhão and Petri, 1996; Simões et al., 1998; Ghilardi and Simões, 2002; Simões et al., 2012; Warren et al., 2015). By a detailed sedimentological and stratigraphic analyses, we define a plausible sedimentary environment for the unit and establish an adequate facies model for depositional systems developed in megalakes with seiche influence and reduced bathymetry. The integration of such data allowed delineating a novel depositional model for the Corumbataí Formation, with relevant implications for understanding megalake sedimentation and part of the depositional history of the Gondwanan Paleozoic basins.

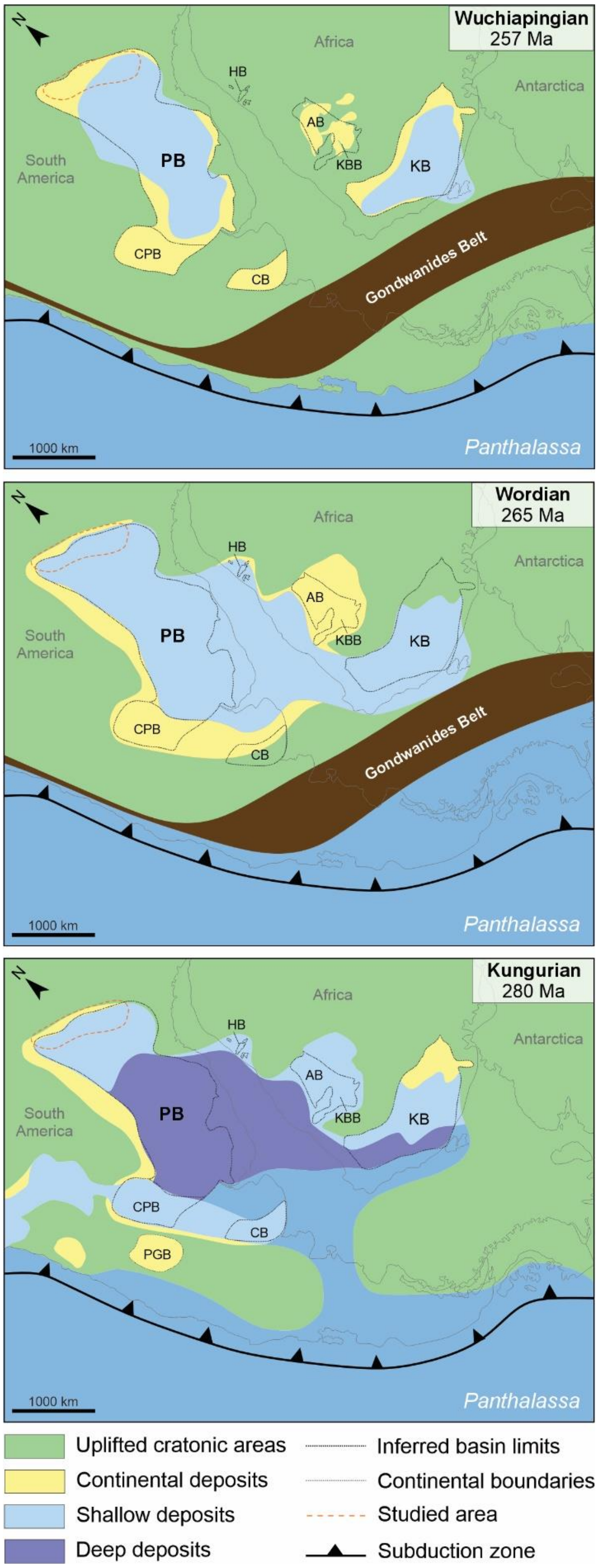

Figure 1 - Permian (Kungurian–Wuchiapingian) paleogeographic maps showing the progressive isolation of the Paraná Basin and coeval depositional areas in Gondwana (modified from Bastos et al., 2021). Explanation: PB - Paraná Basin; HB - Huab Basin; AB - Aranos Basin; KBB - Karasburg Basin; KB - Karoo Basin; CB – Claromecó Basin; CPB - Chaco-Paraná Basin; PGB - Paganzo Basin.

2.2. Geological Setting

The Paraná Basin is an intracratonic basin developed between the Middle Ordovician and Upper Cretaceous periods (Milani et al., 2007). This huge sedimentary basin, located in southernmost Brazil and north/northwestern Uruguay, parts of Paraguay and Argentina, encompasses at least six second-order stratigraphic sequences, including sedimentary and volcanic rocks (Milani et al., 2007).

The sedimentary record of the transition from marine to continental environments encompasses the mixed siliciclastic-carbonate succession of the Passa Dois Group (Irati, Serra Alta, Corumbataí/Teresina and Rio do Rasto formations, Fig. 2), corresponding to the upper part of the Gondwana I Supersequence (Milani et al., 2007). The organic-rich Irati Formation constitute the basal unit of the Passa Dois Group, characterized by organic-rich, black shales interbedded with dolomites (Brito et al., 2023). Above, the organic-poor, fine-grained succession of the Serra Alta Formation is interpreted to be deposited in a closed epeiric sea under dysoxic to anoxic conditions (Holz et al., 2010; Warren et al., 2015), and corresponds to the last basin-scale transgressive event (third-order) during the Permian (Warren et al., 2015). The presence of endemic bivalves and the absence of marine fossils (Runnegar and Newell, 1971; Maranhão and Petri, 1996; Simões et al., 1998; Ghilardi and Simões, 2002) constitute strong evidence that the Irati and Serra Alta formations were already isolated from the Panthalassa at this time (Simões et al., 2012; Warren et al., 2015), although geochemical data points to the punctual presence of marine planktonic organisms (Reis et al., 2018; Bastos et al., 2021).

The overlying mixed siliciclastic-carbonate succession of the Teresina Formation represents the transition from the deeper water setting of the Serra Alta Formation to a fully oxic, and shallow depositional environment (Holz et al., 2010; Warren et al., 2015; Matos et al., 2017; Ng et al., 2019). Due to a marked lateral facies variation, this unit is recognized as the Corumbataí Formation in the northeast of São Paulo, Mato Grosso, and Goiás states (Rohn, 1994) (Fig. 2). According to subsurface correlations between profiles from São Paulo and Paraná states, the upper part of both Corumbataí and Teresina formations are incomplete due to the erosive contact with the overlapping Jurassic units (i.e., Pirambóia Formation in the São Paulo State and Botucatu Formation in the Goiás and Mato Grosso states; Holz et al., 2010; Christofoletti et al., 2021).

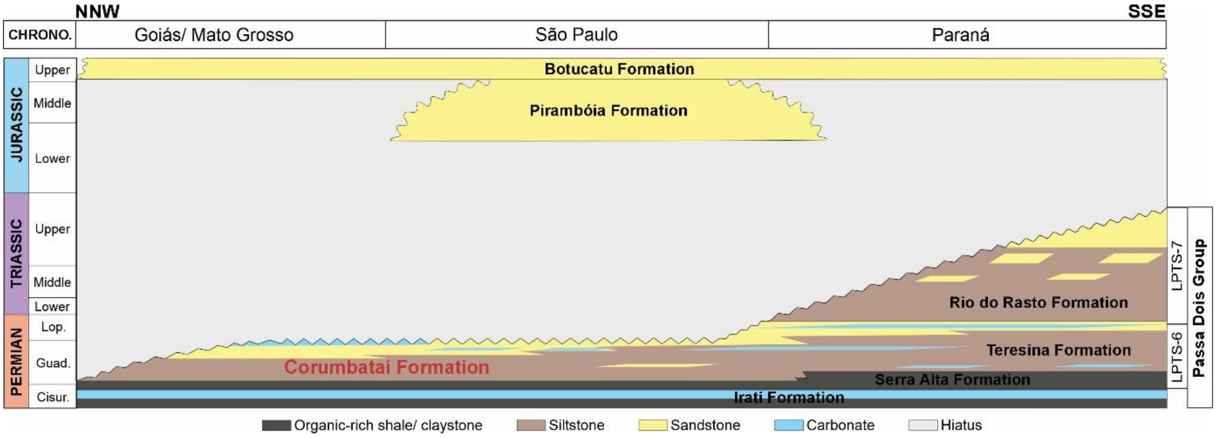

Figure 2 - Permian third-order sequences from the Paraná Basin, highlighting the studied interval (Corumbataí Formation) (modified from Holz et al., 2010). Explanation: CHRONO - Chronostratigraphy; Lop. - Lopingian; Guad. - Guadalupian; Cisur. - Cisuralian; LPTS - Late Paleozoic Third-Order Sequences.

Since the mid-20th century, the Corumbataí Formation has been interpreted as deposited in several different scenarios, including shallow and restricted marine environment, epicontinental sea, tidal flat, and storm-influenced lake (Washburne, 1930; Moraes Rego, 1940; Mendes, 1952; Beurlen, 1954, 1955; Barbosa and Gomes, 1958; Salamuni, 1963; Northfleet et al., 1969; Vieira, 1973; Suguio et al., 1974; Schneider et al., 1974; Fúlfaro et al., 1978; Gama Jr., 1979; Fúlfaro et al., 1980; Zaine, 1980; Petri and Coimbra, 1982; Petri and Fúlfaro, 1983; Sousa, 1985; Lavina 1991; Rohn, 1994) (Table 1). It is important to note that, besides the Gordon Jr. (1947) and Schneider et al. (1974) lithostratigraphic proposal, some authors also used the obsolete name Estrada Nova Formation for part of the succession above the Irati Formation. The use of this outdated nomenclature caused some confusion in the literature since the regional lithostratigraphic expression of the Estrada Nova Formation is variable and may be equivalent to the Serra Alta and Teresina formations; Serra Alta, Teresina and Rio do Rasto (Serrinha Member) formations; Teresina and Rio do Rasto (Serrinha Member) formations; or only to the Teresina Formation (Rohn, 1988; 1994). Thus, in this work we adopted the proposal of Warren et al. (2015) in which the Teresina and Corumbataí formations were lateral equivalents, both presenting lower transitional contact with the underlying Serra Alta Formation and upper erosive contact with the Jurassic units (Pirambóia or Botucatu formations, see Fig. 2; Christofoletti et al., 2021).

Finally, in the south of Paraná Basin (Southern Brazil), the Rio do Rasto Formation overlies the Teresina Formation (Holz et al., 2010). The Rio do Rasto Formation is divided into the Serrinha and Morro Pelado members, representing sedimentation in shallow water setting influenced by river dominated deltas (Warren et al., 2008; Kern et al., 2021). Towards the top, there is an increase in fluvial and eolian deposits, culminating in the complete filling of the water body and continentalization of the Paraná Basin (Warren et al., 2008).

Table 1 - Previous works on the depositional system of the Corumbataí Formation.

Author	Unit	Depositional System
Washburne (1930); Moraes Rego (1940)	Estrada Nova Formation (currently Serra Alta, Teresina, Corumbataí, and Rio do Rasto formations)	Hypersaline shallow water setting
Beurlen (1954 and 1955); Barbosa and Gomes (1958); Vieira (1973)	Teresina Formation	Epicontinental sea, saline water without evidence of connection with the Panthalassa. Sedimentation in storm-influenced proximal settings
Mendes (1952)	Corumbataí Formation	Continental environment, based on the presence of plant remains and absence of diagnostic marine fossil
Salamuni (1963); Northfleet et al. (1969); Schneider et al. (1974); Fúlfaro et al. (1978); Gama Jr. (1979); Fúlfaro et al. (1980); Zaine (1980)	Teresina / Corumbataí formations	Tidal flats, based on the presence of mud cracks, intraformational breccia, and heterolithic bedding
Suguio et al. (1974); Petri and Coimbra (1982)	Estrada Nova Formation	Restricted, shallow water marine or lacustrine setting affected by storms
Petri and Fúlfaro (1983)	"Teresina facies"	Lagoon, with restricted connection with the Panthalassa. The occasional subaerial exposition was related to pluvial fluctuations
Sousa (1985)	Corumbataí Formation	Macrotidal-dominated depositional system
Lavina (1991)	Teresina Formation	Vast epeiric sea (or lake), with base level variations and influenced by storms
Rohn (1994)	Teresina Formation	"Sea-lake", without connection with the Panthalassa. Shallow water setting frequently affected by storms, punctuated by episodes of intense evaporation. Variation in water level were controlled by pluvial fluctuations

2.3. Material and Methods

A detailed sedimentological and stratigraphic study was conducted through the detailed (1:50 scale) measurement of 25 columnar sections in the Middle Permian mixed siliciclastic-carbonate deposits of the Corumbataí Formation, in the northeast and northern part of the Paraná Basin, Brazil (Fig. 3). The sedimentary facies were determined based on bed geometry, grain texture, sedimentary structures, and trace fossil content following the protocol of Miall (2006). All facies represented in columnar sections had their particular depositional processes defined and were associated in distinct facies associations, according to the vertical association of groups of facies, genetically related to each other according to their environmental significance (see Dalrymple, 2010b).

The macroscopic and petrographic description of the carbonate facies was based on the classifications proposed by Dunham (1962) and Embry & Klovan (1972). The basic description of trace fossils followed the conceptual framework summarized in Buatois & Mángano (2011). The degree of bioturbation was estimated based on the Taylor & Goldring (1993) scheme, which defined a bioturbation index (BI), ranging from zero (no bioturbation) to six (completely bioturbated).

Stacking and correlation of columnar sections were based mainly on the identification of stratigraphic surfaces and correlation of facies associations. In order to understand the stratigraphic patterns within the Corumbataí Formation and correlate the distinct outcropping areas, three composite sections were built. For this, the most complete and representative sections for each studied region were selected (see Fig 3): Composite Section I – sections 14, 15, 16, 17, 18, 19, 20, and 22; Composite Section II – sections 6, 7, 8, 9, 10, 11, 12, 13 and 21; Composite Section 3 – 0, 1, 2, 3, 4A, 4B, 4C, 4D and 5.

In addition, accommodation curves were developed through Fischer diagrams, which indicate architectural trends in the studied succession and contribute to the correlation of geographically distant sections. Fischer plots are widely used in paleoenvironmental research as graphic representations of sea- and lake-level changes (Ocakoğlu et al., 2012; Muniz and Bosence, 2015; Yang et al., 2018; Cardoso et al., 2019; Brito et al., 2023) through mapping linearly corrected variation of accumulative cycle thickness over cycle number or stratum depth. Fischer (1964) introduced this graphic method of displaying relative sea-level changes (i.e., the sea-level change represented as the sum of subsidence and eustasy) derived from cyclic limestone and dolostone successions. Sadler et al. (1993) reviewed the use of Fisher plots and suggested that, instead of a time scale originally used, the horizontal axis of the plots should be labeled by cycle number, to avoid the problem of poor absolute time control on the stratigraphic record. According to Sadler et al. (1993), the use of at least 50 cycles is recommended to separate non-random (allogenic) from random (autogenic) fluctuations. Following this concept, the number and thicknesses of coarsening-upward successions recorded in the columnar sections of the Corumbataí Formation were identified and Fischer plots were correlated. Aiming to identify the high-frequency base-level fluctuations and defining the key stratigraphic surfaces, the correlation of the composite sections was carried out first in proximal sections and then at basin scale (Fischer, 1964; Read and Goldhammer, 1988; Day, 1997).

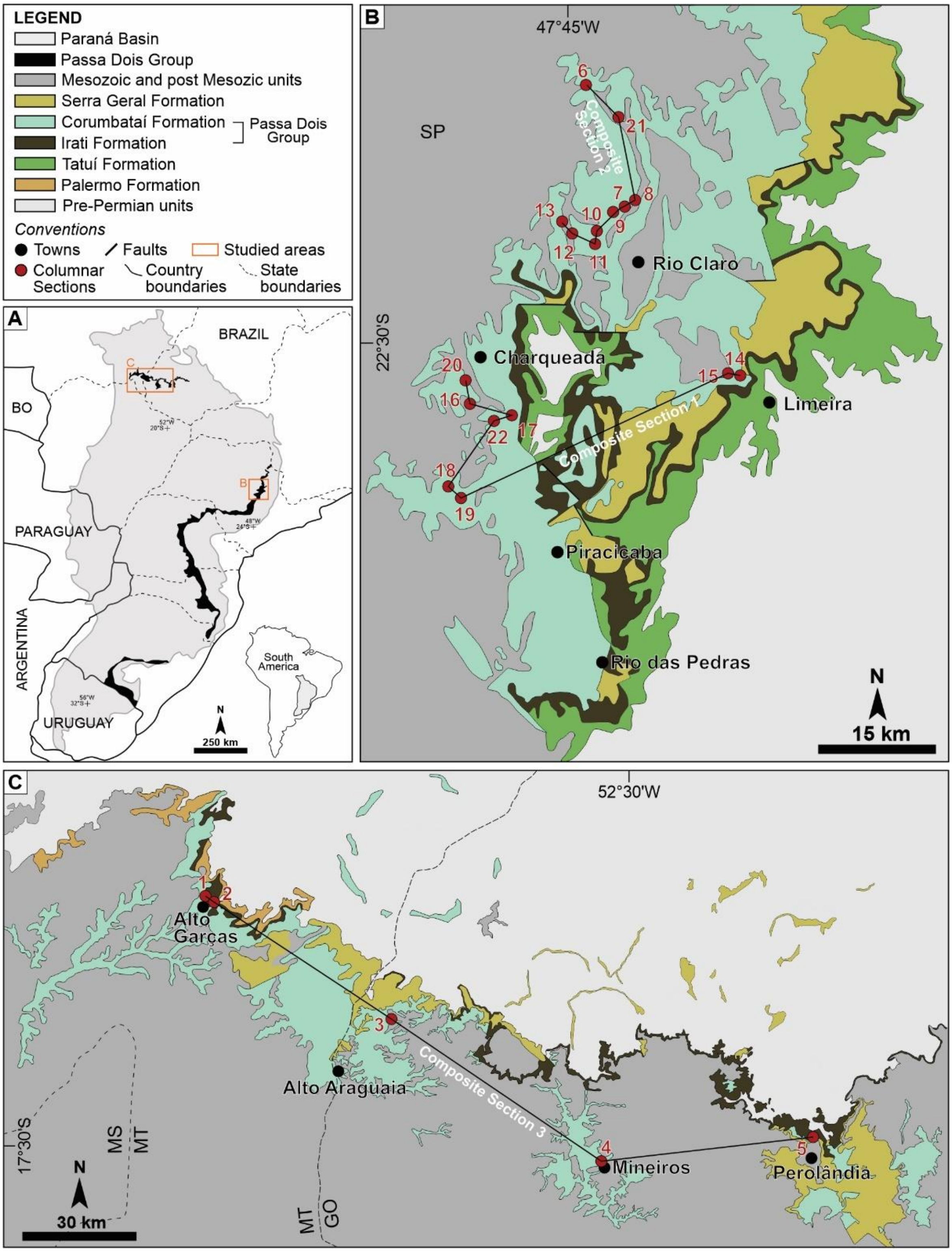

Figure 3 - Location of the studied areas. (A) Outcrop range of the Passa Dois Group in the Paraná Basin, highlighting the studied areas (in orange). (B) Geological map of the studied area in São Paulo State with location of the detailed columnar and composite sections. (C) Geological map of the studied area in Goiás and Mato Grosso states with location of detailed columnar and composite sections. Geological map based on CPRM, 2004. BO - Bolivia; MT - Mato Grosso; MS - Mato Grosso do Sul; SP - São Paulo; GO - Goiás.

2.4. Facies and Facies Associations

The detailed sedimentary description of the Corumbataí Formation allowed the identification of eleven siliciclastic and eight carbonate facies (Table 2), which are grouped into four facies associations: offshore (FA-1), offshore-transition (FA-2), shoreface (FA-3), foreshore (FA-4) and saline flat (FA-5).

Table 2 - Summary of sedimentary facies from the Corumbataí Formation.

Code	Facies	Description	Interpretation
Fm	Massive siltstone/claystone	0.3 to 2 m-thick tabular beds of massive siltstone or claystone, laterally continuous for tens to hundreds of meters. Bioturbation and micro-slumps are locally observed. Presence of sparse and thin (< 1cm-thick) lenses of phosphatic fish remains. **Fm** is more common in the lowermost ~20 m of the Corumbataí Formation and occurs in association with **Fl** facies.	Deposition from suspension in distal, calm, and oxygenated waters. Micro-slumps are interpreted as the product of overload by dense currents in low-gradient settings. Lenses of fish fragments are formed by hyperpycnal currents.
Fl	Laminated siltstone	0.1 to 4 m-thick tabular beds of laminated siltstone, laterally continuous for tens of kilometers. Thin lenses of phosphatic fish fragments and very fine- to fine-grained sandstone are sparsely distributed along laminations. Presence of simple horizontal bioturbation (*Planolites*). Tabular and ptygmatic clastic dykes occur in vertically restricted intervals along the upper part of the succession and are composed of silty to very fine-grained sandstone. The most expressive beds of **Fl** are described in the lower ~20 m of the Corumbataí Formation, but they are present in practically all sections, being the most common facies. In the upper part of the unit, it is generally less thick and occur interbedded with **Sr(s)**.	Settling of fine-grained particles in calm and oxygenated waters. Lenses of phosphatic fossil remains are deposited by long-lasting currents from shallower waters, bringing sand-sized organic particles and fish fragments. The dykes are product of forced upward injection of fluidized sediment, probably induced by seismic activity (seismites), and the occurrence of ptygmatic geometry is related to the effects of later compaction (Riccomini et al., 1992; Riccomini, 1995; Riccomini et al, 2005; Turra et al., 2006; Perinotto et al., 2008; Turra, 2009).
Sm	Structureless sandstone	0.1 to 0.3 m-thick lenticular or tabular beds of very fine- to fine-grained sandstone with massive aspect. Thin lenses of phosphatic fish fragments are dispersed, and horizontal and vertical bioturbation are locally observed. Some of the beds may be silicified. Lenticular bodies are cm-	The massive aspect can be related to 1) obliteration of primary structures by post-depositional processes, such as sediment liquidization; 2) homogeneity of granulometry; 3) rapid deposition of suspended sediments, or 4) intense bioturbation. The close association with fluidized levels within

		scale wide and occur in association with **Fl**.	**Fl**, suggests that the first hypothesis is the most plausible.
Sh	Horizontally laminated sandstone	0.1 to 1 m-thick tabular beds of horizontally laminated, very fine- to fine-grained sandstone, laterally continuous for tens of meters. Occasionally, this facies grades upward to symmetric ripple cross-laminated sandstone (**Sr**). Horizontal bioturbation (*Planolites*) is locally observed.	Transport of sand-sized sediments by traction in planar beds in the upper flow regime. When the Sl grades upward to Sr, the transport occurs under lower flow regime. Dominance of horizontal bioturbation suggests deposition below the fair-weather wave base and above the storm wave base (Seilacher, 1967; Buatois and Mángano, 1995; Buatois and Mángano, 1998).
Sr(s)	Symmetrical ripple cross-laminated sandstone	0.1 to 4 m-thick tabular beds of very fine- to medium-grained sandstone with symmetrical ripple cross-lamination, laterally continuous for tens of meters. The symmetric ripples have cm-scale wavelength and amplitude, and are partially covered by mud drapes, sometimes presenting horizontal to oblique bioturbation, syneresis cracks, and/or millimetric to centimetric mudstone cracks**. Sr(s)** is the most common facies in the upper part of the Corumbataí Formation and normally occurs interbedded with **Fl** and **H**.	Product of deposition under the action of high-frequency oscillatory flow caused by fair-weather waves. During stillstand, mud could settle in the troughs of ripples. Syneresis cracks indicate soft-sediment deformation due to substrate destabilization and/or shrinkage by autogenic (i.e., changes in salinity) or allogenic processes (i.e., earthquakes; Pratt, 1992, 1993, 1998). The presence of mudstone cracks indicates subaerial exposure and desiccation. Bioturbation indicates colonization of the substrate during stillstand.
Sr(a)	Asymmetrical ripple cross-laminated sandstone	Cm to dm-thick tabular beds of very fine to fine quartz-sandstone with asymmetrical cross-lamination. Well-selected sand grains have high sphericity. The climbing ripples present centimeter-wavelength and amplitude.	Migration of ripples under unidirectional tractive flows.
Sp	Planar cross-stratified sandstone	0.5 to 1 m-thick tabular beds, laterally continuous for tens of meters, of fine- to medium-grained sandstone with planar cross-stratification.	Migration of straight-crested dunes (2D dunes) under lower flow regime.
St	Low-angle cross-stratified sandstone	0.1 to 0.3 m-thick tabular beds, laterally continuous for a few meters of light cream to light red, fine- to medium-grained sandstone, with low angle cross-stratification (<15°).	Migration of bedforms with a high wavelength/amplitude ratio in transitional conditions between lower and upper flow regime.
Ss	Swaley cross-stratified sandstone	0.3 to 1 m-thick lenticular and/or amalgamated beds of very fine- to fine-grained sandstone with swaley cross-stratification. Wavelength and amplitude of mounds and swales vary from cm- to dm-scale.	Produced by the interaction of wave- and storm-driven currents parallel to the shoreline (e.g., longshore drift), and shore-normal currents generated by translatory flow (combined-flow oscillation and current interference) associated with plunging waves.

Sb	Bioclastic sandstone	0.1 to 0.8 m-thick tabular beds of very fine- to coarse-grained massive sandstone with disarticulated and fragmented bivalve shells. The loosely dispersed bioclasts are typically oriented obliquely or perpendicularly relative to the bedding plane. Sometimes bioturbation and siltstone intraclasts are observed.	Proximal concentrations produced by very fast accumulation events and occasional reworking during, and after storm events (Simões and Kowalewski, 1998).
H	Heterolithic bedding	0.2 to 2.5 m-thick tabular beds of heterolithic bedding (wavy, linsen, and flaser), marked by the alternation of thinly laminated fine-grained sandstone and claystone/siltstone. Locally, sandstone lamina present symmetric ripple cross-lamination. Syneresis cracks and mudstone cracks (mostly in flaser/wavy beddings) are common in the claystone/siltstone laminae. Abundance of horizontal and vertical bioturbation. Phosphatic fish fragments occur locally in thin lenses. **H** commonly transitions to **Sr(s)** and **Sh** in the upper part of the Corumbataí Formation.	Alternation of tractive flow and silt deposition from suspension in the absence of water flow. The variation from flaser to linsen bedding is related to the amount of mud in suspension and the time available for settling. Mudstone cracks indicate subaerial exposure of the muddy sediment and syneresis cracks indicates soft-sediment deformation due to substrate destabilization and/or shrinkage by autogenic or allogenic processes. Bioturbation indicate animal colonization of the oxic substrate during periods of slack water.
Gn	Normal graded conglomerate	Lenticular beds (4 cm x 70 cm) with erosive base and wavy top of clast-supported conglomerate, composed of rounded to angular silicified intraclasts, varying in size from granule to coarse sand, that presenting normal grading.	Deceleration of high-energy, tractive flow (e.g., storm flows). Deposition of the coarse-grained beds took place in two stages: 1) storm-generated flows with transport from foreshore to offshore, followed by 2) reworking and selective sorting of bed material by asymmetrical oscillatory currents generated by shoaling swell waves propagating onshore (Hart and Plint, 1989).
Gp	Peloidal grainstone	0.2 to 0.3 m-thick tabular beds, laterally continuous for tens of meters, of ripple cross-laminated (**Gpr**), horizontally laminated (**Gpl**), or massive grainstone (**Gpm**). Peloids are ~40% of the framework. Ostracods (~5%) occur chaotically dispersed (articulated and disarticulated). Well sorted angular to subangular quartz grains (silt and very fine sand) are dispersed (~25-30%) or concentrated in specific levels of the lamination (Fig. 4A). The lamination is marked by the deposition of carbonate mud. Microkarst features are locally observed, such as dissolution grooves	Concentric precipitation of carbonate mud (micrite) in a wave-agitated shallow-water setting, with transport under the lower flow regime (ripple and plane bed) punctuaed by moments of slack water and settling of carbonate mud. Massive structure of the **Gpm** microfacies is linked with the local absence of grain size or to rapid deposition during deceleration of high-energy flows. Presence of articulated and disarticulated ostracod shells is indicative of temporal mixing of allochthonous to autochthonous assemblages. Microkarst features are suggestive of subaerial exposure

		and centimeter-sized cavities (funnel-like structures) filled by sparry calcite.	followed by burial and cementation in the meteoric to phreatic zone.
Roi	Inverse graded oncoid rudstone	0.1 to 0.2 m-thick tabular beds laterally continuous for tens of meters. Oncoids are elliptical in shape (type 1) or triangular, showing a convex top and thin basal lamination (type 2), ranging in size from a few mm to up to 4 cm. The nuclei are commonly 80% of the total oncoid size (peloidal intraclast), and occur enveloped by silicified, thin lamination (Fig. 4B). Peloidal grainstone intraclasts (20%) are also part of the framework. Oncoids and intraclasts gradually increase in size towards the top. The silicification process is pervasive.	Oncoids are carbonate-coated grains produced by microorganism activity, commonly cyanobacteria, resulting in the trapping of organic, bioclastic, or lithoclastic nuclei by concentric laminations (Logan et al., 1964; Dahanayake, 1978; Flügel, 2010). The oncoids with spherical shapes (type 1) suggest growth detached from the substrate, and probably with bearing. The concentric biofilm also suggests a homogeneous incidence of light around the oncoid (Rodrigues et al., 2022). The type 2 oncoid (concave top lacking basal lamination) indicates that they were attached to the substrate during growth. The in-situ growth implies in the absence of carbonate production at the oncoid base and may be indicative of reduced light incidence (Rodrigues et al., 2022). The coarsening upward pattern is suggestive of an increase in depositional energy towards the top of the concentration.
Ms	Stromatolites	These are 0.1 to 0.2 m-high isolated morphologies. Laminar accretion can occur as planar, domical, and closed-spaced conical morphologies (Fig. 4C) forms. EPS laminations are characterized by the presence of organic-rich, dark micrite, and pyrite crystals are common. Quartz grains and disarticulated shells of ostracodes in a convex-upward posture are common within planar stromatolites. The fenestral porosities between the laminations present filling by mosaic-type quartz. Silicification is pervasive in some levels of stromatolites bounded by non-silicified beds.	Stromatolites are biosedimentary structures interpreted to be deposited in a highly stressful, evaporitic shallow-water environment, strongly influenced by microbial activity (microbially induced / influenced organomineralization). Conical stromatolites suggests relatively deeper waters in comparison to planar and domical morphologies. Possibly, the stressful conditions and increased space competition of the microbial colonies, would allow the existence of conical stromatolites in shallow waters (Petroff et al., 2010). Silicification is interpreted to be early diagenetic by the increase of pH (>9) solubilizing silica followed by a decrease of pH (Hesse, 1990).
Rb	Bivalve rudstone	0.08 to 0.3 m-thick lenses of bivalve rudstone, laterally continuous for tens meters. Bivalves occur articulated, disarticulated, and fragmented (Fig. 4D), and present fossil elements related to the *Pinzonella illusa* and	Deposits formed by high-energy hydraulic processes, such as landward incoming waves or basinward backwash flows generated during high-energy events (i.e., storms; Simões et al., 2000) or reworking and prolonged exposure of bioclasts at the

		*Pinzonella neotropic*a biozones (Mendes, 1949; 1952).	water/sediment interface, under conditions of low or intermediate sedimentation rates in a proximal environment (above the FWWB) (Simões and Torello, 2003)
Mm	Massive mudstone	0.1 to 0.2 m-thick tabular beds of massive wackestone, laterally continuous for tens of meters. Very fine sand-to-silt-sized grains of angular quartz occur dispersed in the matrix (~5%) (Fig. 4E). Articulated and disarticulated ostracod shells occur scattered in the matrix (<10%).	The settling of carbonate mud suggests very calm depositional conditions (*i.e.*, without significant bottom currents and wave agitation). The presence of both articulated and disarticulated ostracod shells indicate some spatial and temporal mixing of these bioclast grains (Fürsich and Oschmann, 1993). Terrigenous grains points to occasional siliciclastic input carried from proximal to distal areas by currents.
Rp	Phosphate – rudstone	0.1 to 0.2 m-thick, tabular and continuous beds for a few meters of phosphate-rudstone (or bone beds). Composed of poorly-sorted grains (2 µm to 3 mm) of fish fragments (~35%) (coprolites, teeth, ganoid scales), and intraclasts (~5%) (Fig. 4F). Chaotically dispersed articulated and disarticulated ostracod shells also occur. Silicification is pervasive.	Phosphatogenesis was stimulated by the accumulation of bioclastic material rich in Phosphorous (e.g., fish and bivalve fragments, coprolites, and pellets). Chemical conditions and the winnowing process may have played a critical role in the enrichment of the primary phosphate accumulation. Textural classification for phosphatic sediments based on Trappe (2001).
Pe	Evaporitic paleosol	0.3 to 1.5 m-thick tabular beds with massive and mottled aspects, presenting red and white colors. Sometimes is noted the presence of thin veins and lenses filled with calcite and gypsum. The beds are laterally extended for tens of meters. Popcorn crusts, halite hoppers, and stromatolites occur associated. This facies only occurs at the uppermost part of the Corumbataí Formation.	Pedogenesis of previously deposited mud/silt deposits, generating gypsum and calcite during subaerial exposure in high evaporation conditions.

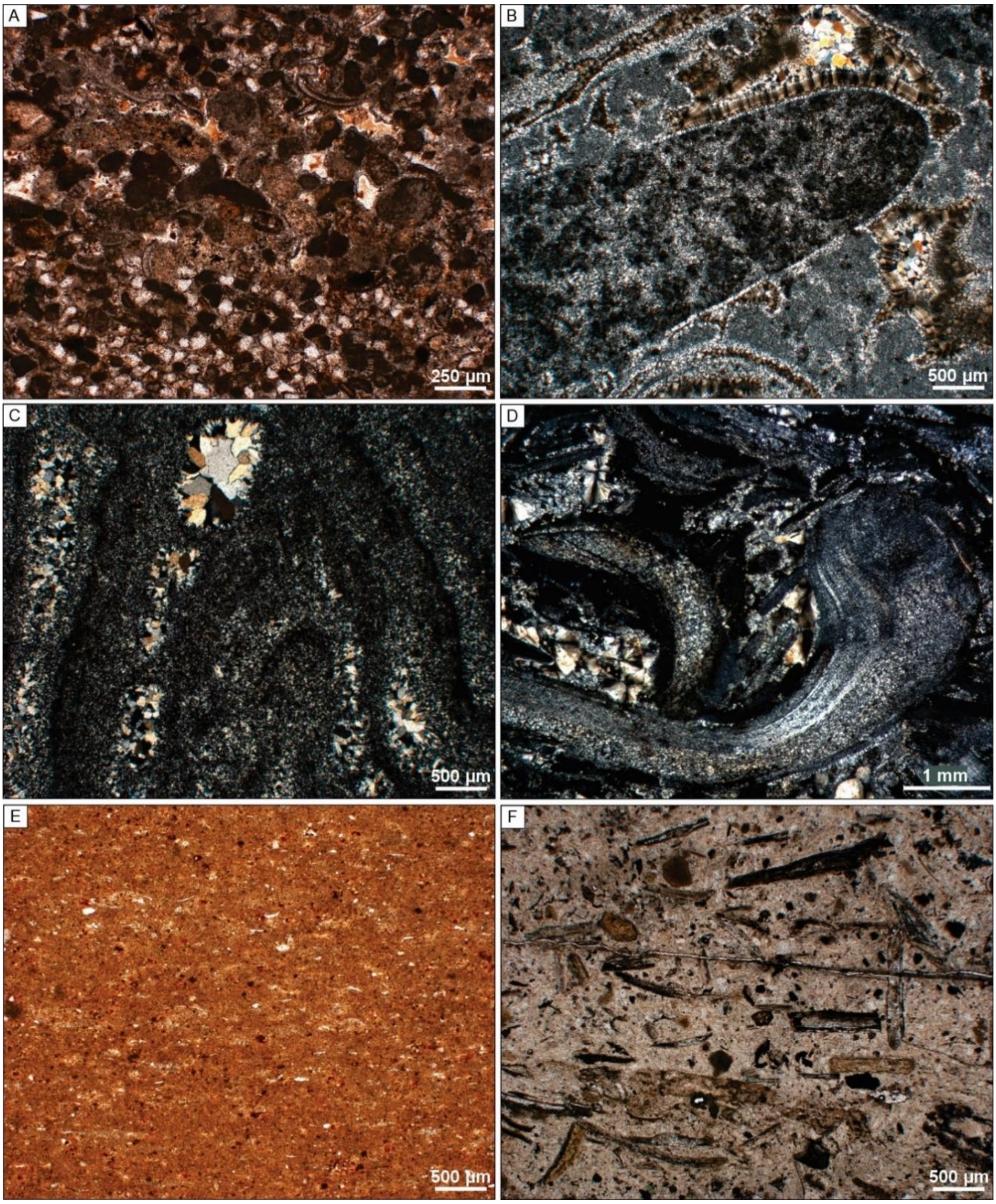

Figure 4 – Carbonate microfacies of the Corumbataí Formation. (A) Peloidal grainstone with sparse ostracod shells. (B) Oncoid rudstone enveloped by thin, wrinkled lamination. Note that the nuclei are ~80% of the total oncoid size. (C) Columnar stromatolite, showing microbial lamination (micrite) and interlaminar spaces filled with mosaic quartz (silicified sample). (D) Bivalve rudstone. (E) Massive wackstone. (F) Phosphate rudstone composed of poorly sorted grains of fish fragments (coprolites, teeth, ganoid scales, among others).

2.4.1. *Offshore (FA-1)*

Description

FA-1 consists of successions of interbedded claystone, siltstone, and sandstone (Fig. 5), with thicknesses between 1 and 6 m and lateral extension in the order of tens of kilometers (Fig. 5A). The facies are predominantly composed of decimeter- to meter-scale tabular beds of grey and reddish-colored **Fm** and **Fl** (Fig. 5B). Very-fine to fine-grained sandstone (**Sh** and **Sr(a)** occur interbedded, composing cm-scale tabular or lenticular beds (Fig. 5C). This interval is characterized by low to moderate bioturbation (BI = 1-2), mainly by simple traces such as *Planolites.* Thin lenses (mm-scale) of phosphatic fish fragments occurs sparsely distributed along **Fl** laminations (Fig. 5D). Interbedded with claystone and siltstone, rare centimeter-scale (5- to 15-cm-thick) bone beds (**Rp**) composed of vertebrate bioclasts (teeth, scales, and bone fragments of paleonisciforms, dipnoiforms, xenacanthiforms, petadolontiforms, and amphibian labyrinthodonts), bivalves fragments, and mudstone intraclasts, are also described by Castro et al. (2001) in these deposits (Fig. 5E).

Interpretation

The dominance and great lateral extension of the fine-grained facies (claystone/siltstone) suggests deposition from suspension in distal and calm waters rarely affected by density currents, hyperpicnal flows, or storms. Although discrete, the presence of the low-diversity traces fossils typifies unconsolidated and permanent subaqueous substrates, in relatively well-oxygenated and stressful, low-energy lake bottoms, periodically affected by episodic sedimentation (Buatois and Mángano, 1995). The occasional presence of fine-grained sandstone with current ripples, with or without fossil fragments, reaffirms the episodic deposition by bottom tractive flows. Residual lag-type bioclastic concentrations indicate that the reworked remains were transported from shallower waters by currents and waves probably induced by storms and concentrated by winnowing. The phosphate rudstone bed (facies **Rp)** of this facies association is interpreted as a concentration deposit formed by the winnowing of P-rich fish and bivalve fragments, coprolites, and fecal pellets.

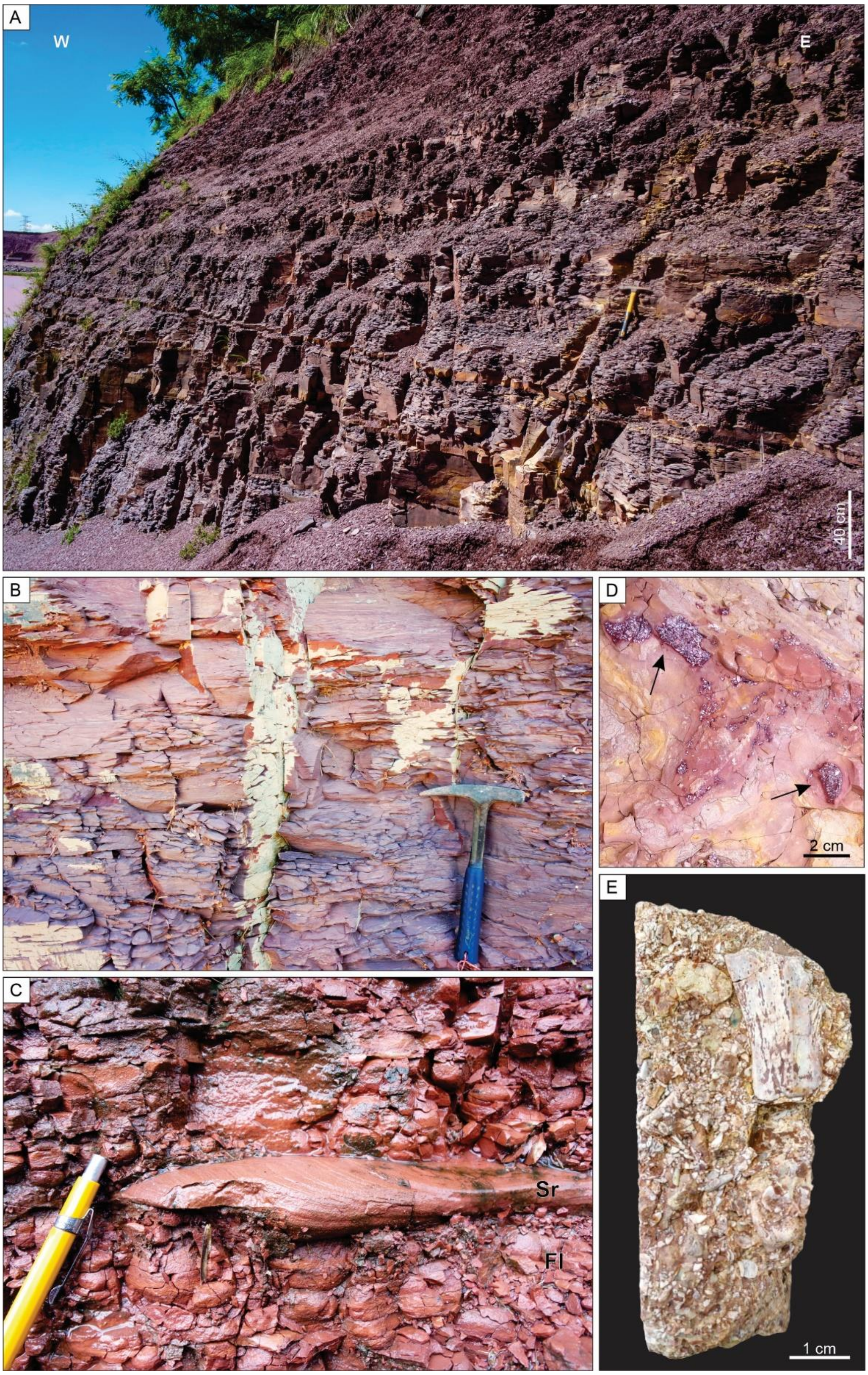

Figure 5 - Offshore deposits (FA-1). (A) General view showing monotonous laminated siltstone interbedded with very fine-grained sandstone. (B) Reddish-colored laminated siltstone. (C) Laminated siltstone interbedded with lenticular bed of very fine-grained sandstone with asymmetrical ripple cross-lamination (**Sr(a)**). (D) Thin lenses of phosphatic fish fragments (black arrows) in plan view. (E) Isolated skeletal elements concentrated in bone bed,

such as teeth, scales, and bone fragments (i.e., paleonisciforms, dipnoiforms, xenacanthiforms, petadolontiforms and labyrinthodonts; Castro et al., 2001). The hammer in A is 25 cm-long and the pencil in B is 8 cm-long.

2.4.2. Offshore-transition (FA-2)

Description

This facies association (Fig. 6) is characterized by 3 to 17 m-thick coarsening-upward successions of interbedded, dm- to m-thick tabular beds of well-sorted sandstone (**Sr**, **Sh,** and **Ss**), laminated siltstone (**Fl**), and heterolithic facies (**Hw** and **Hl**) (Figs. 6A, 6B and 6C). The **Fl**, **Hw** and **Hl** facies present moderate bioturbation index (BI = 3) and characteristically low ichnodiversity of both vertical and horizontal traces (e.g., *Planolites* and *Teichichnus*) (Fig. 6E). Thin lenses (mm-scale) of phosphatic fish fragments are commonly observed within **Fl** and **Hl** facies. Occasionally (Section 3 – Appendix I.III), lenticular beds (4 cm high x 70 cm long) of normally graded, conglomerate (**Gn**) composed of rounded to angular silicified granule-sized siltstone intraclasts may occur, presenting erosive base and wavy top (Fig. 6D). Additionally, lenticular and amalgamated shell beds are observed in the uppermost part of the Corumbataí Formation (Section 13 – Appendix I.II; described in detail by Simões et al., 1996) (Fig. 6F-G).

Abundant clastic dikes are found crosscutting the uppermost part of the Corumbataí Formation, generally confined in well-defined stratigraphic intervals (up to 10 m-thick, Section 15 – Apendix I.I), near the contact with the overlain Pirambóia Formation (see sections 15, 17 and 18 in Apendix I.I), where siltstone and fine-grained sandstone are interbedded (Fig. 6H). The dikes are single or multiple intrusive and are decimeter- to meter-scale wide, with a dominantly quartz sandstone composition. Most parts of the dikes present ptygmatic geometry and upward bifurcations.

Interpretation

This facies association is interpreted to be deposited between the fair-weather and storm wave base due to the occurrence of: (i) swaley cross-stratified sandstone (**Ss**) interbedded with fine-grained deposits (**Fm** and **Fl**); (ii) residual lag-type bioclastic concentrations and shell beds interpreted as tempestites (see Simões et al., 1996 for further discussion); and (iii) absence of mudcracks and other sedimentary structures indicative of subaerial exposure. The occurrence mud-rich heterolithic facies (**Hl** and **Hw**) are interpreted as evidence of the alternation between moments of flow and slack waters, influenced by seiche or storms. The absence of hummocky cross-stratification in the high-frequency finning-upward successions with facies deposited under upper (**Sh**) and lower flow (**Sr**) regimes, reinforces the predominance of bottom density currents from the shallowest parts of the aqueous body. In this context, the generation of these hyperpycnal flows could be related to the effect of the sloshing back of the water column by seiche, that enhance the transport of dense, sand-rich currents from shoreface to offshore-transition (Pritchard and Hogg, 2003).

The deposition of the intraclastic coarse-grained lenticular beds (facies **Gn**) also reinforces the existence of high-frequency oscillations of the water level, as this facies is interpreted to develop in two stages: (i) offshore-ward transport by strong meteorological-generated flows (e.g., seiche and storms), followed by (ii) erosion, reworking and selective sorting of bottom sediment by asymmetrical oscillatory currents by shoaling swell waves propagating onshore (Hart and Plint, 1989).

As for the shell beds (**Rb** facies), their depositional history is interpreted to represent a complex interplay between background and episodic sedimentation, including storm-induced (bellow SWB) reworking (Simões and Kowalewski, 1998).

Finally, the presence of clastic dikes in a well-defined interval at the upper part of the Corumbataí Formation is interpreted as product of the destabilization of unlithified sediments by extensional stress and passive fill of fissures by ascending sediments (Perinotto et al., 2008; Turra 2009). The ptygmatic aspect of some clastic dikes is related to the vertical compaction before sediment lithification that is, upward injection of fluidized sand followed by post-depositional compaction of soft sediment. Recently, clastic dikes and discordant soft-sediment deformation structures present in the upper part of the Corumbataí Formation were associated with seismicity produced during the mega-earthquake triggered by the Araguainha impact event (Tohver et al., 2018). However, the hypothesis that associates these structures to the seismicity produced by intraplate reactivation of continental-scale lithospheric faults (Riccomini et al., 1992) is most probable due to the presence of many intervals with clastic dykes, separated by non-deformed beds.

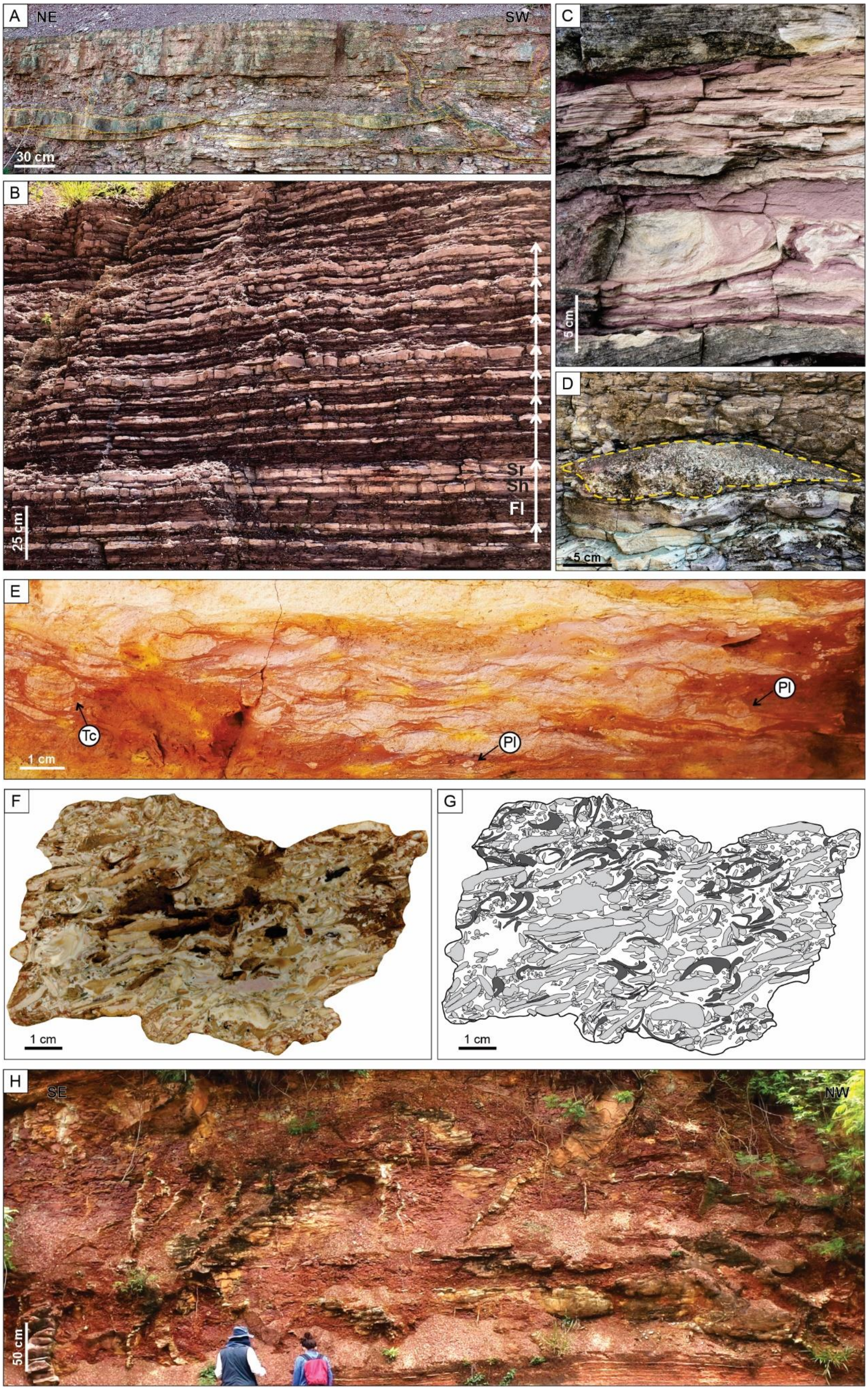
A
NE
SW
30 cm
B
Sr
Sh
Fl
25 cm
C
5 cm
D
5 cm
E
Tc
Pl
Pl
1 cm
F
1 cm
G
1 cm
H
SE
NW
50 cm

Figure 6 – Offshore-transition deposits (FA-2). (A) Swaley cross-stratification and clastic dykes (yellow dashed line) interbedded with **Fl** facies. (B) Typical coarsening-upward successions (vertical white arrows) of **Fl** grading to **Sh** and **Sr.** (C) Mud-rich heterolithic facies (**Hl** and **Hw**). (D) Lenticular bed of granule conglomerate with normal gradation (yellow dashed line). (E) Detail of the highly bioturbated heterolithic facies. Pl – *Planolites*; Tc – *Teichichnus*. (F) Polished cross-section showing the intense silicification and the distribution of clasts and shells of the Batalha shell bed (Section 8, Apendix I.II). (G) Sketch of the sample in F. The flat pebbles are shown in light gray, and the bivalve shells in dark gray. (H) Clastic dykes crosscutting **Fl** and **Sr** facies.

2.4.3. Shoreface (FA-3)

Description

This facies association is characterized by up to 10 m-thick coarsening-upward succession of interbedded tabular beds of siltstone, heterolithic facies and sandstone (Fig. 7). Heterolithic facies of dominant wavy and flaser beddings (**Hw** and **Hf,** Fig. 7A) are common in the lower part of the FA-3, displaying abundant mm- to cm-scale mudstone (Fig. 7B) or syneresis cracks (Fig. 7C) and moderate to high bioturbation index (BI: 4-5). Bioturbation is dominated by structureless vertical U-shapped and horizontal burrow and consist of sediments lithologically different from the host matrix (Figs. 7D). Thin lenses and tabular beds of **Fl** (centimeter-scale) usually occurs interbedded with **Hw**, decreasing in thickness towards the top of the facies association. The facies **Sr** dominates in the upper part of FA-3, and commonly occur as 0.1 to 3 m-thick tabular beds that are laterally continuous for tens to hundreds of meters (Fig. 7E). Millimeter to centimeter-scale mudstone drapes, presenting horizontal bioturbation (e.g., *Planolites*) and vertical U-shapped (e.g., *Arenicolites*) is commonly developed in the troughs of the ripple marks.

Dense accumulations of bivalve shell beds (**Rb**) and bioclastic sandstone (**Sb**) occur as up to 5 cm-thick lenticular beds with lateral extension of tens of meters (Fig. 7F). In these deposits, the bivalve shells are completely disarticulated and dominantly disposed in a convex-upward posture. Fragments of comminuted shells are also observed. Bioclastic fine- to medium-grained sandstone usually displays fragmented bivalve shells chaotically dispersed in the rock framework.

Interpretation

This facies association is interpreted as a low-energy setting developed in a gentle ramp above the fair-weather wave base (Schwarz and Howell, 2005). The dominant presence of symmetrical ripple cross-lamination is interpreted to be the result of the migration of wave ripple marks near the shoreline. The occurrence of mudstone in the troughs of these ripple marks suggests the existence of oscillatory flows generating periods of stillstand and settling of mud particles. In this context, the occurrence of wavy and flaser beddings suggests that during moments of increase in the water-level, mud particles settled above ripple marks in the new slack water condition. During periods of decrease in water-level, ripple marks migrated underwater, and the previously deposited mud was subjected to subaerial exposure generating mudcracks.

The taphonomic characteristics of the **Rb** and **Sb** suggest exhumation, reworking and prolonged exposure of bioclasts at the water/sediment interface, under conditions of low or intermediate sedimentation rates in a proximal environment (above the fair weather wave base) (see discussion in Simões and Torello, 2003).

Figure 7 – Shoreface facies association (FA-3). (A) Interbedded wavy and flaser beddings with fine-grained sandstone with symmetric ripples. (B) Three different beds with mudstone cracks (orange arrows) in heterolithic facies. (C) Syneresis cracks in a mudstone drape. (D) Wavy bedding with *Planolites* (Pl) and *Arenicolites* (Ar) bioturbations. (E) Sandstone with symmetric ripples covered by mud drapes. (F) Polished section of shell bed constituted by bivalves from the *Pinzonella illusa* Biozone (Section 3 – Córrego Cuiabano). The scale in A and D is 5 cm long. The hammer in D is 30 cm long.

2.4.4. Foreshore (FA-4)

Description

Although low expressive, this facies association consists of very-fine to medium grained sandstones with planar cross-stratification **(Sp)**, low-angle cross-stratification **(St)** and horizontal lamination **(Sh)** (Fig. 8A-B), with tabular geometry, thicknesses between 0.2 to 1 m, and lateral extension in the order of few meters. This interval is characterized by low (BI:1) or absence index of bioturbation.

Interpretation

This facies association is interpreted as a high-energy setting developed in a foreshore. The presence of horizontal lamination and cross-stratification (dunes migration) indicates upper-flow regime conditions. The absence of bioturbation suggest that the foreshore was a high-energy, turbulent and stressful environment that inhibited organism colonization (Maceachern and Pemberton, 1992). In a marine setting, that occurs within the intertidal section where swash and back-swash processes, associated with breaking waves (Masselink and Puleo, 2006). In the case of Corumbataí Formation, the foreshore represents the sedimentation above the lower boundary of the saline flat setting, that represents the maximum inundation by seiche and storms. The low expression of FA-4 could be explained by the reworking of the sediments by the swash and backwash of the waves.

Figure 8 – Foreshore facies association (FA-4). (A) Tabular bed of horizontally laminated sandstone (Sh). (B) General view showing foreshore facies (FA-4) overlying the shoreface facies (FA-3).

2.4.5. Saline Flat (FA-5)

Description

An up to 8 m-thick succession of interbedded laminated siltstone, sandstone, grainstone, and silicified stromatolites showing evaporitic features such as breccia, popcorn crusts, and halite hopper characterizes the FA-5 (Fig. 9). This facies association is only present in the upper part of the Corumbataí Formation. In the São Paulo State, the FA-5 is represented by 2-m-thick successions of interbedded **Wm**, **Gr** and **Ms** (Fig. 9A) that are commonly associated to microkarst and dissolution features (Fig. 9B). Microbialite facies are commonly found in the upper part of the FA-5 as silicified domal and planar stromatolites. Additionally, in the Goiás and Mato Grosso states, centimeter-scale, silicified conical stromatolites (Fig. 9C), and planar stromatolites with brecciated top were also observed. Centimeter-scale tabular beds of ostracod wackestone and rudstone are commonly associated to silicified halite hopper (Fig. 9D) and popcorn crust (Fig. 9E). Decimeter-scale successions of evaporitic paleosoil (**Pe**) interbedded with **Rd** (Fig. 9F), mudstone cracks (Fig. 9G), and teepees are also common.

Interpretation

This facies association is interpreted to have been deposited in a saline flat, based on: (i) the predominance of widespread evaporitic paleosoil indicating subaerial exposure; (ii) profusion of silicified evaporitic features such as halite hopper, breccia and popcorn crust, indicating increased salinity towards the upper part of the Corumbataí Formation, and (iii) presence of oncoids, ooids and stromatolites indicating deposition in very shallow water conditions. The formation of saline water bodies (saline pans) is suggestive of the occurrence of moments of flooding interspersed with periods of subaerial exposure of the coastal areas during stronger seiche events, reinforcing the existence of high-frequency oscillations of the water level such as observed in the shoreface facies association (FA-3). In other words, seiche and storms should influence the flooding of the area and, when these events stopped, the day-by-day is marked by the drying and formation of paleosols and evaporite crusts.The existence of a marked tendency of aridization during the end of the Permian (Lavina, 1991; Rohn, 1994; Warren et al., 2008), led to the ideal conditions for the establishment of highly evaporative conditions, concentrating brines, changing pH conditions, and providing suitable settings for the development of microbialites and others evaporitic facies.

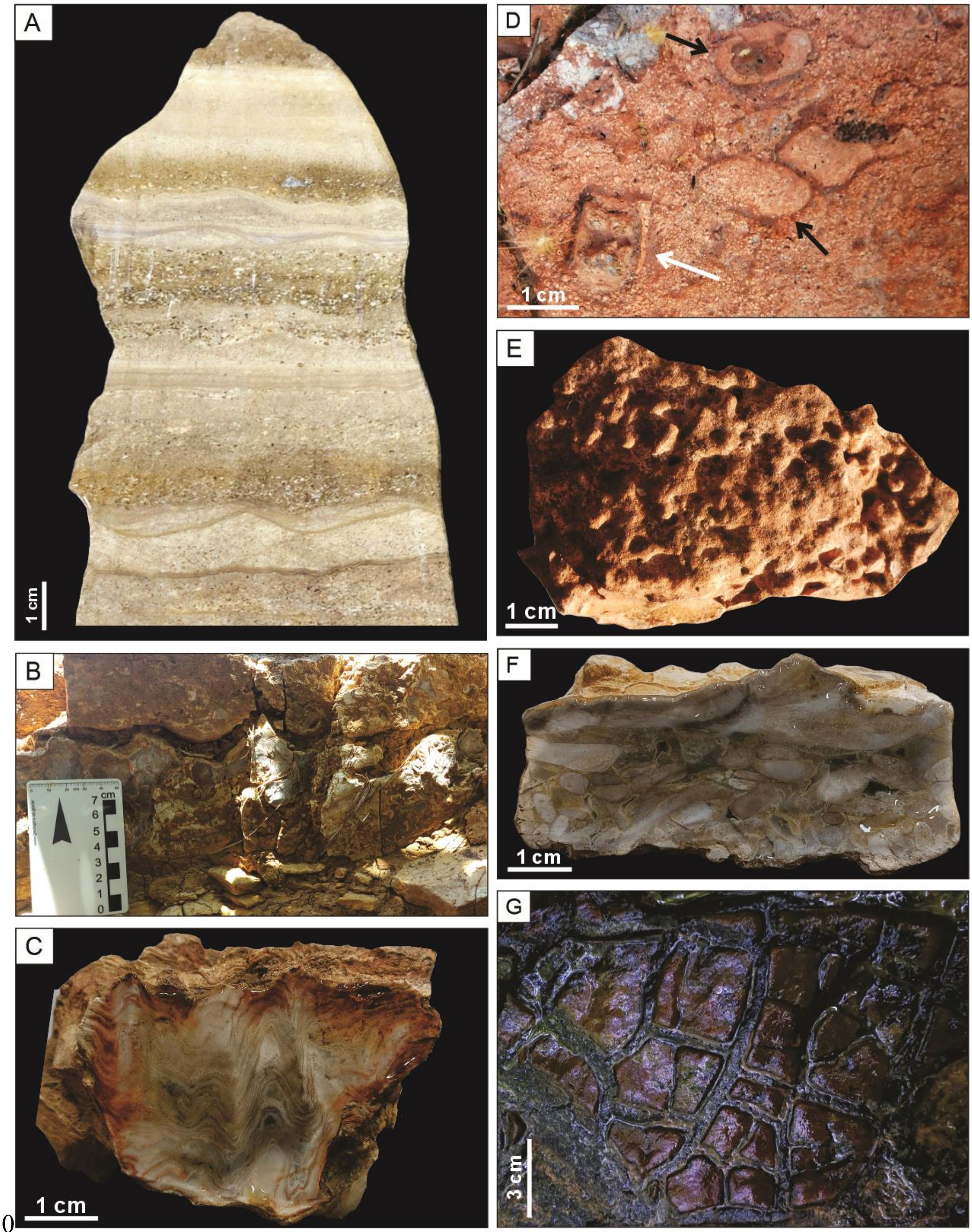

0

Figure 9 – Saline Flat facies association (FA-5) from the upper part of the Corumbataí Formation. (A) Silicified ripple cross-laminated grainstone. (B) Silicified microkarst and dissolution features. (C) Silicified conical stromatolite. (D) Grainstone with oncoids (black arrows) and halite hopper (white arrows). (E) Silicified popcorn crust. (F) Oncoid rudstone. (G) Mudcracks in silicified mudstone.

2.5. Discussion

2.5.1. Sequence Stratigraphic Framework

The studied succession encompasses a third order stratigraphic sequence (Holz et al., 2010), characterized by mixed deposition of siltstone, sandstone, heterolithic facies, carbonate and evaporite rocks in a shallow lacustrine environment (Fig. 10). The sequence is bounded at base by a paraconformity (correlative conformity) with the Irati Formation, marked by the occurrence of phosphatic bone beds (facies **Rp**, interpreted as condensation deposit), and at top by a subaerial unconformity with the Pirambóia (São Paulo State) and Botucatu (Goiás/Mato Grosso states) formations. In this context, the Serra Alta Formation corresponds to the 3rd transgressive systems tract (TST_3; see Warren et al., 2015), while the Corumbataí Formation comprises the 3rd regressive systems tract (RST_3), marked by the major inflection between the rise and fall of the accommodation curve in the upper part of the Serra Alta Formation succession (i.e., maximum flooding surface – MFS_3, as proposed by Holz et al., 2010, Fig. 10).

High-frequency sequences (4th to 6th order; sensu Catuneanu et al., 2009, 2011) were recognized based on the definition of the stacking patterns in distinct scales (Fig. 10). The 6th order sequences are organized into asymmetric progradational pattern, which are traceable across all the studied succession, while the 5th order sequences present asymmetric retrogradational and symmetrical progradational patterns. Two 4th order stratigraphic sequences are identified, comprehending transgressive (TST_{4-1} and TST_{4-2}) and regressive (RST_{4-1} and RST_{4-2}) systems tracts.

The Serra Alta Formation comprise the first transgressive system tract (TST_{4-1}), representing the transition from shoreface-offshore transition to offshore settings. The inflection of the accommodation curve point to the maximum flood surface (MFS_{4-1}) and represents the shift from a predominantly retrogradational architectural pattern (Serra Alta Formation) to a progradational one (top of the Serra Alta Formation and base of the Corumbataí Formation). The first regressive systems tract (RST_{4-1}) is characterized by the constant decrease of the accommodation curve (see Fischer Plots; Fig. 10) added to progradational stacking patterns from offshore-transition to shoreface facies associations (change of color between the dark gray siltstone from Serra Alta Formation and the reddish and bioturbated siltstone of the Corumbataí Formation, rippled sandstones, and heterolithic facies), suggesting progressively shallower and oxygenated depositional conditions (Warren et al. 2015).

The second 4th order stratigraphic sequence begin with the second 4th order transgressive systems tract (TST_{4-2}), where the accommodation curve presents a significant rise in the middle part of the Corumbataí Formation, been more pronounced in the CS-3 (Goiás/Mato Grosso states), and not visible in the CS-1 (São Paulo State). Interestingly, there is a clear dominance of proximal facies in the CS-3 and of distal facies in the CS-1 and CS-2, with a retrogradational pattern observed in all sections. Finally, a significant increase in thickness of sandstone packages and the presence of carbonate and evaporitic facies are related to the progradational architecture of the RST_{4-2}.

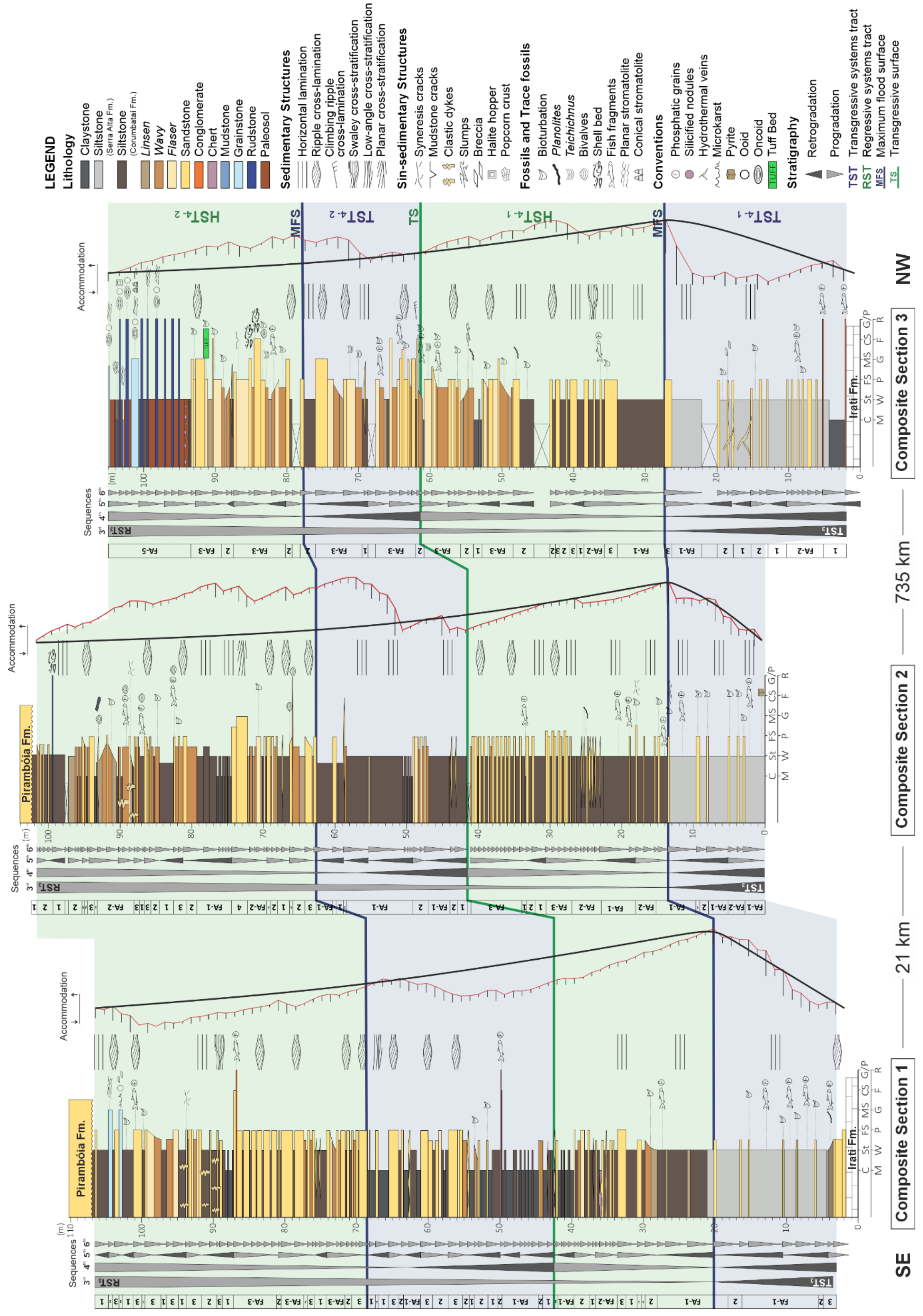

Figure 10 – Composite sections of the Corumbataí Formation along the Paraná Basin with indication of the systems tracts, facies associations and accommodation curve (Fischer Plot). The red accommodation curve refers

to 4th order stratigraphic sequence and the black line refers to 3rd order. C - Clay; St - Silt; FS - Fine Sand; MS - Medium Sand; CS - Coarse Sand; G/P – Granule/Pebble; M – Mudstone; W – Wackstone; P – Packstone; G – Grainstone; F – Floatstone; R – Rudstone; FA – Facies association.

2.5.2. Stages of megalake evolution

The long-term preservation of sediments in lacustrine basins is mainly controlled by subsidence, whereas the short-term changes in accommodation is a result of the interplay between subsidence and water balance (Caroll and Bohacs, 1999). The water balance in lakes, is more complex than in marine settings since it is a function of the relationship between water and sediment supply by rivers, incoming groundwater, evaporation, and subaerial/subsurface water outflow. Regardless the size, the maximum lake level is controlled by the lake spill point over which the lake cannot rise even during an excess of inflowing water. If the lake level has not reached the maximum level, it will operate as a closed or endorheic lake, and any difference in the water balance can result in drastic lake-level variations (Carroll and Bohacs, 1999; Bohacs et al., 2000; Carroll and Bohacs, 2001; Bohacs et al., 2003).

Additionally, in lakes and other climatically influenced/controlled depositional settings, the relative base level variation is a function between the precipitation and evaporation and directly influence the lake architecture (underfilled, balanced-fill, overfilled; Bohacs et al., 2000). If unconsolidated sediments are available in the source areas, an increase in precipitation will condition an equal increase in both water and sediment supply. Thus, if the precipitation/evaporation ratio is positive, a relative rise in the lake level will occur (humid phase). In contrast, if the precipitation/evaporation ratio decreases, the result is a relative fall of the lake level (arid phase).

In this section, we seek to approach the distinct controls of subsidence, lake-level variation and sedimentation, integrating the facies stackings in district parts of the Serra Alta and Corumbataí formations within a sequence stratigraphic framework. Data suggests that these units were deposited in an endorheic megalake that went through balanced-fill to overfilled stages, intimately associated to the transgressive and regressive systems tracts (Figs. 11, 12, 13 and 14). Although this mega lake has experienced overfilled conditions, the absence of fluvial/ deltaic facies associations even in the most marginal regions of the basin, suggests that the lake receive most of the freshwater from precipitation. Furthermore, at this time, the Paraná Basin was compartmentalized by probable structural highs (i.e., Anhembi Dome; Soares, 1991; Riccomini et al., 1992; Rostirolla et al., 2003; Etchebehere et al., 2007; Perinotto et al., 2008;

Cavallaro, 2013; Warren et al., 2015; Varejão et al., 2022), and disconnected from the global ocean. Thus, the mega lake level reflects the equilibrium point between water inflow (precipitation + groundwater, and subordinately, river discharge) and outflow (evaporation), attesting endorheic conditions for this system.

Stage 1: Freshwater ballanced-fill lake

In closed lakes, a common linkage exists between sediment supply and lake level (Schumm, 1977; Perlmutter and Matthews, 1989). The joint increase in sediment and water supply usually results in the landward migration of the coastline (lake transgression), especially in low-gradient lacustrine basins, as is the example of the Serra Alta Formation (TST_{4-1}).

The TST_{4-1} is dominated by grey silty shales cyclic interbedded with fine-grained sandstone in a dominantly offshore setting (Fig.11). During this stage, prevailed the alternation between suspension fallout and low-density turbidity currents (or hyperpicnal/bottom currents), when detrital components are punctually delivered to the deep basin (Warren et al., 2015; Zavala et al. 2022, Peng et al., 2022), as evidenced by the thin beds of sandstone and the common occurrence of condensed levels (phosphate concentrations). These hyperpycnal flows are originated and sustained by the continuous "pumping" from small fluvial systems (without generation/preservation of deltaic systems) and, depending on the duration of sedimentary discharges, they can be maintained for days, weeks, or even months (Zavala et al., 2006; Zavala, 2020).

The lake was getting increasingly deeper to the top of the succession, as evidenced by the increase in the thickness of the muddier beds, and the presence of pyrite crystals, the better preservation of organic matter and the occasional incidence of bioturbation suggest deposition under predominantly reducing conditions (anoxic to dysoxic) (Warren et al., 2015).

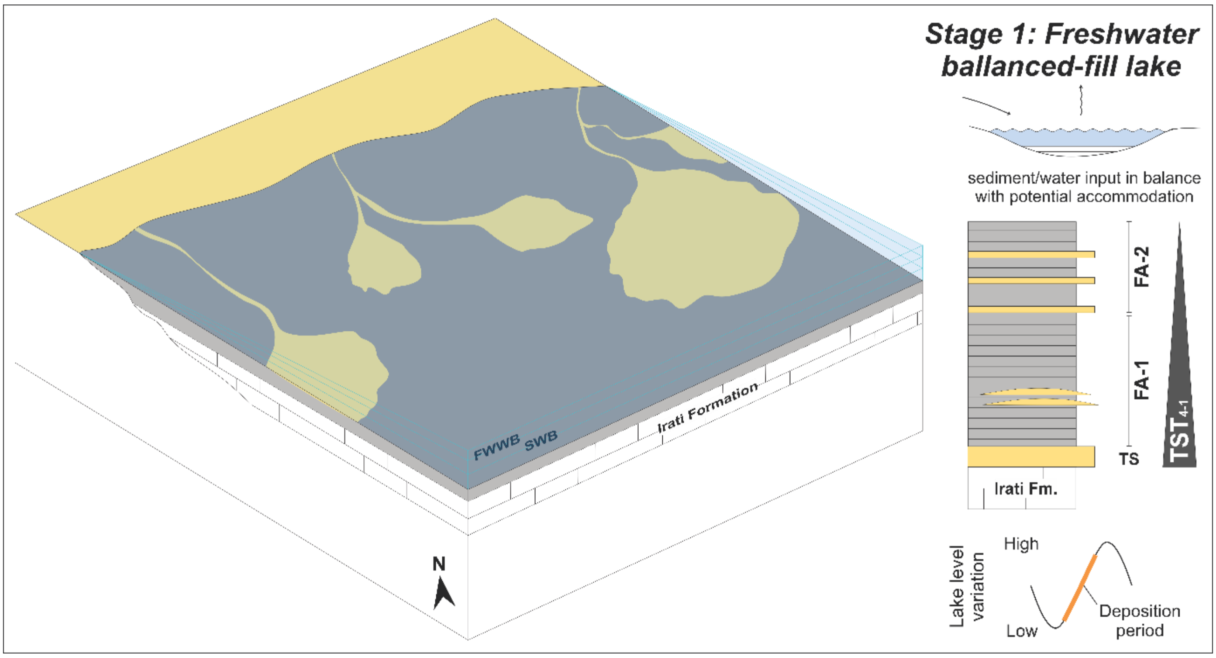

Figure 11 – Stage 1 of the Sedimentary evolution of the Corumbataí Formation. Deposition in a freshwater balanced-fill lake with relatively calm waters, only affected by episodic storm and hyperpycnal flows. The columnar section indicates the sedimentary facies succession distribution in this stage with the respective system tract (TST_{4-1}) (see Fig. 14 for legend). Explanation: TS – Transgressive Surface.

Stage 2: Freshwater overfilled lake

Once the lake achieves maximum level (i.e., maximum flooding surface), the introduction of sediment will inevitably result in the progradation of coastal system (lake regression). In this context, the relatively uniform and slow subsidence expected for extensive, low gradient shallow lakes (or intracontinental basins) (Zalán et al, 1991; Rohn et al., 1994; Milani, 1997; Xie and Heller, 2009) favored a climate-induced basinward migration of the coastline during deposition of the RST_{4-1}.

During this stage, the lake was moderately oxygenated (as indicated by the reduced bioturbation index), and presented relatively calm waters, only affected by episodic storms and seiche. Sedimentation probably occurred under a relatively humid climate (Rees et al., 1999; Spalletti et al., 2003), and a moderate sediment supply as evidenced by the facies associations and the high-frequency transgressive-regressive shallowing upward successions (Fig. 12). This resulted in deposition of offshore to shoreface-offshore transition (CS-1 and 2) and shoreface (CS-3) successions in a progradational arrange. The gradual increase in sandstone beds at this stage reinforces the reduction in water depth and accommodation fall, a consequence of the increase in sediment input.

The absence of carbonate and evaporite facies, in the Stage 2 suggests a permanent freshwater lake, probably with similar characteristics as the modern huge water bodies such as Caspian or Black seas (Hinds et al., 2004; Boomer et al., 2005; Abdullayey et al., 2012).

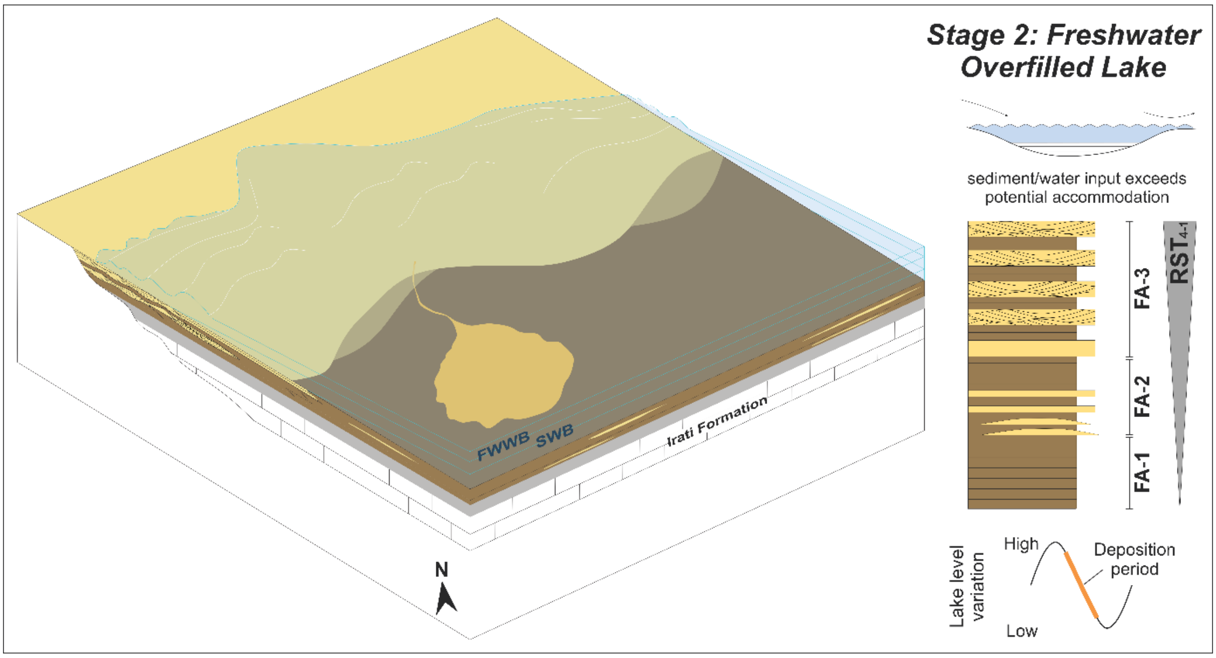

Figure 12 - Stage 2 of the sedimentary evolution of the Corumbataí Formation. The lake level variations promoted the deposition in freshwater overfilled lake dominated by waves and currents, with intercalation of shoreface to offshore -transitions facies associations. The columnar section indicates the sedimentary facies succession distribution in this stage with the respective system tract (RST_{4-1}) (see Fig. 14 for legend).

Stage 3: Brackish water balanced-fill lake

During the deposition of the TST_{4-2}, a positive water balance (precipitation) allowed the rise of the lake level to rise accommodation, resulting in the landward migration of the system and the deposition of offshore-transition deposits over the shoreface facies from RST_{4-1} (Fig. 13). Nonetheless, the sediment supply to the basin contributed again to the transgression of the coastal systems. The wet-dry climatic cycles probably influenced the lake-level and the deposition of the succession by controlling the relationship between evaporation and precipitation, also changing the sediment supply by affecting the denudation. Thus, wet-cycles often result in rising lake-level and increasing sediment supply, in contrast to dry-cycles (Wang et al., 2009; Sztanó et al., 2013; Gong et al., 2019; Zhang et al., 2020).

The commonly bioturbed heterolithic facies observed in the CS-3 suggest great oxygenation and availability of substrate nutrients allowing the proliferation of benthic organisms. The *Teichichnus* assemblage, forming monospecific suites or associated with

Planolites, is common in restricted and heterolithic facies with synaeresis and/or mudstone cracks, pointing to the brackish water (Buatois et al., 2005) character of the Stage 3.

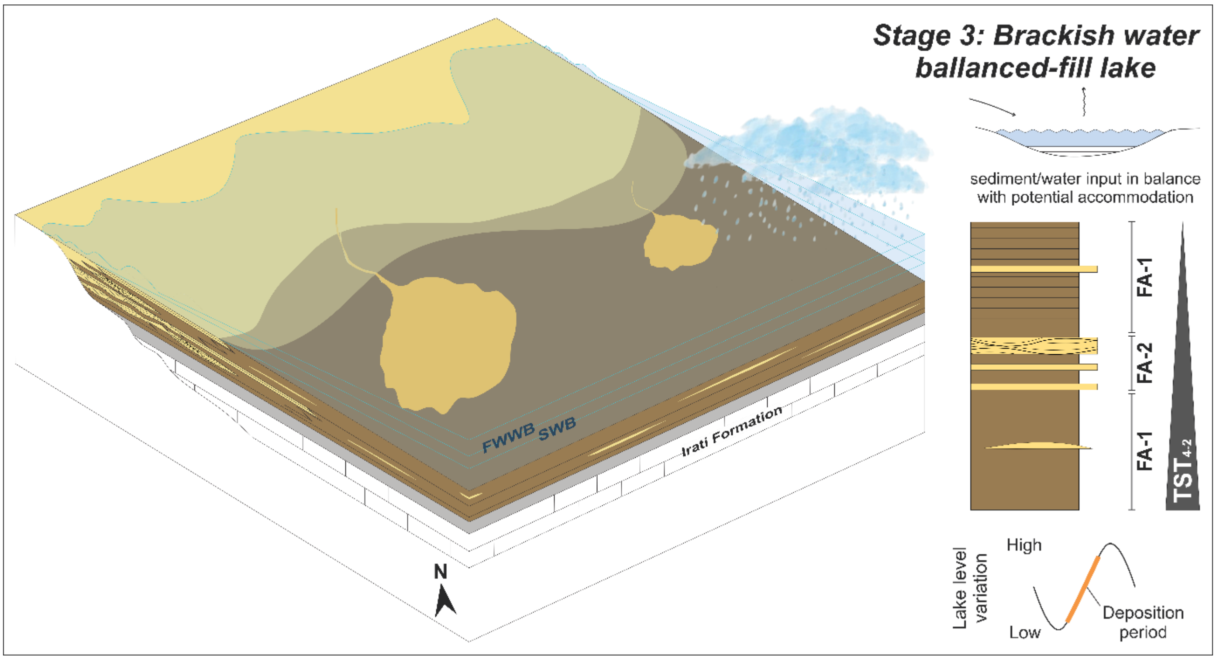

Figure 13 - Stage 3 of the sedimentary evolution of the Corumbataí Formation. The positive water balance (precipitation) allowed the landward migration of the system and the deposition of offshore-transition deposits over the shoreface facies associations, in a brackish water balanced-fill lake. The columnar section indicates the sedimentary facies succession distribution in this stage with the respective system tract (TST_{4-2}) (see Fig. 14 for legend).

Stage 4: Saline overfilled lake

During this stage, the Corumbataí Formation was characterized by the progressive intensification of arid climate and a relatively shallow water level conditions (Fig. 14). The progradational (RST_{4-2}) tendency is evidenced by the marked decrease of accommodation (see Fig. 10) and the presence of evaporite deposits (saline flat facies association – FA-5), in the upper part of the succession. Sandier and heterolithic facies dominate in this part of the lake evolution and attest the advancement of proximal systems. At this time, the shallower water conditions of the megalake evolution allowed the intensification of the day-by-day seiche actuation in the deposition of the heterolithic facies and substrate oxidation (higher bioturbation index), very similar to the depositional conditions of the astronomical tidal flat.

In the final progradational phase, the relatively lower siliciclastic input, and the hydrological deficit due to increase evaporation rates in the endorheic basin led to the increase of alkalinity, favoring carbonate precipitation. During this interval, the progressive clogging of the aquatic body formed small and isolated ponds in marginal areas, prone to high evaporation rates and consequently high salinity, supporting sedimentation of carbonate mud, increase in stressful ecological conditions, proliferation of biomats and formation of microbialites (Fig. 14), formation of evaporitic deposits and expressive subaerial exposure of marginal areas (as indicated by the presence of paleosoils and brecciated beds). The most intense seiche could also be responsible for the temporary flooding of dry areas (storm surges and other strong metereological events, that make it possible the flood of the "backshore" region) originating isolated ponds and reworking sediments by waves and currents, occasionally transporting them to deeper parts of the basin.

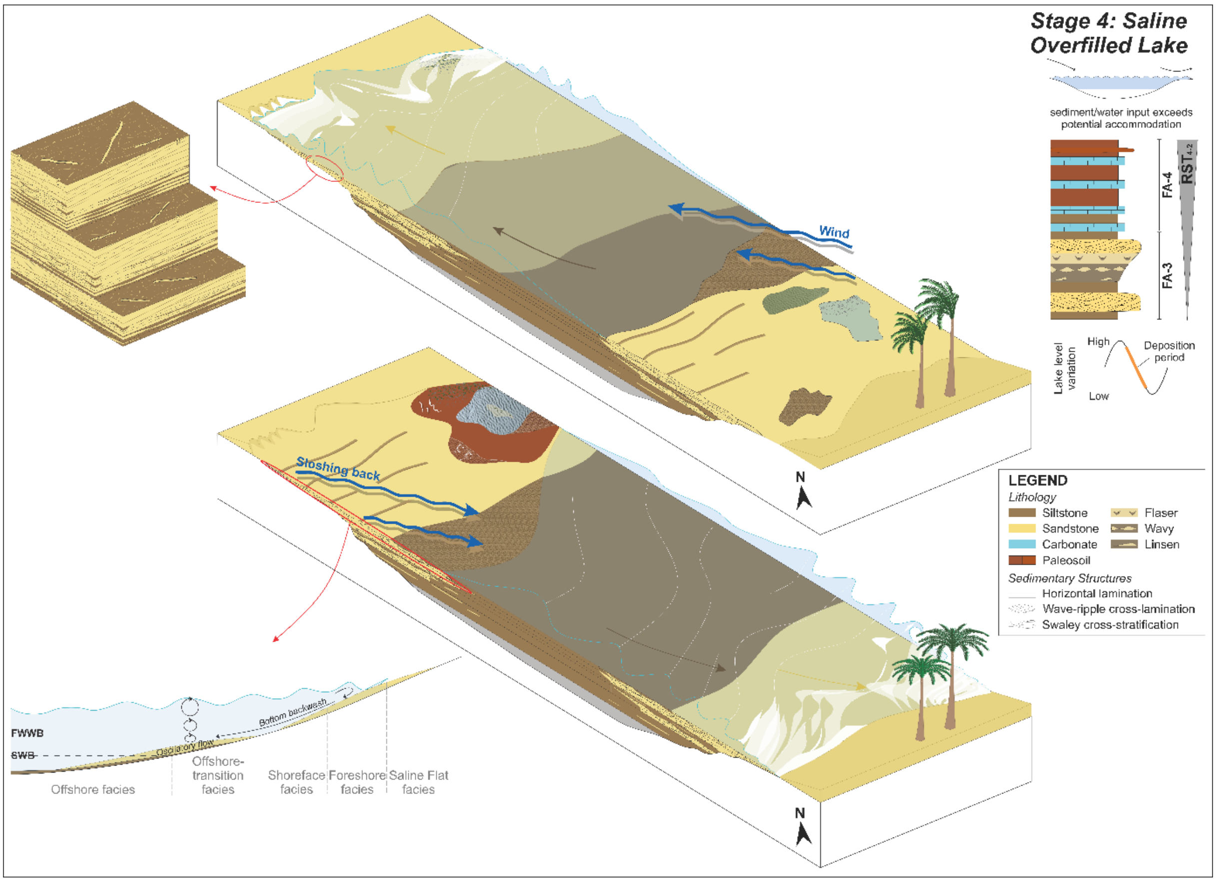

Figure 14 – Stage 4 of the sedimentary evolution of the Corumbataí Formation. The intensification of the arid climate promoted the fall of the lake level and the deposition in a saline overfilled lake under the influence of seiche. Note the movement of the water column that flood/exposure large marginal areas, as well as transport the sediments from distal (deeper) to proximal (shallower) areas. The area in reddish color refers to the evaporitic and carbonate facies described in the states of Goiás and Mato Grosso (northern part of the studied area). The block diagram shows a detail of the heterolithic facies grading to rippled sandstone with bioturbation and mudstone cracks formed by the alternation of floods and exposure caused by seiche. The columnar section indicates the sedimentary facies succession distribution in the stage with the respective system tract (TST_{4-2}).

2.5.2. Controls on the sedimentary dynamic

Allogenic processes are related to external controls in the sedimentation that acted in the entire basin such as tectonics and climate (Beerbower, 1964; Cecil et al., 2011). On the other hand, autogenic processes will result in high-frequency changes in the depositional conditions associated with the internal dynamics of the sedimentary system (e.g., carbonate factory, seiche, storms, internal sediment redistribution, channel avulsions) (Beerbower, 1964; Cecil et al., 2011). From this perspective, it is a hard task to differentiate autogenic and allogenic controls in the sedimentary record since lateral facies variations, changes in bed thickness and punctual differences in cycles/parasequences are expected.

Allogenic processes

Over the evolution of the Paraná Basin, the subsidence seems to have been related to the tectonic regimes established on the Gondwana margin, with periods of low depositional rate followed by long erosive intervals (Assine et al., 1994; Milani, 1997). However, climate changes have been described as an important mechanism for the origin of most cyclicity observed at the outcrop scale (Wu et al., 2013; Hilgen et al., 2015).

During most of the Phanerozoic, the southern region of the Gondwana was tectonically active under a compressive stress regime between the cratonic part of the supercontinent and the Panthalassic oceanic crust (Coira et al., 1982; Milani and Ramos, 1998). In this scenario, the Patagonia figured as an allochthonous microcontinent (Ramos et al., 1984; 1986; 2008) that was amalgamated with the supercontinent during the late Permian Sanrafelic Orogeny (Ramos, 1988; Ramos, 2008). The collision, deformation and subsequent uplift of a high-altitude cordillera (i.e., Gondwanides Belt, Keidel, 1916) caused the isolation of the Paraná and Karoo basins from the Panthalassic Ocean (Warren et al., 2008; Holz et al., 2010) forming a continental-scale megalake, which has been exposed to progressive continentalization and aridization (Milani et al., 2007; Limarino et al., 2013).

Characterized by a long-term transition from icehouse to extreme greenhouse-hothouse conditions, the late Paleozoic paleoclimatic evolution was a unique period in Earth's history (Gastaldo et al., 1996; Spalletti and Limarino, 2017). During the Guadalupian and the beginning of the Lopingian, when the Paraná and Karoo basins were already isolated from the Panthalassic Ocean (Runnegar and Newell, 1971; Maranhão and Petri, 1996; Simões et al., 1998; Ghilardi and Simões 2002; Simões et al., 2012), the climate in the SW Gondwana was probably warm temperate (Rees et al., 1999). At the end of the Permian, subtropical regions extended into higher latitudes, resulting in the disappearance of cool temperate and polar regions, followed by increasingly drier conditions, and ultimately arid climate (Spalletti et al., 2003) (Fig. 15). This progressive aridification was accompanied by the establishment of the long-lived continental Choiyoi Magmatism in southwestern Gondwana (Spalletti and Limarino, 2017), coinciding with the eruption of the continental flood basalts of the Siberian Traps and the most important mass extinction in the Phanerozoic Geological Record (Renne et al., 1995; Kamo et al., 2003; Wignall, 2001; Benton, 2003; Benton and Twitchett, 2003; Sauders and Reichow, 2009; Shen et al., 2011; Chen and Benton, 2012).

The absence of significant basin slope, added to the reduced water depth of this Permian megalake system, restricted the generation of accommodation (Lindsay et al., 1993) and conditioned the progressive basin filling by sediment coming from eroded continental areas (Warren et al., 2008). The combination of low depositional rates (Sloss, 1996), and reduced bathymetry, also caused pronounced variations in the relative base level producing flooding or subaerial exposure of huge marginal areas (Lavina, 1991).

The 3rd order stratigraphic sequence that comprehends the Serra Alta and Corumbataí formations was deposited entirely during the last efforts related to the subsidence pulse associated with the Sanrafaelic Orogeny (Milani and Ramos, 1998; Ramos, 2008) (Fig. 15). The end of the Sanrafelic Orogeny at the late Guadalupian, led to the isostatic readjustment of the crust (Ramos, 2008) and a general decrease in the intracontinental subsidence.

The presence of clastic dykes in the last 4th order RST ($RST_{4\text{-}2}$) is interpreted as related to the reactivation of lithospheric faults associated with seismic activity during the deposition of the Teresina/Corumbataí Formation (paleo-earthquakes with estimated magnitudes >6ML, Riccomini et al., 1992; Perinotto et al., 2008; Turra, 2009; Warren et al., 2015; Matos et al., 2017). At this time, the Tietê Lineament and related discontinuities were active resulting in uplifting of structural highs (i.e., Anhembi Dome; Soares, 1991; Riccomini et al., 1992; Rostirolla et al., 2003; Etchebehere et al., 2007; Perinotto et al., 2008; Cavallaro, 2013) and also produced a series of soft-sediment deformation structures, such as syn-sedimentary faults, sand volcanoes, breccias, thixotropic wedges and hydrothermal exudation recorded in these units (Riccomini et al., 1992; Perinotto et al., 2008; Turra, 2009; Warren et al., 2015; Matos et al., 2017; Varejão et al., 2021). However, it is interesting that this tectonic reactivation did not produce major changes in basin accommodation tendency. A small increase in the curve is only noted in CS-1 (geographically closer to the structural high) just above the interval with clastic dykes. Since the architectural pattern indicative of increase in accommodation is not observed in the others study area (Fig. 10), it is plausible that the intense seismicity may be related to the local generation of accommodation only in the ENE part of the Paraná Basin, in a less distant area from the compressive margin of Gondwana (Ramos et al., 1986; 1998; 2008).

Despite local variations, the widespread reduction in the generation of accommodation in the late Permian resulted in a progradational cycle of the Paraná Basin materialized by the almost entire succession of the Corumbataí Formation (Fig. 10). The decrease in the water supply, related to a more arid climate condition (Rees et al., 1999; Spalletti et al., 2003; Spalletti and Limarino, 2017), maximize the regression of the megalake margins and the basin-scale progradation. This culminated with the deposition of the shallow coastal lacustrine environments with subaerial exposure and saline and carbonate deposition. Considering the vast extent of megalake, the marked presence of evaporites at the upper part of the Corumbataí Formation in the northern sections (Goiás and Mato Grosso states) and shallow coastal deposits in southern sections (São Paulo State) is probably related to different paleoclimate zones at the time of deposition (Rees et al., 1999).

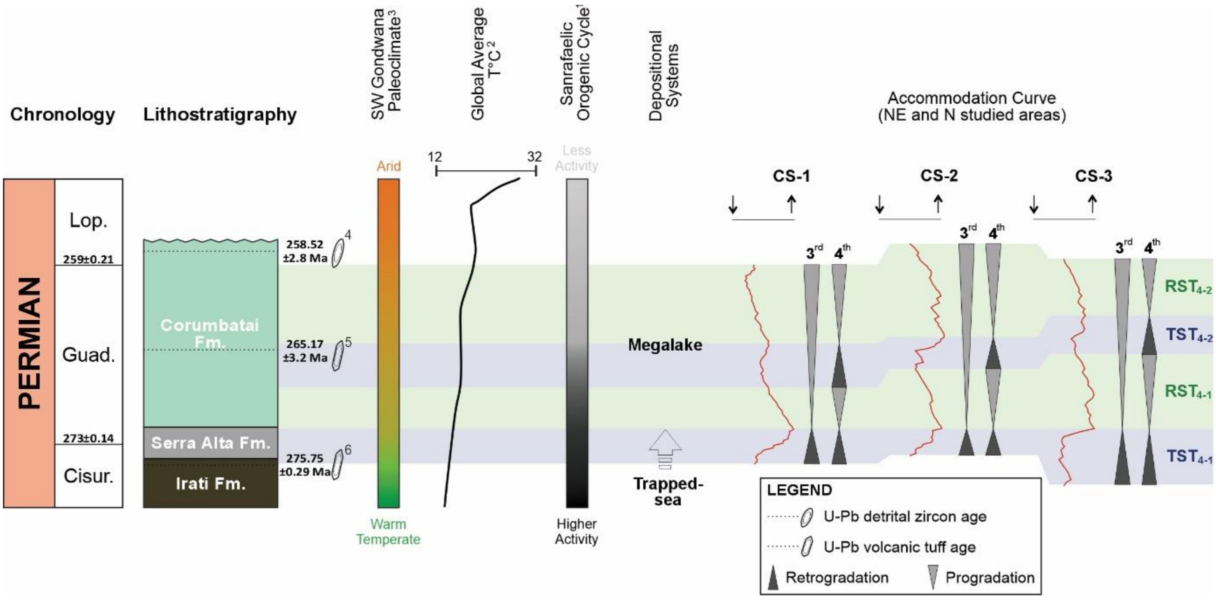

Figure 15 - Tectonic and climatic controls during the deposition of the Permian succession of the Paraná Basin, correlated with the depositional systems evolution in Paraná Basin and accommodation curve obtained for the Corumbataí Formation (this work). U-Pb ages of detrital zircons according to Tohver et al. (2018); Volcanic tuff ages for the Irati Formation according to Cagliari et al. (2022); Ages of volcanic tuff for the Corumbataí Formation according to Christofoletti et al. (2023). 1 – Ramos (2008); 2 – Scotese et al. (2021); 3 – Rees et al. (1999) and Spalletti et al. (2003). CS-1 - Composite section 1; CS-2 - Composite section 2; CS-3 - Composite section 3, shown in Fig. 10; Fm. - Formation; Lop. - Lopingian; Guad. - Guadalupian; Cisur. - Cisuralian.

Autogenic processes

High-frequency changes in the depositional conditions are mainly associated with the internal dynamics of each sedimentary system (Cecil et al., 2011). Thus, in geographically close sections and outcrops it is expected that lateral variations would be much more controlled by autogenic (local) factors than allogenic (regional) variations. Similarly, the effects of the autogenic control are more perceptible in high-resolution sequences (Zecchin, 2007; Catuneanu and Zecchin, 2013). Separating the autogenic from the allogenic signal is a difficult task, by but this can be tentatively made through curves of corrected accumulative thickness of coarsening-upward successions representing increases and decreases in accommodation (Sadler et al., 1993; Ocakoğlu et al., 2012; Muniz et al., 2015; Yang et al., 2018, among others).

These local depositional conditions in Corumbataí Formation can be illustrated by: (i) the absence of lateral correlation of foreshore facies (FA-4). The low preservation potential could be explained by the dinamic of erosion/deposition promoted by the waves (see Fig. 14); (ii) the formation of saline flats at the top of the CS-1, which is very close to offshore-transition facies, reflecting large local changes in sedimentation/accomodation; (iii) the casual existence of shell beds are interpreted as a tsunamite deposit (Batalha Secction; Rodrigues, 2024) differing of other bioclastic-rich concentrations of the Corumbataí Formation that are proximal or distal tempestites (Simões et al., 1996, 1998); (iv) hyperpycnal flows that transport different amounts of sand to the offshore region.

2.5.4. Recognizing seiche in the Permian Corumbatai megalake

Several facies such as heterolithic beds, sigmoidal stratification recovered by mud drapes, herringbone cross-stratification (Nio and Yang, 1989), as well as desiccation cracks (DeVries Klein, 1985), and mud-sand pairs (Dalrymple, 2010a), were tentatively interpreted as diagnostic criteria to define tidally influenced environments. However, despite most of these deposits can be directly related to astronomical forcing (Visser, 1980; Nio et al., 1981), they also have been frequently described in both modern and ancient environments without influence of astronomic tides (Table 3). Thus, a key implication of this is that the classic "tidally" produced sedimentary structures recognized in ancient rock successions should not automatically be attributed to astronomical or marine tidal currents, since meteorological processes (e.g., seiche) in continental environments can generate similar structures.

Table 3 - Synthesis of the occurrence of some sedimentary criteria frequently related to tidal or lacustrine environments and their relationship with the depositional model proposed for the Corumbataí Formation. 1 - Ichaso

and Dalrymple (2009); 2 - Ainsworth et al. (2012); 3 – Dalrymple (1992); 4- Renaut and Gierlowski-Kordesch (2010); 5 – Garzanti (1991); 6 - Andeskie et al., 2018; 7 – Plummer and Gostin (1981); 8 -Flemming et al. (1992); 9 – Longhitano (2011); 10 – Oliveira et al. (2019); 11 – Olivito and Souza (2020); 12 – Wright (1984); 13 – Platt and Wright (1991).

Properties (sedimentological criteria)	Depositional Settings		
	Tidal	Lake	Corumbataí Formation (this work)
Fluid mud	X[1]	X[1]	X
Sandy bundles with mud drapes	X[3]	X[2]	
Rhythmite	X[4]	X[4]	X
Heterolithic bedding	X[4]	X[2]	X
Heterolithic bedding with reduced bioturbation	X[4]		
Rip-up clasts	X[5]	X[6]	X
Mudstone cracks	X[7]	X[7]	X
Subaqueous sedimentary cracks	X[7]	X[7]	X
Bioclastic lags	X[8, 9]	X[10, 11]	X
Finning upward cycles	X[4]		
Coarsening upward cycles			X
Evaporitic facies	X[12]	X[13]	X

During a seiche event, the water level variations can occur in different temporal and spatial scales as a response to changes in the water depth, air pressure and surface wind (or other external forces such as storms). For example, in some of the Great Canadian Lakes and other large water bodies, the period between the "high" and "low" seiche can be as much as four to seven hours, which is very similar to the period between a high and low tide in open oceans (NOAA; Dalrymple, 2010a; Ainsworth et al., 2012). The oscillations at the resonance frequencies in Azov Sea (Ukraine and Russian Federation), corresponding to one-, two, three-, four-, and five-node seiches and are characterized by periods of 38.4, 23.7, 12.1, 8.8, and 5.1h, respectively (Matishov and Inzhebeikin, 2009). In the Caspian Sea, resonance frequencies also vary in function to one, two, three, four, five, and six-node seiches, with respective periods of 13.9, 9.5, 6.1, 4.7, 3.6, and 3h (Medvedev et al., 2019). The Table 4 summarizes the day-by-day variations in water level range triggered by seiche in different enclosed or semi-enclosed basins. Special attention is given to storm season in the Caspian Sea, when significant land areas (ca. 50 km) are inundated, and vast coastal shallow areas (ca. 15 km) are dried during negative surges (Medvedev et al., 2019).

Table 4 – Day-by-day and punctual storm variations in water level triggered by seiches in different enclosed or semi-enclosed basins.

Location	Water level variation (m)	Author
Lake Erie	0.3 – 0.9 m (normal daily range), and 3 – 6 m during storms	Trebitz, 2006; NOAA; NOS
Lake Huron	0.2 – 0.5 m (normal daily range)	Trebitz, 2006
Lake Michigan	0.1 – 0.4 m (normal daily range)	Trebitz, 2006
Lake Ontario	0.05 – 0.2 m (normal daily range)	Trebitz, 2006
Lake Superior	0.1 – 0.3 m (normal daily range)	Trebitz, 2006
Caspian Sea	~0.7 m (normal daily range), and 3 – 4.5 m during storms	Medvedev et al., 2019
Azov Sea	0.1 – 0.7 m (normal daily range)	Matishov & Inzhebeikin, 2009
Venice	0.05 – 0.21 m (normal daily range), and 0.4 m during storms	Ferrarin et al., 2022

The seiches, as well as the astronomical tides, produce the alternation of tractive flows with periods of calm waters, which favor sedimentation of interbedded sand and silt (or heterolithic facies). Thus, it is plausible that this oscillatory phenomenon has a proved sedimentation potential (Bloesch, 1995; Shteinman et al., 1997; Chapon et al., 1999; Pritchard and Hogg, 2003), similar to astronomical tides (Ainsworth et al., 2012) and is capable of originating heterolithic facies and sand-mud pairs as observed in the example of the Permian Corumbataí Formation. The exposure/flooding of large coastal areas provide the ideal conditions for the formation of mudstone cracks and the development of pans and paleosoil, as observed in Stage 4 of the evolution of the Permian megalake here discussed (Fig. 14). In fact, wind-generated waves can also produce a similar scenario in reduced bathymetry, however the exposure/flooding of large coastal areas during, and after, storms seem to be significantly smaller than during seiche.

Another characteristics of the sediment transport and deposition related to seiche include: (i) when the flow (wind/seiche) is parallel to a basin axis, the sediment is transported exclusively from the more distal zones to shallower parts of the basin (Pritchard and Hogg, 2003); (ii) when the flow is radial, the deposition in the center of the basin is reduced and dominated by settling of mud, while there is an increase in the coastal deposition and the erosion of the intermediate part between the distal and coastal zones (Pritchard and Hogg, 2003); (iii) the of erosion and deposition processes are strongly influenced by the grain size of the sediment, which controls the time taken for the suspended sediment concentration to respond to changes in the fluid velocity. This offers the possibility of seiching as a mechanism to explain the segregation of different types of sediment (Pritchard and Hogg, 2003), and (iv) seiches may produce important changes in fine-sand bed forms significantly increasing the sedimentation rate (centimeters per hour; Pritchard and Hogg, 2003). These facts can explain the transport of the silt fraction sediments of the distal to proximal areas during the seiche event, that forming the heterolithic facies. The increase of the sand fraction matches perfectly with what was observed in the Corumbataí formation: heterolithic facies exhibit an increase in the sand/silt ratio (linsen, wavy, flaser, in that order) and the coarsening-upward cycles culminated in wave-rippled sandstone with mud drapes.

Since the 1970s, the depositional environment of the Corumabatái Formation has been attributed to tidal flats based on the presence of heterolithic and wave-rippled sandstone with mudstone cracks. However, the Permian geographical isolation between the Corumbataí megalake and the Panthalassic Ocean, reaffirmed by the fossil content (Mendes, 1952; Beurlen, 1954; 1957; Runnegar and Newell, 1971; Rohn, 1994; Maranhão and Petri, 1996; Simões et al., 1998; Ghilardi and Simões, 2002; Simões et al., 2012; Warren et al., 2015), would make the influence of astronomical tides impossible. Thus, all the sedimentary structures and bedding characteristics present in the Corumbataí Formation, and listed in the Table 3, are suggestive of a tidal response, except that the dominant tide is of meteorological and not astronomical origin.

Thus, in large and shallow lakes, as the Permian Corumbataí megalake, the most important internal dynamics that controls the sedimentation are waves, currents and seiches (Imboden, 2004), being tidal effects negligible even in large water bodies (Renaut and Gierlowski-Kordesch, 2010). Waves tend to move sand-grained sediment along the shoreline and transport fine sediment offshore by processes analogous to those that acted along marine shorelines (Renaut and Gierlowski-Kordesch, 2010) (Fig. 12). As in the modern oceans, geostrophic effects also deflected water currents in large lakes – to the right in the North hemisphere and to the left in the South (Renaut and Gierlowski-Kordesch, 2010) – which can induce circulation, upwelling, and underflows that redistribute the sediment. Seiche was responsible to coastal water-level variations and produced the sedimentation of heterolithic facies, which were covered by exposure deposits such as mudstone with mud cracks. Thus, during events of pronounced oscillation of the water level by the seiche (i.e., storm surges), extensive coastal plains would be alternately flooded, receiving sediment in the sand fraction, or exposed, providing the formation of cracked surfaces with the water retreat (Fig. 14). During periods of calm waters, that is, without the action of strong winds capable of promote large variations in the amplitude of the seiche (day-by-day variations), silt and sand sedimentation would be possible (Fig. 14).

2.6. Conclusion

A new depositional model for the sedimentary evolution of the Permian Corumbataí Formation, Paraná Basin, is proposed based on sedimentological, stratigraphic and ichnological data. According to the gathered data, the depositional sequence encompassing this unit records five facies associations: offshore (FA-1), offshore-transition (FA-2), shoreface (FA-3), foreshore (FA-4) linked to siliciclastic-dominated deposits, while carbonate-dominated successions record deposition in a saline flat (FA-5). The Fischer diagrams indicated architectural trends, provide the accommodation curves of the studied succession and contributed to the correlation of geographically distant sections. These data were integrated to provide an overall stratigraphic framework, and four 4^{th} order systems tracts were recognized (TST_{4-1}; RST_{4-1}; TST_{4-2} and RST_{4-2}), indicating a high-frequency variation in the accommodation of the basin. The autogenic processes associated with combined climatic, tectonic and eustatic variations (allogenic factors) resulted in the deposition in a megalake that evolved from balanced-fill to overfilled stages, fluctuating between freshwater to brackish/saline conditions.

Thus, the Corumbataí Formation presents a typical shallowing-upward pattern and constitutes a wave-dominated shallow lacustrine system strongly affected by meteorological phenomena. In an enclosed basin, not influenced by meso or macro-tides, the deposition by storms or seiche events are likely and could explain the presence of heterolithic facies in shoreface to offshore-transition settings, since water mass movements produced by seiche in coastal plains, of an enclosed or semi enclosed water body, is like astronomic tides. The presence of the coastal saline pan towards the top of the unit attests the regressive pattern of the succession and a progressive aridization during the Late Permian, culminating in the desiccation of this megalake in the SW Gondwana and complete continentalization of the Paraná Basin.

Acknowledgements

We would like to thank the Msc. Paloma Promenzio for assistance during the field activities. B. Christofoletti is a fellow of the master's scholarship of the Training of Human Resources in Petroleum Geology Program - UNESP - PRH 40-ANP, supported with financial investment of oil companies qualified in the P, D&I Clause of ANP Resolution N° 50/2015. Lucas V. Warren, Marcello G. Simões and Mario L. Assine are research fellows of the CNPq.

2.7. References

Ainsworth, R.B., Hasiotis, S.T., Amos, K.J., Krapf, C.B.E., Payenberg, T.H.D., Sandstrom, M.L., Vakarelov, B.K. and Lang, S.C. (2012) Tidal signatures in an intracratonic playa lake. *Geology*, 40, 607–610.

Abdullayev, N.R., Riley, G.W. and Bowman, A.P. (2012) Regional controls on lacustrine sandstone reservoirs: the Pliocene of the South Caspian basin. In: O.W. Baganz, Y. Bartov, K. Bohacs, D. Nummedal (Eds.), Lacustrine Sandstone Reservoirs and Hydrocarbon Systems. *American Association of Petroleum Geologists*, 71-98.

Andeskie, A.S., Benison, K.C., Eichenlaub, L.A., Raine, R. (2018) Acid-saline-lake Systems of the Triassic Mercia Mudstone Group, County Antrim, Northern Ireland. *Journal of Sedimentary Research*, 88, 385–398.

Assine, M.L., Soares, P.C. and Milani, E.J. (1994) Sequências tectono-sedimentares mesopaleozóicas da Bacia do Paraná, Sul do Brasil. Revista Brasileira de Geociências, 24:77-89.

Barbosa, O. and Gomes, F.A. (1958) Pesquisa de petróleo da bacia do Rio Corumbataí, Estado de São Paulo. *Boletim DNPM*, 171, 40p.

Bastos, L.P.H., Rodrigues, R., Pereira, E., Bergamaschi, S., Alferes, C.L.F., Augland, L.E., Domeier, M., Planke, S. and Svensen, H.H. (2021) The birth and demise of the vast epicontinental Permian Irati-Whitehill Sea: evidence from organic geochemistry, geochronology, and paleogeography. *Palaeogeogr. Palaeoclimatol. Palaeoecol*., 562, Article 110103.

Beerbower, J.R. (1964) Cyclothems and cyclic depositional mechanisms in alluvial plain sedimentation. *Kansas State Geol. Surv. Bull.,* 169, 32–42.

Benton, M.J. (2003) When Life Nearly Died. The Greatest Mass Extinction of All Time. Thames & Hudson, London, 336 p.

Benton, M.J. and Twitchett, R.J. (2003) How to kill (almost) all life: the end-Permian extinction event. *Trends in Ecology & Evolution*, 18, 358-365.

Beurlen, K. (1954) As faunas de lamelibrânquios do Sistema Gonduânico no Paraná. In: *Volume Comemorativo do 1° Centenário do Estado do Paraná* (ed. F.W. Lange), Curitiba, pp. 107–136.

Beurlen, K. (1955) As formações Gondwânicas do sul do Estado do Paraná. *Boletim da Divisão de Geologia e Mineralogia*, 153, 52 p.

Bloesch, J. (1995) Mechanisms, measurement and importance of sediment resuspension in lakes. *Marine and Freshwater Research,* 46, 295 – 304.

Bohacs, K.M. (1999) Sequence stratigraphy of lake basins; unraveling the influence of climate and tectonics. *American Association of Petroleum Geologists Bulletin*, 83, p. 1878.

Bohacs, K.M., Carroll, A.R., Neal, J.E. and Mankiewicz, P.J. (2000) Lake basin type, source potential, and hydrocarbon character: an integrated sequence-stratigraphic-geochemical framework. In: *Lake Basins through Space and Time* (Eds. E.H. Gierlowski-Kordesch, K.R. Kelts). *AAPG Studies in Geology*, 46, 3-33.

Bohacs, K.M., Carroll, A.R. and Neal, J.E. (2000a) Lessons from large lake systems—Thresholds, nonlinearity, and strange attractors. *Geological Society of America Abstracts with Programs*, 32, p. A-312.

Bohacs, K.M., Neal, J.E., Carroll, A.R. and Reynolds. D.J. (2000c) Lakes are not small oceans! Sequence stratigraphy in lacustrine basins. *American Association of Petroleum Geologists Annual Meeting Expanded Abstracts*, 9, p. 14.

Bohacs, K.M., Carroll, A.R. and Neal, J.E. (2003) Lessons from large lake systems-thresholds, nonlinearity, and strange attractors. *Special Papers-Geological Society of America*, 75-90.

Boomer, I., von Grafenstein, U., Guichard, F. and Bieda, S. (2005) Modern and Holocene sublittoral ostracod assemblages (Crustacea) from the Caspian Sea: a unique brackish, deep-water environment. *Palaeogeography, Palaeoclimatology, Palaeoecology*, 225, 173-186.

Brito, A.S., Nogueira, A.C.R., de Almeida, L.T.G. and de Lima, S.G. (2023) Orbital-scale cyclicity and organic matter production in a Permian shallow mixed carbonate-siliciclastic system: Paraná Basin, Brazil. *Marine and Petroleum Geology*, 147, 105987.

Buatois, L.A. and Mángano, M.G. (1995) The paleoenvironmental and paleoecological significance of the lacustrine Mermia ichnofacies: an archetypical subaqueous nonmarine trace fossil assemblage. *Ichnos: An International Journal of Plant & Animal*, 4, 151-161.

Buatois, L.A. and Mángano, M.G. (1998). Trace fossil analysis of lacustrine facies and basins. *Palaeogeography, Palaeoclimatology, Palaeoecology,* 140, 367–382.

Buatois, L.A. and Mángano, M.G. (2011) *Ichnology: Organism–Substrate Interactions in Space and Time*. Cambridge University Press, Cambridge, 358 pp.

Buatois, L.A., Gingras, M.K., MacEachern, J., Mángano, M.G., Zonneveld, J.P., Pemberton, S.G., Netto, R.G. and Martin, A. (2005) Colonization of brackish-water systems through time: evidence from the trace-fossil record. *Palaios*, 20, 321-347.

Buoniconti, M.R. (2001) The role of lake level dynamics in lacustrine stratal architecture and sequence development: Evidence for the Songwe delta, Lake Malawi, east Africa. *American Association of Petroleum Geologists Abstracts with Program*, 10, p. A-25.

Cagliari, J., Serratt, H., Cassel, M. C., Schmitz, M. D. and Chemale Jr, F. (2022) New high-precision U-Pb zircon age of the Irati Formation (Paraná Basin) and implications for the timing of the Kungurian anoxic events recorded in southern Gondwana. *Gond. Res.*, 107, 134-145.

Cardoso, A.R., Nogueira, A.C.R. and Rabelo, C.E.N. (2019) Lake cyclicity as response to thermal subsidence: A post-CAMP scenario in the Parnaíba Basin, NE Brazil. *Sediment. Geol.*, 385, 96–109.

Carroll, A.R. and Bohacs, K.M. (1999) Stratigraphic classification of ancient lakes: Balancing tectonic and climatic controls. *Geology*, 27, 99-102.

Carroll, A.R. and Bohacs, K.M. (2001) Lake-type controls on petroleum source rock potential in nonmarine basins. *AAPG bulletin*, 85, 1033-1053.

Castro, J.C.D., Rohn, R., Castro, M.R.D. and Toledo, C.E.V. (2001) Camadas de tempestito grosso (coarse grained storm beds): exemplos do Permiano da bacia do Paraná. *Rem: Revista Escola de Minas*, 54, 179-184.

Catuneanu, O., Abreu, V., Bhattacharya, J. P., Blum, M. D., Dalrymple, R. W., Eriksson, P. G., Fielding, C.R., Fisher, W.L., Galloway, W.E., Gibling, M.R., Giles, K.A., Holbrook, J.M., Jordan, R., Kendall, C.G.St.C., Macurda, B., Martinsen, O.J., Miall, A.D., Neal, J.E., Nummedal, D., Pomar, L. and Winker, C. (2009) Towards the standardization of sequence stratigraphy. *Earth-Science Reviews*, 92, 1-33.

Catuneanu, O., Galloway, W.E., Kendall, C.G.St.C., Miall, A.D., Posamentier, H.W., Strasser, A and Tucker, M.E. (2011) Sequence stratigraphy: methodology and nomenclature. *Newsletters on Stratigraphy*, 44, 173-245.

Catuneanu, O. and Zecchin, M. (2013) High-resolution sequence stratigraphy of clastic shelves II: controls on sequence development. *Marine and Petroleum Geology*, 39, 26-38.

Cavallaro, F.A. (2013) Investigação geofísica no Alto Estrutural de Anhembi. Unpublished PhD Thesis. Institute of Geosciences, University of São Paulo, 148p.

Cecil, C.B., DiMichele, W., Fedorko, N., Skema, V. (2011) Autocyclic and allocyclic controls on the origin of the Dunkard Group. In: *Geology of the Pennsylvanian-Permian in the Dunkard Basin* (Ed. J.A. Harper). 76th Annual Field Conference of Pennsylvania Geologists, Washington, pp. 26–45.

Chapon, E., Beck, C., Pourchet, M. and Deconinck, J.-F. (1999) 1822 earthquake-triggered homogenite in Lake Le Bourget (NW Alps). *Terra Nova*, 11, 86 – 92.

Chen, Z.Q. and Benton, M.J. (2012) The timing and pattern of biotic recovery following the end-Permian mass extinction. *Nature Geoscience,* 5, 375-383.

Christofoletti, B., Peixoto, B.C.P.M., Warren, L.V., Inglez, L., Fernandes, M.A., Alessandretti, L., Perinotto, J.A.J., Simões, M.G. and Assine, M.L. (2021) Dinos among the dunes: Dinoturbation in the Pirambóia Formation (Paraná Basin), São Paulo State and comments on cross-section tracks. *J. S. Am. Earth Sci.,* 109, Article 103252.

Christofoletti, B; Warren, L.V., Varejão, F.G, Simões, M.G., Gómez-Peral, L.E., Lana, C., Rodrigues, M.G., Assine, M.L. 2023. Rising mollusk bivalves from the ashes: geologic, biostratigraphic and evolutionary implications from tuff data in the Permian Corumbataí Formation, Paraná Basin, Brazil. *Pre-Proof Article.*

Coira, B., Davidson, J., Mpodozis, C. and Ramos, V. (1982) Tectonic and magmatic evolution of the Andes of northern Argentina and Chile. *Earth-Science Reviews*, 18, 303-332.

CPRM – SERVIÇO GEOLÓGICO DO BRASIL. 2004. Cartas geológicas do Brasil ao milionésimo

Dahanayake, K. (1978) Sequential position and environmental significance of different types of oncoids. *Sed. Geol.*, 20, 301-316.

Day, P.I. (1997). The Fischer diagram in the depth domain: a tool for sequence stratigraphy. *J. Sed. Res.*, 67, 982–984.

Della Fávera, J.C. (2001) Fundamentos de estratigrafia moderna. Ed. UERJ, Rio de Janeiro, 264p.
Dalrymple, R.W. (1992) Tidal depositional systems. Facies models response to sea-level change, 195-218.
Dalrymple, R.W. (2010a) Tidal depositional systems. In: James, N.P. and Dalrymple, R.W., eds., Facies Models 4, Geotext, p. 201–231.
Dalrymple, R.W. (2010b). Interpreting sedimentary successions: facies, facies analysis and facies models. In: James, N.P and Dalrymple, R.W., eds., Facies Models 4, Geotext, p. 3-18.
DeVries Klein, G. (1985) Intertidal f ats and intertidal sand bodies. In: Davis, R.A., Jr., ed., Coastal Sedimentary Environments: New York, Springer-Verlag, p. 187–224.
Donovan, R.N. and Foster, R.J. (1972) Subaqueous shrinkage cracks from the Caithness Flagstone Series (middle Devonian) of northeast Scotland. *J. Sed. Res*., 42, 309-317.
Dunham, R.J. (1962) Classification of carbonate rocks according to depositional textures.
Embry, A.F. and Klovan, J.E. (1972) Absolute water depth limits of Late Devonian paleoecological zones. *Geol. Rundsch.,* 61, 672-686.
Etchebehere, M.L.C., Saad, A.R., Fulfaro, J.V. (2007). Análise de bacia aplicada a prospecção de água subterrânea no Planalto Ocidental Paulista, SP. *Geociências*, 26, 229–247.
Fischer, A.G. (1964) The Lofer cyclothems of the Alpine Triassic. *Geological Survey of Kansas Bulletin*, 169, 107-149.
Ferrarin, C., Lionello, P., Orlić, M., Raicich, F. and Salvadori, G. (2022) Venice as a paradigm of coastal flooding under multiple compound drivers. *Sci. Rep*., 12, Article 5754.
Flemming, B.W., Schubert, H., Hertweck, G., Müller, K. (1992) Bioclastic tidal-channel lag deposits: a genetic model. *Senckenbergiana Maritima*, 22, 109-129.
Flügel, E. (2010) Microfacies of Carbonate Rocks. Cham: Springer.
Fulfaro, V.J., Saad, A.R., Campanha, V.A. and Canuto, J.R. (1978) Considerações sobre a gênese da Formação Estrada Nova (P) da Bacia do Paraná. *Anais do Congresso Brasileiro de Geologia*, 30, pp.158
Fulfaro, V.J., Gama Jr. E.G. and Soares, P.C. (1980) Revisão estratigráfica da Bacia do Paraná. *Relatório BP 008/80*, Paulipetro, São Paulo, 115p.
Fürsich, F.T. and Oschmann, W. (1993) Shell beds as tools in basin analysis: the Jurassic of Kachchh, western India. *J. Geol. Soc*., 150, 169-185.
Gama Jr., E.G. (1979) A sedimentação do Grupo Passa Dois (exclusive Formação Irati): um modelo geomórfico. *Revista Brasileira de Geociências*, 9, 1-16.
Garzanti, E. (1991) Non-carbonate intrabasinal grains in arenites; their recognition, significance, and relationship to eustatic cycles and tectonic setting. *Journal of Sedimentary Research*, 61, 959-975.
Gastaldo, R., DiMichele, W. and Pfefferkorn, H. (1996) Out of the icehouse into the greenhouse: a late Paleozoic analogue for modern global vegetational change *GSA Today*, 10, 1-7.
Ghilardi, R.P. and Simões, M.G. (2002) Foram os bivalves do Grupo Passa Dois (exclusive Formação Rio do Rasto) moluscos dulcícolas? *Pesquisas em Geociências*, 29, 91-92.
Gierlowski-Kordesch, E. and Kelts, K. (1994) Global geological record of lake basins. Cambridge University Press, vol. 1, 427 p.
Gong, C., Sztanó, O., Steel, R. J., Xian, B., Galloway, W. E. and Bada, G. (2019) Critical differences in sediment delivery and partitioning between marine and lacustrine basins: A comparison of marine and lacustrine aggradational to progradational clinothem pairs. *Bulletin*, 131 , 766-781.
Gordon Jr., M. (1947) Classificação das formações gondwânicas do Paraná Santa Catarina e Rio Grande do Sul. Brasil. *Notas Preliminares e Estudos DNPM-DGM*, 38, 1-20.
Hart, B.S. and Plint, A.G. (1989) Gravelly shoreface deposits: a comparison of modern and ancient facies sequences. *Sedimentology*, 36, 551-557.
Hesse, R. (1990). Silica diagenesis: origin of inorganic and replacement cherts. In: Mcllreath, A., Morrow, D.W. (Eds.), Diagenesis. Geoscience of Canada, vol. 4, GAC, Canada, pp. 253-275.
Hilgen, F.J., Hinnov, L.A., Abdul Aziz, H., Abels, H.A., Batenburg, S., Bosmans, J.H.C., de Boer, B., Hüsing, S.K., Kuiper, K.F., Lourens, L.J., Rivera, T., Tuenter, E., Van de Wal, R.S.W., Wotzlaw, J.F. and Zeeden, C. (2015) Stratigraphic continuity and fragmentary sedimentation: the success of cyclostratigraphy as part of integrated stratigraphy. *Geol. Soc. London Special Publications*, 404, 157-197.

Hinds, D. J., Aliyeva, E., Allen, M. B., Davies, C. E., Kroonenberg, S. B., Simmons, M. D. and Vincent, S. J. (2004) Sedimentation in a discharge dominated fluvial-lacustrine system: the Neogene Productive Series of the South Caspian Basin, Azerbaijan. *Marine and Petroleum Geology*, 21, 613-638.

Holz, M., França, A.B., Souza, P.A., Iannuzzi, R. and Rohn, R. (2010) A stratigraphic chart of the late Carboniferous/Permian succession of the eastern border of the Paraná Basin, Brazil, South America. *J. S. Am. Earth Sci.,* 29, 381-399.

Ichaso, A.A. and Dalrymple, R.W. (2009) Tide- and wave-generated fluid mud deposits in the Tilje Formation (Jurassic), offshore Norway. *Geology*, 37,539–542

Ichinose, G.A., Anderson, J.G., Satake, K., Schweickert, R.A. and Lahren, M.M. (2000) The potential hazard from tsunami and seiche waves generated by large earthquakes within Lake Tahoe, California-Nevada. *Geophysical Research Letters*, 27, 1203-1206.

Imboden, D.M. (2004) The motion of lake waters. In: *The Lakes Handbook: Limnology and Limnetic Ecology* (Eds. P.E. O'Sullivan and C.S. Reynolds) 1st edn, pp. 115 – 152. Malden: Blackwell.

Kamo, S.L., Czamanske, G.K., Amelin, Y., Fedorenko, V.A., Davis, D.W. and Trofimov, V.R. (2003) Rapid eruption of Siberian flood-volcanic rocks and evidence for coincidence with the Permian-Triassic boundary and mass extinction at 251 Ma. *Earth Planet. Sci. Lett*., 214, 75-91.

Keidel, J. (1916) La geología de las Sierras de la Provincia de Buenos Aires y sus relaciones con las montañas de Sudáfrica y Los Andes. *Ministerio de Agricultura de La Nación, Sección Geología, Mineralogía y Minería*, 11, 1-78.

Kern, H.P., Lavina, E.L.C., Paim, P.S.G., Girelli, T.J. and Lana, C. (2021). Paleogeographic evolution of the southern Paraná Basin during the Late Permian and its relation to the Gondwanides. *Sedimentary Geology*, 415, Article 105808.

Kosyan, R.D. and Krylenko, M.V. (2019) Modern state and dynamics of the Sea of Azov coasts. *Estuarine, Coastal and Shelf Science*, 224, 314-323.

Kutzbach, J.E. and Gallimore, R.G. (1989) Pangaean climates: megamonsoons of the megacontinent. *Journal of Geophysical Research: Atmospheres*, 94, 3341-3357.

Lavina, E.L. (1991) Geologia sedimentar e paleogeografa do Neopermiano e Eotriássico (intervalo Kazaniano–Citiano) da Bacia do Paraná. PhD Thesis, Universidade Federal do Rio Grande do Sul.

Limarino, C.O., Césari, S.N., , L.A., Taboada, A.C., Isbell, J.L., Geuna, S. and Gulbranson, E.L. (2013) A paleoclimatic review of southern South America during the late Paleozoic: a record from icehouse to extreme greenhouse conditions. *Gond. Res.*, 25, 1396-1421.

Lindsay, J.F, Kennard, J.M. and Southgate, P.N. (1993) Application of sequence stratigraphy in an intracratonic setting, Amadeus Basin, central Australia. *Sequence stratigraphy and facies associations*, 605-631.

Logan B.W., Rezak R. and Ginsburg R.N. (1964) Classification and Environmental significance of algal stromatolites. *J. Geol*., 72, 68-83.

Longhitano, S.G. (2011) The record of tidal cycles in mixed silici–bioclastic deposits: examples from small Plio–Pleistocene peripheral basins of the microtidal Central Mediterranean Sea. *Sedimentology*, 58, 691-719.

Maceachern, J.A. and Pemberton, S.G. (1992) Ichnological aspects of cretaceous shoreface succession and shoreface variability in the western interior seaway of north America. *In:* Pemberton, S.G. ed., Applications of Ichnology to Petroleum Exploration. SEPM Core Workshop, 17, 57–84.

Maranhão, M.S.A.S. and Petri, S. (1996). Novas ocorrências de fósseis nas formações Corumbataí e Estrada Nova do Estado de São Paulo e considerações preliminares sobre seus significados paleontológicos e bioestratigráficos. *Revista do Instituto Geológico*, 17, 33-54.

Matishov, G.G. and Inzhebeikin, Y.I. (2009) Numerical study of the Azov Sea level seiche oscillations. *Oceanology*, 49, 445-452.

Matos, S.A., Warren, L.V., Varejão, F.G., Assine, M.L. and Simões, M.G. (2017) Permian endemic bivalves of the "Irati anoxic event", Paraná Basin, Brazil: Taphonomical, paleogeographical and evolutionary implications. *Paleogeogr., Paleoclimatol., Paleoecol*., 469, 18–33.

Medvedev, I.P., Kulikov, E.A., Fine, I.V. and Kulikov, A.E. (2019) Numerical modeling of sea level oscillations in the Caspian Sea. *Russian Meteorology and Hydrology*, 44, 529-539.

Meglhioratti, T. (2006) Estratigrafia de sequências das formações Serra Alta, Teresina e Rio do Rasto (Permiano, Bacia do Paraná) na porção nordeste do Paraná e Centro-Sul de São Paulo. Unpublished Master Dissertation, Universidade Estadual Paulista, 147p.

Mendes, J.C. (1949) Novos Lamelibrânquios fósseis da Série Passa Dois, sul do Brasil. *Boletim da Divisão de Geologia e Mineralogia*, 133, 1–40.

Mendes, J.C. (1952) A Formação Corumbataí na região do Rio Corumbataí: Estratigrafia e descrição dos lamelibrânquios. *Boletim USP*, 145, 119p.

Masselink, G. and Puleo, J.A. (2006) Swash-zone morphodynamics. *Continental Shelf Research*, 26, 661–680.

Miall, A.D. (2006) Reconstructing the architecture and sequence stratigraphy of the preserved fluvial record as a tool for reservoir development: A reality check. *AAPG bulletin*, 90, 989-1002.

Milani, E.J. (1997) Evolução tectono-estratigráfica da Bacia do Paraná e seu relacionamento com a geodinâmica fanerozóica do Gondwana sul-ocidental. PhD Thesis, Universidade Federal do Rio Grande do Sul.

Milani, E.J. and Ramos, V.A. (1998) Orogenias paleozóicas no domínio sul-ocidental do Gondwana e os ciclos de subsidência da Bacia do Paraná. *Revista Brasileira de Geociências*, 28, 473-484.

Milani, E.J., Melo, J.H.G, Souza, P.A., Fernades, L.A. and França, A.B. (2007) Bacia do Paraná. *Boletim de Geociências da Petrobrás*, 15, 265–287.

Moraes Rego, L.F. (1940) A geologia do Estado de São Paulo. *Boletim do Departamento de Estradas de Rodagem (DER)*, 2, 155-174.

Muniz, M.C. and Bosence, D.W.J. (2015) Pre-salt microbialites from the Campos Basin (offshore Brazil): image log facies, facies model and cyclicity in lacustrine carbonates. *Geological Society of London Special Publications*, 418, 221-242.

Ng, C., Vega, C.S. and Maranhão, M.S.A.S. (2019) Mixed carbonate-siliciclastic microfacies from Permian deposits of Western Gondwana: evidence of gradual marine to continental transition or episodes of marine ingressions? *Sediment. Geol*., 390, 62-82.

Nio, S.D., Shuttenhelm, R.T.E., van Weering, Tj.C.E. (1981) Holocene Marine Sedimentation in the North Sea Basin. International Association of Sedimentologists Special Publication 5, 515 p.

Nio, S.D., and Yang, C.S. (1989) Recognition of tidally influenced facies and environments: Short Course Note Series 1: Leiderdorp, Netherlands, InterGeos, 83 p.

NOAA. What is a seiche? National Ocean Service website, https://oceanservice.noaa.gov/facts/seiche.html

Northfleet, A.A., Medeiros, R.A. and Muhlmann, H. (1969) Reavaliação dos dados geológicos do Paraná. *Boletim Técnico da Petrobrás*, 12, 291-346.

Ocakoğlu, F., Açıkalın, S., Yılmaz, İÖ., Şafak, Ü. and Gökçeoğlu, C. (2012) Evidence of orbital forcing in lake-level fluctuations in the Middle Eocene oil shale-bearing lacustrine successions in the Mudurnu-Göynük Basin, NW Anatolia (Turkey). *J. Asian Earth Sci.,* 56, 54–72.

Oliveira, V.C.B., Assis Silva, C.M., Borghi, L.F., Souza, I.C. (2019) Lacustrine coquinas and hybrid deposits from rift phase: Pre-Salt, lower Cretaceous, Campos Basin, Brazil. *Journal of South American Earth Sciences*, 95, 102254.

Olivito, J.P.R. and Souza, F.J. (2020) Depositional model of early Cretaceous lacustrine carbonate reservoirs of the Coqueiros formation - Northern Campos Basin, southeastern Brazil. *Marine and Petroleum Geology*, 111, 414-439.

Overeem, I., Kroonenberg, S.B., Veldkamp, A., Groenesteijn, K., Rusakov, G.V. and Svitoch, A.A. (2003) Small-scale stratigraphy in a large ramp delta: recent and Holocene sedimentation in the Volga delta, Caspian Sea. *Sedimentary Geology*, 159, 133–157.

Palcu, D.V., Patina, I.S., Ş D.V., I., Lazarev, S., Vasiliev, I., Stoica, M. and Krijgsman, W. (2021) Late Miocene megalake regressions in Eurasia. *Scientific Rep*., 11, 11471.

Parrish, J. T. (1993) Climate of the supercontinent Pangea. *The Journal of Geology*, 101, 215-233.

Peng, J., Hu, Z., Feng, D. and Wang, Q. (2022). Sedimentology and sequence stratigraphy of lacustrine deep-water fine-grained sedimentary rocks: The Lower Jurassic Dongyuemiao Formation in the Sichuan Basin, Western China. *Marine and Petroleum Geology*, 146, 105933.

Petri, S. and Coimbra, A.M. (1982) Estruturas sedimentares das Formações Irati e Estrada Nova (Permiano) e sua contribuição para elucidação dos seus paleoambientes geradores. *Congresso Latinoamericano de Geologia*, 5, 353-371.

Petri, S. and Fulfaro, V.J. (1983) Geologia do Brasil (Fanerozoico). Ed. Universidade de São Paulo, São Paulo, 631p.

Perinotto, J.A.D.J., Etchebehere, M.L.D.C., Simões, L.S.A. and Zanardo, A. (2008) Diques clásticos na Formação Corumbataí (P) no nordeste da Bacia do Paraná, SP: Análise sistemática e significações estratigráficas, sedimentológicas e tectônicas. *Geociências*, 27, 469-491.

Perlmutter, M.A. and Matthews, M.D. (1989) Global cyclostratigraphy—a model. In: Cross, T.A. (Ed.), Quantitative Dynamic Stratigraphy. Prentice Hall, Englewood Cliffs, pp. 233–260.

Petroff, A. P., Sim, M. S., Maslov, A., Krupenin, M., Rothman, D. H., and Bosak, T. (2010) Biophysical basis for the geometry of conical stromatolites. *Proceedings of the National Academy of Sciences*, 107, 9956-9961.

Platt, N. H. and Wright, V. P. (1991) Lacustrine carbonates: facies models, facies distributions and hydrocarbon aspects. Lacustrine facies analysis, 57-74.

Plummer, P.S. and Gostin, V.A. (1981) Shrinkage cracks: desiccation or synaeresis?. *Journal of Sedimentary Research*, 51, 1147-1156.

Pratt, B.R. (1992) Shrinkage features (“molar tooth” structure) in Proterozoic limestones—new model for their origin through synsedimentary earthquake-induced dewatering. *Geological Society of America Abstracts with Programs*, 24, pp. 53.

Pratt, B.R. (1993) Proterozoic syneresis cracks and molar-tooth structure: Formation by synsedimentary seismicity. *Geological Association of Canada, Annual Meeting, Program with Abstracts*, pp. 85

Pratt, B.R. (1998) Syneresis cracks: Subaqueous shrinkage in argillaceous sediments caused by earthquake-induced dewatering. *Sedimentary Geology*, 117, 1–10.

Pritchard, D. and Hogg, A. J. (2003) Suspended sediment transport under seiches in circular and elliptical basins. *Coastal Engineering*, 49, 43-70.

Posamentier, H., Jervey, M. and Vail, P. (1988) Eustatic controls on clastic deposition I-conceptual framework. In: Wilgus, C., Hastings, B.S., Kendall, C.G.S. C., Posamentier, H.W., Ross, C.A., Van Wagoner, J.C. (Eds.), Sea Level Changes: An Integrated Approach. *SEPM Special Publication*, 42, 109–124.

Quade, J., Dente, E., Armon, M., Ben Dor, Y., Morin, E., Adam, O., Enzel, Y. (2018) Megalakes in the Sahara? A Review. *Quaternary Research*, 90, 253-275.

Ramos, V.A., Jordan, T.E., Allmendinger, R.W., Kay, S.M., Cortés, J.M. and Palma, M.A. (1984) Chilenia: un terreno alóctono en la evolución paleozoica de los Andes Centrales. *Congreso Geológico Argentino*, 9, 84-106.

Ramos, V.A., Jordan, T., Allmendinger, R., Mpodozis, C., Kay, S., Cortez, J. and Palma, M. (1986) Paleozoic terranes of the central Argentina–Chilean Andes. *Tectonics*, 5, 855–880.

Ramos, V.A. (1988) Tectonics of the Late Proterozoic–Early Paleozoic: a collisional history of Southern South America. *Episodes*, 11, 168–174.

Ramos, V.A. (2008) Patagonia: A paleozoic continente adrift? *J. S. Am. Earth Sci*., 26, 235-251.

Read, J.F. and Goldhammer, R.K. (1988). Use of Fischer plots to define third-order sea-level curves in peritidal carbonates, Ordovician, Appalachians. *Geology*, 16, 895-899.

Rees, P.M.A., Gibbs, M.T., Ziegler, A.M., Kutzbach, J.E. and Behling, P.J. (1999) Permian climates: evaluating model predictions using global paleobotanical data. *Geology*, 27, 891-894.

Reis, D. E., Rodrigues, R., Moldowan, J. M., Jones, C. M., Brito, M., da Costa Cavalcante, D., and Portela, H. A. (2018) Biomarkers stratigraphy of Irati Formation (Lower Permian) in the southern portion of Paraná Basin (Brazil). *Marine and Petroleum Geology*, 95, 110-138.

Renaut, W.R. and Gierlowski-Kordesch, E.H. (2010) Lakes. In: *Facies Model* (Eds. N.P. James and R.W. Dalrymple) 4th ed., pp. 541 – 572. Geological Association of Canadá, Canadá.

Renne, P.R., Zhang, Z., Richardson, M.A., Black, M.T. and Basu, A.R. (1995) Synchrony and causal relations between Permian-Triassic boundary crises and Siberian flood volcanism. *Science*, 269, 1413-1416.

Riccomini, C., Chamani, M.A.C., Agena, S.S., Fambrini, G.L., Fairchild, T.R. and Coimbra, A.M. (1992) Earthquake-induced liquefaction features in the Corumbataí Formation (Permian, Paraná Basin, Brazil) and the dynamics of Gondwana. *Anais da Academia Brasileira de Ciências*, 64, pp. 210.

Riccomini, C. (1995) Tectonismo gerador e deformador dos depósitos sedimentares Pós-Gondwânicos da porção centro-oriental do Estado de São Paulo e áreas vizinhas. Tese de Livre-Docência, Universidade de São Paulo, 100p.

Riccomini, C., Almeida, R.P., Turra, B.B., Chamani, M.A.C., Fairchild, T.R. and Hachiro, J. (2005) Reativação de falha do embasamento causa sismicidade no Permotriássico da Bacia do Paraná. *Boletim de Resumos Expandidos*, 18-20.

Rodrigues, A.C., Santos, L.D.R., Cury, L.F. and Rumbelsperger, A.B. (2022). Continental freshwater carbonate coated grains: oncoids in Quaternary deposits of the Serra da Bodoquena region, Central-West Brazil. *Brazilian Journal of Geology*, 52, Article e2021042.

Rodrigues, M.G. 2024. Modelo tafonômico de concentrações bioclásticas em mares interiores rasos: exemplos do Cretáceo e Permiano do Brasil. Unpublished PhD Thesis, Universidade Estadual Paulista, Rio Claro.

Rohn, R. (1988) Bioestratigrafia e paleoambientes da Formação Rio do Rasto na Borda leste da Bacia do Paraná (Permiano Superior, Estado do Paraná). Unpublished Master Dissertation, Universidade de São Paulo, São Paulo.

Rohn, R. (1994) Evolução Ambiental da Bacia do Paraná durante o Neopermiano no leste de Santa Catarina e do Paraná. Ph.D thesis, Universidade de São Paulo, São Paulo.

Rohn, R. (2001) A estratigrafia da Formação Teresina (Permiano, Bacia do Paraná) de acordo com furos de sondagem entre Anhembi (SP) e Ortigueira (PR). *Ciência Técnica- Petróleo*, 20, 209-218.

Rostirolla, S.P., Mancini, F., Rigoti, A., Kraft, R.P. (2003) Structural styles of the intracratonic reactivation of the Perimbó fault zone, Paraná Basin, Brazil. *J. S. Am. Earth Sci*., 16, 287–300.

Runnegar, B. and Newell, N.D. (1971) Caspian-like relict molluscan fauna in the South American Permian. *Bull. Am. Mus. Nat. Hist.,* 146, 1–66.

Sadler, P.M., Osleger, D.A. and Montanez, I.P. (1993) On the labeling, length, and objective basis of Fischer plots. *Journal of Sedimentary Research*, 63, 360-368.

Salamuni, R. (1963) Estruturas sedimentares singenéticas e sua significação na Série Passa Dois, Paraná. *Boletim do Instituto Geológico*, 12, 89p.

Sauders, A. and Reichow, M. (2009) The Siberian Traps and the End-Permian mass extinction: a critical review. *Chinese Science Bulletin,* 54, 20-37.

Schneider, R.L., Mühlmann, H., Tomassi, E., Medeiros, R.A., Daemon, R.F. and Nogueira, A.A. (1974) Revisão Estratigráfica da Bacia do Paraná. Anais do Congresso Brasileiro de Geologia, 28, 41–65.

Schwarz, E. and Howell, J.A. (2005) Sedimentary evolution and depositional architecture of a lowstand sequence set: the Lower Cretaceous Mulichinco Formation, Neuquén Basin, Argentina. *Geol. Soc. London Special Publications*, 252, 109-138.

Schumm, S.A. (1977) The Fluvial System. John Wiley & Sons, New York. 338 pp.

Scotese, C. R., Song, H., Mills, B. J. and van der Meer, D. G. (2021) Phanerozoic paleotemperatures: The earth's changing climate during the last 540 million years. *Earth-Science Reviews*, 215, 103503.

Seilacher, A. (1967). Bathymetry of trace fossils. Marine Geology, 5, 413–428.

Shen, S., Crowley, J.L., Wang, Y., Bowring, S.A., Erwin, D.H., Sadler, P.M., Cao, C., Rothman, D.H., Henderson, C.M., Ramezani, J., Zhang, H., Shen, Y., Wang, X., Wang, W., Mu, L., Li, W., Tang, Y., Liu, X., Liu, L., Zeng, Y., Jiang, Y. and Jin, Y. (2011) Calibrating the End-Permian mass extinction. *Science*, 334, 1367-1372.

Shteinman, B., Eckert, W., Kaganowsky, S. and Zohary, T. (1997) Seiche-induced resuspension in Lake Kinneret: a fluorescent tracer experiment. *Water, Air and Soil Pollution,* 99, 123 – 131.

Simões, M.G., Torello, F.F. and Rocha-Campos, A.C. (1996) Gênese e classificação da coquina de Camaquã (assembléia de Pinzonella neotropica), Formação Corumbataí (Permiano Superior), Rio Claro, SP. *Anais Academia Brasileira de Ciências*, 68, 545-557.

Simões, M.G. and Kowalewski, M. (1998) Shell beds as paleoecological puzzles: a case study from the Upper Permian of the Paraná Basin, Brazil. *Facies*, 38, 175-195.

Simões, M.G., Rocha-Campos, A.C. and Anelli, L.E. (1998) Paleoecology and evolution of Permian pelecypod assemblages (Paraná Basin) from Brazil. In: *Bivalves – An Eon of Evolution- Paleobiological Studies Honoring Norman D. Newell* (Eds. P.A. Johnston and J.W. Haggart). University of Calgary Press, Calgary, pp. 443–452.

Simões, M.G., Torello, F.F., Mello, L.H.C. and Ghilardi, R.P. (2000) O conteúdo fossilífero de novos afloramentos do Grupo Passa Dois (Neopermiano), nas porções centro-sul e nordeste do Estado de São Paulo: implicações bioestratigráficas e paleoecológicas. *Acta Geol. Leopold*., 23, 61-90.

Simões, M.G., Quaglio, F., Warren, L.V., Anelli, L.E., Stone, P., Riccomini, C., Grohmann, C.H. and Chamani, M.A.C. (2012) Permian non marine bivalves of the Falkland Islands and their paleoenvironmental significance. *Alcheringa*, 36, 543-554.

Sladen, C.P. (1994) Key elements during the search for hydrocarbons in lake systems. In: Gierlowski-Kordesch, E. and Kelts, K., Global geological record of lake basins, vol. 1: Cambridge, Cambridge University Press, 3–17.

Sloss, L.L. (1996) Sequence stratigraphy on the craton: Caveat emptor. *Geological Society of America Special Papers*, 306, 425-434.

Soares, P.C. (1991) Tectonica sinsedimentar cíclica na Bacia do Paraná. Unpublished PhD dissertation. Federal University of Paraná, 141p.

Sousa, S.H.M. (1985) Fácies sedimentares das formações Estrada Nova e Corumbataí no Estado de São Paulo. Master Dissertation, Universidade de São Paulo, São Paulo.

Spalletti, L.A., Artabe, A.E. and Morel, E.M. (2003) Geological factors and evolution of southwestern Gondwana Triassic plants. *Gond. Res*., 6, 119-134.

Spalletti, L.A. and Limarino, C.O. (2017) The Choiyoi magmatism in southwestern Gondwana: implications for the end-Permian mass extinction - a review. *Andean Geology*, 44, 328-338.

Suguio, K., Salati, C. and Barcelos, J.H. (1974) Calcários oolíticos de Taguaí, SP e seu possível significado paleoambeintal na deposição da Formação Estrada Nova. *Revista Brasileira de Geociências*, 4, 142-160.

Sztanó, O., Szafián, P., Magyar, I., Horányi, A., Bada, G., Hughes, D. W., Hoyer, D. and Wallis, R. J. (2013) Aggradation and progradation controlled clinothems and deep-water sand delivery model in the Neogene Lake Pannon, Makó Trough, Pannonian Basin, SE Hungary. *Global and Planetary Change*, 103, 149-167.

Taylor, A.M. and Goldring, R. (1993) Description and analysis of bioturbation and ichnofabric. *J. Geol. Soc., London*, 150, 141–148.

Trappe, J. (2001) A nomenclature system for granular phosphate rocks according to depositional texture. *Sed. Geol*., 145, 135-150.

Trebitz, A.S. (2006) Characterizing seiche and tide-driven daily water level fluctuations affecting coastal ecosystems of the Great Lakes. *Journal of Great Lakes Research*, 32, 102-116.

Tohver, E., Schmieder, M., Lana, C., Mendes, P.S., Jourdan, F., Warren, L. and Riccomini, C. (2018) End-Permian impactogenic earthquake and tsunami deposits in the intracratonic Paraná Basin of Brazil. *GSA Bulletin*, 130, 1099-1120.

Turra, B.B., Riccomini, C. and Almeida, R.P. (2006) Significado tectônico dos sismitos permotriássicos da Bacia do Paraná. Anais do Congresso Brasileiro de Geologia, 43, pp. 111.

Turra, B.B. (2009) Diques clásticos da Formação Corumbataí, Bacia do Paraná, no contexto da Tectônica Permotriássica do Gondwana Ocidental. Master Dissertation, Universidade de São Paulo, São Paulo, 96p.

Varejão, F.G., Warren, L.V., Alessandretti, L., Rodrigues, M.G., Ricomini, C., Assine, M.L., Cury, L.F., Faleiros, F.M., Simões, M.G. (2022) Late Permian siliceous hot springs developed on the margin of a restricted epeiric sea: Insights into strata-confined silicification in mixed siliciclastic-carbonate successions. *Palaeogeography, Palaeoclimatology, Palaeoecology*, 604, 111213.

Vieira, A.J. (1973) Geologia do centro e nordeste do Paraná e centro-sul de São Paulo. *Anais do Congresso Brasileiro de Geologia*, 27, 259-277.

Visser, M.J. (1980) Neap-spring cycles refl ected in Holocene subtidal large-scale bedform deposits: A preliminary note. Geology, 8, 543–546,

Wang, J., Zheng, H., Xiao, H., Zhong, G., Steel, R. and Yin, P. (2009) A climatic sequence stratigraphic model in the terrestrial lacustrine basin: A case study of Green River formation, Uinta Basin, USA. *Acta Geologica Sinica-English Edition*, 83, 130-135.

Warren, L.V., Almeida, R.P., Hachiro, J., Machado, R., Roldan, L.F., Steiner, S.S. and Chamani, M.A.C. (2008) Evolução Sedimentar da Formação Rio do Rasto (Permo-Triássico da Bacia do Paraná) na porção centro-sul do Estado de Santa Catarina, Brasil. *Revista Brasileira de Geociências*, 38, 213–227.

Warren, L.V., Assine, M.L., Simões, M.G., Riccomini, C. and Anelli, L.E. (2015) A Formação Serra Alta, Permiano, no centro-leste do Estado de São Paulo, Bacia do Paraná, Brasil. *Brazilian Journal of Geology*, 45, 109-126.

Washburne, C.W. (1930) Petroleum geology of the State of São Paulo. *Boletim Comissão Geográfica e Geológica*, 22, 272p.

Wignall, P.B. (2001) Large igneous provinces and mass extinctions. *Earth- Sci. Rev*., 53, 1-33.

Wright, V. P. (1984) Peritidal carbonate facies models: a review. *Geological Journal*, 19, 309-325.

Wu, H., Zhang, S., Hinnov, L.A., Jiang, G., Feng, Q., Li, H. and Yang, T. (2013) Time calibrated Milankovitch cycles for the late Permian. *Nature Communications*, 4, Article 2452.

Xie, X. and Heller, P. L. (2009) Plate tectonics and basin subsidence history. *Geological Society of America Bulletin*, 121, 55-64.

Yang, D., Huang, Y., Guo, W., Huang, Q., Ren, Y. and Wang, C. (2018) Late Santonian-early Campanian lake-level fluctuations in the Songliao Basin, NE China and their relationship to coeval eustatic changes. *Cretac. Res.*, 92, 138-149.

Zaine, M.F. (1980) Uma barreira geográfica no Paleozoico Superior na região de Fartura, SP. Master Dissertation, Instituto de Geociências, Universidade de São Paulo, São Paulo.

Zalán, P.V., Wolf, S., Conceição, J.C., Astolfí, A.M., Vieira, I.S., Appi, V.T., Zanotto, O.A. and Marques, A. (1991) Tectonics and sedimentation of the Paraná Basin. *7th Proceedings of the Gondwana, Universidade de São Paulo*, pp. 83–117.

Zavala, C., Ponce, J.J., Arcuri, M., Drittanti, D., Freije, H. and Asensio, M. (2006) Ancient lacustrine hyperpycnites: a depositional model from a case study in the Rayoso Formation (Cretaceous) of west-central Argentina. *Journal of Sedimentary Research*, 76, 41–59.

Zavala, C. (2020) Hyperpycnal (over density) flows and deposits. *Journal of Palaeogeography*, 9, 1–21.

Zavala, C., Liu, H., Li, X., Arcuri, M., Di Meglio, M., Zorzano, A., Otharán, G., Hoa, B., Wang, Y. (2022) Lacustrine sequence stratigraphy: hew insights from the study of the Yanchang Formation (Middle-Late Triassic), Ordos Basin, China. In: *The Ordos Basin* (Eds. R. Yang, A.J. Van Loon). Sedimentological Research for Hydrocarbons Exploration, Elsevier, Amsterdam, pp. 309-335.

Zecchin, M. (2007). The architectural variability of small-scale cycles in shelf and ramp clastic systems: the controlling factors. *Earth-Science Reviews*, 84, 21-55.

Zhang, J., Olariu, C., Steel, R. and Kim, W. (2020) Climatically controlled lacustrine clinoforms: Theory and modelling results. *Basin Research*, 32, 240-250.

2. DEPÓSITO DE CINZAS VULCÂNICAS NA FORMAÇÃO CORUMBATAÍ: IMPLICAÇÕES GEOCRONÓLOGICAS, BIOESTRATIGRÁFICAS E EVOLUTIVAS

Depósitos de cinzas vulcânicas, ou tufos, são excelentes para a determinação de idades deposicionais de alta precisão de seus sedimentos hospedeiros. Graças à presença de níveis de tufo na sucessão do Permiano Inferior da Bacia do Paraná, muitas idades radioisotópicas absolutas puderam ser publicadas (Maynard et al., 1996; Rocha-Campos et al., 2006; Santos et al., 2006; Silva et al., 2017; Rocha-Campos et al., 2019; Cagliari et al., 2022). No entanto, mesmo após mais de 100 anos de sua definição original pela Comissão Geográfica e Geológica do Estado de São Paulo (1916), a idade da Formação Corumbataí permanece em debate.

Portanto, estabelecer uma idade precisa para a Formação Corumbataí é fundamental para refinar e estabelecer lito- e biocorrelações confiáveis. Neste contexto, novas idades U-Pb, bem como dados isotópicos contribuem para a compreensão da evolução geológica do Gondwana ocidental durante o final do Paleozóico, incluindo aspectos como taxa de sedimentação da unidade, área de origem destas cinzas vulcânicas e o padrão de dispersão atmosférica. Mais importante ainda, precisar os dados geocronológicos e cronoestratigráficos é fundamental para traçar um cenário mais realista da evolução *in situ* dos moluscos da Formação Corumbataí e aprimorar o aproveitamento desses macrofósseis na bioestratigrafia do Grupo Passa Dois, algo que vem sendo tentado desde Von Huene (1928). Assim, os parte dos dados desta pesquisa constituem o manuscrito intitulado *"Rising mollusk bivalves from the ashes: geologic, biostratigraphic and evolutionary implications from tuff data in the Permian Corumbataí Formation, Paraná Basin, Brazil"*.

Referências

Cagliari, J., Serratt, H., Cassel, M. C., Schmitz, M. D., Chemale Jr, F. 2022. New high-precision U-Pb zircon age of the Irati Formation (Paraná Basin) and implications for the timing of the Kungurian anoxic events recorded in southern Gondwana. Gondwana Research, 107, 134-145.

Maynard, J.B., Chocyk-Jaminski, M., Gaines, R.R., Huff, W.D., Krekeler, M.P., Prokopenko, M., Summers, A.M. 1996. Bentonites in the Late Permian (Tatarian) Irati Formation of Brazil; geochemistry and potential for stratigraphic correlation. *In*: Geological Society of America, Abstracts with Programs 28, 280.

Rocha-Campos, A.C., Basei, M.A.S., Nutman, A.P., Santos, P.D. 2006. SHRIMP U-Pb zircon geochronological calibration of the late Paleozoic supersequence, Paraná Basin, Brazil. *In:* 5th South American Symposium on Isotope Geology, Buenos Aires, Argentina.

Rocha-Campos, A.C., Basei, M.A.S., Nutman, A.P., Santos, P.R.D., Passarelli, C.R., Canile, F.M., Rosa, O.C.R., Fernandes, M.T., Santa Ana, H., Veroslavsky, G. 2019. U-Pb zircon dating of ash fall 78 deposits from the paleozoic Paraná basin of Brazil and Uruguay: a reevaluation of the stratigraphic correlations. The Journal of Geology, 127, 167-182.

Santos, R.V., Souza, P.A., de Alvarenga, C.J.S., Dantas, E.L., Pimentel, M.M., de Oliveira, C.G., de Araújo, L.M. 2006. Shrimp U–Pb zircon dating and palynology of bentonitic layers from the Permian Irati Formation, Paraná Basin, Brazil. Gondwana Research, 9, 456-463.

Silva, A.F., Dani, N., Remus, M.V.D., Sommer, M.G., Horn, B.L.D., 2017. Bentonitas da Formação Irati no setor sul da Bacia do Paraná. Geologia USP 17, 75-88.

Von Huene, F. 1928. Aphorismen über die Stratigraphie des brasilianisch Staates Sao Paulo. Separat-Abdruck aus dem Centralblatt für Mineralogie, Geologie und Paläontologie, 10, 524–531 (German).

Rising mollusk bivalves from the ashes: geologic, biostratigraphic and evolutionary implications from tuff data in the Permian Corumbataí Formation, Paraná Basin, Brazil

Abstract

During the Permian, the southwestern Gondwana margin experienced episodes of intense volcanism tied to the Choiyoi magmatism. Several ash-fall horizons related to this magmatic event are preserved within the Late Paleozoic lake-sea sedimentary record of the Paraná Basin. Furthermore, near the Permian-Triassic boundary, a meteor fell in the northern border of the basin, generating unshocked zircon grains preserved in a stratigraphic marker called the Porangaba Bed. In this study, a new U-Pb zircon age of 265.17 ± 3.2 Ma is presented for a volcanic tuff in the upper part of the Corumbataí Formation, near the stratigraphic interval of the Porangaba Bed. In addition, Lu-Hf isotopic compositions of the zircon grains, whole-rock geochemistry, and atmospheric circulation data indicate the affinity of the ash-fall horizon with the Frontal Cordillera source. The combination of these new and previous U-Pb ages allowed us to draw a more realistic scenario of the evolution of bivalve mollusk of the Corumbataí Formation and to improve the use of these macrofossils in the biostratigraphy of the Permian succession of the Paraná Basin. In this context, we established the lower limit of the *Pinzonella neotropica*-*Jacquesia brasiliensis* Association Biozone between 262.38 ±5.7 Ma and 257.5 ±2.2 Ma. Hence, in the north and central Paraná Basin the local resolution of this biozone is of ~5 Ma. Moreover, the range of this biozone indicates that the endemic bivalves survived the end-Guadalupian (ca. 259 Ma) extinction event unscathed.

Keywords: U-Pb age; volcanic ash; Choiyoi magmatism; lake-sea; biostratigraphy.

3.1. Introduction

The precise age of the Corumbataí Formation in the upper part of the Permian Passa Dois Group, Paraná Basin, southeastern and central Brazil, is one of the main issues of the Brazilian Gondwana geology. Since the benchmark monography of Runnegar and Newell (1971), the unit has become known worldwide for its endemic fauna of well-preserved, silicified bivalves that evolved in a large and isolate inland basin (Simões et al., 1998; Wesselingh, 2007). Therefore, establishing the precise age, and reliable litho- and bio-correlations in the Corumbataí Formation are of fundamental importance for our understandings of the geological evolution of the western Gondwana during the end of the Paleozoic, including aspects such as sedimentation rate, source area and atmospheric dispersion pattern. The new geochronological and chronostratigraphic data is also fundamental to draw a more realistic scenario of that in situ mollusk evolution and to improve the use of those macrofossils in the biostratigraphy of the Passa Dois Group, something that has been attempted since Von Huene (1928).

Since the seminal works of Mendes (1952), a late Permian age is widely accepted for the Corumbataí Formation exclusively grounded on bivalve assemblages and palynological data (Daemon, 1974). Over the years, these fossils occurrences and biostratigraphy have been revised a few times (Rohn and Rösler, 1987; Sohn and Rocha-Campos, 1990; Rohn and Lavina, 1993), which seems to confirm the late Permian age (or even Permo-Triassic age, see Runnegar, 1977) for the deposition of the unit. However, the bivalves of the Passa Dois Group, including those of the Corumbataí Formation, are endemic (Mendes, 1952), and without other geochronological dating calibrations they cannot be used to improve the age associated with these geological units. This problem was partially solved by dating the ash beds in the underlying Irati Formation (Cagliari et al., 2022) resulting in a lower depositional limit of 275 Ma for the Corumbataí Formation. However, the absence of datable tuff beds at the upper part of this unit has made it extremely difficult to define the upper limit of the bivalve biozones and especially if the deposition of the Corumbataí Formation extends beyond the Permian. Hence, it is noteworthy that even after more than 100 years of studies (the Corumbataí Formation was originally defined in 1916 by the Geographical and Geological Commission of the State of São Paulo, Morais-Rego, 1930) the age of this unit remains under dispute.

Given the context above, in this contribution an accurate and precise age for the Corumbataí Formation is presented based on tuffaceous material from the State of Goiás, Central Brazil. This is relevant to our understandings of the age and time elapsed in the sedimentation of this unit. Even more significant, this new discovery raises another issue related to the magmatic source of the Permian volcanic ash recorded in the Paraná Basin. Exclusively grounded on age comparisons, the source of the ash falls has been generically assigned to the Choiyoi magmatism (Coutinho and Hachiro, 2005; Guerra-Sommer et al., 2008; Rocha-Campos et al., 2011; Silva et al., 2017), the largest magmatic event in the western margin of Gondwana (from the western Andean Cordillera to the Sierra Australes). Although the Choiyoi magmatism is widely accepted as the source of these deposits (Rocha-Campos et al., 2011), the exact location of the volcanism is still debated. Yet, it opens a series of new avenues to discuss the age of the endemic bivalve fauna of the Passa Dois Group, the temporal resolution of its biozones, and the bivalve species duration, with wide geochronological and evolutionary applications. Hence, in these context, (i) a new high-precision U-Pb radioisotope age for the Corumbataí Formation, northern Paraná Basin is presented; (ii) a Lu-Hf isotope analysis and whole rock geochemistry (including REY) is shown, offering us a unique opportunity to identify with precision the source of the volcanic ash preserved in this unit and, (iii) a relative dating pinpointing the age of the bivalve biozones of the Corumbataí Formation is constrained for the first time. These biozones are the main tool for surficial interbasinal stratigraphic correlations between sedimentary successions that are also tracked outside the Brazilian part of the Paraná Basin (i.e., Paraguay), thus, providing the foundation for continental-scale geological and paleontological interpretations.

3.2. Geological Setting

The intracratonic Paraná Basin extends over 1,700,000 km^2 in the central and southern Brazil, eastern Paraguay, northeastern Argentina, and northern Uruguay (Fig. 1A). This huge sedimentary basin encompasses at least six second-order stratigraphic sequences deposited between the Middle Ordovician and Upper Cretaceous periods, including sedimentary and volcanic successions bounded by regional unconformities (Milani et al., 2007). The Paleozoic successions comprise marine and continental rocks deposited over complete transgressive-regressive sequences (Schneider et al., 1974; Milani, 1997; Milani et al., 1998; 2007; Warren et al., 2008; Holz et al., 2010). Following this tendency, the SW Gondwana experienced a progressive continentalization and aridization during the Permian (Milani et al., 2007; Limarino et al., 2013) induced by the end of the marine connections between the southward Panthalassa and the Paraná and Karoo basins (Warren et al., 2008; Holz et al., 2010). The development of an orographic barrier (Gondwanides Belt; Keidel, 1916) during the assembling of the Patagonia plate against the Gondwana supercontinent (San Rafaelica orogeny; Ramos et al., 1986), led to the restriction of the above cited basins forming a continental-scale trapped lake-sea (sensu Palcu et al., 2021). In this huge, enclosed water body were deposited the Irati, Serra Alta, Teresina/Corumbataí and Rio do Rasto formations, from the Passa Dois Group (part of the Gondwana I supersequence; Milani et al., 2007).

In the northern/northeastern part of the Paraná Basin (São Paulo, Mato Grosso, and Goiás states), the stratigraphic interval that encompasses the Teresina Formation in the southern and southeastern Brazil, is usually designated as the Corumbataí Formation (Schneider et al., 1974; Warren et al., 2015). In the Goiás and São Paulo states, a well-marked breccia interval with regional scale significance stands out in the upper part of the Corumbataí and Teresina formations. This marker bed is called the Porangaba Bed (Matos and Coimbra, 1998; Tohver et al., 2018). Although its origin is under dispute (e.g., paleosol or tsunamite), unshocked zircon grains provide one of the few absolute ages for the Corumbataí Formation (ca. 254 Ma, Late Permian; Tohver et al., 2018).

In the Goiás and Mato Grosso states, the Corumbataí Formation is bounded at the base by the Serra Alta Formation (Petrobras boreholes – 2-AG-1-MT and 2-JA-1-GO) and at the top by a disconformity with the Botucatu Formation (Fig. 1B). In these localities, the Corumbataí Formation has a typical coarsening-upward pattern (Fig. 1C), with a monotonous succession of claystone and siltstone interbedded with cm-thick beds of swaley cross-stratified and wave-rippled fine-grained sandstone at its base. Highly bioturbated, tabular beds (cm- to m-scale-thick) of siltstone, heterolithic facies, wave-rippled fine-grained sandstone, and bivalve shell beds transitionally overlapped the basal succession (Ng et al., 2019). In the upper part of the unit, fine sandstone and heterolithic facies with mudstone cracks are common, while the presence of siltstone deposits significantly decreases. Carbonate facies (including microbialites), bivalve-dominated shell beds, evaporitic breccia with halite pseudomorphs, tepees and saline crusts are also observed (Ng et al., 2019).

Since the mid-20th century, multiple paleoenvironmental scenarios have been proposed for the Corumbataí Formation, including shallow restricted marine, lacustrine and tide-influenced settings (Schneider et al., 1974; Suguio et al., 1974; Petri and Coimbra, 1982; Sousa, 1985; Rohn, 1994). Based on recent studies (Warren et al., 2015) and sedimentological data from the southern and northern part of Paraná Basin (this contribution), the interpretation is that the Corumbataí Formation were deposited in a vast, almost flat, and shallow, trapped lake-sea, without connection with the Panthalassa (Mendes, 1984; Rohn, 1994, 2007; Simões et al., 1998). Paleobiological evidence suggests that the salinity was variable and that the endemic taxa was not typically freshwater or marine (Mendes, 1952; Beurlen, 1954; 1957; Runnegar and Newell, 1971; Sousa, 1985; Sohn and Rocha-Campos, 1990; Simões, 1992; Rohn, 1994; Maranhão, 1995; Matos, 1995; Simões et al., 1998; Ghilardi and Simões, 2002). This huge intraplate, confined water body was frequently affected by storms, and marked by periods of intense evaporation and hypersalinity with punctual influence of freshwater input (Suguio et al., 1974; Sousa, 1985; Sohn and Rocha-Campos, 1990; Simões, 1992; Rohn, 1994; Maranhão, 1995; Matos, 1995; Simões and Rocha-Campos, 1996; Simões et al., 1998; Ghilardi and Simões, 2002).

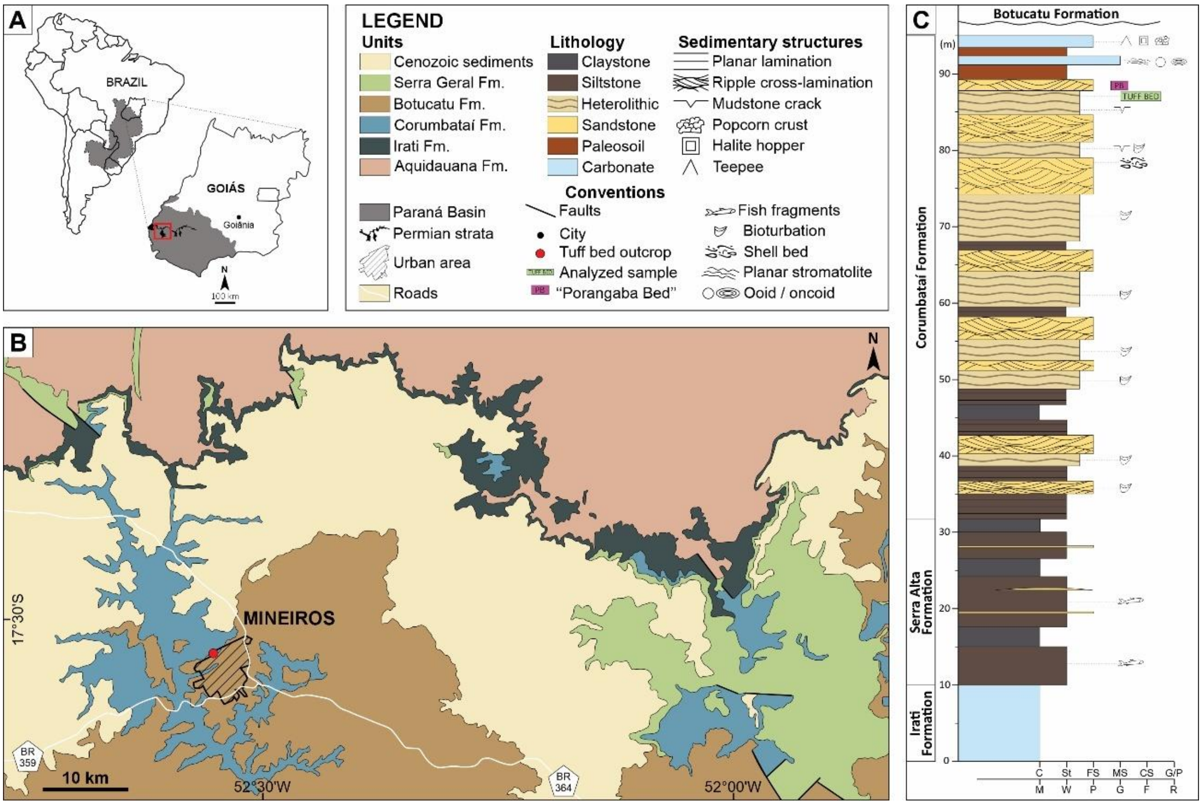

Figure 1 – Study area and general stratigraphy of the Corumbataí Formation and tuff-bearing succession. (A) Location of the studied area in the Paraná Basin. (B) Simplified geologic map (modified from CPRM, 2006) with the location of the tuff bed outcrop (17°32.607'S / 52°33.931'W). (C) Simplified stratigraphic column of the Corumbataí Formation showing the precise vertical position of the tuff bed in the upper part of the unit. Explanation: Fm. - Formation; C – claystone; St – siltstone; FS – fine sandstone; MS – medium sandstone; CS – coarse sandstone; G/P – granule/pebble; M – mudstone; W – wackestone; G – grainstone; B – boundstone; R – rudstone. Porangaba Bed according to Tohver et al. (2018).

3.2.1. On the age of the Corumbataí Formation

Given the presence of *Stereosternum tumidum* and *Mesosaurus brasiliensis* in the underlying Irati Formation, and *Licopodiopsis derbyi* (see Mendes, 1952, and references therein) in the Corumbataí Formation, a Late Paleozoic age was assigned to the sedimentary succession of the Passa Dois Group, even prior to its formal designation as the Passa Dois Series by White (1908). Until 1927, a Permian age was accepted to the Passa Dois Group, but during the famous geological comparison between South America and Africa, Du Toit (1927) referred the upper part of the group to the Triassic. Bivalves collected by him in the State of Paraná were erroneously referred to as the Mesozoic bivalve genera *Myophoriopsis* (= *Jacquesia*) and *Pachycardia* (= *Pinzonella*) by Reed (1929; 1932; 1935). Du Toit (1927) had access to Reed's data before the publication of his studies. These facts introduced strong confusion into the chronology of the Corumbataí beds.

Mendes (1952) revised the bivalves of the Corumbataí Formation based on fossils from the State of São Paulo, again recognizing a Permian age for the formation. In addition to the presence of *Glossopteris* and arborescent lycophytes (Mendes, 1967), the occurrence of striated dissaccate pollen grains (e.g., *Striamonosaccites* cf. *S. morondavensis*) from subsurface samples of the Corumbataí Formation in the State of São Paulo indicates a latest Permian age for the unit (Tatarian stage of the European Zechstein Sea, or Capitanian to basal Wuchiapingian) (Daemon, 1974). An upper Permian (i.e., Kazanian-Tatarian or nearly Capitanian-Wuchiapingian age) was accepted for the Corumbataí Formation for a long time by various authors (e.g., Daemon and Quadros, 1970; Rohn and Rösler, 1987; Sohn and Rocha-Campos, 1990; Rohn and Lavina, 1993). However, based on a pattern of alternating reverse and normal geomagnetic polarity, Valencio et al. (1975) had proposed a Late Permian or even younger (Triassic) paleomagnetic age for the Corumbataí Formation in São Paulo State. In turn, Runnegar (1977) considered the Passa Dois bivalves to be representative of a Permo-Triassic benthic biota.

A Triassic age was again suggested for the Corumbataí Formation by Ragonha (1984), based on fossil remains of *Xenacanthus moorei*, a cosmopolitan shark that occurs in Triassic deposits of Europe, India, and North America. Similarly, Daemon et al. (1996), on the ground of palynological content, invertebrates and vertebrates considered the Corumbataí Formation as Triassic in age. On the other hand, ostracod taxa described from occurrences in the Goiás and Mato Grosso states (Tomassi, 2009) have been reported from Changhsingian (Late Permian) based in similar forms found in coeval successions in China (Shu and Utting, 1990; Crasquin et al., 2010). Hence, for a long time, the age of the Corumbataí Formation was mainly inferred based on its micro and macrofossil content, and its contact relationships with the underlying Serra Alta and Irati formations and the overlying Pirambóia Formation, as well as its lateral correlation with the Teresina Formation in the southern Brazil. This was until recently, when Rocha-Campos et al. (2019) dated some probable ash fall layers and published U-Pb zircon ages, suggesting an age of 257±2.2 Ma. (only 3 zircon grains) and 266±7.1 Ma. for the Corumbataí and Teresina formations, respectively. However, the authors themselves point out that these data present little confidence and can be placed in establishing the age of the units, due to the scarce number of data.

Thanks to the presence of tuff layers in the Lower Permian succession of the Paraná Basin, also including the Irati Formation, some published absolute radioisotope ages are now available (Maynard et al., 1996; Rocha-Campos et al., 2006; Santos et al., 2006; Silva et al., 2017; Bastos et al., 2019; Rocha-Campos et al., 2019; Cagliari et al., 2022). These ash-fall tuffs are crucial because they usually contain a representative zircon population, which is product of a volcanic event and can be used to provide a precise U-Pb depositional age for the host sediments.

3.3. Material and Methods

During a detailed geological survey in the Corumbataí Formation at the northwestern part of the Paraná Basin, one tuff bed was founded and sampled in a road cut at the Mineiros town, State of Goiás, Brazil (17°32.607'S / 52°33.931'W). The tuff bed was stratigraphically constrained at the upper succession of the Corumbataí Formation, ~10 m below the upper erosive boundary with the Botucatu Formation (Fig. 1C). A detailed (1:50) columnar section was measurement including the description of the lithology, sedimentary structures, and fossil content (Fig. 2), and one sample (~2kg) of the tuff bed was collected.

3.3.1. Zircon U-Pb geochronology

The zircon grains were separated from rock sample (2 kg) using standard techniques encompassing crushing, sieving and separation by heavy liquid (bromoform). Zircon grains (~430 grains) were handpicked under a binocular stereomicroscope, mounted on adhesive tape, and enclosed in epoxy resin mounts. These were polished to about half their sizes and imaged by cathodoluminescence (Fig. 3A; JEOL 6510 Scanning at DEGEO/UFOP), aiming to characterize internal features (recrystallization rings, fractures, inclusions) of the individual zircon grains. The zircon description and typology followed the protocol in Pupin (1980).

U-Pb analyses (see Supplementary Material) were carried out at the Isotopic Geochemistry Laboratory (Federal University of Ouro Preto – UFOP) using a Thermo-Finnegan Neptune multi-collector ICP-MS coupled with a Photon-Machines 193 nm excimer laser system (LA-MC-ICP-MS). Data were acquired using automatic mode with background measurement during 20 s, zircon ablation during 40 s and 20 µm spot size. The GJ-1 zircon standard (Jackson et al., 2004) was used as a primary standard for this study with the Plešovice zircon standard ($^{206}Pb/^{238}U$ = 337 Ma, $^{207}Pb/^{235}U$ = 337 Ma and $^{207}Pb/^{206}Pb$ = 339 Ma; Sláma et al., 2008) as a secondary standard. Data reduction was done in SATURN® Software (Silva et al., 2022), whereas the concordance, probability, radial and Concordia diagrams, and the weighted average ages were generated by the Excel Isoplot software (Ludwig, 2003).

3.3.2. Lu-Hf isotope analyses

The Hf isotope ratios were determined on seventeen previously selected zircon crystals showing reliable U-Pb ages with low analytical error (see Supplementary Material). The analysis were carried out in a multi-collector MC-ICP-MS Thermo-Scientific Neptune Plus system, coupled to a Photon Machines 193 (λ=193 nm) ArF Excimer laser ablation system, hosted in the Isotopic Geochemistry Laboratory (Federal University of Ouro Preto – UFOP). Data were collected in static mode during 60 s of ablation with a spot size of 40 µm. The spots were drilled with a repetition rate of 6Hz and 0.3 He gas.

The accuracy and external reproducibility were verified by analyses of the standard zircons Blue Berry $^{176}Hf/^{177}Hf$ =0.281692 ± 0.000017 (n = 10), Mud Tank $^{176}Hf/^{177}Hf$ =0.282516 ± 0.000015 (n = 10), GJ-1 $^{176}Hf/^{177}Hf$ = 0.282005 ± 0.000019 (n = 10) and Temora $^{176}Hf/^{177}Hf$ = 0.28260 ± 0.000014 (n = 10) (all errors are ± 2σ SD). These ratios are in good agreement with the accepted ratios data of 0.281674 ± 0.000018 (Blue Berry; Santos et al., 2017), 0.282504 ± 0.000044 (Mud Tank; Black and Gulson, 1978; Woodhead and Hergt, 2005), 0.282000 ± 0.000005 (GJ-1; Jackson et al., 2004), and 0.282680 ± 0.000031 (Temora; Black et al., 2003; Wu et al., 2006).

For the calculation of the εHf(t) values, the chondritic values reported by Chauvel et al. (2008) of $^{176}Hf/^{177}Hf$ = 0.283164 and $^{176}Lu/^{177}Hf$ = 0.0270 were used. To calculate the model ages (TDM) based on a depleted mantled source, the present-day ratios of $^{176}Hf/^{177}Hf$ = 0.282313 and $^{176}Lu/^{177}Hf$ = 0.000311 were used (Blichert-Toft et al., 2008). The λ decay constant for ^{176}Lu applied was 1.867x10−11/yr (Söderlund et al., 2004).

3.3.3. Whole-rock mineralogy and ICP-MS-geochemistry

Whole-rock and clay mineralogy of the tuff bed sample was determined from XRD patterns. Analyses were run on a PANalytical X'Pert PRO difractometer in the Centro de

Investigaciones Geológicas (CIG CONICET-UNLP, La Plata, Argentina), using Cu radiation (Kα=1.5 Å) and a Ni filter, and generation settings of 40 kV and 40 mA. Routine air-dried mounts were run between 2 and 32°2θ at a scan speed of 2°2θ/min. Samples were ethylene glycol-solvated without saturation pre-treatment and heated to 550 °C, and they were run from 2 to 27°2θ and 3–15°2θ, respectively, at a scan speed of 2°2θ/min. The methodology used for sample preparation follows Brown and Brindley (1980), and semi-quantification of the minerals was obtained considering the intensity of the main peak for each mineral (Biscaye, 1965; Moore and Reynolds, 1999 including laboratory patterns).

Rare-earth elements and yttrium (REY) contents, expressed in ppm, were obtained from the sample of tuff using a Perkin-Elmer quadrupole inductively coupled plasma mass spectrometry (ICP-MS) fitted with a Meinhardt concentric nebulizer at the CIG. In preparation for elemental analyses, aliquots of whole powder were digested for 2 h in trace metal grade 2% HNO_3. REE concentrations were normalized to chondrite values (Sun and McDonough, 1989) and compared to REE pattern of the rhyolite certificated geo-standard (RGM-1).

3.4. Results

3.4.1. Tuff-bearing succession

The tuff-bearing section (Fig. 2) is organized in up to 3 m-thick, coarsening-upward successions composed of dm-scale beds of siltstone with horizontal lamination interbedded with ripple cross-laminated, fine-grained sandstone in the base, which transitions to sandstone with flaser and wavy bedding at the middle, and to fine-grained sandstone with ripple cross-lamination and horizontal lamination at the top (Fig. 2D). The volcanic bed is a low-density, whitish claystone (Fig. 2C) that conforms an approximately >5 m-wide and 5 to 10 cm-thick lens within a siltstone bed between ripple cross-laminated and horizontally laminated fine-grained sandstone. To the top of the succession, interbedded laminated siltstone and silicified horizontally laminated stromatolites occur.

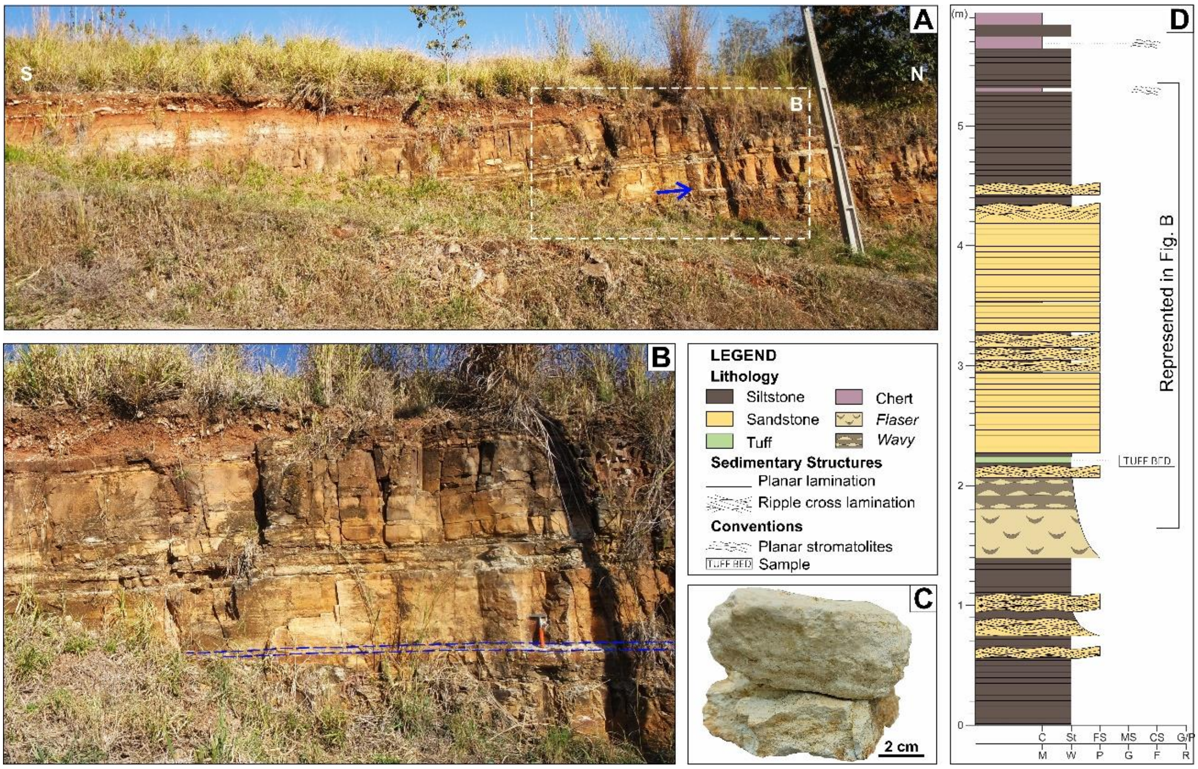

Figure 2 - Tuff bed and associated sedimentary facies. (A) General view of the outcrop. (B) Detail of the volcanic ash bed (blue dashed line indicates the sampled layer). (C) Part of the sampled ash bed. (D) Columnar section showing the position of the tuff bed within the sedimentary facies succession. Explanation: C – claystone; St – siltstone; FS – fine sandstone; MS – medium sandstone; CS – coarse sandstone; G/P – granule/pebble; M - mudstone; W - wackestone; G - grainstone; B - boundstone; R – rudstone. The hammer in B is 30-cm-long.

3.4.2. *Volcanic zircon U-Pb ages*

A total of 430 zircons were analyzed under cathodoluminescence. Of these, 43 euhedral volcanic grains were randomly selected for dating by LA-ICPMS (Fig. 3A).

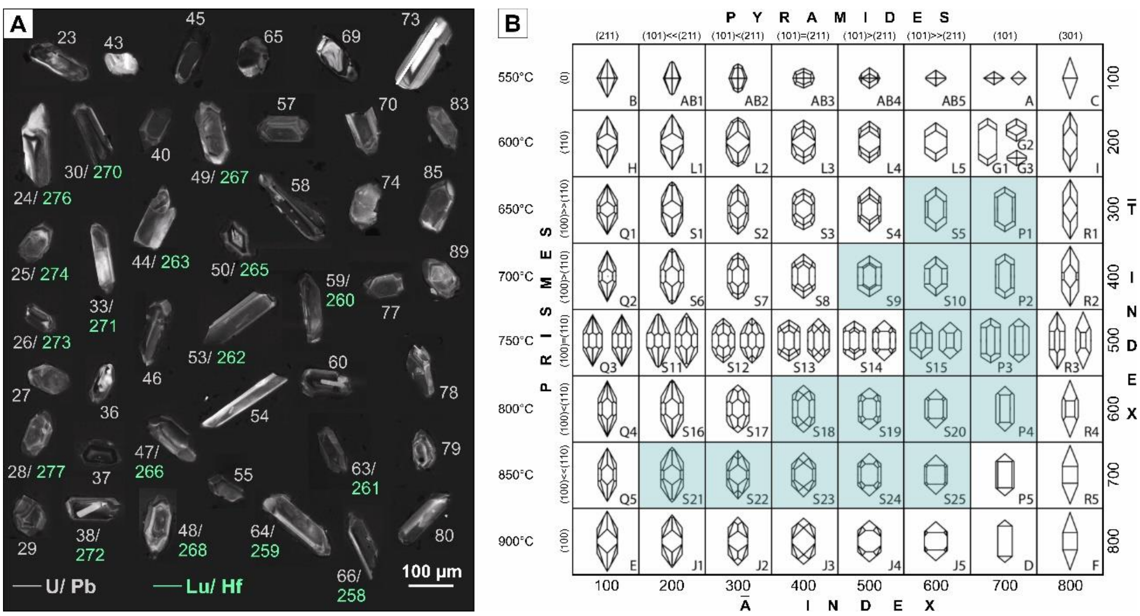

Figure 3 – Zircon morphology. (A) Cathodoluminescence image of the selected volcanic zircons for the LA-ICP-MS dating (grey number refer to the zircon identification in Supplementary Material) and Lu-Hf analysis (green number refer to the zircon identification in Supplementary Material). Numbers. (B) Zircon crystal typological classification diagram (Pupin, 1980). The blue subtypes refer to the analyzed zircon population.

The 37 analyzed zircons have prismatic and euhedral morphologies ranging in size from 56 to 176 µm (Fig. 3A), with medium sizes around 80 to 110 µm. Almost all zircons correspond to dipyramidal grains with well-developed prismatic faces, corresponding to the subtypes P1-4, S5, 9, 10, 15, 18-25 of Pupin (1980) (Fig. 3B).

About 86% of the analyzed zircon population have a late Permian age, varying between a minimum of 261.6 ± 8.0 Ma and a maximum of 267.8 ± 2.5 Ma (Capitanian to Roadian ages). The $^{206}Pb/^{238}U$ weighted mean age of 265.0 ± 0.5 Ma with a mean square of weighted deviation (MSWD) of 0.76 and a probability of 0.85 (95% of confidence, Fig. 4A) and the $^{206}Pb/^{238}U$ concordia age of 265.17 ± 3.2 Ma (Fig. 4B) confirm a Wordian age for the analyzed zircon population. Six zircon grains (4% of the zircon population; numbers 23 to 73 in Fig. 3A) are rounded to subrounded (sizes vary between 70 to 137 µm), having Cambrian (558.3±15.5 Ma, Fortunian) to Paleoproterozoic ages (2018.8±24.1 Ma, Orosian).

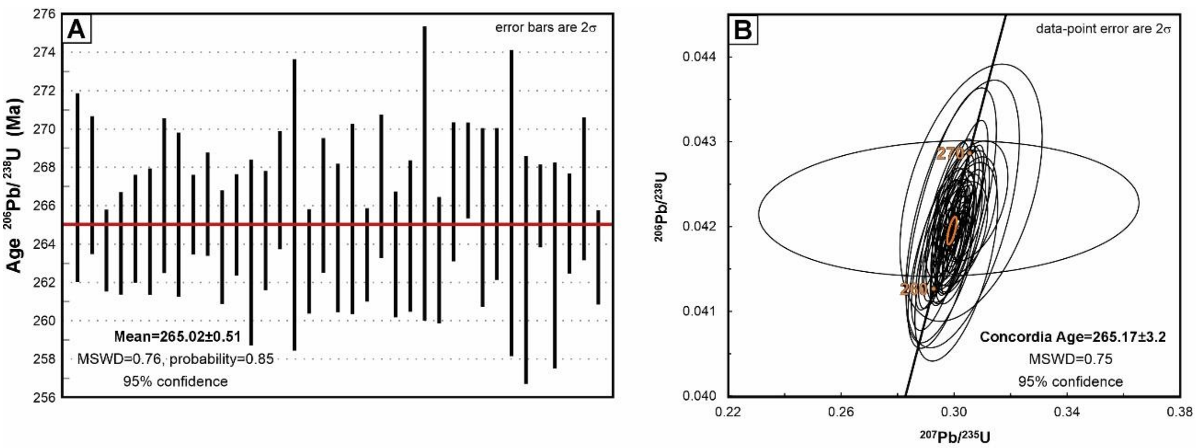

Figure 4 - U-Pb LA-ICP-MS results of the analyzed volcanic zircon grains. (A) $^{206}Pb/^{238}U$ weighted mean age of the LA-ICP-MS dated grains. (B) Concordia diagram illustrating LA-ICP-MS dated grains. MSWD: mean square of weighted deviates.

3.4.3. Volcanic Zircon Lu-Hf analysis

Among the 37 Permian-age zircon grains, 17 were randomly selected and subjected to isotopic analyzes of Lu-Hf. The εHf(t) vs. time diagram (Fig. 5) shows that most volcanic zircon grains have negative values between −5.5 and −0.9 and TDM ages from 1.3 to 1.5 Ga. Only two grains have positive εHf values of 0.9 and 1.0, and TDM ages between 1.2 and 1.1 Ga.

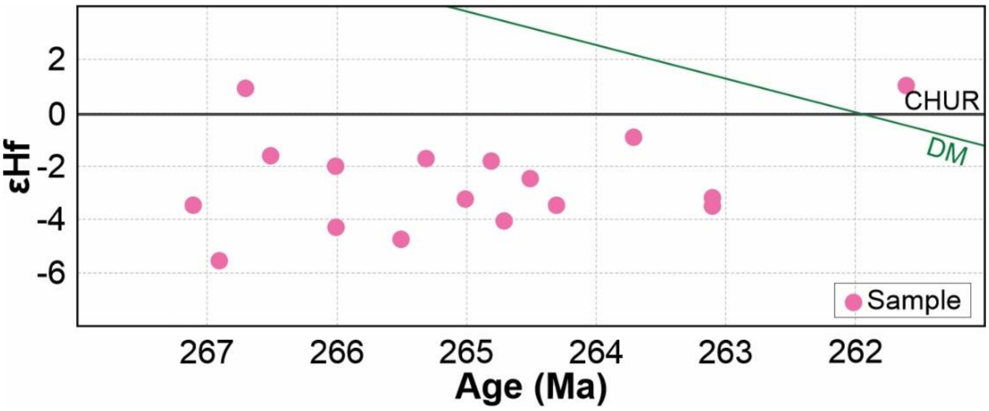

Figure 5 - Lu-Hf isotope analyses of the zircon grains indicated in Figure 3. CHUR: chondritic values; DM: depleted mantle.

3.4.4. Whole-rock mineralogy and ICP-MS-geochemistry

The whole-rock XRD compositional data of the tuff sample shows that quartz is the prevalent mineral (37%); followed by K-feldspar (23.5%), plagioclase (18.5%), tridymite-cristobalite (12%), pyroxene (7%), and clay minerals (3%) (Fig. 6A). Clay-fraction (<2 µm), XRD analysis (less than 3% of the whole rock) shows smectite and in less proportion mixed layered illite–smectite (IS) (Fig. 6B). In the analyzed sample, clays are mostly the product of very scarcely altered glass.

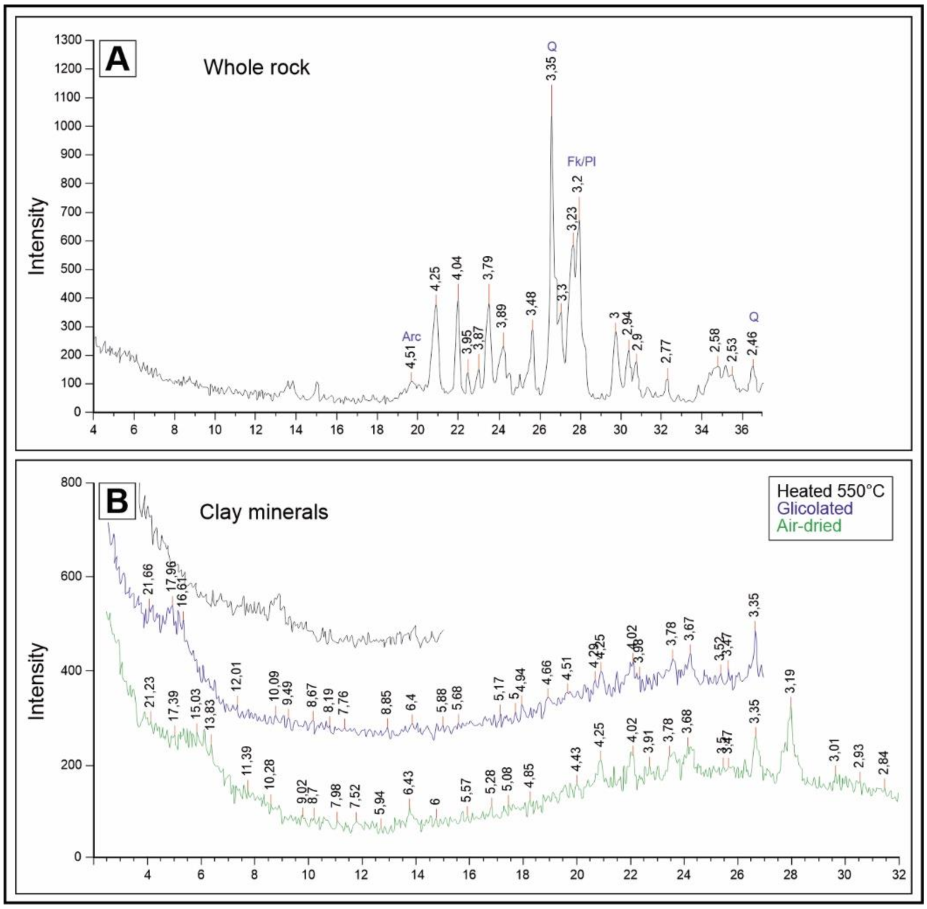

Figure 6 - XRD-diffractograms. (A) Tuff sample mineral composition. (B) Tuff sample in < 2µm fraction. Q: quartz; FK: alkaline feldspar; Pl: plagioclase; Arc: clays.

3.5. Discussion

3.5.1. The age of the Corumbataí Formation and the nature of Porangaba Bed

The $^{206}Pb/^{238}U$ age of 265.17±3.2 Ma (Wordian, Cohen et al., 2013; updated), in the upper part of the Corumbataí Formation in the Góias State, clearly indicates that this unit is older than previously realized. The low degree of dispersion in the dataset (the Cambrian and Paleoproterozoic zircons were considered detrital grains from an older source that got mixed in during the deposition of the tuff layer in the depositional environment) and the unusual abundance of euhedral zircon reinforces that the dated grains are non-reworked and correspond to the same original magmatic population. Thus, the age obtained approximately correspond to the age of ash ejection and tuff deposition.

In other words, the unit is neither Triassic nor Tatarian (i.e., Changhsingian) (Fig. 7), as previously suggested by Ragonha (1984) and Quadros et al. (1996), among others. On the other hand, the ca. 265.17±3.2 Ma age is in accordance with a Kazanian age (270.5–260.4 Ma) or Roadian-Capitanian age, already suggested by various authors (Daemon and Quadros, 1970; Rohn and Rösler, 1987; Sohn and Rocha-Campos, 1990; Rohn and Lavina, 1993). As shown in Figure 7, only the upper part of the Corumbataí Formation is Capitanian to basal Wuchiapingian, an age that is also in accordance with some pollen grains (i.e., *Striamonosaccites* cf. *S. morondavensis*) recorded in subsurface samples from the Corumbataí Formation in the São Paulo State (Daemon, 1974).

Previous paleomagnetic studies indicate that the Corumbataí Formation was entirely deposited after the end of the Kiaman Superchron at 262–265 Ma (Capitanian-Wordian) (Valencio et al., 1975). However, recent paleomagnetic data, constrained by U-Pb ages in zircons, from the Porangaba Bed (Tohver et al., 2018), contest this depositional age and pointed to a deposition between ca. 274–254 Ma (Kungurian-Changhsingian; Aragão and Scardia, 2021).

The Porangaba Bed is defined by a matrix-supported breccia grading upward to a light gray to dark-red, massive, poorly sorted silty sandstone with free-floating, angular lithic clasts of white, altered chert or ocher siltstone (Matos, 1995; Matos and Coimbra, 1997). This bed was first described at the contact between the Passa Dois Group and the overlying Pirambóia Formation, in São Paulo State (Brazil) (Matos, 1995; Matos and Coimbra, 1997). Tohver et al. (2018) reported a breccia bed in a single location in the State of Goiás and attributed this facies to the same Porangaba Bed described in the São Paulo State by Matos (1995). This deposit has been interpreted either as the product of pedogenesis (Matos and Coimbra, 1997) or more recently, as a result of a high energy episode related to the late Permian Araguainha impact event (Tohver et al., 2018).

Tohver et al. (2018) dated unshocked detrital zircon grains from this breccia bed providing a SHRIMP U-Pb maximum depositional age (youngest population; n=12) of 253.0±3.0 (Changhsingian). Compiling only the ages of grains collected exclusively in the northern part of the Paraná Basin by Tohver et al. (2018), in the same stratigraphic interval and just 60 km away from the tuff bed studied here, the concordia age of the Permian population of zircons reaches 262.38 Ma±5.7 Ma (Tohver et al., 2018) (Fig. 7).

When compared, the columnar sections of the tuff bed outcrop and that of the Porangaba Bed (Tohver et al., 2018), it is clear that: (i) the "Porangaba Bed" described by Tohver et al. (2018) in Goiás State is stratigraphically located a few meters (~10 m) below the top of the

Corumbataí Formation; (ii) the Porangaba Bed is almost at the same stratigraphic level as the tuff bed studied here; (iii) in the northern part of the Paraná Basin, the upper part of the Corumbataí Formation was eroded and overlain by the Botucatu Formation, and (iv) in the SP-280 highway, central part of the São Paulo State, limestone with bivalves of the *Pinzonella neotropica-Jacquesia brasiliensis* Association Biozone in the upper part of the Teresina Formation are recorded ~14 m above the Porangaba Bed, almost in the contact with the overlying Pirambóia Formation. Thus, at least in theory, the breccia facies of the Porangaba Bed occur at a stratigraphically well-delimited single level and could not have been formed at different ages (neither by pedogenesis, nor by impact, or even a fault reactivation).

However, even considering dating errors (2 to 5 Ma), the ages obtained by Tohver et al. (2018) for the breccia bed described in Goiás State (and associated by these authors to the Porangaba Bed) are older than those obtained for the Porangaba Bed in the São Paulo State. Thus, the breccias observed in the Goiás State are probably not part of the Poranbaga Bed described for the Teresina/Corumbataí Formation from the São Paulo State, which the origin of breccias is probably associated to the Permian reactivation of the Jacutinga Fault, by intraplate stress propagation associated to the Sanrafaelica Orogeny (Riccomini, 1992; Rostirola et al., 2003; Turra, 2009; Varejão et al., 2022). Alternatively, these breccia levels may compose an interval ("Porangaba Bed Interval") related to distinct triggering events.

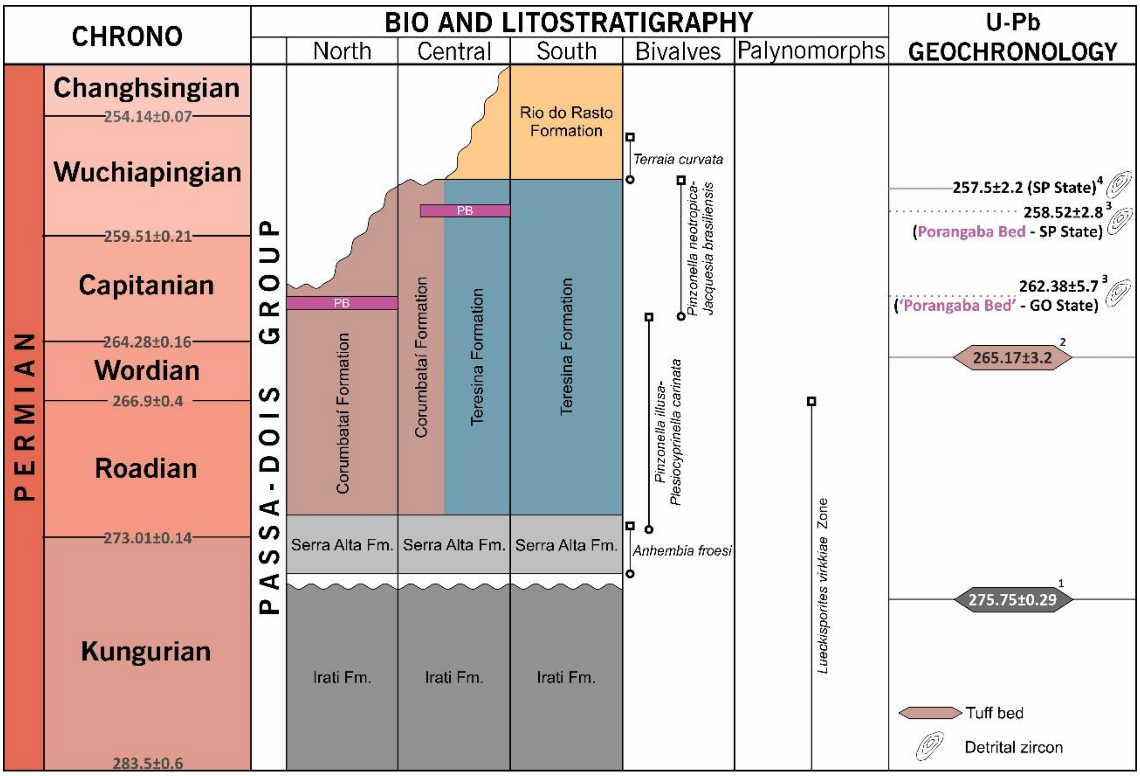

Figure 7 – Chronostratigraphic correlation of the Passa Dois Group in the south, central and north parts of the Paraná Basin. Palynozones, bivalve association biozones, and the main available U-Pb ages are highlighted. The chronostratigraphy is according to the International Commission on Stratigraphy 2022/10 chart (Cohen et al., 2013; updated). Radiometric ages from: 1 – Cagliari et al. (2022); 2 – This contribution; 3 – Tohver et al. (2018); 4 – Rocha-Campos et al. (2019). Palynological and biostratigraphic data from Daemon and Quadros (1970), Barberena et al. (1985), and Simões et al. (2020). Explanation: Fm.: Formation; PB: Porangaba Bed.

3.5.2. Permian volcanism and related sources

During the early to middle Permian (280-260 Ma), the southwestern Gondwana margin experienced episodes of intense volcanism. In the inner part of the supercontinent, these events were recorded as rare tuffaceous horizons deposited in the Paraná Basin (Brazil, Paraguay, and Uruguay) (Coutinho et al., 1988; Milani and Ramos, 1998; López-Gamundí, 2006; Rocha-Campos et al., 2011). Due to age and geochemical characteristics, many of these tuff levels have been associated with the multiple magmatic events related to the Permian-Triassic Choiyoi Orogeny that occurred between 280 and 250 Ma (Milani and Ramos, 1998; Rocha-Campos et al., 2011). Thus, this large volcano-plutonic complex characterized by lava flows, ignimbrites, pyroclastic, and sub-volcanic rocks cropping out in the current central Chile and western Argentina was the main source for the ashes deposited in the intracontinental basins (Kay et al., 1989; Kleiman and Japas, 2009; Fanning et al., 2011).

Since the chemical characteristics of the crystallization play an important role in the origin and growth of zircon grains, it is possible to suggest a preliminary petrogenetic classification based on external morphology (Pupin and Turco, 1975; Pupin, 1976;1980). As previously mentioned, the analyzed zircon population fits well in the morphological subtypes P1-4; S5, 9, 10, 15, 18-25 (see Fig. 3B; Pupin, 1980), commonly related to granite of crustal + mantle affinity (orogenic granite, leucogranite, monzogranite, granodiorite and sienogranite). Additionally, most of the analyzed Permian zircons with ages between 267-262 Ma have minimum and maximum negative εHf values of -5.5 to -0.9, respectively (Figs. 4 and 5). This suggests a strong crustal influence in the genesis of the granitoid rocks (Faure, 1986).

The Permian age of the analyzed zircon and the mostly negative εHf values are consistent with geochronological and geochemical data from the Choiyoi igneous province. Negative εHf values (-15.3 to -0.08) were reported in the Permian (ca. 260 – 269 Ma) igneous rocks from the Frontal Cordillera (Central Andes) (Poma et al., 2014; Peper et al., 2016; Capaldi et al., 2021), North Patagonia Massif (258 – 269 Ma, εHf values between -32.9 to – 2.8, Fanning et al., 2011; Chernicoff et al., 2013; Peper et al., 2016; Castillo et al., 2017), igneous rocks from Northern

Antarctic Peninsula (ca. 263 – 269 Ma, εHf values -20 to – 7, Fanning et al., 2011), and Tierra del Fuego (ca. 260 – 262 Ma, εHf values -12.2 to – 9.5, Castillo et al., 2017) (Fig. 8).

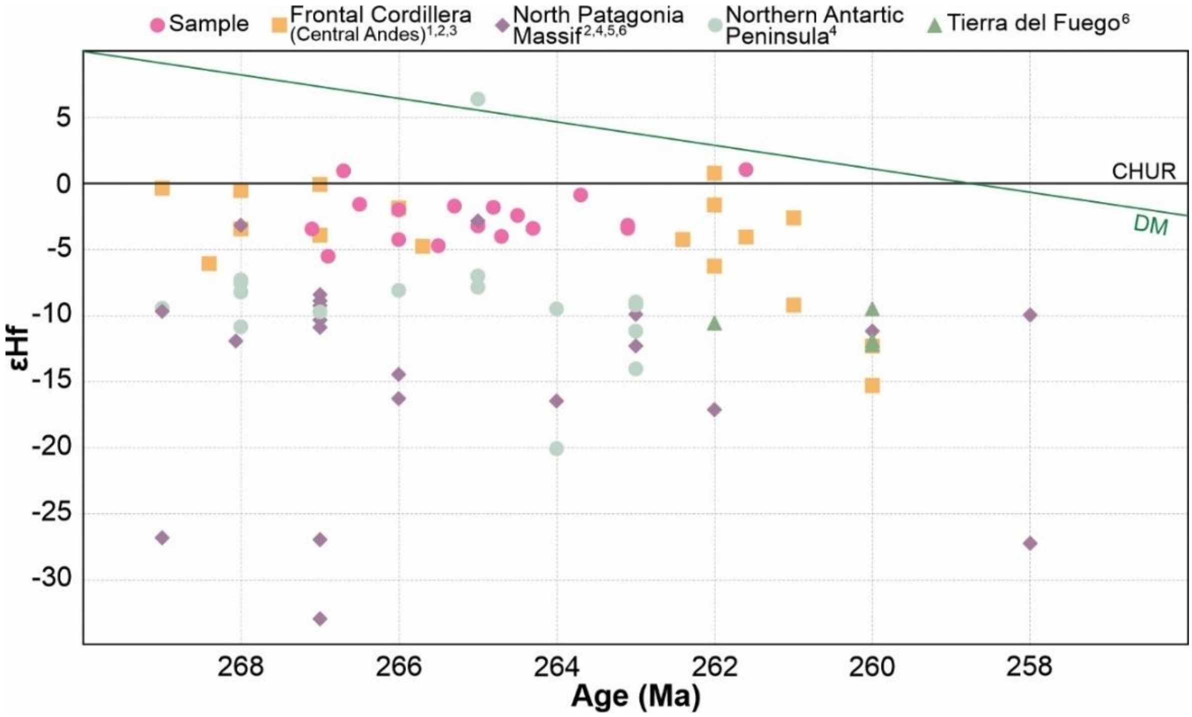

Figure 8 - Lu-Hf comparison of the Permian tuff bed from the upper Corumbataí Formation and multiple magmatic provinces associated to the Choiyoi Orogeny. 1 – Poma et al. (2014); 2 – Peper et al. (2016); 3 – Capaldi et al. (2021); 4 – Fanning et al. (2011); 5 – Chernicoff et al. (2013); 6 – Castillo et al. (2017). Explanation: CHUR: chondritic values; DM: depleted mantle.

When compared with the available data from the Choiyoi Province (Fig. 8), the age dispersion indicate affinity with Frontal Cordillera and North Patagonia Massif, while the εHf values are more similar to those found in the Frontal Cordillera. On the other hand, the Northern Antarctic Peninsula and Tierra del Fuego showed more negative εHf values and less compatibility with the tuff studied here.

Analyzing the atmospheric circulation pattern that prevailed during the Upper Permian, it is noteworthy the presence of a high-pressure cell developed during summers in the southern hemisphere (Fig. 9; Parrish and Curtis, 1982). Thus, as pointed by the ages and Lu-Hf data, it is plausible that winds blowing from SW to NE carried ashes from the Frontal Cordillera or North Patagonia Massif to the Paraná Basin depositional site located about 2000 km from the magmatic source area (Fig. 9).

Acceptance of the Choiyoi igneous province vents as the source for Paraná Basin tuff beds would imply in dispersion of volcanic ash clouds transportation for distances from over

2000 km. Rocha-Campos et al. (2011) compared the Toba eruption event (Indonesia, 75 ka) that left a blanket over an area of about 4,000,000 km^2 (over 20.5 times the Paraná Basin area) up to 3000 km away (Rose and Chesner, 1987), charactering a large scale explosive eruption of plinian to ultraplinian intensity. In largest eruptions the ash clouds typically develop diameters greater than 600 km and up to 6000 km in the most powerful supereruptions, thus explaining why areas of continental size can be covered with volcanic ash (Baines and Sparks, 2005). Furthermore, models of dispersion of volcanic ash clouds indicate that particles with sizes varying between 30-100 µm can reach distances of up to 3000 km from the source area (Beckett et al., 2015), which is compatible with the size of zircon grains from the tuffaceous bed here analyzed.

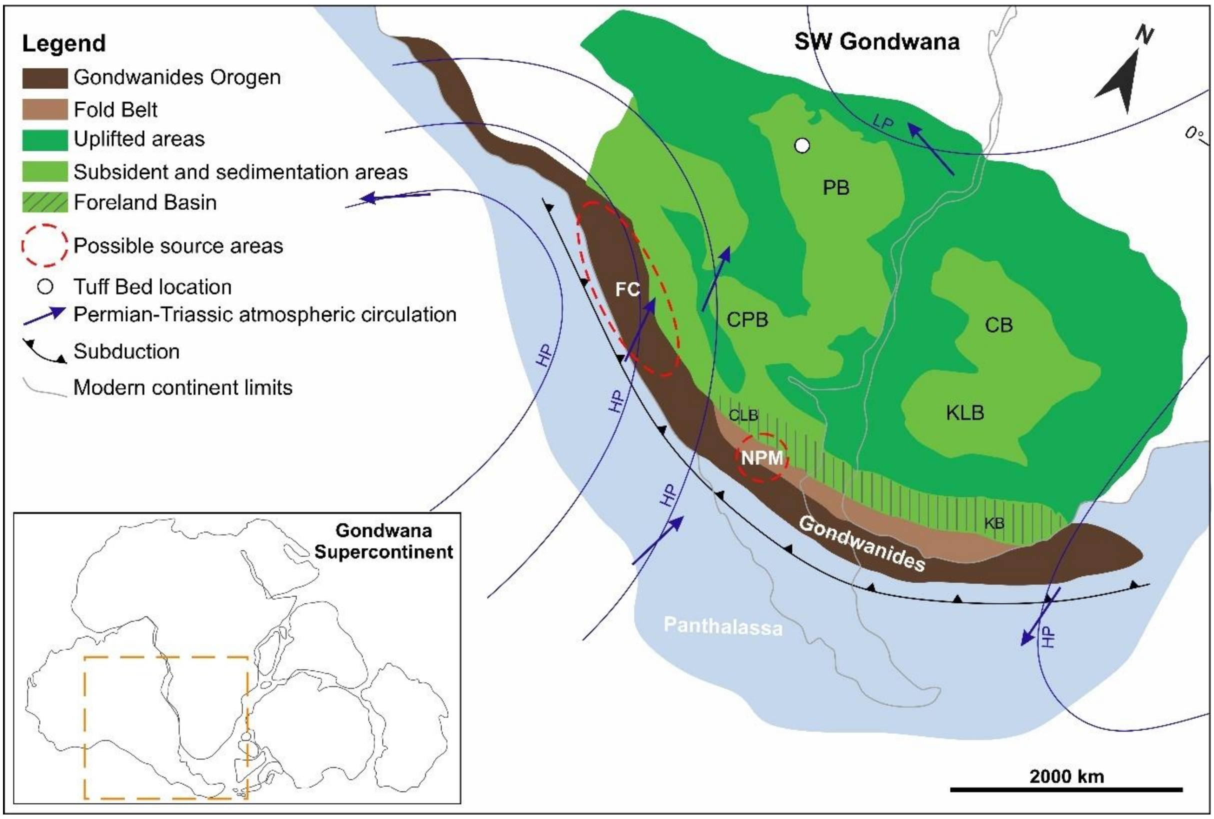

Figure 9 - Reconstruction of the Permian-Triassic paleogeography and atmospheric circulation of the SW Gondwana showing possible source areas and the depositional site of the Corumbataí Formation tuff bed in the Paraná Basin. Explanation: PB – Paraná Basin; CPB – Chaco-Paraná Basin; CB – Congo Basin; KLB – Kalahari Basin; CLM – Claromecó Basin; KB – Kalahari Basin; FC – Frontal Cordillera; NPM – North Patagonia Massif; HP – High-pressure; LP – Low-pressure. Paleogeography reconstruction modified from Faure and Cole (1999); atmospheric circulation pattern based on Parrish and Curtis (1982).

REEs are useful tracers for petrogenetic processes, and they are commonly used for characterization of rocks (Rollinson, 1993). In this sense, the REE concentrations of the tuff were normalized to the chondrite values (Boynton, 1984) and the total REE abundance obtained was in sum 135 ppm. As seen in Figure 10, REE pattern of the tuff is similar to the geo-standard RGM-1. It is characterized by LREE enrichment (La_N/Sm_N = 5.32) and relatively flat to depleted in HREE (Gd_N/Yb_N = 2.26). They also show absence to slightly negative Eu anomalies (Eu/Eu* = 0.81).

According to Rollinson (1993), Eu anomalies are chiefly controlled by feldspar; particularly in felsic magmas and the removal of feldspar from a felsic melt by crystal fractionation give rise to a negative Eu anomaly. However, negative Eu anomalies is not recognized in the REE patterns of the tuff (Fig. 10), the LREE-enriched and relatively flat HREE.

The compatibility of the Corumbataí Formation ash fall layer and the Frontal Cordillera were also tested by comparing their rare earth elements (REE) and depict a great compatibility (data from Poma et al., 2014; Rocher et al., 2015), indicating similar origin and evolution (Fig. 10). Rare earth elements sum of the tuff sample (135 ppm) is in the range of that reported by the same vulcanism (119-234 ppm; Rocher et al., 2015). The REEs normalized to the chondrite patterns obtained for these authors show moderate slopes, with slightly enriched light REEs, presence of negative Eu anomalies of variable magnitude, and relatively flat patterns in heavy REEs.

Added to all this geochemical data, the grain sizes of the zircons are another specific evidence of congruence between the Frontal Cordillera magmatism and the Corumbataí tuff bed. The zircons of the Llullaillaco Unit (Frontal Cordillera) exhibit 80 µm to 200 µm long (Poma et al., 2014) compatible with the mean grain size obtained here (80 to 110 µm).

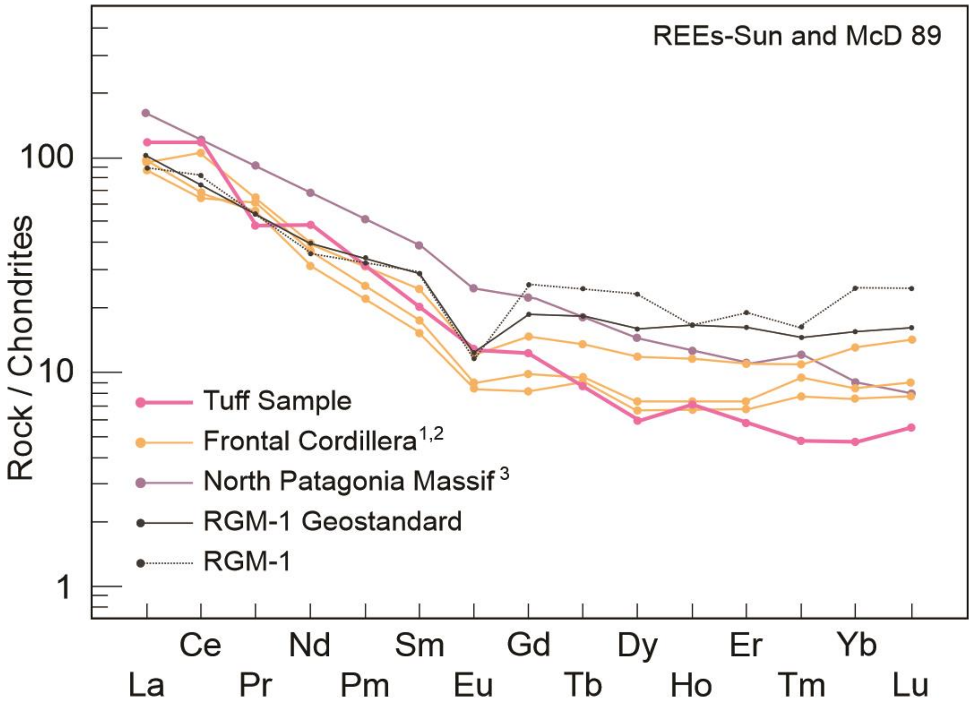

Figure 10 - Chondrite-normalized REE patterns of the tuff (Boynton, 1984), Frontal Cordillera (1 - Poma et al., 2014; 2 - Rocher et al., 2015), North Patagonia Massif (3 – Gregory et al., 2021), theorical RGM-1 geostandard and RGM-1 geostandard analysed in this work (black dashed line).

3.5.3. Sedimentation rate

The chronologic constraints based on the age of the most recent volcanic tuff of the Irati Formation (275.75 Ma; Cagliari et al., 2022) and the age for the top of the Corumbataí Formation presented here (265.17 Ma) provide insights about the sedimentation rates in the north sector of the Paraná Basin. The Serra Alta and Corumbataí formations are ~80 m-thick in the studied area. In our model, these units were deposited over 10.6 Myr at ca. 7.5 m/Myr rates. These data fits well with the rates of ca. 8 m/Myr for the northeastern sector of the Paraná Basin, proposed by Aragão and Scardia (2021) and is within subsidence curves patterns for intracratonic basins, which corresponds to subsidence rates as low as 5 to 50 m/Myr (Perron et al., 2021). Although the duration for the deposition of the Serra Alta and Teresina formations are comparable, our values are lower than those proposed by previous authors, such as 42 m/Myr (Quintas et al., 1999), and 62.5 m/Myr (Holz et al., 2010). This discrepancy in the sedimentation rate is expected in the large Paraná Basin and, our estimates should be considered representative of the proximal sector of the basin (north margin of the basin), with is more subject to erosion than in the depocenter.

3.5.4. Biostratigraphic implications

The radiometric ages now available are extremely relevant to better constrain the bivalve species duration and the relative ages of some bivalve Association Biozones of the Corumbataí Formation, the most important benthic macrofossils for biostratigraphy and intra and interbasinal correlations in the Passa Dois Group (Simões and Kowalewski, 1998; Simões et al., 1998). Although the vertical amplitude of some bivalves can transcend the lower and upper limits of bivalve biozones, the first and last appearance data of index bivalve species are vertically well marked. The *Pinzonella neotropica*-*Jacquesia brasiliensis* Association Biozone is one example (Fig. 11) that is well-recognized by various authors in the Corumbataí and Teresina formations (see Rohn, 1994, and references therein). The biozone is defined by the vertical amplitude of *Pinzonella neotropica*, with the lower limit marked by the first stratigraphic appearance of *P. neotropica*, *Jacquesia brasiliensis*, and the last stratigraphic appearance of *Ferrazia cardinalis* (Rohn, 1944). The upper limit is defined by the last stratigraphic appearance of *P. neotropica* and *Cowperesia anceps* (Rohn, 1994). The main associated bivalve species is *Naiadopsis lamellosus*, a very derived Pachydomiidae bivalve. The vertical distribution of the *Pinzonella neotropica*-*Jacquesia brasilensis* is shown in Figure 11. Note that the lower limit of this biozone is slightly older than 262.38 ±5.7 Ma and the upper limit is ca. 257.5 ±2.2 Ma. Hence, in the north and central Paraná Basin the local resolution of the *Pinzonella neotropica*-*Jacquesia brasiliensis* Association Biozone is of ~5 Ma. Just to remember, this biozone can be tracked from Brazil to Paraguay, and our data offers an age for a layer that extends laterally for hundreds of kilometers.

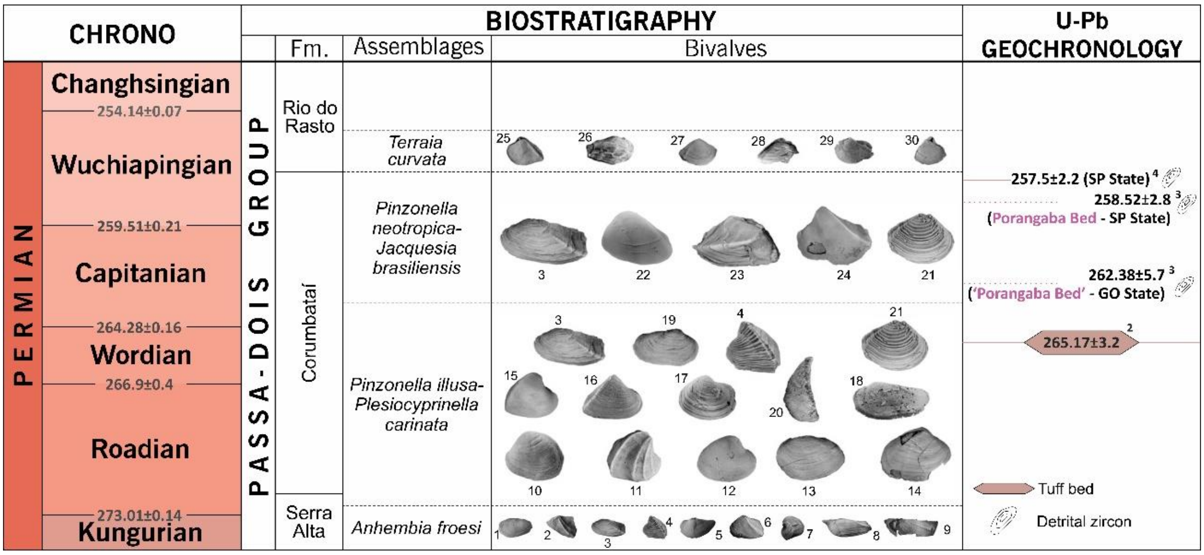

Figure 11 – Chrono and biostratigraphy chart showing the main bivalve assemblages and associated species, which are recorded in the Serra Alta, Corumbataí and Rio do Rasto formations. Species composition (not to scale): 1-

Kidodia cf. K. stockleyi; 2 - *Barbosaia angulata*; 3 - *Holdhausiella elongata*; 4 - *Tambaquyra camargoi*; 5 - *Rioclaroa lefevrei*; 6 - *Maackia contorta*; 7 - *Ferrazia simplicicarinata*; 8 - *Anhembia gigantea*; 9 - *Anhembia froesi*; 10 - *Pinzonella illusa*; 11 - *Ferrazia cardinalis*; 12 - *Casterella gratiosa*; 13 - *Angatubia cowperesioides*; 14 - *Othonella araguaiana*; 15 - *Plesiocyprinella carinata*; 16 - *Terraia aequilateralis*; 17 - *Runnegariella fragilis*; 18 - *Favalia arcuata*; 19 - *Roxoa corumbataiensis*; 20 - *Coxesia mezzalirai*; 21 - *Cowperesia anceps*; 22 - *Pinzonella neotropica*; 23 - *Naiadopsis lamellosus*; 24 - *Jaquesia brasiliensis;* 25 - *Terraia curvata*; 26 - *Beurlenella elongatella*; 27 - *Cowperesia emerita*; 28 - *"Leinzia" curta*; 29 - *Terraia bipleura*; 30 - *Astartellopsis prosoclina*. Data from Mendes (1952), Runnegar and Newell (1971), Simões et al. (1998), Matos et al. (2017), Guerrini et al. (2019), and Simões et al. (2020). Compiled U-Pb geochronological data from Tohver et al. (2018); Rocha-Campos et al. (2019). The chronostratigraphy is according to the International Commission on Stratigraphy 2022/10 chart (Cohen et al., 2013; updated). Explanation: Fm.: Formation.

3.5.5. Evolutionary implications

Bivalve species durations

The concept of bivalve species duration has application in both biostratigraphy and in evolutionary studies (Koch, 1980). Indeed, the maximum temporal bivalve species duration may have an important chronostratigraphic significance, but given the low availability of accurate radiometric ages, only a few information is found in the literature on this topic (see Koch, 1980; Rohn, 1994). Our newly obtained age allows us to, for the first time, evaluate the maximum temporal bivalve species duration of the *Pinzonella neotropica-Jacquesia brasiliensis* Association Biozone, as well as the exclusive species that coexisted in this biozone (*Naiadopsis lamellous*), and about some species that are recorded across various biozones (i.e., *Cowperesia anceps*).

Average bivalve species duration varies with time, environment, life habit, and geographic distribution (Koch, 1980; Stanley, 1990; Rohn, 1994). The average total duration of the marine bivalve species is approximately 10 Ma (Stanley, 1990). However, this value changes significantly for those bivalve species that thrived in interior (lake-sea) basins, given the high speciation and extinction rates coupled to the disturbance in stability in the benthic ecosystems (Koch, 1980; Nevesskaia et al., 1987), characteristic of this type of basin. For example, Koch (1980) investigated the duration of 41 bivalve species, which coexisted in the Western Interior of North America, during the uppermost *Sciponoceras gracile* Zone of the Cenomanian, and found an average species duration of 2 Ma. Nevesskaia et al. (1987) has also found values lower than 10 Ma for the total duration of bivalve species that flourished in Cenozoic marine half-closed and nearly closed brackish basins during Oligocene-Pliocene of the Paratethys (see also Nevesskaia et al., 2009). Notably, the duration of *Pinzonella neotropica*, *Jacquesia brasiliensis*, and *Naiadopsis lamellosus* is ~5 Ma, corresponding to an age interval substantially lower than those found by Stanley (1990) for marine settings. In turn, *Cowperesia* *anceps* that is recorded throughout the Teresina and Corumbataí formations (*Pinzonella illusa*-*Plesiocyprinella carinata* and *Pinzonella neotropica*-*Jacquesia brasiliensis* biozones) had a total species duration of ~16 Ma substantially larger than that found by Stanley (1990). One possible explanation is that those endemic species were eurythopic.

From local to global Permian bioevents

The transition between the *Pinzonella illusa*-*Plesiocyprinella carinata* and *Pinzonella neotropica*-*Jacquesia brasiliensis* biozones encompasses one of the main faunal turnovers in the fossil record of the Permian Passa Dois Group. Bivalve diversity and abundance dropped significantly at this time (see Simões et al., 2015, p. 23, fig. 6). Hence, if our geochronological data is correct, this marked faunal change has occurred between ~265-262Ma (i.e., Wordian-Capitanian transition). However, the main benthic faunal turnover in the Passa Dois Group is recorded between the *Pinzonella neotropica*-*Jacquesia brasiliensis* and the *Terraia curvata* assemblage, in the Serrinha Member of the Rio do Rasto Formation (Simões et al., 2015, p. 23, Fig. 11). This faunal change is marked by the end of the *Pinzonella*-dominated bivalve assemblages of the Corumbataí-Teresina formations and its substitution by the *Terraia*-dominated assemblages in the overlying Rio do Rasto Formation (Simões et al., 2015). The species composition, abundance, and dominance in the *Terraia curvata* assemblage differ significantly from the preceding *Pinzonella*-dominated assemblages. Notably, bivalve abundance has never been like that of Corumbataí times. The radiometric ages available (Fig. 11) indicate that this bioevent can now be constrained to ~257.5 Ma, in the middle of the Wuchiapingian.

On the other hand, the ca. 262 Ma to 257 Ma of the total local range of the *Pinzonella neotropica*-*Jacquesia brasiliensis* indicates that the endemic bivalves survived the end-Guadalupian (ca. 259 Ma) extinction event unscathed. Marine tropical taxa, including the fusulinids, giant bivalves (i.e., family *Alatoconchidae*), and rugose corals that thrived in the Panthalassa and Paleo-Tethys were severely affected by this event (see Arefifard and Payne, 2020, and references therein). Global warming-induced failure of marine associations following the Emeishan volcanism is the main trigger evocated for the end-Guadalupian extinct event (Arefifard and Payne, 2020). Protected within an isolate, continental-scale, inland aquatic system in the Gondwana supercontinent, the Corumbataí-Teresina bivalves were away from this Guadalupian/Lopingian benthic marine biotic crises, showing how the open oceans and the coeval inland seas (lake-seas) have very distinct ecological and evolutionary responses.

3.6. Conclusion

The tuff bed sample collected in the upper part of the Corumbataí Formation, in the northernmost Paraná Basin (Goiás State), has a Wordian depositional age of 265.17±3.2 Ma. This U-Pb age with Lu-Hf isotopic data, whole-rock geochemistry, and atmospheric circulation data, allows us to pinpoint the source of this ash with confidence and related it to the Frontal Cordillera magmatism (ca. 260 – 269 Ma). The chronologic constraints based on the age of the most recent volcanic tuff of the Irati Formation (275.75 Ma; Cagliari et al., 2022) and the age for the top of the Corumbataí Formation presented here (265.17 Ma) provide a sedimentation rate of ca. 7.5 m/Myr for the Serra Alta and Corumbataí formations, in the northern part of Paraná Basin.

This radiometric age is important to constrain the bivalve species duration and the relative ages of some bivalve Association Biozones of the Corumbataí Formation, the most important benthic macrofossils for biostratigraphy and intra and interbasinal correlations in the Passa Dois Group. The vertical distribution of the *Pinzonella neotropica-Jacquesia brasilensis* is ~5 Ma (262.38 Ma to 257.5 Ma), substantially lower than the age interval proposed by Stanley (1990) for marine environments.

Finally, our geochronological data allow for the transition of the bivalve diversity that fall between the *Pinzonella illusa-Plesiocyprinella carinata* and *Pinzonella neotropica-Jacquesia brasiliensis* biozones to be constrained between ~265-262Ma (i.e., Wordian-Capitanian transition); and, in turn, the biggest faunal change in the Passa Dois Group between the *Pinzonella neotropica-Jacquesia brasiliensis* and the *Terraia curvata* assemblage can now be constrained to ~257.5 Ma (middle Wuchiapingian). It is important to note that *Pinzonella neotropica-Jacquesia brasiliensis* assemblage are contemporaneous with the end-Guadalupian (ca. 259 Ma) extinct event that severely affected the Panthalassa and Paleo-Tethys biota. However, the Corumbataí-Teresina bivalves were protected within an isolate, continental-scale, inland aquatic system, confirming how very distinct the ecological and evolutionary dynamics were in this late Paleozoic megalake.

Acknowledgements

We would like to thank Paloma Promenzio for field assistance and detrital zircon preparations. B. Christofoletti is a fellow of the master's scholarship of the Training of Human Resources in Petroleum Geology Program - UNESP - PRH 40-ANP, supported with financial investment of oil companies qualified in the P, D&I Clause of ANP Resolution No. 50/2015. Lucas V. Warren, Marcello G. Simões and Mario L. Assine are research fellows of the CNPq. Our acknowledgements are extending to financial support from PICT 2018-4022 to Lucía Gómez Peral (FONCYT), and the Centro de Investigaciones Geológicas (CIG) laboratories especially to G. Kurten, L. Vigiani and V. Liegl for their assistance in XRD analysis, and to C. Cavarozzi and V. García for ICP-MS analysis.

3.7. References

Aragão M and Scardia G (2021) Middle–Late Permian magnetostratigraphy and the onset of the Illawarra Reversals in the northeastern Parana Basin, South America. *Geophysical Journal International* **225**, 860-871. https://doi.org/10.1093/gji/ggab011

Arefifard S and Payne JL (2020) End-Guadalupian extinction of larger fusulinids in central Iran and implications for the global biotic crisis. *Palaeogeography, Palaeoclimatology, Palaeoecology* 550, Article 109743. https://doi.org/10.1016/j.palaeo.2020.109743

Baines PG and Sparks RSJ (2005) Dynamics of giant volcanic ash clouds from supervolcanic eruptions. *Geophysical Research Letters* **32**, Article L24808. https://doi.org/10.1029/2005GL024597

Bastos LPH, Rodrigues R, Pereira E, Bergamaschi S, Alferes CLF, Augland LE, Domeier M, Planke S and Svensen HH (2021) The birth and demise of the vast epicontinental Permian Irati-Whitehill sea: Evidence from organic geochemistry, geochronology, and paleogeography. *Palaeogeography, Palaeoclimatology, Palaeoecology* **562**, Article 110103. https://doi.org/10.1016/j.palaeo.2020.11010

Beckett FM, Witham CS, Hort MC, Stevenson JA, Bonadonna C and Millington SC (2015) Sensitivity of dispersion model forecasts of volcanic ash clouds to the physical characteristics of the particles. *Journal of Geophysical Research: Atmospheres* **120**, 11-636. https://doi.org/10.1002/2015JD023609**Beurlen K** (1954) Horizontes fossilíferos das Camadas Serra Alta do Paraná. *Boletim DGM-DNPM* **152**, 1-30.

Beurlen K (1957) Faunas salobras fósseis e o tipo ecológico-paleogeográfico das faunas Gondwânicas no Brasil. *Anais da Academia Brasileira de Ciências* **29**, 229-241.

Biscaye PE (1965) Mineralogy and Sedimentation of Recent Deep-Sea Clay in the Atlantic Ocean and Adjacent Seas and Oceans. *Geological Society of America Bulletin* **76**, 803–832. https://doi.org/10.1130/0016-7606(1965)76[803:MASORD]2.0.CO;2

Black LP and Gulson BL (1978) The age of the Mud Tank carbonatite, Strangeways Range, Northern Territory. *BMR Journal of Australian Geology and Geophysics* **3**, 227–232.

Black LP, Kamo SL, Allen CM, Aleinikoff JN, Davis DW, Korsch RJ, Foudoulis C (2003) TEMORA 1: a new zircon standard for Phanerozoic U–Pb geochronology. *Chemical Geology* **200**, 155-170. https://doi.org/10.1016/S0009-2541(03)00165-7

Blichert-Toft J (2008) The Hf isotopic composition of zircon reference material 91500. *Chemical Geology* **253**, 252-257. https://doi.org/10.1016/j.chemgeo.2008.05.014

Boynton WV (1984) Cosmochemistry of the rare earth elements; meteorite studies. In: Henderson, P. (Ed.), Rare Earth Element Geochemistry. *Elsevier*, Amsterdam, pp. 63–114.

Brown G and Brindley GW (1980) X-ray diffraction procedures for clay mineral identification. In: Crystal structures of clay minerals and their X-ray identification (G.W. Brindley and G. Brown ed.). *Mineralogical Society of Great Britain and Ireland*, pp. 305-359.

Cagliari J, Serratt H, Cassel MC, Schmitz MD and Chemale Jr F (2022) New high-precision U-Pb zircon age of the Irati Formation (Paraná Basin) and implications for the timing of the Kungurian anoxic events recorded in southern Gondwana. *Gondwana Research* **107**, 134-145. https://doi.org/10.1016/j.gr.2022.03.004

Capaldi TN, McKenzie NR, Horton BK, Mackaman-Lofland C, Colleps CL and Stockli DF (2021) Detrital zircon record of Phanerozoic magmatism in the southern Central Andes. *Geosphere* **17**, 876-897. https://doi.org/10.1130/GES02346.1

Castillo P, Fanning CM, Hervé F and Lacassie JP (2017) Characterisation and tracing of Permian magmatism in the south-western segment of the Gondwanan margin; U–Pb age, Lu–Hf and O isotopic compositions of detrital zircons from metasedimentary complexes of northern Antarctic Peninsula and western Patagonia. *Gondwana Research* **36**, 1-13. https://doi.org/10.1016/j.gr.2015.07.014

Chauvel C, Lewin E, Carpentier M, Arndt NT and Marini JC (2008) Role of recycled oceanic basalt and sediment in generating the Hf–Nd mantle array. *Nature Geoscience* **1**, 64-67. https://doi.org/10.1038/ngeo.2007.51

Chernicoff CJ, Zappettini EO., Santos JOS, McNaughton NJ and Belousova E (2013) Combined U-Pb SHRIMP and Hf isotope study of the Late Paleozoic Yaminué Complex, Rio Negro Province, Argentina: Implications for the origin and evolution of the Patagonia composite terrane. *Geoscience Frontiers* **4**, 37–56. https://doi.org/10.1016/j.gsf.2012.06.003

Cohen KM, Finney SC, Gibbard PL and Fan JX (2013, updated) The ICS International Chronostratigraphic Chart. *Episodes* **36**, 199-204.

Coutinho JMV, Dos Santos PR and Coimbra AM (1988) Ash-fall derived vitroclastic tuffaceous sediments in the Permian of the Paraná Basin and its provenance. *Abstracts of the International Gondwana Symposium* **7**, p.78.

Coutinho JMV and Hachiro J (2005) Distribution, mineralogy, petrography, provenance and significance of Permian ash-carrying deposits in the Paraná Basin. *Geologia USP* **5**, 29-39. https://doi.org/10.5327/S1519-874X2005000100003

CPRM – SERVIÇO GEOLÓGICO DO BRASIL. 2006. Cartas geológicas do Brasil ao milionésimo

Crasquin S, Forel MB, Feng Q, Yuan A, Baudin F and Collin PY (2010) Ostracods (Crustacea) through the Permian-Triassic boundary in South China: The Meishan stratotype (Zhejiang Province). *Journal of Systematic Palaeontology* **8**, 331–370. https://doi.org/10.1080/14772011003784992

Daemon RF and Quadros LP (1970) Bioestratigrafia do Neopaleozóico da Bacia do Paraná. *Anais do Congresso Brasileiro de Geologia*, **24**.

Daemon RF (1974) Integragação dos resultados palinológicos aos de fauna e flora de camadas fossiliferas do Neopaleozóico da Bacia do Paraná-Implicações estratigráficas-paleogeográficas. *Revista UNIMAR* **1**, 25-41.

Daemon RF, Casaletti PL and Ciguel JHG (1996) Biopaleogeografia da Bacia do Paraná. *Simpósio Sulamericano do Siluro-Devoniano*, pp.55-99.

Du Toit AL (1927) Comparação geológica entre a América do Sul e África do Sul. *DNPM-SGM*, Rio de Janeiro, 179p.

Fanning CM, Hervé F, Pankhurst RJ, Rapela CW, Kleiman LE, Yaxley GM and Castillo P (2011) Lu–Hf isotope evidence for the provenance of Permian detritus in accretionary complexes of western Patagonia and the northern Antarctic Peninsula region. *Journal of South American Earth Sciences* **32**, 485-496. https://doi.org/10.1016/j.jsames.2011.03.007

Faure G (1986) Isotope systematics in two-component mixtures. *Principles of Isotope Geology*, pp.141-153.

Faure K and Cole D (1999). Geochemical evidence for lacustrine microbial blooms in the vast Permian Main Karoo, Paraná, Falkland Islands and Huab basins of southwestern Gondwana. *Palaeogeography, Palaeoclimatology, Palaeoecology* **152**, 189-213. https://doi.org/10.1016/S0031-0182(99)00062-0

Ghilardi RP and Simões MG (2002) Foram os bivalves do Grupo Passa Dois (exclusive Formação Rio do Rasto), Neopermiano, invertebrados tipicamente dulcícolas? *Pesquisas em Geociências* **29**, 83-95.

Gregori DA, Strazzere L, Barros M, Benedini L, Marcos P and Kostadinoff J (2021) The Mencué batholith: Permian episodic arc-related magmatism in the western North Patagonian Massif, Argentina. *International Geology Review* **63**, 317-341. https://doi.org/10.1080/00206814.2019.1710865

Guerra-Sommer M, Cazzulo-Klepzig M, Santos JOS, Hartmann LA, Ketzer JM and Formoso MLL (2008) Radiometric age determination of tonsteins and stratigraphic constraints for the Lower Permian coal succession in southern Paraná Basin, Brazil. *International Journal of Coal Geology* **74**, 13-27. https://doi.org/10.1016/j.coal.2007.09.005

Guerrini VB, Matos SA, Rohn R, Varejão FG, Warren LVand Simões MG (2020) The last chapter of 30 million years of molluscan evolution: Permian non-marine bivalves of the Rio do Rasto Formation, Paraná Basin, Brazil. *PalZ* **94**, 487-512. https://doi.org/10.1007/s12542-019-00455-0

Holz M, França AB, Souza PA, Iannuzzi R and Rohn R (2010) A stratigraphic chart of the Late Carboniferous/Permian succession of the eastern border of the Paraná Basin, Brazil, South America. *Journal of South American Earth Sciences* **29**, 381–399. https://doi.org/10.1016/j.jsames.2009.04.004

Jackson SE, Pearson NJ, Griffin WL and Belousova EA (2004) The application of laser ablation-inductively coupled plasma-mass spectrometry to in-situ U-Pb zircon geochronology. *Chemical Geology* **211**, 47–69. https://doi.org/10.1016/j.chemgeo.2004.06.017

Kay SM, Ramos VA, Mpodozis C and Sruoga P (1989) Late Paleozoic to Jurassic silicic magmatism at the Gondwana margin: analogy to the Middle Proterozoic in North America. *Geology* **17**, 324–328. https://doi.org/10.1130/0091-7613(1989)017<0324:LPTJSM>2.3.CO;2

Keidel H (1916) La geología de las sierras de la provincia de Buenos Aires y sus relaciones con las montañas de Sud Africa y los Andes. *Talleres gráficos del Ministerio de agricultura de la nación*.

Kleiman LE and Japas MS (2009) The Choiyoi volcanic province at 34°–36°S (San Rafael, Mendoza, Argentina): implications for the late Paleozoic evolution of the southwestern margin of Gondwana. *Tectonophysics* **473**, 283–299. https://doi.org/10.1016/j.tecto.2009.02.046

Koch CF (1980) Bivalve species duration, areal extent, and population size in a Cretaceous Sea. *Paleobiology* **6**, 184-192. https://doi.org/10.1017/S0094837300006746

Limarino CO, Césari SN, Spalletti LA, Taboada AC, Isbell JL, Geuna S and Gulbranson, EL (2014) A paleoclimatic review of southern South America during the late Paleozoic: a record from icehouse to extreme greenhouse conditions. *Gondwana Research* **25**, 1396-1421. https://doi.org/10.1016/j.gr.2012.12.022

López-Gamundi OR (2006) Permian plate margin volcanism and tuffs in adjacent basins of west Gondwana: age constrains and common characteristics. *Journal of South American Earth Sciences* **22**, 227–238. https://doi.org/10.1016/j.jsames.2006.09.012

Ludwig KR (2003) User's Manual for Isoplot 3.00: A Geochronological Toolkit for Microsoft Excel. *Berkeley Geochronology Center, Special Publication*, 1–70.

Maranhão MSAS (1995) Fósseis das formações Corumbataí e Estrada Nova do Estado de São Paulo: subsídios ao conhecimento paleontológico e bioestratigráfico. PhD thesis, Universidade de São Paulo.

Maranhão MSAS and Petri S (1996) Novas ocorrências de fósseis nas formações Corumbataí e Estrada Nova de São Paulo e considerações sobre o seu significado paleontológico e bioestratigráfico. *Revista do Instituto Geológico* **17**, 33–54.

Matos SLF (1995) O contato entre o Grupo Passa Dois e a Formação Piramboia na borda Leste da Bacia do Paraná no Estado de São Paulo. MSc thesis, Universidade de São Paulo.

Matos SLF and Coimbra AM (1997) Sucessão de Fácies na Camada Porangaba, Grupo Passa Dois, Estado de São Paulo. *Revista Brasileira de Geociências* **27**, 377-386.

Matos SA, Warren LV, Fürsich FT, Alessandretti L, Assine ML, Riccomini C and Simoes MG (2017) Paleoecology and paleoenvironments of Permian bivalves of the Serra Alta Formation, Brazil: Ordinary suspension feeders or Late Paleozoic Gondwana seep organisms? *Journal of South American Earth Sciences* **77**, 21-41. https://doi.org/10.1016/j.jsames.2017.04.007

Maynard JB, Chocyk-Jaminski M, Gaines RR, Huff WD, Krekeler MP, Prokopenko M and Summers AM (1996) Bentonites in the Late Permian (Tatarian) Irati Formation of Brazil; geochemistry and potential for stratigraphic correlation. *Geological Society of America, Abstracts with Programs* **28**, pp. 280.

Mendes JC (1949) Novos Lamelibrânquios fósseis da Série Passa Dois, sul do Brasil. *Divisão Geológica e Mineralógica do Brasil* **133**, 1–40.

Mendes JC (1952) A Formação Corumbataí na região do Rio Corumbataí. Estratigrafia e descrição dos lamelibrânquios. *Boletim USP* **145**, pp. 119.

Mendes JC (1967) The Passa Dois Group (the Brazilian portion of the Parana Basin). In: *Problems in Brazilian Gondwana Geology* (JJ Bigarella, RD Becker, ID Pinto Eds.), Curitiba, 119-166.

Mendes JC (1984) Sobre os paleoambientes deposicionais do Grupo Passa Dois. *Revista do Instituto Geológico* **5**, 15-24.

Milani EJ (1997) Evolução tectono-estratigráfica da Bacia do Paraná e seu relacionamento com a geodinâmica fanerozóica do Gondwana sul-ocidental. PhD thesis, Universidade Federal do Rio Grande do Sul.

Milani EJ and Ramos VA (1998) Orogenias paleozóicas no domínio sul-ocidental do Gondwana e os ciclos de subsidência da Bacia do Paraná. *Revista Brasileira de Geociências* **28**, 473-484.

Milani EJ, Araujo LM, Cupertino JA, Faccini UF and Scherer CM (1998) Sequences and stratigraphic hierarchy of the Parana Basin (Ordovician Cretaceous), Southern Brazil. *Boletim IG-USP* **29**.

Milani EJ, Melo JHG, Souza PA, Fernades LA and França AB (2007) Bacia do Paraná. *Boletim de Geociências da Petrobrás* **15**, 265–287.

Moore DM and Reynolds Jr RC (1997) X-ray Diffraction and the Identification and Analysis of Clay Minerals, 2nd. Oxford University Press, Oxford.

Moraes Rego LF (1930) A geologia do petróleo no Estado de São Paulo. *Boletim do Serviço Geológico e Mineral Brasileiro*, Rio de Janeiro, 110 p.

Mori ALO, Souza PA, Marques JC and Cunha Lopes R (2012) A new U–Pb zircon age dating and palynological data from a Lower Permian section of the southernmost Paraná Basin, Brazil: biochronostratigraphical and geochronological implications for Gondwanan correlations. *Gondwana Research* **21**, 654-669. https://doi.org/10.1016/j.gr.2011.05.019

Neregato R, Souza PAD and Rohn R (2008) Registros palinológicos inéditos nas formações Teresina e Rio do Rasto (Permiano, Grupo Passa Dois, Bacia do Paraná): implicações biocronoestratigráficas e paleoambientais. *Pesquisas em Geociências* **35**, 9-21.

Nevesskaia LA, Iljina LB and Paramonova NP (1987) Evolutionary Transformations of Mollusks in Basins of Different Types. *Paleontological Journal* **4**, 5–15.

Nevesskaia LA, Goncharova I, Il'ina LB and Popov SV (2009) Evolutionary transformations of the malacofaunas in the Neogene basins of Paratethys as an example of development of the ecosystems of insular type. *Zhurnal Obshcheĭ Biologii* **70**, 396-414. (In Russian).

Ng C, Vega CS and Maranhão MDSAS (2019) Mixed carbonate-siliciclastic microfacies from Permian deposits of Western Gondwana: Evidence of gradual marine to continental transition or episodes of marine transgression? *Sedimentary Geology* **390**, 62-82. https://doi.org/10.1016/j.sedgeo.2019.07.006

Palcu DV, Patina IS, Șandric I, Lazarev S, Vasiliev I, Stoica M and Krijgsman W (2021) Late Miocene megalake regressions in Eurasia. *Scientific Reports* **11**, Article 11471. https://doi.org/10.1038/s41598-021-91001-z

Parrish JT and Curtis RL (1982) Atmospheric circulation, upwelling, and organic-rich rocks in the Mesozoic and Cenozoic eras. *Palaeogeography, Palaeoclimatology, Palaeoecology* **40**, 31-66. https://doi.org/10.1016/0031-0182(82)90084-0

Pepper M, Gehrels G, Pullen A, Ibanez-Mejia M, Ward KM and Kapp P (2016) Magmatic history and crustal genesis of western South America: Constraints from U-Pb ages and Hf isotopes of detrital zircons in modern rivers. *Geosphere* **12**, 1532–1555. https://doi.org/10.1130/GES01315.1

Perron P, Le Pourhiet L, Guiraud M, Vennin E, Moretti I, Portier É and Konaté M (2021) Control of inherited accreted lithospheric heterogeneity on the architecture and the low, long-term subsidence rate of intracratonic basins. *Bulletin de la Société Géologique de France*, 192.

Petri S and Coimbra AM (1982) Estruturas sedimentares das Formações Irati e Estrada Nova (Permiano) e sua contribuição para elucidação dos seus paleoambientes geradores. *Congresso Latino-americano de Geologia* **5**, 353-371.

Poma S, Zappettini EO, Quenardelle S, Santos JO, Koukharsky M, Belousova E and McNaughton N (2014) Geochemistry, U-Pb SHRIMP zircon dating and Hf isotopes of the Gondwanan magmatism in NW

Argentina: petrogenesis and geodynamic implications. *Andean Geology* **41**, 267-292. https://doi.org/10.5027/andgeoV41n2-a01

Pupin JP and Turco G (1975) Typologie de zircon accessoire dans les roches plutoniques dioritiques, granitiques et syenitiques, Facteurs essentiels determinant les variations typologiques. *Petrologie* **1**, 139-156.

Pupin JP (1976) Signification des caractgres morphologiques du zircon commun des roches en petrologie. Base de la methode typologique. Applications. PhD thesis, Nice University.

Pupin JP (1980) Zircon and granite petrology. *Contributions to mineralogy and petrology* **73**, 207-220.

Quintas MCL, Mantovani MSM and Zalán PV (1999) Contribuição ao estudo da evolução mecânica da Bacia do Paraná. *Revista Brasileira de Geociências* 29, 217–226.

Ragonha EW (1984) Taxionomia de dentes e espinhos isolados de Xenacanfhodii (condrichfhyes, elasmobranchii) da Formação Corumbataí: considerações cronológicas e paleoambientais. PhD thesis, Universidade de São Paulo.

Ramos VA, Jordan TE, Allmendinger RW, Mpodozis C, Kay SM, Cortés JM and Palma M (1986) Paleozoic terranes of the central Argentine-Chilean Andes. *Tectonics* **5**, 855-880. https://doi.org/10.1029/TC005i006p00855

Reed FRC (1929) Faunas triássicas do Brasil. *Serviço Geológico Minerário do Brasil* **9**, 1-97.

Reed FRC (1932) Triassic fossils from Brazil. *The Annals & Magazine of Natural History* **2**, 39-48.

Reed FRC (1935) Some triassic lamellibranchs from Brazil and Paraguay. *Geological Magazine* **72**, 33-42. https://doi.org/10.1017/S0016756800092311

Riccomini C, Chamani MAC, Agena SS, Fambrini GL, Fairchild TR and Coimbra AM (1992) Earthquake-induced liquefaction features in the Corumbataí Formation (Permian, Paraná Basin, Brazil) and the dynamics of Gondwana. *Anais da Academia Brasileira de Ciências* **64**, pp. 210.

Rocha HDV, Mendes M, Pereira Z, Rodrigues C, Fernandes P, Lopes G, Santa'Anna LG, Tassinari CCG and Sousa ML (2020) New palynostratigraphic data of the Irati (Assistência Member) and the Corumbataí formations, Paraná Basin, Brazil, and correlation with other south American basins. *Journal of South American Earth Sciences* **102**, Article 102631. https://doi.org/10.1016/j.jsames.2020.102631

Rocha-Campos AC, Basei MAS, Nutman AP and Santos PD (2006) SHRIMP U-Pb zircon geochronological calibration of the late Paleozoic supersequence, Paraná Basin, Brazil. In: *5th South American Symposium on Isotope Geology*, Buenos Aires, Argentina.

Rocha-Campos AC, Basei MA, Nutman AP, Kleiman LE, Varela R, Llambias E, Canile FM and Da Rosa ODC (2011) 30 million years of Permian volcanism recorded in the Choiyoi igneous province (W Argentina) and their source for younger ash fall deposits in the Paraná Basin: SHRIMP U–Pb zircon geochronology evidence. *Gondwana Research* **19**, 509-523. https://doi.org/10.1016/j.gr.2010.07.003

Rocha-Campos AC, Basei MAS, Nutman AP, Santos PRD, Passarelli CR, Canile FM, Rosa OCR, Fernandes MT, Santa Ana H and Veroslavsky G (2019) U-Pb zircon dating of ash fall deposits from the paleozoic Paraná basin of Brazil and Uruguay: a reevaluation of the stratigraphic correlations. *The Journal of Geology* **127**, 167-182. https://doi.org/10.1086/701254

Rocher S, Vallecillo B and Alasino P (2015) El Grupo Choiyoi (Pérmico temprano-medio) en la Cordillera Frontal de Calingasta, San Juan, Argentina: volcanismo de arco asociado a extensión. *Revista Mexicana de Ciencias Geológicas* **32**, 415-432.

Rohn R and Rösler O (1987) Relações entre a Flora Permiana do Gondwana e as floras das províncias setentrionais. *Congresso Brasileiro de Paleontologia* 10, 885-899.

Rohn R and Lavina EL (1993) Cronoestratigrafia do Grupo Passa Dois. Simpósio de Cronoestratigrafia da Bacia do Paraná, 77-80.

Rohn R (1994) Evolução ambiental da Bacia do Paraná durante o Neo-Permiano no leste de Santa Catarina e do Paraná. PhD thesis, Universidade de São Paulo.

Rohn R (2007) The Passa Dois Group (Paraná Basin, Permian): investigations in progress. *Extended abstracts from 1st Workshop on Problems in Western Gondwana Geology*, 151–157.

Rollinson HR (1993) Using trace element data, part 4. *Using Geochemical Data Book: Evaluation, Presentation, Interpretation*. JohnWiley & Sons Inc., New York, 352 pp.

Rose WL and Chesner CA (1987) Dispersal of ash in the great Toba eruption, 75 ka. *Geology* **15**, 913–917. https://doi.org/10.1130/0091-7613(1987)15<913:DOAITG>2.0.CO;2

Rostirolla SP, Mancini F, Rigoti A and Kraft RP (2003) Structural styles of the intracratonic reactivation of the Perimbó fault zone, Paraná basin, Brazil. *Journal of South American Earth Sciences* **16**, 287-300. https://doi.org/10.1016/S0895-9811(03)00065-8

Runnegar B and Newell ND (1971) Caspian-like relict molluscan fauna in South American Permian. *Bulletin of American Museum of Natural History* **146**, 1-66.

Runnegar B (1977) Marine fossil invertebrates of the Gondwanaland: paleogeographic implications. *Papers of the International Gondwana Symposium*, **4**, 305-339.

Santos RV, Souza PA, de Alvarenga CJS, Dantas EL, Pimentel MM, de Oliveira CG and de Araújo LM (2006) Shrimp U–Pb zircon dating and palynology of bentonitic layers from the Permian Irati Formation, Paraná Basin, Brazil. *Gondwana Research* **9**, 456-463. https://doi.org/10.1016/j.gr.2005.12.001

Santos MM, Lana C, Scholz R, Buick I, Schmitz MD, Kamo SL, Gerdes A, Corfu F, Tapster S, Lancaster P, Storey CD, Basei MAS, Tohver E, Alkmim A, Nalini H, Krambrock K, Fantini C and Wiedenbeck M (2017) A new appraisal of Sri Lankan BB zircon as a reference material for LA-ICP-MS U-Pb geochronology and Lu-Hf isotope tracing. *Geostandards and Geoanalytical Research* **41**, 335-358. https://doi.org/10.1111/ggr.12167

Schneider RL, Mühlmann H, Tommasi E, Medeiros RA, Daemon RF and Nogueira AA (1974) Revisão estratigráfca da Bacia do Paraná. In: *28° Congresso Brasileiro de Geologia*, Porto Alegre, 41–66.

Shu O and Utting J (1990) Palynology of Upper Permian and Lower Triassic rocks, Meishan, Changxing County, Zhejiang Province, China. *Review of Palaeobotany and Palynology* **66**, 65–103. https://doi.org/10.1016/0034-6667(90)90029-I

Silva AF, Dani N, Remus MVD, Sommer MG and Horn BLD (2017) Bentonitas da Formação Irati no setor sul da Bacia do Paraná. *Geologia USP* **17**, 75-88. https://doi.org/10.11606/issn.2316-9095.v17-368

Silva JP, Lana C, Mazoz A, Buick I and Scholz R (2022) U-Pb Saturn: New U-Pb/Pb-Pb Data Reduction Software for LA-ICP-MS. *Geostandards and Geoanalytical Research* **47**, 49-66. https://doi.org/10.1111/ggr.12474

Simões MG (1992) Pelecípodes da Formação Palermo (Permiano) de São Sepé (RS) e Guiratinga (MT): implicações na evolução da fauna neopaleozóica da Bacia do Paraná. PhD thesis, Universidade de São Paulo.

Simões MG and Kowalewski M (1998) Shell beds as paleoecological puzzles: a case study from the Upper Permian of the Paraná Basin, Brazil. *Facies* **38**, 175-195. https://doi.org/10.1007/BF02537364

Simões MG, Rocha-Campos AC and Anelli LE (1998) Paleoecology and evolution of Permian pelecypod assemblages (Paraná Basin) from Brazil. In: *Bivalves – An Eon of Evolution- Paleobiological Studies Honoring Norman D. Newell* (PA, Johnston and JW Haggart Eds), University of Calgary Press, Calgary, 443–452.

Simões MG, Torello FF, Mello LHC and Ghilardi RP (2000) O conteúdo fossilífero de novos afloramentos do Grupo Passa Dois (Neopermiano), nas porções centro-sul e nordeste do Estado de São Paulo: implicações bioestratigráficas e paleoecológicas. *Acta Geologica Leopoldensia* **23**, 61-90.

Simões MG, Matos SA, Anelli LE, Rohn R, Warren LV and David JM (2015) A new Permian bivalve-dominated assemblage in the Rio do Rasto Formation, Paraná Basin, Brazil: faunal turnover driven by regional-scale environmental changes in a vast epeiric sea. *Journal of South American Earth Sciences* **64**, 14-26. https://doi.org/10.1016/j.jsames.2015.09.009

Simões MG, Guerrini VB, Matos SA and Rohn R (2020) Morphology and taxonomic position of the bizarre Permian pachydomid bivalve Leinzia from Western Gondwana. *Acta Palaeontologica Polonica* **65**, 291-303. https://doi.org/10.4202/app.00665.2019

Sláma J, Košler J, Condon DJ, Crowley JL, Gerdes A, Hanchar JM, Horstwood MSS, Morris GA, Lutz N, Norberg N, Schaltegger U, Schoene B, Tubrett MN and Whitehouse MJ (2008) Plešovice zircon—a new natural reference material for U–Pb and Hf isotopic microanalysis. *Chemical Geology* **249**, 1-3. https://doi.org/10.1016/j.chemgeo.2007.11.005

Söderlund U, Patchett PJ, Vervoort JD and Isachsen CE (2004) The 176Lu decay constant determined by Lu–Hf and U–Pb isotope systematics of Precambrian mafic intrusions. *Earth and Planetary Science Letters* **219**, 311-324. https://doi.org/10.1016/S0012-821X(04)00012-3

Sohn IG and Rocha-Campos AC (1990) Late Paleozoic (Gondwanan) ostracodes in the Corumbataí Formation, Paraná Basin, Brazil. *Journal of Paleontology* **64**, 116–128. https://doi.org/10.1017/S0022336000042293

Sousa SHM (1985) Fácies sedimentares das formações Estrada Nova e Corumbataí no Estado de São Paulo. MSc thesis, Universidade de São Paulo.

Souza PA and Marques-Toigo M (2005) Progress on the palynostratigraphy of the Permian strata in Rio Grande do Sul State, Paraná basin, Brazil. *Anais da Academia Brasileira de Ciências* **77**, 353-365.

Stanley SM (1990) The general correlation between rate of speciation and rate of extinction: fortuitous causal linkages. In: *Causes of Evolution: A Paleontological Perspective* (RM Ross and WD Allmon Eds.). Chicago University Press, Chicago, 103– 172.

Suguio K, Salati C and Barcelos JH (1974) Calcários oolíticos de Taguaí, SP e seu possível significado paleoambiental na deposição da Formação Estrada Nova. *Revista Brasileira de Geociências* **4**, 142-160.

Sun S and McDonough WF (1989) Chemical and Isotopic Systematics of Oceanic Basalts: Implications for Mantle Composition and Processes. In: Magmatism in the Ocean Basins (AD, Saunders and MJ Norry Eds.). *Geological Society of London Special Publications* **42**, 313–345.

Tohver E, Schmieder M, Lana C, Mendes PS, Jourdan F, Warren LV and Riccomini C (2018) End-Permian impactogenic earthquake and tsunami deposits in the intracratonic Paraná Basin of Brazil. *GSA Bulletin* **130**, 1099-1120. https://doi.org/10.1130/B31626.1

Tomassi HZ (2009) Taxonomia, Tafonomia e Paleoecologia de Ostracodes (Crustacea) da Formação Corumbataí, Permiano da Bacia do Paraná, Estado de Goiás, Brasil. MSc. Thesis, Universidade de Brasília.

Turra BB (2009) Diques clásticos da Formação Corumbataí, Bacia do Paraná, no contexto da tectônica permotriássica do Gondwana Ocidental. MSc thesis, Universidade de São Paulo.

Valencio DA, Rocha-Campos AC and Pacca IG (1975) Paleomagnetism of some sedimentary rocks of the late Paleozoic Tubarão and Passa Dois Groups from the Paraná Basin, Brazil. *Revista Brasileira de Geociencias* **5**, 186–197.

Varejão FG, Warren LV, Alessandretti L, Rodrigues MG, Riccomini C, Assine M, Cury LF, Faleiros FM and Simões MG (2022) Late Permian siliceous hot springs developed on the margin of a restricted epeiric sea: Insights into strata-confined silicification in mixed siliciclastic-carbonate successions. *Palaeogeography, Palaeoclimatology, Palaeoecology* **604**, Article 111213. https://doi.org/10.1016/j.palaeo.2022.111213

Von Huene F (1928) Aphorismen über die Stratigraphie des brasilianisch Staates Sao Paulo. Separat-Abdruck aus dem Centralblatt für Mineralogie, *Geologie und Paläontologie* **10**, 524–531 (German).

Warren LV, Almeida RP, Hachiro J, Machado R, Roldan LF, Steiner SS and Chamani MAC (2008) Evolução Sedimentar da Formação Rio do Rasto (Permo-Triássico da Bacia do Paraná) na porção centro-sul do Estado de Santa Catarina, Brasil. *Revista Brasileira de Geociências* **38**, 213–227.

Warren LV, Assine ML, Simões MG, Riccomini C and Anelli LE (2015) A Formação Serra Alta, Permiano, no centro-leste do Estado de São Paulo, Bacia do Paraná, Brasil. *Brazilian Journal of Geology* **45**, 109-126. https://doi.org/10.1590/23174889201500010008

Wesselingh FP (2007) Long-lived Lake molluscs as island faunas: a bivalve perspective. In: *Biogeography, time, and place: distributions, barriers and islands* (W Renema Eds.). Dordrecht: Springer, 275-314.

White IC (1908) Relatório sobre as Coal Measures e rochas associadas do Sul do Brasil. *Relatório final da Comissão dos Estudos das Minas de Pedra do Brasil*, Rio de Janeiro.

Woodhead JD and Hergt JM (2005) A preliminary appraisal of seven natural zircon reference materials for in situ Hf isotope determination. *Geostandards and Geoanalytical Research* **29**, 183-195. https://doi.org/10.1111/j.1751-908X.2005.tb00891.x

Wu FY, Yang YH, Xie LW, Yang JH and Xu, P (2006) Hf isotopic compositions of the standard zircons and baddeleyites used in U–Pb geochronology. *Chemical Geology* **234**, 105-126. https://doi.org/10.1016/j.chemgeo.2006.05.003

4. CONCLUSÃO

Na presente dissertação foi abordada de forma integrada a sedimentação mista siliciclástica-carbonática da Formação Corumbataí, tendo como meta: (1) caracterizar a arquitetura deposicional e a evolução paleogeográfica da unidade; (2) identificar e interpretar os controles na sedimentação e acomodação; (3) estabelecer a correlação estratigráfica; (4) investigar a idade e origem do nível de cinzas vulcânica presentes na unidade; e (5) balizar cronológicamente a duração das espécies de bivalves e as idades relativas de algumas biozonas presentes na unidade.

A Formação Corumbataí (Bacia do Paraná) regista cinco associações de fácies: *offshore* (FA-1), *offshore-transition* (FA-2), *shoreface* (FA-3), *foreshore* (FA-4) ligadas a depósitos dominantemente siliclásticos, enquanto sucessões dominadas por carbonato são registradas nas *saline flats* (FA-5). Nesse contexto, os resultados obtidos nesta dissertação suportam interpretação de deposição em um mega lago, inaugurando importante linha de pesquisa sobre estratigrafia lacustre e seus controles na Bacia do Paraná. Além disso, a aplicação dos diagramas de Fischer foram eficazes e indicaram tendências arquitetônicas e curvas de acomodação da sucessão estudada, contribuindo para a correlação de trechos geograficamente distantes.

A integração dos dados permitiu o reconhecimento de sequências estratigráficas de 3ª ordem já descritos previamente na literatura - tratos trangressivo (TST_3), referente a Formação Serra Alta, e regressivo (RST_3), que abrange toda a Formação Corumbataí – além de quatro tratos de sistemas de 4ª ordem. Estes, estão diretamente relacionados com os estágios de evolução propostos para a Formação Corumbataí e indicam variação de alta frequência na acomodação da bacia: $TST_{4\text{-}1}$ caracterizado por fácies de offshore depositadas em um lago de água doce com enchimento balanceado (*ballanced fill*). Este primeiro estágio compreende a Formação Serra Alta; $RST_{4\text{-}1}$ representado pela progradação do sistema costeiro com fácies de offshore-transition e shoreface, depositados num estágio *overfilled*; $TST_{4\text{-}2}$ registra a retrogradação do sistema e a deposição de fácies de offshore-transition sobre shoreface. O balanço hídrico positivo permitiu a elevação do nível do lago e o aumento na acomodação, resultando em em um novo estágio *ballanced-fill*; $RST_{4\text{-}2}$ marca o estágio do lago salino *overfilled*, caracterizado pela aridização e condições de nível de água relativamente raso, evidenciado pela presença de fácies carbonáticas e feições evaporíticas, além da dominância da fácies *shoreface*.

Diferentemente de bacias de margem passiva, os lagos endorreicos (como o caso estudado) apresentam baixa taxa de subsidência, a qual controlaria a acomodação da bacia a longo prazo. Assim, as mudanças de curto prazo na acomodação são resultado da interação entre a o equilíbrio hídrico e subsidência. O balanço hídrico nos lagos é uma função da relação entre o abastecimento de água e sedimentos pelos rios, a entrada de águas subterrâneas, precipatação e evaporação. Dessa forma, o nível de base é muito sensível e pode experimentar grandes variações que influenciam influencia diretamente a arquitetura do lago. Para o caso da Formação Corumbataí, os processos autogênicos associados a variações climáticas, tectônicas e eustáticas combinadas (fatores alogênicos) resultaram na deposição em um mega lago que evoluiu de estágios de enchimento balanceado (*ballanced-fill*) para transbordamento (*overfilled*), flutuando entre condições de água doce a salobra. Ainda, a Formação Corumbataí representa importante registro da influência de seiche na sedimentação de mega lagos de reduzida batimetria.

Somado as características sedimentólogicas, a descoberta do nível de cinza vulcânica trouxe implicações relevantes aos aspectos paleogeográficos e paleoecológicos do Permiano do sudoeste de Gondwana. A nova idade U-Pb de 265,17±3,2 Ma, aliado aos dados isotópicos de Lu-Hf, geoquímica de toda a rocha e dados de circulação atmosférica, permitiu atribuir a origem das cinzas ao magmatismo da Cordilheira Frontal. Esta idade também foi importante para restringir a duração das espécies de bivalves e as idades relativas de algumas Biozonas da Associação de bivalves da Formação Corumbataí: a distribuição vertical de *Pinzonella neotropica-Jacquesia brasilensis* é de ~5 Ma (262,38 Ma a 257,5 Ma); a transição da diversidade de bivalves entre as biozonas *Pinzonella illusa-Plesiocyprinella carinata* e *Pinzonella neotropica-Jacquesia brasiliensis* pôde ser restringida entre ~265-262Ma (transição Wordiano-Capitaniana); e a maior mudança faunística no Grupo Passa Dois entre a assembleia de *Pinzonella neotropica-Jacquesia brasiliensis* e *Terraia curvata* (Formação Rio do Rasto) pode agora ser restringida a ~257,5 Ma (Wuchiapingiano médio). Tal distribuição cronólogica das biozonas implica que os bivalves das formações Corumbataí-Teresina não foram afetados oela extinção Permo-Triássica, corroborando com a hipótese de que estes estavam protegidos dentro de um mega lago com as dinâmicas ecológica e evolutiva distintas dos oceanos globais.

APÊNDICE I

Seções Colunares

Apêndice I.I - Seções colunares utilizadas para o empilhamento da seção composta 1. FA: associação de fácies. Escala granulométrica: C: argila; St: silte; FS: areia fina; MS: areia média; CS: areia grossa; G/P: grânulo/ seixo; M: *mudstone*; W: *wackstone*; F: *packstone*; G: *grainstone*; F: *floatstone*; R: *rudstone*.

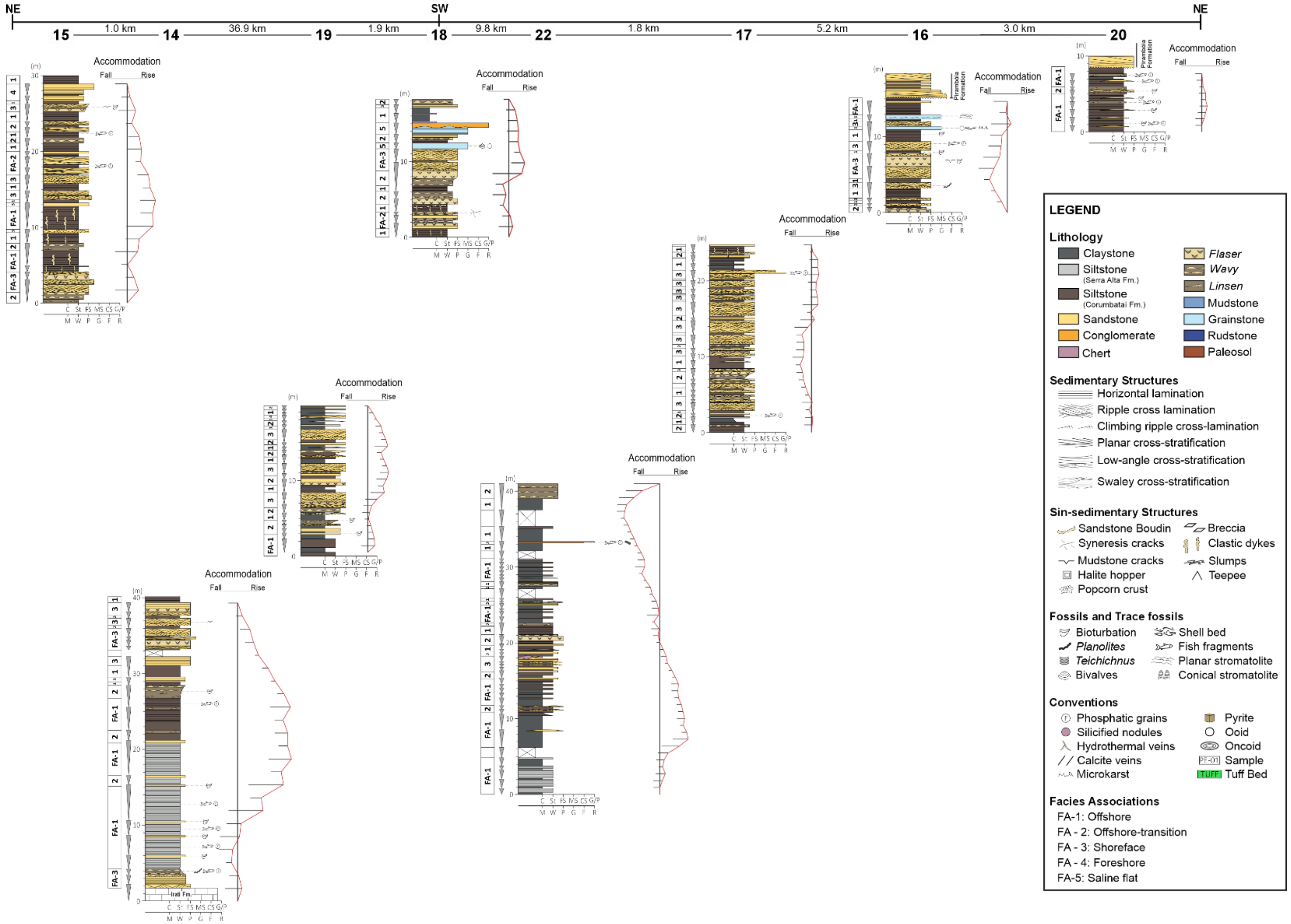

Apêndice I.II - Seções colunares utilizadas para o empilhamento da seção composta 2. FA: associação de fácies. Escala granulométrica: C: argila; St: silte; FS: areia fina; MS: areia média; CS: areia grossa; G/P: grânulo/ seixo; M: *mudstone*; W: *wackstone*; F: *packstone*; G: *grainstone*; F: *floatstone*; R: *rudstone*.

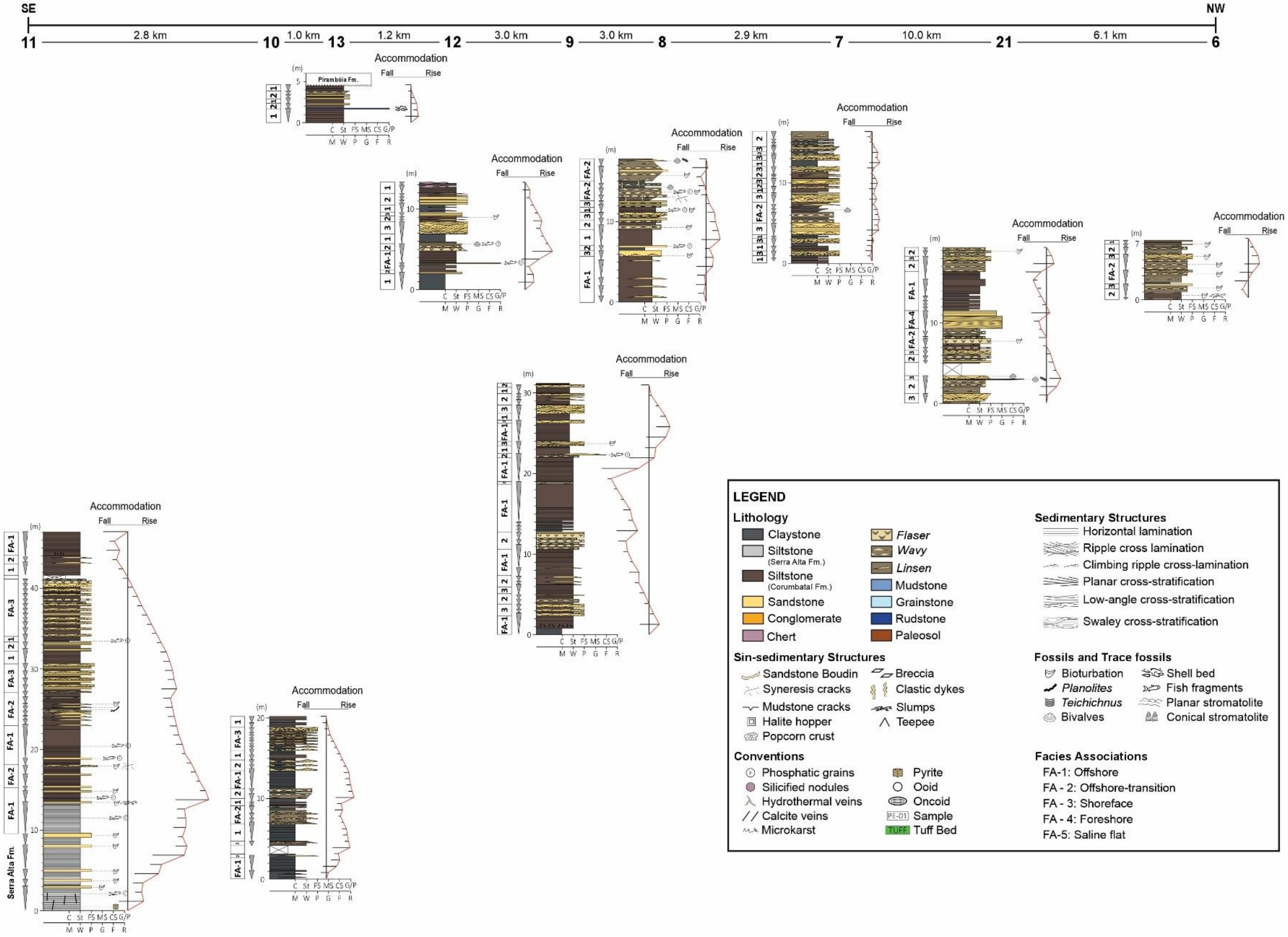

Apêndice I.III - Seções colunares utilizadas para o empilhamento da seção composta 3. FA: associação de fácies. Escala granulométrica: C: argila; St: silte; FS: areia fina; MS: areia média; CS: areia grossa; G/P: grânulo/ seixo; M: *mudstone*; W: *wackstone*; F: *packstone*; G: *grainstone*; F: *floatstone*; R: *rudstone*.

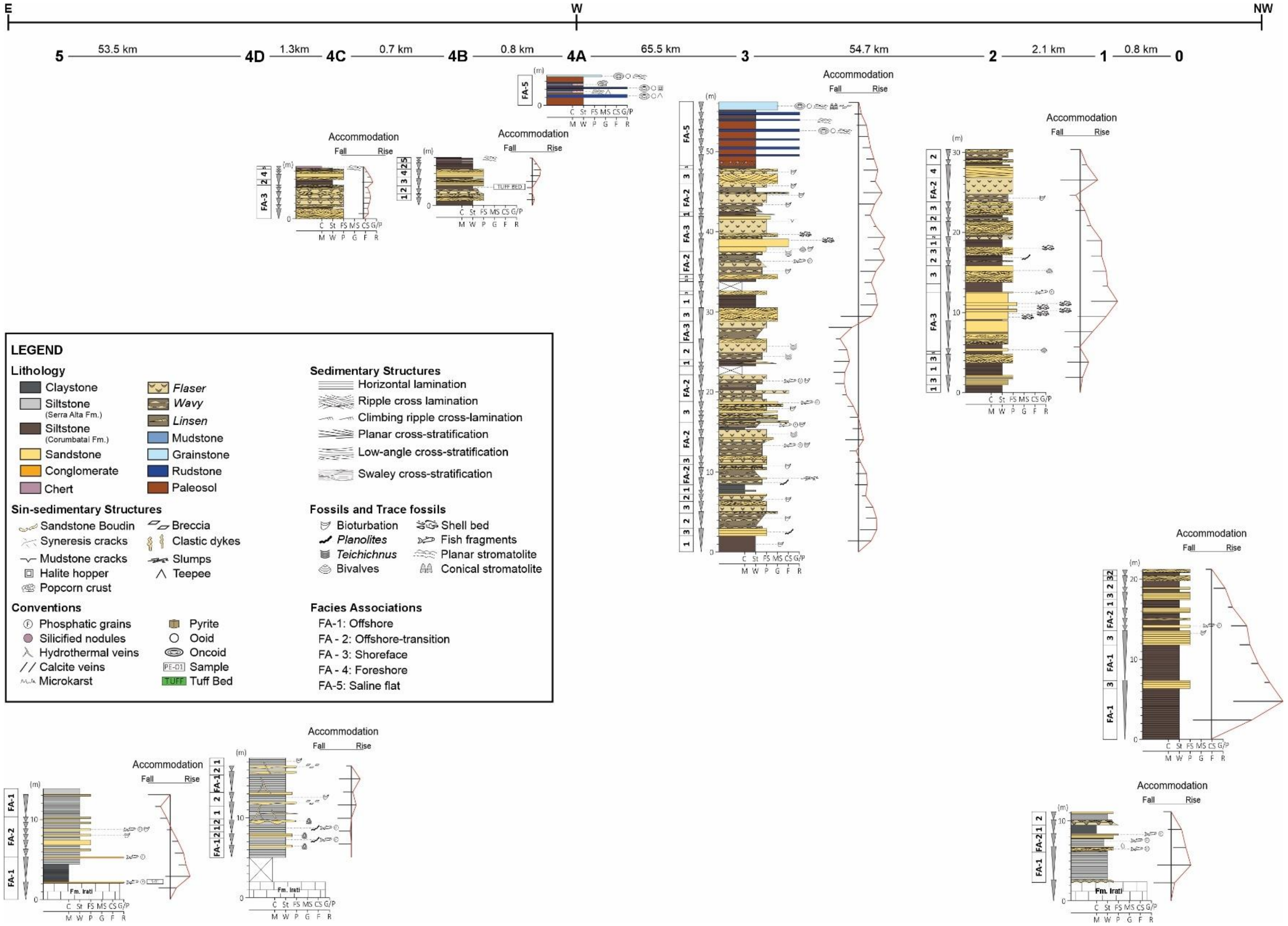

APÊNDICE II

Dados U-Pb, Lu-Hf, REE e elementos traços

Apêndice II.I - Dados U-Pb dos grãos de zircão obtidos por LA-ICP-MS. Em vermelho: grãos desconsiderados da curva concórdia, por apresentarem idades muito discrepantes dos demais e, provavelmente, serem grãos herdados.

Coord: 17°32.607'S / 52°33.931'W (Mineiros - GO)
Summary of U-Pb in situ zircon data of sample, obtained by LA-ICP-MS

Spot number	Isotope ratios							Ages (Ma)						% Conc.	Best age	
	$^{207}Pb^{*}/^{235}U$	2σ	$^{206}Pb^{*}/^{238}U$	2σ	Rho	$^{207}Pb^{*}/^{206}Pb$	2σ	$^{206}Pb/^{238}U$	±	$^{207}Pb/^{235}U$	±	$^{207}Pb/^{206}Pb$	±		(Ma)	±
24	0.873	1.298	0.102	1.181	0.910	0.062	0.538	266.9	4.9	268.5	6.1	282.3	37.7	99.4	**266.9**	4.9
25	0.306	3.489	0.042	1.375	0.394	0.052	3.207	267.1	3.6	271.0	8.6	305.4	74.8	98.5	**267.1**	3.6
26	0.298	1.106	0.042	0.826	0.746	0.052	0.736	263.7	2.1	264.9	2.8	276.1	17.0	99.5	**263.7**	2.1
27	0.293	1.217	0.042	1.034	0.849	0.051	0.643	264.0	2.7	261.0	3.0	233.7	14.9	101.2	**264.0**	2.7
28	0.301	1.311	0.042	1.083	0.826	0.052	0.740	264.8	2.8	266.9	3.3	285.7	17.0	99.2	**264.8**	2.8
29	0.299	2.097	0.042	1.270	0.606	0.052	1.669	264.7	3.3	266.0	5.2	277.6	38.7	99.5	**264.7**	3.3
30	0.298	18.459	0.042	1.546	0.084	0.051	18.394	266.5	4.0	264.9	44.2	251.0	489.4	100.6	**266.5**	4.0
33	0.303	2.641	0.042	1.643	0.622	0.052	2.068	265.5	4.3	268.5	6.5	294.5	47.9	98.9	**265.5**	4.3
36	0.305	1.737	0.042	1.031	0.594	0.052	1.398	266.1	2.7	270.1	4.4	304.7	32.2	98.5	**266.1**	2.7
37	0.300	1.571	0.042	1.147	0.730	0.052	1.074	263.8	3.0	266.2	3.9	286.9	24.7	99.1	**263.8**	3.0
38	0.299	1.256	0.042	1.020	0.812	0.052	0.734	265.0	2.6	265.8	3.2	272.6	16.9	99.7	**265.0**	2.6
40	0.295	2.769	0.042	1.878	0.678	0.051	2.035	263.6	4.9	262.4	6.7	251.6	47.5	100.5	**263.6**	4.9
44	0.302	2.670	0.042	1.199	0.449	0.052	2.385	264.7	3.1	267.9	6.5	296.3	55.4	98.8	**264.7**	3.1
46	0.301	1.801	0.042	1.178	0.654	0.052	1.362	266.8	3.1	266.9	4.5	267.6	31.6	100.0	**266.8**	3.1
47	0.299	4.356	0.042	2.914	0.669	0.051	3.238	266.0	7.6	265.6	10.5	262.1	76.1	100.2	**266.0**	7.6
48	0.295	1.477	0.042	1.055	0.714	0.051	1.034	263.1	2.7	262.1	3.7	253.3	24.0	100.4	**263.1**	2.7
49	0.305	2.693	0.042	1.346	0.500	0.053	2.333	266.0	3.5	270.3	6.7	307.8	54.0	98.4	**266.0**	3.5
50	0.302	2.249	0.042	1.494	0.664	0.052	1.681	264.3	3.9	267.7	5.5	297.3	38.8	98.7	**264.3**	3.9
53	0.296	2.469	0.042	1.908	0.773	0.051	1.568	265.3	5.0	263.5	6.0	247.7	36.5	100.7	**265.3**	5.0
54	0.300	1.660	0.042	0.943	0.568	0.052	1.366	263.4	2.4	266.5	4.1	293.1	31.5	98.9	**263.4**	2.4
55	0.300	2.102	0.042	1.430	0.680	0.051	1.541	267.0	3.7	266.3	5.2	260.3	35.8	100.3	**267.0**	3.7
57	0.298	1.804	0.042	1.271	0.704	0.052	1.281	263.5	3.3	264.9	4.5	277.6	29.6	99.5	**263.5**	3.3
58	0.300	2.107	0.042	1.523	0.723	0.052	1.456	264.4	3.9	266.1	5.2	281.1	33.7	99.4	**264.4**	3.9
59	0.315	1.924	0.042	1.247	0.648	0.055	1.466	264.5	3.2	278.0	4.9	393.4	33.2	95.1	**264.5**	3.2

60	0.306	6.723	0.042	2.922	0.435	0.052	6.055	267.7	7.7	271.1	16.4	300.4	144.3	98.8	**267.7**	7.7
63	0.293	1.808	0.042	1.277	0.706	0.051	1.280	263.2	3.3	260.8	4.4	239.3	29.8	100.9	**263.2**	3.3
64	0.304	1.807	0.042	1.387	0.768	0.052	1.158	266.7	3.6	269.4	4.5	292.5	26.7	99.0	**266.7**	3.6
66	0.309	1.491	0.041	0.960	0.644	0.054	1.141	261.6	2.5	273.4	3.8	374.9	25.9	95.7	**261.6**	2.5
70	0.303	1.596	0.042	0.934	0.585	0.052	1.294	267.8	2.5	268.7	4.0	276.8	29.9	99.7	**267.8**	2.5
74	0.300	2.726	0.042	1.792	0.657	0.052	2.054	265.4	4.7	266.5	6.6	276.1	47.7	99.6	**265.4**	4.7
77	0.297	1.932	0.042	1.117	0.578	0.051	1.576	265.0	2.9	264.1	4.7	255.3	36.6	100.4	**265.0**	2.9
78	0.303	5.420	0.042	3.060	0.565	0.052	4.474	266.1	8.0	268.7	13.1	291.4	105.5	99.0	**266.1**	8.0
79	0.301	3.982	0.042	2.303	0.578	0.052	3.249	262.7	5.9	267.0	9.6	305.3	75.8	98.4	**262.7**	5.9
80	0.298	1.314	0.042	0.830	0.632	0.051	1.019	266.0	2.2	264.6	3.3	252.4	23.6	100.5	**266.0**	2.2
83	0.296	3.330	0.042	2.080	0.625	0.052	2.600	262.9	5.4	263.1	8.0	264.7	60.8	99.9	**262.9**	5.4
85	0.302	1.286	0.042	1.004	0.781	0.052	0.803	265.1	2.6	268.2	3.3	295.3	18.4	98.8	**265.1**	2.6
89	0.300	1.197	0.042	0.953	0.796	0.052	0.724	263.3	2.5	266.4	3.0	293.4	16.6	98.8	**263.3**	2.5
23	0.873	1.298	0.102	1.181	0.910	0.062	0.538	624.4	7.0	637.0	6.7	681.8	11.5	98.0	624.4	7.0
43	0.758	3.122	0.090	2.892	0.926	0.061	1.177	558.4	15.5	572.7	14.3	629.8	25.6	97.5	558.4	15.5
45	1.259	5.427	0.134	4.962	0.914	0.068	2.198	808.7	37.8	827.7	31.9	879.1	46.1	97.7	808.7	37.8
56	14.555	5.637	0.162	3.833	0.680	0.650	4.133	970.6	34.6	2786.6	57.5	4623.2	61.1	34.8	970.6	34.6
65	6.425	1.611	0.368	1.386	0.861	0.127	0.820	2018.8	24.1	2035.7	16.1	2052.9	14.6	99.2	2018.8	24.1
69	5.349	1.508	0.326	1.223	0.811	0.119	0.882	1818.7	19.4	1876.8	14.7	1941.6	15.9	96.9	1818.7	19.4
73	0.767	1.005	0.093	0.636	0.633	0.060	0.778	572.0	3.5	578.0	5.0	601.6	16.9	99.0	572.0	3.5
90	7.703	5.702	0.109	3.292	0.577	0.515	4.655	664.2	20.8	2196.9	54.5	4284.1	70.2	30.2	664.2	20.8

Apêndice II.II - Dados isotópicos de Lu-Hf dos grãos de zircão obtidos por LA-MC-ICPMS

LA-MC-ICPMS Lu-Hf isotope data of zircon from sample of tuff - Corumbataí Formation (Paraná Basin) in Goiás state

		Sample (present day ratios)				**Sample (initial ratios)**			**TDM (Ga)**	
N° spot	**U-Pb Age (Ma)**	**±2σ**	**^{176}Hf/^{177}Hf**	**±2σ**	**^{176}Hf/^{177}Hf**	**±2σ**	**^{176}Hf/^{177}Hf(t)**	**eHf(t)**	**Felsic**	**Mafic**
258	**261.6**	94	0.00214	22	1.46745	1.19416	0.282649711	1.0	1.1	0.9
259	**266.7**	75	0.00213	21	1.46759	1.132425	0.282643138	0.9	1.2	0.9
260	**264.5**	36	0.00108	7	1.46743	1.405806	0.282549501	-2.4	1.3	1.1
261	**263.1**	37	0.00131	9	1.46746	1.035543	0.282529684	-3.2	1.4	1.1
262	**265.3**	49	0.00114	12	1.46725	1.270833	0.282569729	-1.7	1.3	1.1
263	**264.7**	33	0.00093	7	1.46747	1.319691	0.282504225	-4.0	1.4	1.2
265	**264.3**	32	0.00096	6	1.46742	1.630264	0.282521672	-3.4	1.4	1.2
266	**266**	42	0.00099	7	1.46717	1.495581	0.282561409	-2.0	1.3	1.1
267	**266**	35	0.00084	6	1.46740	1.406608	0.282497002	-4.3	1.4	1.2
268	**263.1**	29	0.00108	7	1.46737	1.392565	0.282522793	-3.4	1.4	1.1
270	**266.5**	43	0.00139	10	1.46740	0.972437	0.282572207	-1.6	1.3	1.1
271	**265.5**	44	0.00159	10	1.46778	1.591088	0.282484124	-4.7	1.5	1.2
272	**265**	40	0.00116	8	1.46746	1.851061	0.282527446	-3.2	1.4	1.1
273	**263.7**	62	0.00204	15	1.46759	1.69603	0.282593548	-0.9	1.3	1.0
274	**267.1**	36	0.00127	9	1.46749	1.194235	0.282519338	-3.5	1.4	1.2
276	**266.9**	28	0.00098	6	1.46742	1.364845	0.282461225	-5.5	1.5	1.3
277	**264.8**	38	0.00113	9	1.46729	1.403353	0.282567244	-1.8	1.3	1.1

Apêndice II.III - Elementos terras raras (REE), expressos em ppm, obtidos da amostra de tufo por ICP-MS.

REE data from sample of tuff - Corumbataí Formation (Paraná Basin) in Goiás State

SAMPLE	TUFF*	RGM-1*	RGM-1
La	27,43	24,00	21,42
La*	88,48	77,42	69,09
Ce	69,45	47,00	45,16
Ce*	85,95	58,17	55,89
Pr	4,54	4,70	4,82
Pr*	37,17	38,52	31,29
Nd	22,82	19,00	19,23
Nd*	38,04	31,67	32,05
Sm	3,24	4,30	4,42
Sm*	16,63	22,05	22,67
Eu	0,78	0,66	0,66
Eu*	10,62	8,98	8,99
Gd	2,63	3,70	3,84
Gd*	10,17	14,29	14,81
Tb	0,32	0,67	0,70
Tb*	6,69	14,05	14,72
Dy	1,70	4,08	4,16
Dy*	5,28	12,67	12,92
Ho	0,40	0,95	0,91
Ho*	5,54	13,23	12,71
Er	0,72	2,60	2,67
Er*	3,41	12,38	12,74
Tm	0,12	0,37	0,33
Tm*	3,84	11,56	10,20
Yb	0,94	2,60	2,22
Yb*	4,49	12,44	10,63
Lu	0,14	0,41	0,44
Lu*	4,23	12,73	13,59
Sm*xGd*	169,02	315,02	335,78
raiz	13,00	17,75	18,32
SREE	135,22	115,04	109,97
Eu/Eu*	0,82	0,51	0,49
La*/Sm*	5,32	3,51	3,05
Gd*/Yb*	2,26	1,15	1,39
La*/Yb*	19,71	6,22	6,50

Apêndice II.IV - Elementos traço e teores de ítrio, expressos em ppm, obtidos da amostra de tufo por ICP-MS

Trace elements data from sample of tuff - Corumbataí Formation (Paraná Basin) in Goiás State

Sample	RGM-1*	Tuff *	RGM-1 Gstdr
Li	59,81	62,03	57,00
Be	3,00	1,38	2,37
Sc	4,39	6,03	4,40
V	16,20	18,65	13,00
Cr	6,02	1,55	3,70
Co	2,58	26,90	2,00
Ni	4,43	12,08	4,40
Cu	7,09	12,20	11,60
Zn	38,61	64,07	32,00
Ga	19,77	42,92	15,00
Rb	139,13	195,98	149,00
Sr	105,44	338,08	108,00
Y	25,63	7,88	25,00
Zr	285,68	133,03	219,00
Nb	11,48	17,92	8,90
Cs	41,62	12,24	47,00
Hf	6,12	8,84	6,20
Tl	0,66	1,60	0,93
Pb	26,00	21,58	24,00
Bi	0,20	0,57	0,27
Th	12,21	37,16	15,10
U	4,92	10,90	5,80
Nb/Y	0,45	2,28	0,36

APÊNDICE III

Journal of South American Earth Sciences 134 (2024) 104750

Contents lists available at ScienceDirect

Journal of South American Earth Sciences

journal homepage: www.elsevier.com/locate/jsames

Rising mollusk bivalves from the ashes: Geologic, biostratigraphic and evolutionary implications from tuff data in the Permian Corumbataí Formation, Paraná Basin, Brazil

B. Christofoletti [a,*], L.V. Warren [a], F.G. Varejão [b], M.G. Simões [c], L.E. Gómez-Peral [d], C. Lana [b], M.G. Rodrigues [a], M.L. Assine [a,e]

[a] Departament of Geology, São Paulo State University, Rio Claro, SP, 13506-900, Brazil
[b] Departament of Geology, Ouro Preto Federal University, Ouro Preto, MG, 35402-163, Brazil
[c] Department of Zoology, São Paulo State University, Botucatu, SP, 18618-000, Brazil
[d] Centro de Investigaciones Geológicas – CONICET – FCNyM (UNLP), La Plata, Diagonal 113 N°275, Argentina
[e] Institute of Geosciences, University of Brasilia, Brasilia, DF, 70910-900, Brazil

ARTICLE INFO

Keywords:
U-Pb age
Volcanic ash
Choiyoi magmatism
Megalake
Biostratigraphy

ABSTRACT

During the Permian, the southwestern Gondwana margin experienced episodes of intense volcanism tied to the Choiyoi magmatism. Several ash-fall horizons related to this magmatic event are preserved within the Late Paleozoic lake-sea sedimentary record of the Paraná Basin. Furthermore, near the Permian-Triassic boundary, a meteor fell in the northern border of the basin, generating unshocked zircon grains preserved in a stratigraphic marker called the Porangaba Bed. In this study, a new U-Pb zircon age of 265.17 ± 3.2 Ma is presented for a volcanic tuff in the upper part of the Corumbataí Formation, near the stratigraphic interval of the Porangaba Bed. In addition, Lu-Hf isotopic compositions of the zircon grains, whole-rock geochemistry, and atmospheric circulation data indicate the affinity of the ash-fall horizon with the Frontal Cordillera source. The combination of these new and previous U-Pb ages allowed us to draw a more realistic scenario of the evolution of bivalve mollusk of the Corumbataí Formation and to improve the use of these macrofossils in the biostratigraphy of the Permian succession of the Paraná Basin. In this context, we established the limits of the *Pinzonella neotropica-Jacquesia brasiliensis* Association Biozone between 262.38 ± 5.7 Ma and 257.5 ± 2.2 Ma. Hence, in the north and central Paraná Basin the local resolution of this biozone is of ~5 Ma. Moreover, the range of this biozone indicates that the endemic bivalves survived the end-Guadalupian (ca. 259 Ma) extinction event unscathed.

1. Introduction

The precise age of the Corumbataí Formation in the upper part of the Permian Passa Dois Group, Paraná Basin, southeastern and central Brazil, is one of the main issues of the Brazilian Gondwana geology. Since the benchmark monography of Runnegar and Newell (1971), the unit has become known worldwide for its endemic fauna of well-preserved, silicified bivalves that evolved in a large and isolate inland basin (Simões et al., 1998; Wesselingh, 2007). Therefore, establishing the precise age, and reliable litho- and bio-correlations in the Corumbataí Formation are of fundamental importance for our understandings of the geological evolution of the western Gondwana during the end of the Paleozoic, including aspects such as sedimentation rate, source area and atmospheric dispersion pattern. The new geochronological and chronostratigraphic data is also fundamental to draw a more realistic scenario of that in situ mollusk evolution and to improve the use of those macrofossils in the biostratigraphy of the Passa Dois Group, something that has been attempted since Von Huene (1928).

Since the seminal works of Mendes (1952), a late Permian age is widely accepted for the Corumbataí Formation exclusively grounded on bivalve assemblages and palynological data (Daemon, 1974). Over the years, these fossils occurrences and biostratigraphy have been revised a few times (Rohn and Rösler, 1987; Sohn and Rocha-Campos, 1990; Rohn and Lavina, 1993), which seems to confirm the late Permian age (or even Permo-Triassic age, see Runnegar, 1977) for the deposition of the unit.

* Corresponding author.
E-mail address: beatriz.christofoletti@unesp.br (B. Christofoletti).

https://doi.org/10.1016/j.jsames.2023.104750
Received 14 November 2023; Received in revised form 18 December 2023; Accepted 18 December 2023
Available online 24 December 2023
0895-9811/

However, the bivalves of the Passa Dois Group, including those of the Corumbataí Formation, are endemic (Mendes, 1952), and without other geochronological dating calibrations they cannot be used to improve the age associated with these geological units. This problem was partially solved by dating the ash beds in the underlying Irati Formation (Cagliari et al., 2022) resulting in a lower depositional limit of 275 Ma for the Corumbataí Formation. However, the absence of datable tuff beds at the upper part of this unit has made it extremely difficult to define the upper limit of the bivalve biozones and especially if the deposition of the Corumbataí Formation extends beyond the Permian. Hence, it is noteworthy that even after more than 100 years of studies (the Corumbataí Formation was originally defined in 1916 by the Geographical and Geological Commission of the State of São Paulo, Moraes Rego, 1930) the age of this unit remains under dispute.

Given the context above, in this contribution an accurate and precise age for the Corumbataí Formation is presented based on tuffaceous material from the State of Goiás, Central Brazil. This is relevant to our understandings of the age and time elapsed in the sedimentation of this unit. Even more significant, this new discovery raises another issue related to the magmatic source of the Permian volcanic ash recorded in the Paraná Basin. Exclusively grounded on age comparisons, the source of the ash falls has been generically assigned to the Choiyoi magmatism (Coutinho and Hachiro, 2005; Guerra-Sommer et al., 2008; Rocha-Campos et al., 2011; Silva et al., 2017), the largest magmatic event in the western margin of Gondwana (from the western Andean Cordillera to the Sierra Australes). Although the Choiyoi magmatism is widely accepted as the source of these deposits (Rocha-Campos et al., 2011), the exact location of the volcanism is still debated. Yet, it opens a series of new avenues to discuss the age of the endemic bivalve fauna of the Passa Dois Group, the temporal resolution of its biozones, and the bivalve species duration, with wide geochronological and evolutionary applications. Hence, in these context, (i) a new high-precision U-Pb radioisotope age for the Corumbataí Formation, northern Paraná Basin is presented; (ii) a Lu-Hf isotope analysis and whole rock geochemistry (including REY) is shown, offering us a unique opportunity to identify with precision the source of the volcanic ash preserved in this unit and, (iii) a relative dating pinpointing the age of the bivalve biozones of the Corumbataí Formation is constrained for the first time. These biozones are the main tool for surficial interbasinal stratigraphic correlations between sedimentary successions that are also tracked outside the Brazilian part of the Paraná Basin (i.e., Paraguay), thus, providing the foundation for continental-scale geological and paleontological interpretations.

2. Geological setting

The intracratonic Paraná Basin extends over 1,700,000 km^2 in the central and southern Brazil, eastern Paraguay, northeastern Argentina, and northern Uruguay (Fig. 1A). This huge sedimentary basin encompasses at least 6 s-order stratigraphic sequences deposited between the Middle Ordovician and Upper Cretaceous periods, including sedimentary and volcanic successions bounded by regional unconformities

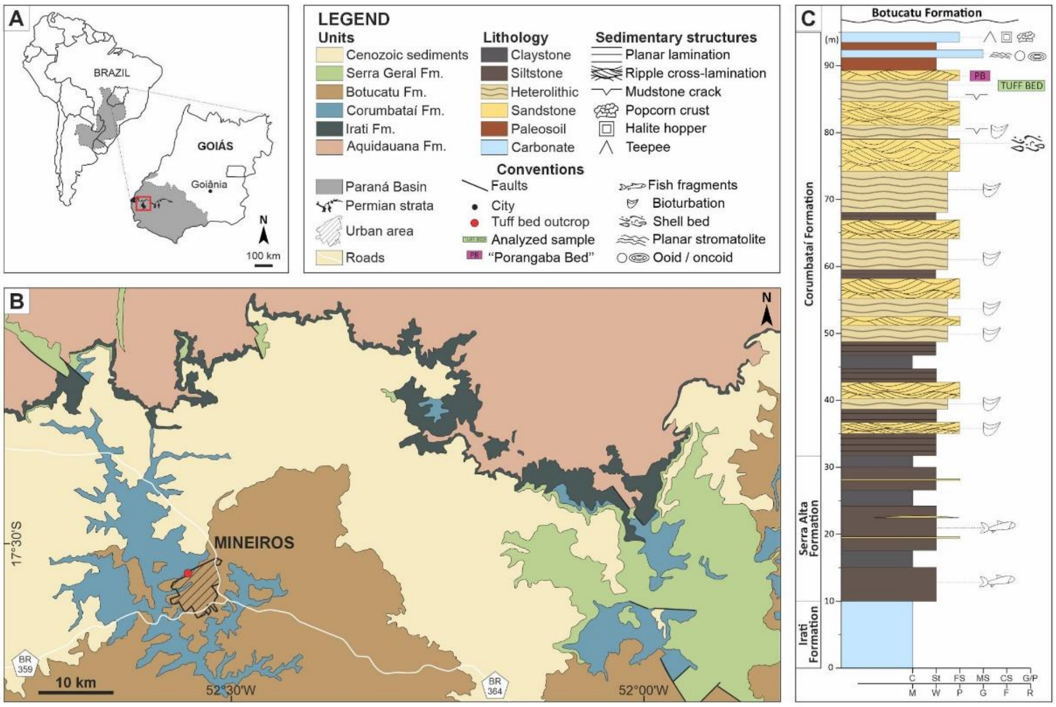

Fig. 1. Study area and general stratigraphy of the Corumbataí Formation and tuff-bearing succession. (A) Location of the studied area in the Paraná Basin. (B) Simplified geologic map (modified from CPRM – Serviço Geológico do Brasil, 2006) with the location of the tuff bed outcrop (17°32.607′S/52°33.931′W). (C) Simplified stratigraphic column of the Corumbataí Formation showing the precise vertical position of the tuff bed in the upper part of the unit. Explanation: Fm. - Formation; C – claystone; St – siltstone; FS – fine sandstone; MS – medium sandstone; CS – coarse sandstone; G/P – granule/pebble; M – mudstone; W – wackestone; G – grainstone; B – boundstone; R – rudstone. Porangaba Bed according to Tohver et al. (2018).

(Milani et al., 2007). The Paleozoic successions comprise marine and continental rocks deposited over complete transgressive-regressive sequences (Schneider et al., 1974; Milani, 1997; Milani et al., 1998, 2007; Warren et al., 2008; Holz et al., 2010). Following this tendency, the SW Gondwana experienced a progressive continentalization and aridization during the Permian (Milani et al., 2007; Limarino et al., 2014) induced by the end of the marine connections between the southward Panthalassa and the Paraná and Karoo basins (Warren et al., 2008; Holz et al., 2010). The development of an orographic barrier (Gondwanides Belt; Keidel, 1916) during the assembling of the Patagonia plate against the Gondwana supercontinent (San Rafaelica orogeny; Ramos et al., 1986), led to the restriction of the above cited basins forming a continental-scale megalake (sensu Palcu et al., 2021). In this huge, enclosed water body were deposited the Irati, Serra Alta, Teresina/Corumbataí and Rio do Rasto formations, from the Passa Dois Group (part of the Gondwana I supersequence; Milani et al., 2007).

In the northern/northeastern part of the Paraná Basin (São Paulo, Mato Grosso, and Goiás states), the stratigraphic interval that encompasses the Teresina Formation in the southern and southeastern Brazil, is usually designated as the Corumbataí Formation (Schneider et al., 1974; Warren et al., 2015). In the Goiás and São Paulo states, a well-marked breccia interval with regional scale significance stands out in the upper part of the Corumbataí and Teresina formations. This marker bed is called the Porangaba Bed (Matos and Coimbra, 1997; Tohver et al., 2018). Although its origin is under dispute (e.g., paleosol or tsunamite), unshocked zircon grains provide one of the few absolute ages for the Corumbataí Formation (ca. 254 Ma, Late Permian; Tohver et al., 2018).

In the Goiás and Mato Grosso states, the Corumbataí Formation is bounded at the base by the Serra Alta Formation (Petrobras boreholes – 2-AG-1-MT and 2-JA-1-GO) and at the top by a disconformity with the Botucatu Formation (Fig. 1B). In these localities, the Corumbataí Formation has a typical coarsening-upward pattern (Fig. 1C), with a monotonous succession of claystone and siltstone interbedded with cm-thick beds of swaley cross-stratified and wave-rippled fine-grained sandstone at its base. Highly bioturbated, tabular beds (cm-to m-scale-thick) of siltstone, heterolithic facies, wave-rippled fine-grained sandstone, and bivalve shell beds transitionally overlapped the basal succession (Ng et al., 2019). In the upper part of the unit, fine sandstone and heterolithic facies with mudstone cracks are common, while the presence of siltstone deposits significantly decreases. Carbonate facies (including microbialites), bivalve-dominated shell beds, evaporitic breccia with halite pseudomorphs, tepees and saline crusts are also observed (Ng et al., 2019).

Since the mid-20th century, multiple paleoenvironmental scenarios have been proposed for the Corumbataí Formation, including shallow restricted marine, lacustrine and tide-influenced settings (Schneider et al., 1974; Suguio et al., 1974; Petri and Coimbra, 1982; Sousa, 1985; Rohn, 1994). Based on Warren et al. (2015) and sedimentological data from the southern and northern part of Paraná Basin (this contribution), the interpretation is that the Corumbataí Formation were deposited in a shallow megalake (i.e. without connection with the Panthalassa (Mendes, 1984; Rohn, 1994, 2007; Simões et al., 1998)). Paleobiological evidence suggests that the salinity was variable and that the endemic taxa was not typically freshwater or marine (Mendes, 1949, 1952; Beurlen, 1954; 1957; Runnegar and Newell, 1971; Sousa, 1985; Sohn and Rocha-Campos, 1990; Simões, 1992; Rohn, 1994; Maranhão, 1995; Matos, 1995; Maranhão and Petri, 1996; Simões et al., 1998, 2000; Ghilardi and Simões, 2002). This huge intraplate, confined water body was frequently affected by storms, and marked by periods of intense evaporation and hypersalinity with punctual influence of freshwater input (Suguio et al., 1974; Sousa, 1985; Sohn and Rocha-Campos, 1990; Simões, 1992; Rohn, 1994; Maranhão, 1995; Matos, 1995; Maranhão and Petri, 1996; Simões et al., 1996; Simões et al., 1998, 2000; Ghilardi and Simões, 2002).

2.1. On the age of the Corumbataí Formation

Given the presence of *Stereosternum tumidum* and *Mesosaurus brasiliensis* in the underlying Irati Formation, and *Licopodiopsis derbyi* (see Mendes, 1952, and references therein) in the Corumbataí Formation, a Late Paleozoic age was assigned to the sedimentary succession of the Passa Dois Group, even prior to its formal designation as the Passa Dois Series by White (1908). Until 1927, a Permian age was accepted to the Passa Dois Group, but during the famous geological comparison between South America and Africa, Du Toit (1927) referred the upper part of the group to the Triassic. Bivalves collected by him in the State of Paraná were erroneously referred to as the Mesozoic bivalve genera *Myophoriopsis* (=*Jacquesia*) and *Pachycardia* (=*Pinzonella*) by Reed (1929, 1932, 1935). Du Toit (1927) had access to Reed's data before the publication of his studies. These facts introduced strong confusion into the chronology of the Corumbataí beds.

Mendes (1952) revised the bivalves of the Corumbataí Formation based on fossils from the State of São Paulo, again recognizing a Permian age for the formation. In addition to the presence of *Glossopteris* and arborescent lycophytes (Mendes, 1967), the occurrence of striated dissaccate pollen grains (e.g., *Striamonosaccites* cf. *S. morondavensis*) from subsurface samples of the Corumbataí Formation in the State of São Paulo indicates a latest Permian age for the unit (Tatarian stage of the European Zechstein Sea, or Capitanian to basal Wuchiapingian) (Daemon, 1974). An upper Permian (i.e., Kazanian-Tatarian or nearly Capitanian-Wuchiapingian age) was accepted for the Corumbataí Formation for a long time by various authors (e.g., Daemon and Quadros, 1970; Rohn and Rösler, 1987; Sohn and Rocha-Campos, 1990; Rohn and Lavina, 1993).

However, based on a pattern of alternating reverse and normal geomagnetic polarity, Valencio et al. (1975) had proposed a Late Permian or even younger (Triassic) paleomagnetic age for the Corumbataí Formation in São Paulo State. In turn, Runnegar (1977) considered the Passa Dois bivalves to be representative of a Permo-Triassic benthic biota.A Triassic age was again suggested for the Corumbataí Formation by Ragonha (1984), based on fossil remains of *Xenacanthus moorei*, a cosmopolitan shark that occurs in Triassic deposits of Europe, India, and North America. Similarly, Daemon et al. (1996), on the ground of palynological content, invertebrates and vertebrates considered the Corumbataí Formation as Triassic in age.

Although scarce, the palynostratigraphic studies identified the typical species of the *Lueckisporites virkkiae* Zone in the Corumbataí Formation attributing a Cisuralian-Guadalupian age for this unit (Daemon and Quadros, 1970; Maranhão, 1995; Souza and Marques-Toigo, 2005; Neregato et al., 2008; Mori et al., 2012; Rocha et al., 2020).

On the other hand, ostracod taxa described from occurrences in the Goiás and Mato Grosso states (Tomassi, 2009) have been reported from Changhsingian (Late Permian) based in similar forms found in coeval successions in China (Shu and Utting, 1990; Crasquin et al., 2010). Hence, for a long time, the age of the Corumbataí Formation was mainly inferred based on its micro and macrofossil content, and its contact relationships with the underlying Serra Alta and Irati formations and the overlying Pirambóia Formation, as well as its lateral correlation with the Teresina Formation in the southern Brazil. This was until recently, when Rocha-Campos et al. (2019) dated some probable ash fall layers and published U-Pb zircon ages, suggesting an age of 257 ± 2.2 Ma. (only 3 zircon grains) and 266 ± 7.1 Ma for the Corumbataí and Teresina formations, respectively. However, the authors themselves point out that these data present little confidence and can be placed in establishing the age of the units, due to the scarce number of data.

Thanks to the presence of tuff layers in the Lower Permian succession of the Paraná Basin, also including the Irati Formation, some published absolute radioisotope ages are now available (Maynard et al., 1996; Rocha-Campos et al., 2006, 2019; Santos et al., 2006; Silva et al., 2017; Bastos et al., 2021; Cagliari et al., 2022). These ash-fall tuffs are crucial because they usually contain a representative zircon population, which is product of a volcanic event and can be used to provide a precise U-Pb depositional age for the host sediments.

3. Material and methods

During a detailed geological survey in the Corumbataí Formation at the northwestern part of the Paraná Basin, one tuff bed was founded and sampled in a road cut at the Mineiros town, State of Goiás, Brazil (17°32.607′S/52°33.931′W). The tuff bed was stratigraphically constrained at the upper succession of the Corumbataí Formation, ~10 m below the upper erosive boundary with the Botucatu Formation (Fig. 1C). A detailed (1:50) columnar section was measured including the description of the lithology, sedimentary structures, and fossil content (Fig. 2), and one sample (~2 kg) of the tuff bed was collected.

3.1. Zircon U-Pb geochronology

The zircon grains were separated from rock sample (2 kg) using standard techniques encompassing crushing, sieving and separation by heavy liquid (bromoform). Zircon grains (~430 grains) were handpicked under a binocular stereomicroscope, mounted on adhesive tape, and enclosed in epoxy resin mounts. These were polished to about half their sizes and imaged by cathodoluminescence (Fig. 3A; JEOL 6510 Scanning at DEGEO/UFOP), aiming to characterize internal features (recrystallization rings, fractures, inclusions) of the individual zircon grains. The zircon description and typology followed the protocol in Pupin (1980).

U-Pb analyses (see Supplementary Material) were carried out at the Isotopic Geochemistry Laboratory (Federal University of Ouro Preto – UFOP) using a Thermo-Finnegan Neptune multi-collector ICP-MS coupled with a Photon-Machines 193 nm excimer laser system (LA-MC-ICP-MS). Data were acquired using automatic mode with background measurement during 20 s, zircon ablation during 40 s and 20 μm spot size. The GJ-1 zircon standard (Jackson et al., 2004) was used as a primary standard for this study with the Plešovice zircon standard ($^{206}Pb/^{238}U$ = 337 Ma, $^{207}Pb/^{235}U$ = 337 Ma and $^{207}Pb/^{206}Pb$ = 339 Ma; Sláma et al., 2008) as a secondary standard. Data reduction was done in SATURN® Software (Silva et al., 2022), whereas the concordance, probability, radial and Concordia diagrams, and the weighted average ages were generated by the Excel Isoplot software (Ludwig, 2003).

3.2. Lu-Hf isotope analyses

The Hf isotope ratios were determined on seventeen previously selected zircon crystals showing reliable U-Pb ages with low analytical error (see Supplementary Material). The analysis were carried out in a multi-collector MC-ICP-MS Thermo-Scientific Neptune Plus system, coupled to a Photon Machines 193 (λ = 193 nm) ArF Excimer laser ablation system, hosted in the Isotopic Geochemistry Laboratory (Federal University of Ouro Preto – UFOP). Data were collected in static mode during 60 s of ablation with a spot size of 40 μm. The spots were drilled with a repetition rate of 6Hz and 0.3 He gas.

The accuracy and external reproducibility were verified by analyses of the standard zircons Blue Berry $^{176}Hf/^{177}Hf = 0.281692 \pm 0.000017$

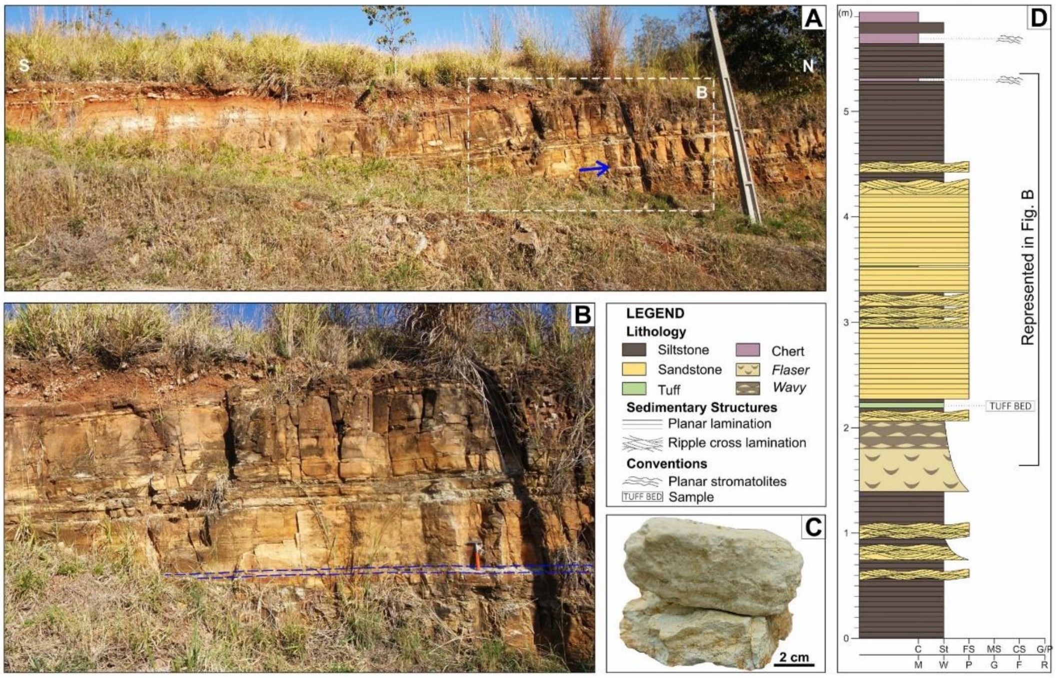

Fig. 2. Tuff bed and associated sedimentary facies. (A) General view of the outcrop. (B) Detail of the volcanic ash bed (blue dashed line indicates the sampled layer). (C) Part of the sampled ash bed. (D) Columnar section showing the position of the tuff bed within the sedimentary facies succession. Explanation: C – claystone; St – siltstone; FS – fine sandstone; MS – medium sandstone; CS – coarse sandstone; G/P – granule/pebble; M – mudstone; W – wackestone; G – grainstone; B – boundstone; R – rudstone. The hammer in B is 30-cm-long.

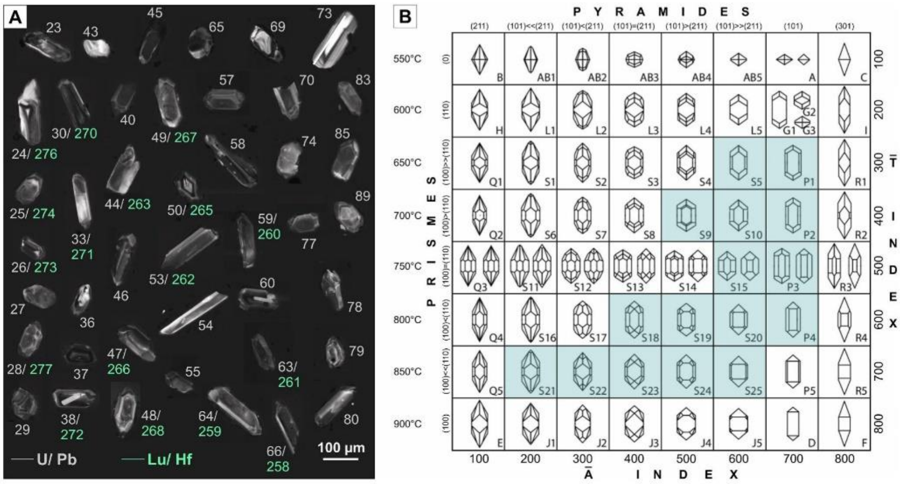

Fig. 3. Zircon morphology. (A) Cathodoluminescence image of the selected volcanic zircons for the LA-ICP-MS dating (grey number refer to the zircon identification in Supplementary Material) and Lu-Hf analysis (green number refer to the zircon identification in Supplementary Material). (B) Zircon crystal typological classification diagram (Pupin, 1980). The blue subtypes refer to the analyzed zircon population.

(n = 10), Mud Tank $^{176}Hf/^{177}Hf = 0.282516 \pm 0.000015$ (n = 10), GJ-1 $^{176}Hf/^{177}Hf = 0.282005 \pm 0.000019$ (n = 10) and Temora $^{176}Hf/^{177}Hf = 0.28260 \pm 0.000014$ (n = 10) (all errors are ± 2σ SD). These ratios are in good agreement with the accepted ratios data of 0.281674 ± 0.000018 (Blue Berry; Santos et al., 2017), 0.282504 ± 0.000044 (Mud Tank; Black and Gulson, 1978; Woodhead and Hergt, 2005), 0.282000 ± 0.000005 (GJ-1; Jackson et al., 2004), and 0.282680 ± 0.000031 (Temora; Black et al., 2003; Wu et al., 2006).

For the calculation of the εHf(t) values, the chondritic values reported by Chauvel et al. (2008) of $^{176}Hf/^{177}Hf = 0.283164$ and $^{176}Lu/^{177}Hf = 0.0270$ were used. To calculate the model ages (TDM) based on a depleted mantled source, the present-day ratios of $^{176}Hf/^{177}Hf = 0.282313$ and $^{176}Lu/^{177}Hf = 0.000311$ were used (Blichert-Toft, 2008). The λ decay constant for ^{176}Lu applied was 1.867 × 10−11/yr (Söderlund et al., 2004).

3.3. Whole-rock mineralogy and ICP-MS-geochemistry

Whole-rock and clay mineralogy of the tuff bed sample was determined from XRD patterns. Analyses were run on a PANalytical X'Pert PRO difractometer in the Centro de Investigaciones Geológicas (CIG CONICET-UNLP, La Plata, Argentina), using Cu radiation (Kα = 1.5 Å) and a Ni filter, and generation settings of 40 kV and 40 mA. Routine air-dried mounts were run between 2 and 32°2θ at a scan speed of 2°2θ/min. Samples were ethylene glycol-solvated without saturation pre-treatment and heated to 550 °C, and they were run from 2 to 27°2θ and 3–15°2θ, respectively, at a scan speed of 2°2θ/min. The methodology used for sample preparation follows Brown and Brindley (1980), and semi-quantification of the minerals was obtained considering the intensity of the main peak for each mineral (Biscaye, 1965; Moore and Reynolds, 1997 including laboratory patterns).

Rare-earth elements and yttrium (REY) contents, expressed in ppm, were obtained from the sample of tuff using a PerkinElmer quadrupole inductively coupled plasma mass spectrometry (ICP-MS) fitted with a Meinhardt concentric nebulizer at the CIG. In preparation for elemental analyses, aliquots of whole powder were digested for 2 h in trace metal grade 2% HNO_3. REE concentrations were normalized to chondrite values (Sun and McDonough, 1989) and compared to REE pattern of the rhyolite certificated geo-standard (RGM-1).

4. Results

4.1. Tuff-bearing succession

The tuff-bearing section (Fig. 2) is organized in up to 3 m-thick, coarsening-upward successions composed of dm-scale beds of siltstone with horizontal lamination interbedded with ripple cross-laminated, fine-grained sandstone in the base, which transitions to sandstone with flaser and wavy bedding at the middle, and to fine-grained sandstone with ripple cross-lamination and horizontal lamination at the top (Fig. 2D). The volcanic bed is a low-density, whitish claystone (Fig. 2C) that conforms an approximately >5 m-wide and 5 to 10 cm-thick lens within a siltstone bed between ripple cross-laminated and horizontally laminated fine-grained sandstone. To the top of the succession, interbedded laminated siltstone and silicified horizontally laminated stromatolites occur.

4.2. Volcanic zircon U-Pb ages

A total of 430 zircons were analyzed under cathodoluminescence. Of these, 43 euhedral volcanic grains were randomly selected for dating by LA-ICPMS (Fig. 3A).

The 37 analyzed zircons have prismatic and euhedral morphologies ranging in size from 56 to 176 µm (Fig. 3A), with medium sizes around 80–110 µm. Almost all zircons correspond to dipyramidal grains with well-developed prismatic faces, corresponding to the subtypes P1-4, S5, 9, 10, 15, 18–25 of Pupin (1980) (Fig. 3B).

About 86% of the analyzed zircon population have a late Permian age, varying between a minimum of 261.6 ± 8.0 Ma and a maximum of 267.8 ± 2.5 Ma (Capitanian to Roadian ages). The $^{206}Pb/^{238}U$ weighted mean age of 265.0 ± 0.5 Ma with a mean square of weighted deviation (MSWD) of 0.76 and a probability of 0.85 (95% of confidence, Fig. 4A) and the $^{206}Pb/^{238}U$ concordia age of 265.17 ± 3.2 Ma (Fig. 4B) confirm a Wordian age for the analyzed zircon population. Six zircon grains (4% of the zircon population; numbers 23 to 73 in Fig. 3A) are rounded to subrounded (sizes vary between 70 and 137 µm), having Cambrian

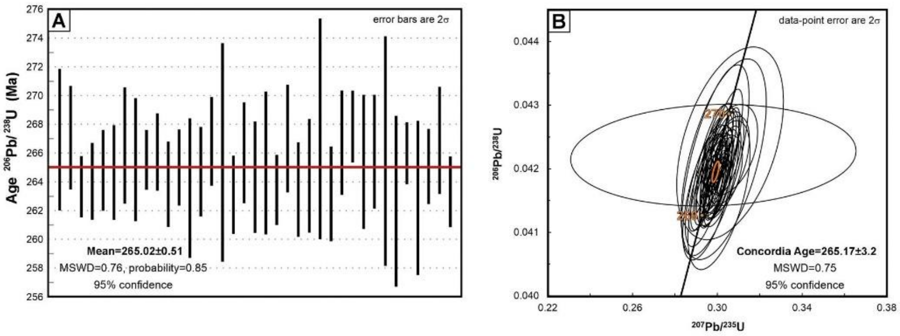

Fig. 4. U-Pb LA-ICP-MS results of the analyzed volcanic zircon grains. (A) $^{206}Pb/^{238}U$ weighted mean age of the LA-ICP-MS dated grains. (B) Concordia diagram illustrating LA-ICP-MS dated grains. MSWD: mean square of weighted deviates.

(558.3 ± 15.5 Ma, Fortunian) to Paleoproterozoic ages (2018.8 ± 24.1 Ma, Orosian).

4.3. Volcanic zircon Lu-Hf analysis

Among the 37 Permian-age zircon grains, 17 were randomly selected and subjected to isotopic analyzes of Lu-Hf. The εHf(t) vs. time diagram (Fig. 5) shows that most volcanic zircon grains have negative values between −5.5 and −0.9 and TDM ages from 1.3 to 1.5 Ga. Only two grains have positive εHf values of 0.9 and 1.0, and TDM ages between 1.2 and 1.1 Ga.

4.4. Whole-rock mineralogy and ICP-MS-geochemistry

The whole-rock XRD compositional data of the tuff sample shows that quartz is the prevalent mineral (37%); followed by K-feldspar (23.5%), plagioclase (18.5%), tridymite-cristobalite (12%), pyroxene (7%), and clay minerals (3%) (Fig. 6A). Clay-fraction (<2 μm), XRD analysis (less than 3% of the whole rock) shows smectite and in less proportion mixed layered illite–smectite (IS) (Fig. 6B). In the analyzed sample, clays are mostly the product of very scarcely altered glass.

5. Discussion

5.1. The age of the Corumbataí Formation and the nature of Porangaba Bed

The $^{206}Pb/^{238}U$ age of 265.17 ± 3.2 Ma (Wordian, Cohen et al., 2013; updated), in the upper part of the Corumbataí Formation in the Góias State, clearly indicates that this unit is older than previously realized. The low degree of dispersion in the dataset (the Cambrian and Paleoproterozoic zircons were considered detrital grains from an older source that got mixed in during the deposition of the tuff layer in the depositional environment) and the unusual abundance of euhedral zircon reinforces that the dated grains are non-reworked and correspond to the same original magmatic population. Thus, the age obtained approximately correspond to the age of ash ejection and tuff deposition.

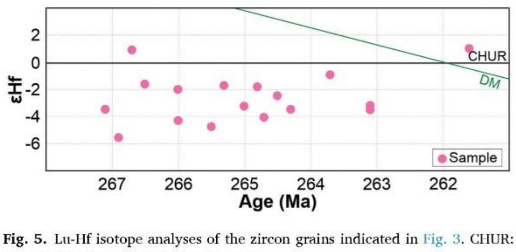

Fig. 5. Lu-Hf isotope analyses of the zircon grains indicated in Fig. 3. CHUR: chondritic values; DM: depleted mantle.

In other words, the unit is neither Triassic nor Tatarian (i.e., Changhsingian) (Fig. 7), as previously suggested by Ragonha (1984) and Daemon et al. (1996), among others. On the other hand, the ca. 265.17 ± 3.2 Ma age is in accordance with a Kazanian age (270.5–260.4 Ma) or Roadian-Capitanian age, already suggested by various authors (Daemon and Quadros, 1970; Rohn and Rösler, 1987; Sohn and Rocha-Campos, 1990; Rohn and Lavina, 1993). As shown in Fig. 7, only the upper part of the Corumbataí Formation is Capitanian to basal Wuchiapingian, an age that is also in accordance with some pollen grains (i.e., *Striamonosaccites* cf. *S. morondavensis*) recorded in subsurface samples from the Corumbataí Formation in the São Paulo State (Daemon, 1974).

Previous paleomagnetic studies indicate that the Corumbataí Formation was entirely deposited after the end of the Kiaman Superchron at 262–265 Ma (Capitanian-Wordian) (Valencio et al., 1975). However, recent paleomagnetic data, constrained by U-Pb ages in zircons, from the Porangaba Bed (Tohver et al., 2018), contest this depositional age and pointed to a deposition between ca. 274–254 Ma (Kungurian-Changhsingian; Aragão and Scardia, 2021).

The Porangaba Bed is defined by a matrix-supported breccia grading upward to a light grey to dark-red, massive, poorly sorted silty sandstone with free-floating, angular lithic clasts of white, altered chert or ocher siltstone (Matos, 1995; Matos and Coimbra, 1997). This bed was first described at the contact between the Passa Dois Group and the overlying Pirambóia Formation, in São Paulo State (Brazil) (Matos, 1995; Matos and Coimbra, 1997). Tohver et al. (2018) reported a breccia bed in a single location in the State of Goiás and attributed this facies to the same Porangaba Bed described in the São Paulo State by Matos (1995). This deposit has been interpreted either as the product of pedogenesis (Matos and Coimbra, 1997) or more recently, as a result of a high energy episode related to the late Permian Araguainha impact event (Tohver et al., 2018).

Tohver et al. (2018) dated unshocked detrital zircon grains from this breccia bed providing a SHRIMP U-Pb maximum depositional age (youngest population; n = 12) of 253.0 ± 3.0 (Changhsingian). Compiling only the ages of grains collected exclusively in the northern part of the Paraná Basin by Tohver et al. (2018), in the same stratigraphic interval and just 60 km away from the tuff bed studied here, the concordia age of the Permian population of zircons reaches 262.38 Ma ±5.7 Ma (Tohver et al., 2018) (Fig. 7).

When compared, the columnar sections of the tuff bed outcrop and that of the Porangaba Bed (Tohver et al., 2018), it is clear that: (i) the

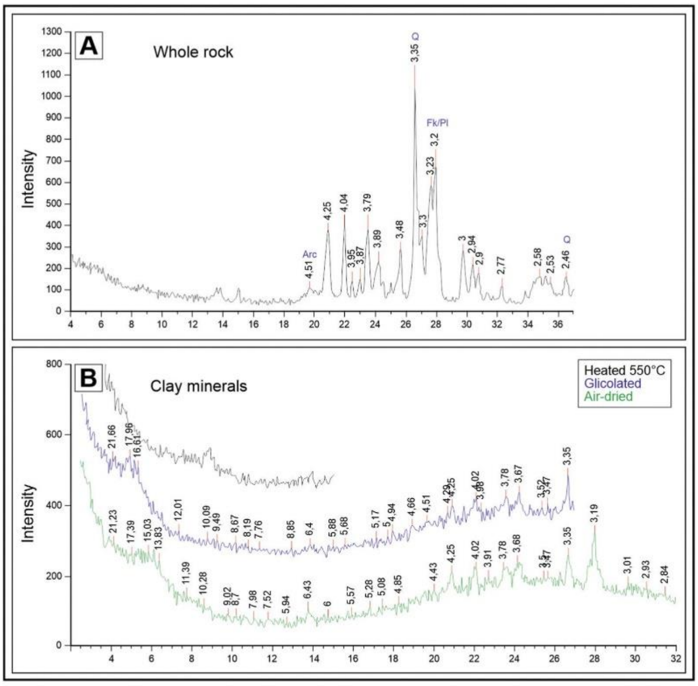

Fig. 6. XRD-diffractograms. (A) Tuff sample mineral composition. (B) Tuff sample in <2 μm fraction. Q: quartz; FK: alkaline feldspar; Pl: plagioclase; Arc: clays.

"Porangaba Bed" described by Tohver et al. (2018) in Goiás State is stratigraphically located a few meters (~10 m) below the top of the Corumbataí Formation; (ii) the Porangaba Bed is almost at the same stratigraphic level as the tuff bed studied here; (iii) in the northern part of the Paraná Basin, the upper part of the Corumbataí Formation was eroded and overlain by the Botucatu Formation, and (iv) in the SP-280 highway, central part of the São Paulo State, limestone with bivalves of the *Pinzonella neotropica-Jacquesia brasiliensis* Association Biozone in the upper part of the Teresina Formation are recorded ~14 m above the Porangaba Bed, almost in the contact with the overlying Pirambóia Formation. Thus, at least in theory, the breccia facies of the Porangaba Bed occur at a stratigraphically well-delimited single level and could not have been formed at different ages (neither by pedogenesis, nor by impact, or even a fault reactivation).

However, even considering dating errors (2–5 Ma), the ages obtained by Tohver et al. (2018) for the breccia bed described in Goiás State (and associated by these authors to the Porangaba Bed) are older than those obtained for the Porangaba Bed in the São Paulo State. Thus, the breccias observed in the Goiás State are probably not part of the Poranbaga Bed described for the Teresina/Corumbataí Formation from the São Paulo State, which the origin of breccias is probably associated to the Permian reactivation of the Jacutinga Fault, by intraplate stress propagation associated to the Sanrafaelica Orogeny (Riccomini et al., 1992; Rostirolla et al., 2003; Turra, 2009; Varejão et al., 2022). Alternatively, these breccia levels may compose an interval ("Porangaba Bed Interval") related to distinct triggering events.

5.2. Permian volcanism and related sources

During the early to middle Permian (280–260 Ma), the southwestern Gondwana margin experienced episodes of intense volcanism. In the inner part of the supercontinent, these events were recorded as rare tuffaceous horizons deposited in the Paraná Basin (Brazil, Paraguay, and Uruguay) (Coutinho et al., 1988; Milani and Ramos, 1998; López-Gamundi, 2006; Rocha-Campos et al., 2011). Due to age and geochemical characteristics, many of these tuff levels have been associated with the multiple magmatic events related to the Permian-Triassic Choiyoi Orogeny that occurred between 280 and 250 Ma (Milani and Ramos, 1998; Rocha-Campos et al., 2011). Thus, this large volcano-plutonic complex characterized by lava flows, ignimbrites, pyroclastic, and sub-volcanic rocks cropping out in the current central Chile and western Argentina was the main source for the ashes deposited in the intracontinental basins (Kay et al., 1989; Kleiman and Japas, 2009; Fanning et al., 2011).

Since the chemical characteristics of the crystallization play an important role in the origin and growth of zircon grains, it is possible to suggest a preliminary petrogenetic classification based on external morphology (Pupin and Turco, 1975; Pupin, 1976, 1980). As previously mentioned, the analyzed zircon population fits well in the morphological subtypes P1-4; S5, 9, 10, 15, 18–25 (see Fig. 3B; Pupin, 1980), commonly related to granite of crustal + mantle affinity (orogenic granite, leucogranite, monzogranite, granodiorite and sienogranite). Additionally, most of the analyzed Permian zircons with ages between 267 and 262 Ma have minimum and maximum negative εHf values of −5.5 to −0.9, respectively (Figs. 4 and 5). This suggests a strong crustal influence in the genesis of the granitoid rocks (Faure, 1986).

The Permian age of the analyzed zircon and the mostly negative εHf values are consistent with geochronological and geochemical data from the Choiyoi igneous province. Negative εHf values (−15.3 to −0.08) were reported in the Permian (ca. 260–269 Ma) igneous rocks from the Frontal Cordillera (Central Andes) (Poma et al., 2014; Pepper et al., 2016; Capaldi et al., 2021), North Patagonia Massif (258–269 Ma, εHf

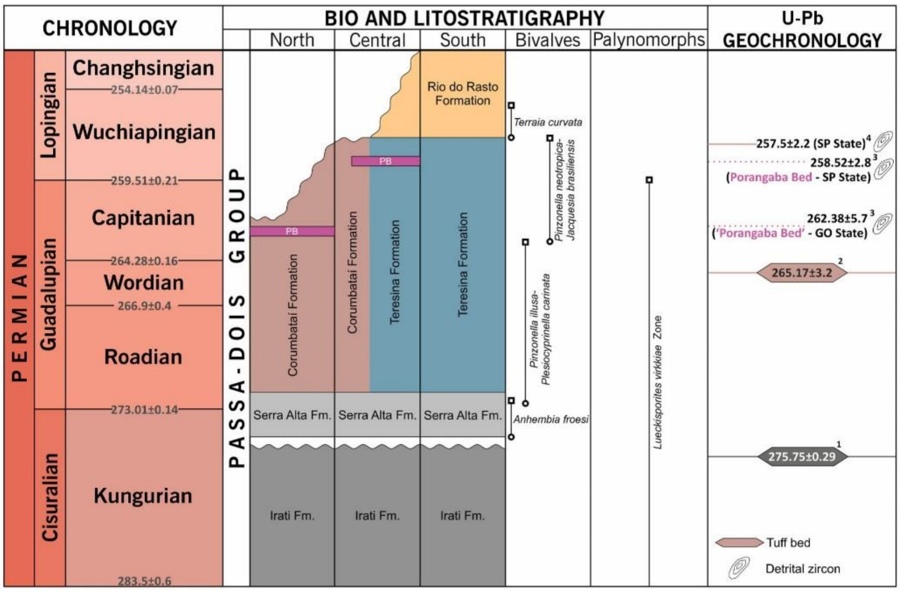

Fig. 7. Chronostratigraphic correlation of the Passa Dois Group in the south, central and north parts of the Paraná Basin. Palynozone, bivalve association biozones, and the main available U-Pb ages are highlighted. The chronostratigraphy is according to the International Commission on Stratigraphy 2022/10 chart (Cohen et al., 2013; updated). Radiometric ages from: 1 – Cagliari et al. (2022); 2 – This contribution; 3 – Tohver et al. (2018); 4 – Rocha-Campos et al. (2019). Palynological data from Rocha et al. (2020) and biostratigraphic data from Simões et al. (2020). Explanation: Fm.: Formation; PB: Porangaba Bed.

values between −32.9 and − 2.8, Fanning et al., 2011; Chernicoff et al., 2013; Pepper et al., 2016; Castillo et al., 2017), igneous rocks from Northern Antarctic Peninsula (ca. 263–269 Ma, εHf values −20 to − 7, Fanning et al., 2011), and Tierra del Fuego (ca. 260–262 Ma, εHf values −12.2 to − 9.5, Castillo et al., 2017) (Fig. 8).

When compared with the available data from the Choiyoi Province (Fig. 8), the age dispersion indicate affinity with Frontal Cordillera and North Patagonia Massif, while the εHf values are more similar to those found in the Frontal Cordillera. On the other hand, the Northern Antarctic Peninsula and Tierra del Fuego showed more negative εHf values and less compatibility with the tuff studied here.

Analyzing the atmospheric circulation pattern that prevailed during the middle and late Permian, it is noteworthy the presence of a high-pressure cell developed during summers in the southern hemisphere (Fig. 9; Parrish and Curtis, 1982). Thus, as pointed by the ages and Lu-Hf data, it is plausible that winds blowing from SW to NE carried ashes from

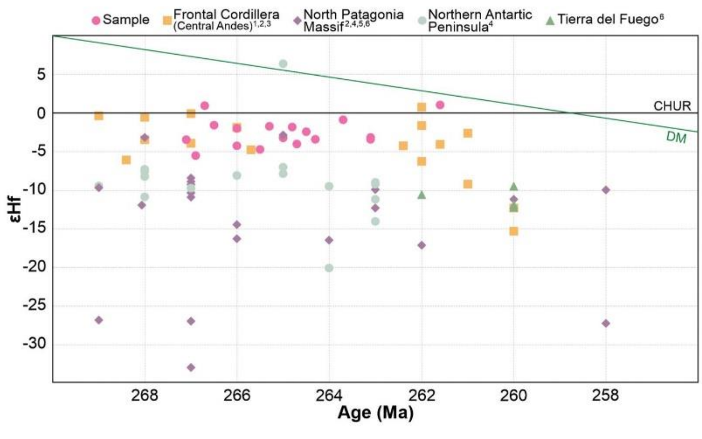

Fig. 8. Lu-Hf comparison of the Permian tuff bed from the upper Corumbataí Formation and multiple magmatic provinces associated to the Choiyoi Orogeny. 1 – Poma et al. (2014); 2 – Pepper et al. (2016); 3 – Capaldi et al. (2021); 4 – Fanning et al. (2011); 5 – Chernicoff et al. (2013); 6 – Castillo et al. (2017). Explanation: CHUR: chondritic values; DM: depleted mantle.

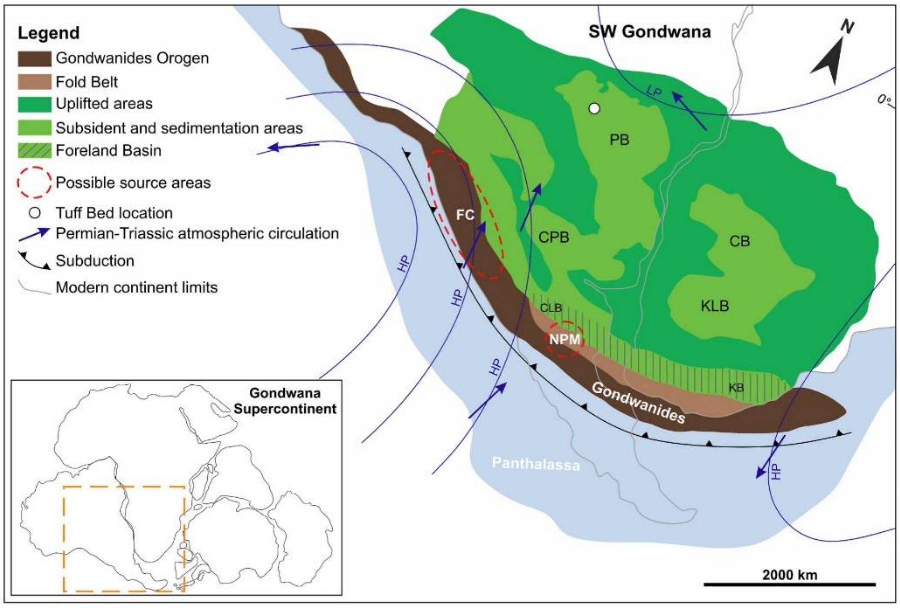

Fig. 9. Reconstruction of the Permian-Triassic paleogeography and atmospheric circulation of the SW Gondwana showing possible source areas and the depositional site of the Corumbataí Formation tuff bed in the Paraná Basin. Explanation: PB – Paraná Basin; CPB – Chaco-Paraná Basin; CB – Congo Basin; KLB – Kalahari Basin; CLM – Claromecó Basin; KB – Kalahari Basin; FC – Frontal Cordillera; NPM – North Patagonia Massif; HP – High-pressure; LP – Low-pressure. Paleogeography reconstruction modified from Faure and Cole (1999); atmospheric circulation pattern based on Parrish and Curtis (1982).

the Frontal Cordillera or North Patagonia Massif to the Paraná Basin depositional site located about 2000 km from the magmatic source area (Fig. 9).

Acceptance of the Choiyoi igneous province vents as the source for Paraná Basin tuff beds would imply in dispersion of volcanic ash clouds transportation for distances from over 2000 km. Rocha-Campos et al. (2011) compared the Toba eruption event (Indonesia, 75 ka) that left a blanket over an area of about 4,000,000 km^2 (over 20.5 times the Paraná Basin area) up to 3000 km away (Rose and Chesner, 1987), characterizing a large scale explosive eruption of plinian to ultraplinian intensity. In largest eruptions the ash clouds typically develop diameters greater than 600 km and up to 6000 km in the most powerful supereruptions, thus explaining why areas of continental size can be covered with volcanic ash (Baines and Sparks, 2005). Furthermore, models of dispersion of volcanic ash clouds indicate that particles with sizes varying between 30 and 100 μm can reach distances of up to 3000 km from the source area (Beckett et al., 2015), which is compatible with the size of zircon grains from the tuffaceous bed here analyzed.

REEs are useful tracers for petrogenetic processes, and they are commonly used for characterization of rocks (Rollinson, 1993). In this sense, the REE concentrations of the tuff were normalized to the chondrite values (Boynton, 1984) and the total REE abundance obtained was in sum 135 ppm. As seen in Fig. 10, REE pattern of the tuff is similar to the geo-standard RGM-1. It is characterized by LREE enrichment ($La_N/Sm_N = 5.32$) and relatively flat to depleted in HREE ($Gd_N/Yb_N = 2.26$). They also show absence to slightly negative Eu anomalies ($Eu/Eu^* = 0.81$).

According to Rollinson (1993), Eu anomalies are chiefly controlled by feldspar; particularly in felsic magmas and the removal of feldspar from a felsic melt by crystal fractionation give rise to a negative Eu anomaly. However, negative Eu anomalies is not recognized in the REE patterns of the tuff (Fig. 10), the LREE-enriched and relatively flat HREE.

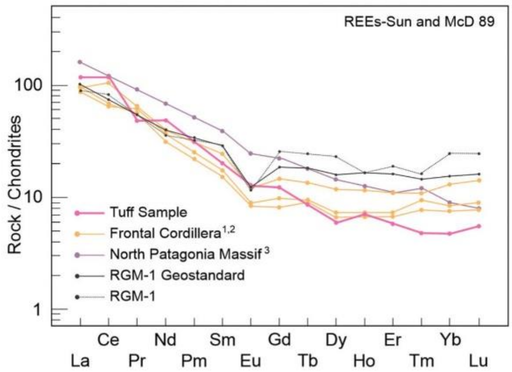

Fig. 10. Chondrite-normalized REE patterns of the tuff (Boynton, 1984), Frontal Cordillera (1 – Poma et al., 2014; 2 – Rocher et al., 2015), North Patagonia Massif (3 – Gregori et al., 2021), theorical RGM-1 geostandard and RGM-1 geostandard analyzed in this work (black dashed line).

The compatibility of the Corumbataí Formation ash fall layer and the Frontal Cordillera were also tested by comparing their rare earth elements (REE) and depict a great compatibility (data from Poma et al., 2014; Rocher et al., 2015), indicating similar origin and evolution (Fig. 10). Rare earth elements sum of the tuff sample (135 ppm) is in the range of that reported by the same vulcanism (119–234 ppm; Rocher et al., 2015). The REEs normalized to the chondrite patterns obtained for these authors show moderate slopes, with slightly enriched light REEs, presence of negative Eu anomalies of variable magnitude, and relatively flat patterns in heavy REEs.

Added to all this geochemical data, the grain sizes of the zircons are another specific evidence of congruence between the Frontal Cordillera magmatism and the Corumbataí tuff bed. The zircons of the Llullaillaco Unit (Frontal Cordillera) exhibit 80 μm–200 μm long (Poma et al., 2014) compatible with the mean grain size obtained here (80–110 μm).

5.3. Biostratigraphic implications

The radiometric ages now available are extremely relevant to better constrain the bivalve species duration and the relative ages of some bivalve Association Biozones of the Corumbataí Formation, the most important benthic macrofossils for biostratigraphy and intra and inter-basinal correlations in the Passa Dois Group (Simões and Kowalewski, 1998; Simões et al., 1998). Although the vertical amplitude of some bivalves can transcend the lower and upper limits of bivalve biozones, the first and last appearance data of index bivalve species are vertically well marked. The *Pinzonella neotropica-Jacquesia brasiliensis* Association Biozone is one example (Fig. 11) that is well-recognized by various authors in the Corumbataí and Teresina formations (see Rohn, 1994, and references therein). The biozone is defined by the vertical amplitude of *Pinzonella neotropica*, with the lower limit marked by the first stratigraphic appearance of *P. neotropica*, *Jacquesia brasiliensis*, and the last stratigraphic appearance of *Ferrazia cardinalis* (Rohn, 1994). The upper limit is defined by the last stratigraphic appearance of *P. neotropica* and *Cowperesia anceps* (Rohn, 1994). Fig. 11 show the vertical distribution of the *Pinzonella neotropica-Jacquesia brasilensis*, in which the lower limit of this biozone is slightly older than 262.38 ± 5.7 Ma and the upper limit is ca. 257.5 ± 2.2 Ma. Hence, in the north and central Paraná Basin the local resolution of the *Pinzonella neotropica-Jacquesia brasiliensis* Association Biozone is of ~5 Ma. Just to remember, this biozone can be tracked from Brazil to Paraguay, and our data offers an age for a layer that extends laterally for hundreds of kilometers.

5.4. Evolutionary implications

5.4.1. Bivalve species duration

The concept of bivalve species duration has application in both biostratigraphy and in evolutionary studies (Koch, 1980). Indeed, the maximum temporal bivalve species duration may have an important chronostratigraphic significance, but given the low availability of accurate radiometric ages, only a few information is found in the literature on this topic (see Koch, 1980; Rohn, 1994). Our newly obtained age allows us to, for the first time, evaluate the maximum temporal bivalve species duration of the *Pinzonella neotropica-Jacquesia brasiliensis* Association Biozone, as well as the exclusive species that coexisted in this biozone (*Naiadopsis lamellous*), and about some species that are recorded across various biozones (i.e., *Cowperesia anceps*).

Average bivalve species duration varies with time, environment, life habit, and geographic distribution (Koch, 1980; Stanley, 1990; Rohn, 1994). The average total duration of the marine bivalve species is approximately 10 Ma (Stanley, 1990). However, this value changes significantly for those bivalve species that thrived in interior (lake-sea) basins, given the high speciation and extinction rates coupled to the disturbance in stability in the benthic ecosystems (Koch, 1980; Nevesskaia et al., 1987), characteristic of this type of basin. For example, Koch (1980) investigated the duration of 41 bivalve species, which coexisted in the Western Interior of North America, during the uppermost *Scipoceras gracile* Zone of the Cenomanian, and found an average species duration of 2 Ma. Nevesskaia et al. (1987) has also found values lower than 10 Ma for the total duration of bivalve species that flourished in Cenozoic marine half-closed and nearly closed brackish basins during Oligocene-Pliocene of the Paratethys (see also Nevesskaia et al., 2009). Notably, the duration of *Pinzonella neotropica*, *Jacquesia brasiliensis*, and *Naiadopsis lamellosus* is ~5 Ma, corresponding to an age interval substantially lower than those found by Stanley (1990) for marine settings. In turn, *Cowperesia anceps* that is recorded throughout the Teresina and Corumbataí formations (*Pinzonella illusa-Plesiocyprinella carinata* and *Pinzonella neotropica-Jacquesia brasiliensis* biozones) had a total species duration of ~16 Ma substantially larger than that found by Stanley (1990). One possible explanation is that those endemic species were

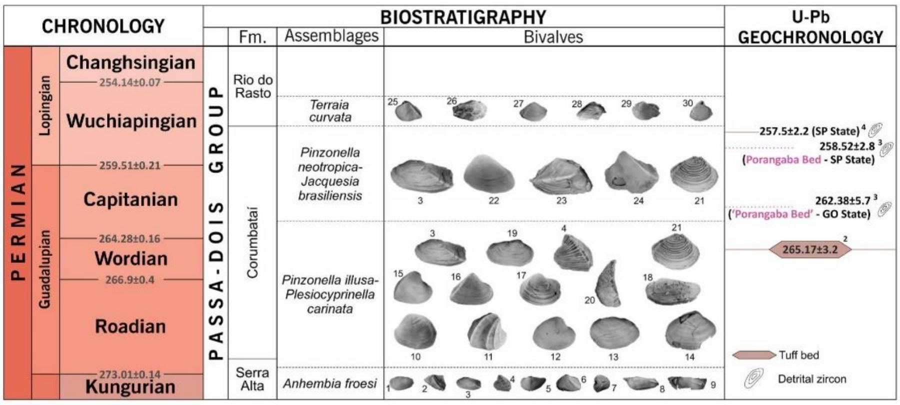

Fig. 11. Chrono and biostratigraphy chart showing the main bivalve assemblages and associated species, which are recorded in the Serra Alta, Corumbataí and Rio do Rasto formations. Species composition (not to scale): 1- *Kidodia* cf. *K. stockleyi*; 2 - *Barbosaia angulata*; 3 - *Holdhausiella elongata*; 4 - *Tambaquyra camargoi*; 5 - *Rioclaroa lefevrei*; 6 - *Maackia contorta*; 7 - *Ferrazia simplicicarinata*; 8 - *Anhembia gigantea*; 9 - *Anhembia froesi*; 10 - *Pinzonella illusa*; 11 - *Ferrazia cardinalis*; 12 - *Casterella gratiosa*; 13 - *Angatubia cowperesioides*; 14 - *Othonella araguaiana*; 15 - *Plesiocyprinella carinata*; 16 - *Terraia aequilateralis*; 17 - *Runnegariella fragilis*; 18 - *Favalia arcuata*; 19 - *Roxoa corumbataiensis*; 20 - *Coxesia mezzalirai*; 21 - *Cowperesia anceps*; 22 - *Pinzonella neotropica*; 23 - *Naiadopsis lamellosus*; 24 - *Jaquesia brasiliensis*; 25 - *Terraia curvata*; 26 - *Beurlenella elongatella*; 27 - *Cowperesia emerita*; 28 - "*Leinzia*" *curta*; 29 - *Terraia bipleura*; 30 - *Astartellopsis prosoclina*. Data from Mendes (1952), Runnegar and Newell (1971), Simões et al. (1998), Matos et al. (2017), Guerrini et al. (2020), and Simões et al. (2020). Compiled U-Pb geochronological data from: 2 – This work; 3 - Tohver et al. (2018); 4 - Rocha-Campos et al. (2019). The chronostratigraphy is according to the International Commission on Stratigraphy 2022/10 chart (Cohen et al., 2013; updated). Explanation: Fm.: Formation.

eurythopic.

5.4.2. From local to global Permian bioevents

The transition between the *Pinzonella illusa-Plesiocyprinella carinata* and *Pinzonella neotropica-Jacquesia brasiliensis* biozones encompasses one of the main faunal turnovers in the fossil record of the Permian Passa Dois Group. Bivalve diversity and abundance dropped significantly at this time (see Simões et al., 2015, p. 23, Fig. 6). Hence, if our geochronological data is correct, this marked faunal change has occurred between ~265 and 262Ma (i.e., Wordian-Capitanian transition). However, the main benthic faunal turnover in the Passa Dois Group is recorded between the *Pinzonella neotropica-Jacquesia brasiliensis* and the *Terraia curvata* assemblage, in the Serrinha Member of the Rio do Rasto Formation (Simões et al., 2015, p. 23, Fig. 11). This faunal change is marked by the end of the *Pinzonella*-dominated bivalve assemblages of the Corumbataí-Teresina formations and its substitution by the *Terraia*-dominated assemblages in the overlying Rio do Rasto Formation (Simões et al., 2015). The species composition, abundance, and dominance in the *Terraia curvata* assemblage differ significantly from the preceding *Pinzonella*-dominated assemblages. Notably, bivalve abundance has never been like that of Corumbataí times. The radiometric ages available (Fig. 11) indicate that this bioevent can now be constrained to ~257.5 Ma, in the middle of the Wuchiapingian.

On the other hand, the ca. 262 Ma to 257 Ma of the total local range of the *Pinzonella neotropica-Jacquesia brasiliensis* indicates that the endemic bivalves survived the end-Guadalupian (ca. 259 Ma) extinction event unscathed. Marine tropical taxa, including the fusulinids, giant bivalves (i.e., family *Alatoconchidae*), and rugose corals that thrived in the Panthalassa and Paleo-Tethys were severely affected by this event (see Arefifard and Payne, 2020, and references therein). Global warming-induced failure of marine associations following the Emeishan volcanism is the main trigger evocated for the end-Guadalupian extinct event (Arefifard and Payne, 2020). Protected within an isolate, continental-scale, inland aquatic system in the Gondwana supercontinent, the Corumbataí-Teresina bivalves were away from this Guadalupian/Lopingian benthic marine biotic crises, showing how the open oceans and the coeval inland seas (or megalakes) have very distinct ecological and evolutionary responses.

6. Conclusion

The tuff bed sample collected in the upper part of the Corumbataí Formation, in the northernmost Paraná Basin (Goiás State), has a Wordian depositional age of 265.17 ± 3.2 Ma. This U-Pb age with Lu-Hf isotopic data, whole-rock geochemistry, and atmospheric circulation data, allows us to pinpoint the source of this ash with confidence and related it to the Frontal Cordillera magmatism (ca. 260–269 Ma). The chronologic constraints based on the age of the most recent volcanic tuff of the Irati Formation (275.75 Ma; Cagliari et al., 2022) and the age for the top of the Corumbataí Formation.

This radiometric age is important to constrain the bivalve species duration and the relative ages of some bivalve Association Biozones of the Corumbataí Formation, the most important benthic macrofossils for biostratigraphy and intra and interbasinal correlations in the Passa Dois Group. The vertical distribution of the *Pinzonella neotropica-Jacquesia brasilensis* is ~5 Ma (262.38 Ma to 257.5 Ma), substantially lower than the age interval proposed by Stanley (1990) for marine environments.

Finally, our geochronological data allow for the transition of the bivalve diversity that fall between the *Pinzonella illusa-Plesiocyprinella carinata* and *Pinzonella neotropica-Jacquesia brasiliensis* biozones to be constrained between ~265 and 262Ma (i.e., Wordian-Capitanian transition); and, in turn, the biggest faunal change in the Passa Dois Group between the *Pinzonella neotropica-Jacquesia brasiliensis* and the *Terraia curvata* assemblage can now be constrained to ~257.5 Ma (middle Wuchiapingian). It is important to note that *Pinzonella neotropica-Jacquesia brasiliensis* assemblage are contemporaneous with the end-Guadalupian (ca. 259 Ma) extinct event that severely affected the Panthalassa and Paleo-Tethys biota. However, the Corumbataí-Teresina bivalves demonstrated a unique ability to adapt and were protected within an isolate, continental-scale, inland aquatic system, confirming how very distinct the ecological and evolutionary dynamics were in this late Paleozoic megalake.

CRediT authorship contribution statement

B. Christofoletti: Writing - review & editing, Writing - original draft, Investigation, Formal analysis, Conceptualization. **L.V. Warren:** Writing - review & editing, Writing - original draft, Validation, Supervision, Resources, Project administration, Investigation, Conceptualization. **F.G. Varejão:** Writing - review & editing, Writing - original draft, Validation, Supervision, Investigation, Formal analysis, Conceptualization. **M.G. Simões:** Writing - review & editing, Validation. **L.E. Gómez-Peral:** Writing - review & editing, Investigation, Formal analysis, Data curation. **C. Lana:** Formal analysis, Data curation. **M.G. Rodrigues:** Writing - review & editing, Data curation. **M.L. Assine:** Writing - review & editing, Data curation.

Declaration of competing interest

The authors declare that they have no known competing financial interests or personal relationships that could have appeared to influence the work reported in this paper.

Data availability

Data will be made available on request.

Acknowledgements

We would like to thank Paloma Promenzio for field assistance and detrital zircon preparations. B. Christofoletti is a fellow of the master's scholarship of the Training of Human Resources in Petroleum Geology Program - UNESP - PRH 40-ANP, supported with financial investment of oil companies qualified in the P, D&I Clause of ANP Resolution No. 50/2015. Lucas V. Warren, Marcello G. Simões and Mario L. Assine are research fellows of the CNPq. The authors would like to acknowledge the National Council for Scientific and Technological Development (CNPq 405521/2021-9) for financial support of the project "Biotic and abiotic interactions in hy- drothermal systems controlling facies variability and heterogeneity in mixed carbonate-siliciclastic successions: Lessons from the Permian of the Paraná Basin, Brazil". Our acknowledgements are extending to financial support from PICT 2018-4022 to Lucía Gómez Peral (FONCYT), and the Centro de Investigaciones Geológicas (CIG) laboratories especially to G. Kurten, L. Vigiani and V. Liegl for their assistance in XRD analysis, and to C. Cavarozzi and V. García for ICP-MS analysis.

Appendix A. Supplementary data

Supplementary data to this article can be found online at https://doi.org/10.1016/j.jsames.2023.104750.

References

Aragão, M., Scardia, G., 2021. Middle–late Permian magnetostratigraphy and the onset of the Illawarra reversals in the northeastern Parana Basin, Aouth America. Geophys. J. Int. 225, 860–871. https://doi.org/10.1093/gji/ggab011.

Arefifard, S., Payne, J.L., 2020. End-Guadalupian extinction of larger fusulinids in central Iran and implications for the global biotic crisis. Palaeogeogr. Palaeoclimatol. Palaeoecol. 550, 109743 https://doi.org/10.1016/j.palaeo.2020.109743.

Baines, P.G., Sparks, R.S.J., 2005. Dynamics of giant volcanic ash clouds from supervolcanic eruptions. Geophys. Res. Lett. 32, L24808 https://doi.org/10.1029/2005GL024597.

Bastos, L.P.H., Rodrigues, R., Pereira, E., Bergamaschi, S., Alferes, C.L.F., Augland, L.E., Domeier, M., Planke, S., Svensen, H.H., 2021. The birth and demise of the vast epicontinental Permian Irati-Whitehill sea: evidence from organic geochemistry, geochronology, and paleogeography. Palaeogeogr. Palaeoclimatol. Palaeoecol. 562, 110103 https://doi.org/10.1016/j.palaeo.2020.11010.

Beckett, F.M., Witham, C.S., Hort, M.C., Stevenson, J.A., Bonadonna, C., Millington, S.C., 2015. Sensitivity of dispersion model forecasts of volcanic ash clouds to the physical characteristics of the particles. J. Geophys. Res. Atmos. 120, 11–636. https://doi.org/10.1002/2015JD023609.

Beurlen, K., 1954. Horizontes fossilíferos das Camadas Serra Alta do Paraná. Boletim DGM-DNPM 152, 1–30.

Beurlen, K., 1957. Faunas salobras fósseis e o tipo ecológico-paleogeográfico das faunas Gondwânicas no Brasil. An Acad. Bras Ciências 29, 229–241.

Biscaye, P.E., 1965. Mineralogy and sedimentation of recent deep-sea clay in the Atlantic ocean and adjacent seas and oceans. Geol. Soc. Am. Bull. 76, 803–832. https://doi.org/10.1130/0016-7606(1965)76[803:MASORD]2.0.CO;2.

Black, L.P., Gulson, B.L., 1978. The age of the Mud Tank carbonatite, Strangeways range, northern territory. BMR (Bur. Miner. Resour.) J. Aust. Geol. Geophys. 3, 227–232.

Black, L.P., Kamo, S.L., Allen, C.M., Aleinikoff, J.N., Davis, D.W., Korsch, R.J., Foudoulis, C., 2003. TEMORA 1: a new zircon standard for Phanerozoic U–Pb geochronology. Chem. Geol. 200, 155–170. https://doi.org/10.1016/S0009-2541(03)00165-7.

Blichert-Toft, J., 2008. The Hf isotopic composition of zircon reference material 91500. Chem. Geol. 253, 252–257. https://doi.org/10.1016/j.chemgeo.2008.05.014.

Boynton, W.V., 1984. Cosmochemistry of the rare earth elements; meteorite studies. In: Henderson, P. (Ed.), Rare Earth Element Geochemistry. Elsevier, Amsterdam, pp. 63–114.

Brown, G., Brindley, G.W., 1980. X-ray diffraction procedures for clay mineral identification. In: Brindley, G.W., Brown, G. (Eds.), Crystal Structures of Clay Minerals and Their X-Ray Identification. Mineralogical Society of Great Britain and Ireland, pp. 305–359.

Cagliari, J., Serratt, H., Cassel, M.C., Schmitz, M.D., Chemale Jr., F., 2022. New high-precision U-Pb zircon age of the Irati Formation (Paraná Basin) and implications for the timing of the Kungurian anoxic events recorded in southern Gondwana. Gondwana Res. 107, 134–145. https://doi.org/10.1016/j.gr.2022.03.004.

Capaldi, T.N., McKenzie, N.R., Horton, B.K., Mackaman-Lofland, C., Colleps, C.L., Stockli, D.F., 2021. Detrital zircon record of Phanerozoic magmatism in the southern Central Andes. Geosphere 17, 876–897. https://doi.org/10.1130/GES02346.1.

Castillo, P., Fanning, C.M., Hervé, F., Lacassie, J.P., 2017. Characterisation and tracing of Permian magmatism in the south-western segment of the Gondwanan margin; U–Pb age, Lu–Hf and O isotopic compositions of detrital zircons from metasedimentary complexes of northern Antarctic Peninsula and western Patagonia. Gondwana Res. 36, 1–13. https://doi.org/10.1016/j.gr.2015.07.014.

Chauvel, C., Lewin, E., Carpentier, M., Arndt, N.T., Marini, J.C., 2008. Role of recycled oceanic basalt and sediment in generating the Hf–Nd mantle array. Nat. Geosci. 1, 64–67. https://doi.org/10.1038/ngeo.2007.51.

Chernicoff, C.J., Zappettini, E.O., Santos, J.O.S., McNaughton, N.J., Belousova, E., 2013. Combined U-Pb SHRIMP and Hf isotope study of the late paleozoic Yaminué complex, Rio Negro province, Argentina: implications for the origin and evolution of the Patagonia composite terrane. Geosci. Front. 4, 37–56. https://doi.org/10.1016/j.gsf.2012.06.003.

Cohen, K.M., Finney, S.C., Gibbard, P.L., Fan, J.X., 2013. The ICS international chronostratigraphic chart. Episodes 36, 199–204.

Coutinho, J.M.V., Dos Santos, P.R., Coimbra, A.M., 1988. Ash-fall derived vitroclastic tuffaceous sediments in the Permian of the Paraná Basin and its provenance. In: Abstracts of the International Gondwana Symposium 7, p. 78.

Coutinho, J.M.V., Hachiro, J., 2005. Distribution, mineralogy, petrography, provenance and significance of Permian ash-carrying deposits in the Paraná Basin. Geologia USP 5, 29–39. https://doi.org/10.5327/S1519-874X2005000100003.

CPRM – Serviço Geológico do Brasil, 2006. Cartas Geológicas Do Brasil Ao Milionésimo.

Crasquin, S., Forel, M.B., Feng, Q., Yuan, A., Baudin, F., Collin, P.Y., 2010. Ostracods (Crustacea) through the Permian-triassic boundary in south China: the Meishan stratotype (Zhejiang province). J. Syst. Palaeontol. 8, 331–370. https://doi.org/10.1080/14772011003784992.

Daemon, R.F., Quadros, L.P., 1970. Bioestratigrafia do Neopaleozóico da Bacia do Paraná. Anais do Congresso Brasileiro de Geologia 24.

Daemon, R.F., 1974. Integragação dos resultados palinológicos aos de fauna e flora de camadas fossiliferas do Neopaleozóico da Bacia do Paraná-Implicações estratigráficas-paleogeográficas. Rev. Unimar 1, 25–41.

Daemon, R.F., Casaletti, P.L., Ciguel, J.H.G., 1996. Biopaleogeografia da Bacia do Paraná. In: Simpósio Sulamericano do Siluro-Devoniano, pp. 55–99.

Du Toit, A.L., 1927. Comparação geológica entre a América do Sul e África do Sul. DNPM-SGM, Rio de Janeiro, p. 179.

Fanning, C.M., Hervé, F., Pankhurst, R.J., Rapela, C.W., Kleiman, L.E., Yaxley, G.M., Castillo, P., 2011. Lu–Hf isotope evidence for the provenance of Permian detritus in accretionary complexes of western Patagonia and the northern Antarctic Peninsula region. J. S. Am. Earth Sci. 32, 485–496. https://doi.org/10.1016/j.jsames.2011.03.007.

Faure, G., 1986. Isotope systematics in two-component mixtures. In: Principles of Isotope Geology, pp. 141–153.

Faure, K., Cole, D., 1999. Geochemical evidence for lacustrine microbial blooms in the vast Permian Main Karoo, Paraná, Falkland Islands and Huab basins of southwestern Gondwana. Palaeogeogr. Palaeoclimatol. Palaeoecol. 152, 189–213. https://doi.org/10.1016/S0031-0182(99)00062-0.

Ghilardi, R.P., Simões, M.G., 2002. Foram os bivalves do Grupo Passa Dois (exclusive Formação Rio do Rasto), Neopermiano, invertebrados tipicamente dulcícolas? Pesqui. em Geociencias 29, 83–95.

Gregori, D.A., Strazzere, L., Barros, M., Benedini, L., Marcos, P., Kostadinoff, J., 2021. The Mencué batholith: Permian episodic arc-related magmatism in the western North Patagonian Massif, Argentina. Int. Geol. Rev. 63, 317–341. https://doi.org/10.1080/00206814.2019.1710865.

Guerra-Sommer, M., Cazzulo-Klepzig, M., Santos, J.O.S., Hartmann, L.A., Ketzer, J.M., Formoso, M.L.L., 2008. Radiometric age determination of tonsteins and stratigraphic constraints for the Lower Permian coal succession in southern Paraná Basin, Brazil. Int. J. Coal Geol. 74, 13–27. https://doi.org/10.1016/j.coal.2007.09.005.

Guerrini, V.B., Matos, S.A., Rohn, R., Varejão, F.G., Warren Lvand Simões, M.G., 2020. The last chapter of 30 million years of molluscan evolution: Permian non-marine bivalves of the Rio do Rasto Formation, Paraná Basin, Brazil. PalZ 94, 487–512. https://doi.org/10.1007/s12542-019-00455-0.

Holz, M., França, A.B., Souza, P.A., Iannuzzi, R., Rohn, R., 2010. A stratigraphic chart of the Late Carboniferous/Permian succession of the eastern border of the Paraná Basin, Brazil, South America. J. S. Am. Earth Sci. 29, 381–399. https://doi.org/10.1016/j.jsames.2009.04.004.

Jackson, S.E., Pearson, N.J., Griffin, W.L., Belousova, E.A., 2004. The application of laser ablation-inductively coupled plasma-mass spectrometry to in-situ U-Pb zircon geochronology. Chem. Geol. 211, 47–69. https://doi.org/10.1016/j.chemgeo.2004.06.017.

Kay, S.M., Ramos, V.A., Mpodozis, C., Sruoga, P., 1989. Late paleozoic to Jurassic silicic magmatism at the Gondwana margin: analogy to the middle Proterozoic in north America. Geology 17, 324–328. https://doi.org/10.1130/0091-7613(1989)017<0324:LPTJSM>2.3.CO.

Keidel, H., 1916. La geología de las sierras de la provincia de Buenos Aires y sus relaciones con las montañas de Sud Africa y los Andes. Talleres gráficos del Ministerio de agricultura de la nación.

Kleiman, L.E., Japas, M.S., 2009. The Choiyoi volcanic province at 34°–36°S (San Rafael, Mendoza, Argentina): implications for the late Paleozoic evolution of the southwestern margin of Gondwana. Tectonophysics 473, 283–299. https://doi.org/10.1016/j.tecto.2009.02.046.

Koch, C.F., 1980. Bivalve species duration, areal extent, and population size in a Cretaceous Sea. Paleobiology 6, 184–192. https://doi.org/10.1017/S0094837300006746.

Limarino, C.O., Césari, S.N., Spalletti, L.A., Taboada, A.C., Isbell, J.L., Geuna, S., Gulbranson, E.L., 2014. A paleoclimatic review of southern South America during the late Paleozoic: a record from icehouse to extreme greenhouse conditions. Gondwana Res. 25, 1396–1421. https://doi.org/10.1016/j.gr.2012.12.022.

López-Gamundi, O.R., 2006. Permian plate margin volcanism and tuffs in adjacent basins of west Gondwana: age constrains and common characteristics. J. S. Am. Earth Sci. 22, 227–238. https://doi.org/10.1016/j.jsames.2006.09.012.

Ludwig, K.R., 2003. User's Manual for Isoplot 3.00: A Geochronological Toolkit for Microsoft Excel. Berkeley Geochronology Center, Special Publication, 1–70.

Maranhão, M.S.A.S., 1995. Fósseis das formações Corumbataí e Estrada Nova do Estado de São Paulo: subsídios ao conhecimento paleontológico e bioestratigráfico. PhD thesis. Universidade de São Paulo.

Maranhão, M.S.A.S., Petri, S., 1996. Novas ocorrências de fósseis nas formações Corumbataí e Estrada Nova de São Paulo e considerações sobre o seu significado paleontológico e bioestratigráfico, 17. Revista do Instituto Geológico, pp. 33–54.

Matos, S.L.F., 1995. O contato entre o Grupo Passa Dois e a Formação Piramboia na borda Leste da Bacia do Paraná no Estado de São Paulo. Universidade de São Paulo. MSc thesis.

Matos, S.L.F., Coimbra, A.M., 1997. Sucessão de Fácies na Camada Porangaba, Grupo Passa Dois, Estado de São Paulo. Rev. Bras. Geociencias 27, 377–386.

Matos, S.A., Warren, L.V., Fürsich, F.T., Alessandretti, L., Assine, M.L., Riccomini, C., Simoes, M.G., 2017. Paleoecology and paleoenvironments of Permian bivalves of the Serra Alta Formation, Brazil: ordinary suspension feeders or late paleozoic Gondwana seep organisms? J. S. Am. Earth Sci. 77, 21–41. https://doi.org/10.1016/j.jsames.2017.04.007.

Maynard, J.B., Chocyk-Jaminski, M., Gaines, R.R., Huff, W.D., Krekeler, M.P., Prokopenko, M., Summers, A.M., 1996. Bentonites in the Late Permian (Tatarian) Irati Formation of Brazil; Geochemistry and Potential for Stratigraphic Correlation, 28. Geological Society of America, Abstracts with Programs, p. 280.

Mendes, J.C., 1949. Novos Lamelibrânquios fósseis da Série Passa Dois, sul do Brasil. Divisão Geológica e Mineralógica do Brasil 133, 1–40.

Mendes, J.C., 1952. A Formação Corumbataí na região do Rio Corumbataí. Estratigrafia e descrição dos lamelibrânquios. Boletim USP 145, 119.

Mendes, J.C., 1967. The Passa Dois group (the Brazilian portion of the Parana basin). In: Bigarella, J.J., Becker, R.D., Pinto, I.D. (Eds.), Problems in Brazilian Gondwana Geology. Curitiba, pp. 119–166.

Mendes, J.C., 1984. Sobre Os Paleoambientes Deposicionais Do Grupo Passa Dois, 5. Revista do Instituto Geológico, pp. 15–24.

Milani, E.J., 1997. Evolução tectono-estratigráfica da Bacia do Paraná e seu relacionamento com a geodinâmica fanerozóica do Gondwana sul-ocidental. Universidade Federal do Rio Grande do Sul. PhD thesis.

Milani, E.J., Ramos, V.A., 1998. Orogenias paleozóicas no domínio sul-ocidental do Gondwana e os ciclos de subsidência da Bacia do Paraná. Rev. Bras. Geociencias 28, 473–484.

Milani, E.J., Araujo, L.M., Cupertino, J.A., Faccini, U.F., Scherer, C.M., 1998. Sequences and Stratigraphic Hierarchy of the Parana Basin (Ordovician Cretaceous), Southern Brazil, 29. Boletim IG-USP.

Milani, E.J., Melo, J.H.G., Souza, P.A., Fernades, L.A., França, A.B., 2007. Bacia do Paraná. Bol. Geociencias Petrobras 15, 265–287.

Moore, D.M., Reynolds Jr., R.C., 1997. X Ray Diffraction and the Identification and Analysis of Clay Minerals, 2nd. Oxford University Press, Oxford.
Moraes Rego, L.F., 1930. A geologia do petróleo no Estado de São Paulo. Boletim do Serviço Geológico e Mineral Brasileiro, Rio de Janeiro, p. 110.
Mori, A.L.O., Souza, P.A., Marques, J.C., Cunha Lopes, R., 2012. A new U–Pb zircon age dating and palynological data from a Lower Permian section of the southernmost Paraná Basin, Brazil: biochronostratigraphical and geochronological implications for Gondwanan correlations. Gondwana Res. 21, 654–669. https://doi.org/10.1016/j.gr.2011.05.019.
Neregato, R., Souza, P.A.D., Rohn, R., 2008. Registros palinológicos inéditos nas formações Teresina e Rio do Rasto (Permiano, Grupo Passa Dois, Bacia do Paraná): implicações biocronoestratigráficas e paleoambientais. Pesqui. em Geociencias 35, 9–21.
Nevesskaia, L.A., Iljina, L.B., Paramonova, N.P., 1987. Evolutionary transformations of mollusks in basins of different types. Paleontol. J. 4, 5–15.
Nevesskaia, L.A., Goncharova, I., Il'ina, L.B., Popov, S.V., 2009. Evolutionary transformations of the malacofaunas in the Neogene basins of Paratethys as an example of development of the ecosystems of insular type. Zh. Obshch. Biol. 70, 396–414 (In Russian).
Ng, C., Vega, C.S., Maranhão, M.D.S.A.S., 2019. Mixed carbonate-siliciclastic microfacies from Permian deposits of Western Gondwana: evidence of gradual marine to continental transition or episodes of marine transgression? Sediment. Geol. 390, 62–82. https://doi.org/10.1016/j.sedgeo.2019.07.006.
Palcu, D.V., Patina, I.S., Şandric, I., Lazarev, S., Vasiliev, I., Stoica, M., Krijgsman, W., 2021. Late miocene megalake regressions in Eurasia. Sci. Rep. 11, 11471 https://doi.org/10.1038/s41598 021 91001 z.
Parrish, J.T., Curtis, R.L., 1982. Atmospheric circulation, upwelling, and organic-rich rocks in the Mesozoic and Cenozoic eras. Palaeogeogr. Palaeoclimatol. Palaeoecol. 40, 31–66. https://doi.org/10.1016/0031-0182(82)90084-0.
Pepper, M., Gehrels, G., Pullen, A., Ibanez-Mejia, M., Ward, K.M., Kapp, P., 2016. Magmatic history and crustal genesis of western South America: constraints from U-Pb ages and Hf isotopes of detrital zircons in modern rivers. Geosphere 12, 1532–1555. https://doi.org/10.1130/GES01315.1.
Petri, S., Coimbra, A.M., 1982. Estruturas sedimentares das Formações Irati e Estrada Nova (Permiano) e sua contribuição para elucidação dos seus paleoambientes geradores. Congresso Latino-Americano de Geologia 5, 353–371.
Poma, S., Zappettini, E.O., Quenardelle, S., Santos, J.O., Koukharsky, M., Belousova, E., McNaughton, N., 2014. Geochemistry, U-Pb SHRIMP zircon dating and Hf isotopes of the Gondwanan magmatism in NW Argentina: petrogenesis and geodynamic implications. Andean Geol. 41, 267–292. https://doi.org/10.5027/andgeoV41n2-a01.
Pupin, J.P., Turco, G., 1975. Typologie de zircon accessoire dans les roches plutoniques dioritiques, granitiques et syenitiques, Facteurs essentiels determinant les variations typologiques. Petrologie 1, 139–156.
Pupin, J.P., 1976. Signification des caractgres morphologiques du zircon commun des roches en petrologie. Base de la methode typologique. Applications. PhD thesis. Nice University.
Pupin, J.P., 1980. Zircon and granite petrology. Contrib. Mineral. Petrol. 73, 207–220.
Ragonha, E.W., 1984. Taxionomia de dentes e espinhos isolados de Xenacanthodii (condrichthyes, elasmobranchii) da Formação Corumbataí: considerações cronológicas e paleoambientais. PhD thesis. Universidade de São Paulo.
Ramos, V.A., Jordan, T.E., Allmendinger, R.W., Mpodozis, C., Kay, S.M., Cortés, J.M., Palma, M., 1986. Paleozoic terranes of the central Argentine-Chilean Andes. Tectonics 5, 855–880. https://doi.org/10.1029/TC005i006p00855.
Reed, F.R.C., 1929. Faunas triássicas do Brasil. Serviço Geológico Minerário do Brasil 9, 1–97.
Reed, F.R.C., 1932. Triassic fossils from Brazil. Ann. Mag. Nat. Hist. 2, 39–48.
Reed, F.R.C., 1935. Some triassic lamellibranchs from Brazil and Paraguay. Geol. Mag. 72, 33–42. https://doi.org/10.1017/S0016756800092311.
Riccomini, C., Chamani, M.A.C., Agena, S.S., Fambrini, G.L., Fairchild, T.R., Coimbra, A.M., 1992. Earthquake-induced liquefaction features in the Corumbataí Formation (Permian, Paraná Basin, Brazil) and the dynamics of Gondwana. An Acad. Bras Ciências 64, 210.
Rocha, H.D.V., Mendes, M., Pereira, Z., Rodrigues, C., Fernandes, P., Lopes, G., Santa'Anna, L.G., Tassinari, C.C.G., Sousa, M.L., 2020. New palynostratigraphic data of the Irati (Assistência Member) and the Corumbataí formations, Paraná Basin, Brazil, and correlation with other south American basins. J. S. Am. Earth Sci. 102, 102631 https://doi.org/10.1016/j.jsames.2020.102631.
Rocha-Campos, A.C., Basei, M.A.S., Nutman, A.P., Santos, P.D., 2006. SHRIMP U-Pb zircon geochronological calibration of the late Paleozoic supersequence, Paraná Basin, Brazil. In: 5th South American Symposium on Isotope Geology, Buenos Aires, Argentina.
Rocha-Campos, A.C., Basei, M.A., Nutman, A.P., Kleiman, L.E., Varela, R., Llambias, E., Canile, F.M., Da Rosa, O.D.C., 2011. 30 million years of Permian volcanism recorded in the Choiyoi igneous province (W Argentina) and their source for younger ash fall deposits in the Paraná Basin: SHRIMP U–Pb zircon geochronology evidence. Gondwana Res. 19, 509–523. https://doi.org/10.1016/j.gr.2010.07.003.
Rocha-Campos, A.C., Basei, M.A.S., Nutman, A.P., Santos, P.R.D., Passarelli, C.R., Canile, F.M., Rosa, O.C.R., Fernandes, M.T., Santa Ana, H., Veroslavsky, G., 2019. U-Pb zircon dating of ash fall deposits from the paleozoic Paraná Basin of Brazil and Uruguay: a reevaluation of the stratigraphic correlations. J. Geol. 127, 167–182. https://doi.org/10.1086/701254.
Rocher, S., Vallecillo, B., Alasino, P., 2015. El Grupo Choiyoi (Pérmico temprano-medio) en la Cordillera Frontal de Calingasta, San Juan, Argentina: volcanismo de arco asociado a extensión. Rev. Mex. Ciencias Geol. 32, 415–432.
Rohn, R., Rösler, O., 1987. Relações entre a Flora Permiana do Gondwana e as floras das províncias setentrionais. Congresso Brasileiro de Paleontologia 10, 885–899.
Rohn, R., Lavina, E.L., 1993. Cronoestratigrafia do Grupo Passa Dois. In: Simpósio de Cronoestratigrafia da Bacia do Paraná, pp. 77–80.
Rohn, R., 1994. Evolução ambiental da Bacia do Paraná durante o Neo-Permiano no leste de Santa Catarina e do Paraná. PhD thesis. Universidade de São Paulo.
Rohn, R., 2007. The Passa Dois group (Paraná Basin, Permian): investigations in progress. In: Extended Abstracts from 1st Workshop on Problems in Western Gondwana Geology, pp. 151–157.
Rollinson, H.R., 1993. Using Trace Element Data, Part 4. *Using Geochemical Data Book: Evaluation, Presentation, Interpretation*. JohnWiley & Sons Inc., New York, p. 352.
Rose, W.I., Chesner, C.A., 1987. Dispersal of ash in the great Toba eruption, 75 ka. Geology 15, 913–917. https://doi.org/10.1130/0091-7613(1987)15<913:DOAITG>2.0.CO.
Rostirolla, S.P., Mancini, F., Rigoti, A., Kraft, R.P., 2003. Structural styles of the intracratonic reactivation of the Perimbó fault zone, Paraná basin, Brazil. J. S. Am. Earth Sci. 16, 287–300. https://doi.org/10.1016/S0895-9811(03)00065-8.
Runnegar, B., Newell, N.D., 1971. Caspian-like relict molluscan fauna in South American Permian. Bull. Am. Mus. Nat. Hist. 146, 1–66.
Runnegar, B., 1977. Marine fossil invertebrates of the Gondwanaland: paleogeographic implications. In: Papers of the International Gondwana Symposium, 4, pp. 305–339.
Santos, R.V., Souza, P.A., de Alvarenga, C.J.S., Dantas, E.L., Pimentel, M.M., de Oliveira, C.G., de Araújo, L.M., 2006. Shrimp U–Pb zircon dating and palynology of bentonitic layers from the Permian Irati Formation, Paraná Basin, Brazil. Gondwana Res. 9, 456–463. https://doi.org/10.1016/j.gr.2005.12.001.
Santos, M.M., Lana, C., Scholz, R., Buick, I., Schmitz, M.D., Kamo, S.L., Gerdes, A., Corfu, F., Tapster, S., Lancaster, P., Storey, C.D., Basei, M.A.S., Tohver, E., Alkmim, A., Nalini, H., Krambrock, K., Fantini, C., Wiedenbeck, M., 2017. A new appraisal of Sri Lankan BB zircon as a reference material for LA-ICP-MS U-Pb geochronology and Lu-Hf isotope tracing. Geostand. Geoanal. Res. 41, 335–358. https://doi.org/10.1111/ggr.12167.
Schneider, R.L., Mühlmann, H., Tommasi, E., Medeiros, R.A., Daemon, R.F., Nogueira, A.A., 1974. Revisão estratigráfca da Bacia do Paraná. In: 28° Congresso Brasileiro de Geologia, Porto Alegre, pp. 41–66.
Shu, O., Utting, J., 1990. Palynology of upper Permian and lower triassic rocks, Meishan, Changxing County, Zhejiang province, China. Rev. Palaeobot. Palynol. 66, 65–103. https://doi.org/10.1016/0034-6667(90)90029-I.
Silva, A.F., Dani, N., Remus, M.V.D., Sommer, M.G., Horn, B.L.D., 2017. Bentonitas da Formação Irati no setor sul da Bacia do Paraná. Geologia USP 17, 75–88. https://doi.org/10.11606/issn.2316-9095.v17-368.
Silva, J.P., Lana, C., Mazoz, A., Buick, I., Scholz, R., 2022. U Pb Saturn: new U-Pb/Pb Pb data reduction software for LA-ICP-MS. Geostand. Geoanal. Res. 47, 49–66. https://doi.org/10.1111/ggr.12474.
Simões, M.G., 1992. Pelecípodes da Formação Palermo (Permiano) de São Sepé (RS) e Guiratinga (MT): implicações na evolução da fauna neopaleozóica da Bacia do Paraná. PhD thesis. Universidade de São Paulo.
Simões, M.G., Kowalewski, M., 1998. Shell beds as paleoecological puzzles: a case study from the Upper Permian of the Paraná Basin, Brazil. Facies 38, 175–195. https://doi.org/10.1007/BF02537364.
Simões, M.G., Rocha Campos, A.C., Anelli, L.E., 1998. Paleoecology and evolution of Permian pelecypod assemblages (Paraná Basin) from Brazil. In: Johnston, (PA, Haggart, J.W. (Eds.), Bivalves – an Eon of Evolution- Paleobiological Studies Honoring Norman D. Newell. University of Calgary Press, Calgary, pp. 443–452.
Simões, M.G., Torello, F.F., Mello, L.H.C., Ghilardi, R.P., 2000. O conteúdo fossilífero de novos afloramentos do Grupo Passa Dois (Neopermiano), nas porções centro-sul e nordeste do Estado de São Paulo: implicações bioestratigráficas e paleoecológicas. Acta Geol. Leopoldensia 23, 61–90.
Simões, M.G., Matos, S.A., Anelli, L.E., Rohn, R., Warren, L.V., David, J.M., 2015. A new Permian bivalve dominated assemblage in the Rio do Rasto Formation, Paraná Basin, Brazil: faunal turnover driven by regional-scale environmental changes in a vast epeiric sea. J. S. Am. Earth Sci. 64, 14–26. https://doi.org/10.1016/j.jsames.2015.09.009.
Simões, M.G., Guerrini, V.B., Matos, S.A., Rohn, R., 2020. Morphology and taxonomic position of the bizarre Permian pachydomid bivalve Leinzia from Western Gondwana. Acta Palaeontol. Pol. 65, 291–303. https://doi.org/10.4202/app.00665.2019.
Simões, M.G., Torello, F.F., Rocha-Campos, A.C., 1996. Gênese e classificação da coquina de Camaquã (assembléia de Pinzonella neotropica), Formação Corumbataí (Permiano Superior), Rio Claro. SP. Anais da Academia Brasileira de Ciências 68, 545–557.
Sláma, J., Košler, J., Condon, D.J., Crowley, J.L., Gerdes, A., Hanchar, J.M., Horstwood, M.S.S., Morris, G.A., Lutz, N., Norberg, N., Schaltegger, U., Schoene, B., Tubrett, M.N., Whitehouse, M.J., 2008. Plešovice zircon—a new natural reference material for U–Pb and Hf isotopic microanalysis. Chem. Geol. 249, 1–3. https://doi.org/10.1016/j.chemgeo.2007.11.005.
Söderlund, U., Patchett, P.J., Vervoort, J.D., Isachsen, C.E., 2004. The 176Lu decay constant determined by Lu–Hf and U–Pb isotope systematics of Precambrian mafic intrusions. Earth Planet Sci. Lett. 219, 311–324. https://doi.org/10.1016/S0012-821X(04)00012-3.
Sohn, I.G., Rocha Campos, A.C., 1990. Late paleozoic (Gondwanan) ostracodes in the Corumbataí Formation, Paraná Basin, Brazil. J. Paleontol. 64, 116–128. https://doi.org/10.1017/S0022336000042293.
Sousa, S.H.M., 1985. Fácies sedimentares das formações Estrada Nova e Corumbataí no Estado de São Paulo. MSc thesis. Universidade de São Paulo.

Souza, P.A., Marques Toigo, M., 2005. Progress on the palynostratigraphy of the Permian strata in Rio Grande do sul state, Paraná Basin, Brazil. An Acad. Bras Ciências 77, 353–365.

Stanley, S.M., 1990. The general correlation between rate of speciation and rate of extinction: fortuitous causal linkages. In: Ross, R.M., Allmon, W.D. (Eds.), Causes of Evolution: A Paleontological Perspective. Chicago University Press, Chicago, pp. 103–172.

Suguio, K., Salati, C., Barcelos, J.H., 1974. Calcários oolíticos de Taguaí, SP e seu possível significado paleoambiental na deposição da Formação Estrada Nova. Rev. Bras. Geociencias 4, 142–160.

Sun, S., McDonough, W.F., 1989. Chemical and isotopic systematics of oceanic Basalts: implications for mantle composition and processes. In: Saunders, A.D., Norry, M.J. (Eds.), Magmatism in the Ocean Basins, 42. Geological Society of London Special Publications, pp. 313–345.

Tohver, E., Schmieder, M., Lana, C., Mendes, P.S., Jourdan, F., Warren, L.V., Riccomini, C., 2018. End Permian impactogenic earthquake and tsunami deposits in the intracratonic Paraná Basin of Brazil. GSA Bull. 130, 1099–1120. https://doi.org/10.1130/B31626.1.

Tomassi, H.Z., 2009. Taxonomia, Tafonomia e Paleoecologia de Ostracodes (Crustacea) da Formação Corumbataí, Permiano da Bacia do Paraná, Estado de Goiás, Brasil. MSc. Thesis. Universidade de Brasília.

Turra, B.B., 2009. Diques clásticos da Formação Corumbataí, Bacia do Paraná, no contexto da tectônica permotriássica do Gondwana Ocidental. MSc thesis. Universidade de São Paulo.

Valencio, D.A., Rocha Campos, A.C., Pacca, I.G., 1975. Paleomagnetism of some sedimentary rocks of the late paleozoic Tubarão and Passa Dois groups from the Paraná Basin, Brazil. Rev. Bras. Geociencias 5, 186–197.

Varejão, F.G., Warren, L.V., Alessandretti, L., Rodrigues, M.G., Riccomini, C., Assine, M., Cury, L.F., Faleiros, F.M., Simões, M.G., 2022. Late Permian siliceous hot springs developed on the margin of a restricted epeiric sea: Insights into strata confined silicification in mixed siliciclastic-carbonate successions. Palaeogeogr. Palaeoclimatol. Palaeoecol. 604, 111213 https://doi.org/10.1016/j.palaeo.2022.111213.

Von Huene, F., 1928. Aphorismen über die Stratigraphie des brasilianisch Staates Sao Paulo. Separat-Abdruck aus dem Centralblatt für Mineralogie. Geologie und Paläontologie 10, 524–531 (German).

Warren, L.V., Almeida, R.P., Hachiro, J., Machado, R., Roldan, L.F., Steiner, S.S., Chamani, M.A.C., 2008. Evolução Sedimentar da Formação Rio do Rasto (Permo-Triássico da Bacia do Paraná) na porção centro sul do Estado de Santa Catarina, Brasil. Rev. Bras. Geociencias 38, 213–227.

Warren, L.V., Assine, M.L., Simões, M.G., Riccomini, C., Anelli, L.E., 2015. A Formação Serra Alta, Permiano, no centro-leste do Estado de São Paulo, Bacia do Paraná, Brasil. Braz. J. Genet. 45, 109–126. https://doi.org/10.1590/23174889201500010008.

Wesselingh, F.P., 2007. Long lived Lake molluscs as island faunas: a bivalve perspective. In: Renema, W. (Ed.), Biogeography, Time, and Place: Distributions, Barriers and Islands. Springer, Dordrecht, pp. 275–314.

White, I.C., 1908. Relatório sobre as Coal Measures e rochas associadas do Sul do Brasil. In: Relatório final da Comissão dos Estudos das Minas de Pedra do Brasil, Rio de Janeiro.

Woodhead, J.D., Hergt, J.M., 2005. A preliminary appraisal of seven natural zircon reference materials for in situ Hf isotope determination. Geostand. Geoanal. Res. 29, 183–195. https://doi.org/10.1111/j.1751-908X.2005.tb00891.x.

Wu, F.Y., Yang, Y.H., Xie, L.W., Yang, J.H., Xu, P., 2006. Hf isotopic compositions of the standard zircons and baddeleyites used in U–Pb geochronology. Chem. Geol. 234, 105–126. https://doi.org/10.1016/j.chemgeo.2006.05.003.